
**Investigation of condensin-related proteins and purification of the
DNA excision machinery in *Paramecium tetraurelia***

Inaugural dissertation
of the Faculty of Science,
University of Bern

presented by

Fukai Zhang

from China

Supervisor of the doctoral thesis:

Prof. Dr. Mariusz Nowacki

Institute of Cell Biology

**Investigation of condensin-related proteins and purification of the
DNA excision machinery in *Paramecium tetraurelia***

Inaugural dissertation
of the Faculty of Science,
University of Bern

presented by

Fukai Zhang

from China

Supervisor of the doctoral thesis:

Prof. Dr. Mariusz Nowacki

Institute of Cell Biology

Accepted by the Faculty of Science.

Bern, 15.11.2022

The Dean

Prof. Dr.

License



Attribution 4.0 International (CC BY 4.0)

<https://creativecommons.org/licenses/by/4.0/>

1. Abstract	6
2. Introduction	7
2.1. The <i>Paramecium tetraurelia</i>	7
2.2. Life cycle and nuclear development in <i>Paramecium tetraurelia</i>	9
2.2.1. Progressive genome rearrangement	11
2.2.2. Scanning models in IES excision	14
2.3. Structural maintenance of chromosomes (SMC)	18
2.3.1. The structure and function of condensin	22
2.3.2. The SMCs in ciliates	27
2.4. PiggyMac, a key protein in IES excisions	28
3. Aim of the thesis	30
4. Results	31
4.1. Part I: Research article: Functional analysis of structural maintenance of chromosomes (SMCs) in internal eliminated sequences (IESs) elimination in <i>Paramecium tetraurelia</i>	31
4.2. Part II: Purification of IES excision machinery by affinity capture and mass spectrometry from <i>Paramecium tetraurelia</i>	61
4.3. Part III: Expression of dominant negative form of PiggyMac in <i>Paramecium tetraurelia</i>	78
5. Conclusions and perspective	83
6. Methods and Materials	86
6.1. <i>Paramecium</i> strain and cultivation	86
6.2. Ethanol fixation and staining for <i>Paramecium</i>	86
6.3. Cloning	86
6.4. Silencing specific gene by dsRNAs feeding	87
6.5. Survival test	88
6.6. Genomic DNA extraction of <i>P. tetraurelia</i> cells	88
6.7. IES retention PCR	88
6.8. Microinjection linearized DNA fragments into the Macronucleus	89
6.9. Dot Blot	91
6.10. Macronuclear DNA isolation	93
6.11. Total RNA extraction with TRI	96
6.12. Analysis of sRNA in denaturing gel	97

6.13.	Co-immunoprecipitation	99
6.14.	SDS-PAGE.....	101
6.15.	Silver staining	103
6.16.	Western blot	104
6.17.	N-6× His-SUMO-PGM Expression	105
6.18.	N-6× His-SUMO-PGM purification	105
6.19.	Denaturing urea polyacrylamide gel electrophoresis	108
6.20.	Primer List.....	109
7.	References	111
8.	Appendix	120
9.	Acknowledgements	160
10.	Declaration of Consent	161
11.	Curriculum vitae	162

1. Abstract

The spatial organization of chromosomes is vital to life at the cellular level. DNA loops formed by condensin are the crucial structure of the meiotic and mitotic genomes which organize chromatin in interphase and metaphase. The structural maintenance of chromosomes (SMCs) protein family, which is now thought to serve as a DNA motor, is central to this organization. *Paramecium tetraurelia* is a ciliate that performs RNA-mediated widely genome rearrangement, mainly Internal Elimination Sequence (IES) excision, during sexual reproduction. The scanning model, which includes two sets of small RNAs (scanRNA and iesRNA), is widely used to explain this process. While the exact mechanism by which interphase and metaphase genome structure interact with IES excision is unknown to date. Given the importance of SMCs to chromosome structure and the poorly reported condensin in *Paramecium tetraurelia*, we explored the function of condensin SMCs in IES elimination and investigated whether their cooperation displayed different effects on this progress. One of the SMC4s in *Paramecium tetraurelia*, SMC4-2, is a novel player of IES elimination. Knockdown of SMC4-2 is lethal and causes the retention of almost all IESs, while the knockdown of SMC2s and SMC4-1 exhibit lethality to progeny without any sign of IES retention. Most interestingly, combining SMC4-2 RNAi with any of the other SMCs mentioned above abolished the retention in SMC4-2 single silencing. The SMC4-1 and SMC4-2 Co-immunoprecipitation and mass spectrometry analysis indicates a possibility that the interactions between SMC4-1 and SMC4-2 are decided by their concentration ratio of them. Additionally, we developed and optimized a purification method for IES-specific *in vivo* DNA binding complexes. The exact players of IES excision, especial the complexes that perform recognizing, binding and cleaving, are still unclear. This method allows us to purify specific-IES binding excision machinery from the new developing MAC where the old MAC contamination can be excluded. After that, we also tried to analyse the PiggyMac (PGM) interacting proteins by using Flag-HA tagged PGM 3A mutant. We were unable to enrich the PGM 3A-Flag-HA on anti-HA beads. However, we still provide some hints which could be helpful to further study.

2. Introduction

2.1. The *Paramecium tetraurelia*

Paramecium tetraurelia (*P. tetraurelia*) is an abundant, free-living, unicellular organism that is simple to cultivate in a lab. Generally, *P. tetraurelia* lives in various freshwater environments where it feeds on algae, yeast or bacteria¹. As a very popular studied ciliated which provides a fascinating viewpoint on the fundamental molecular and cellular processes of eukaryotic life² due to its location within Alveolate (Figure 1), which is distinct from the models that are most frequently employed³. There are several organelles in this foot-shaped cell containing in other eukaryotes, such as ribosomes, mitochondria, endoplasmic reticulum, a Golgi apparatus, a phagosome-lysosome system, an endocytic system of shuttle vesicles, and enveloped nucleus⁴. In the meantime, its huge body (approximately 120 μm long, 50 μm broad) and nuclear size (3 μm to 40 μm) make *P. tetraurelia* an ideal subject of cellular and molecular biology research. The occurrence of two different nuclei inside the same cell is a defining feature of ciliate genetics: the micronucleus (MIC) is diploid and the macronucleus (MAC) is highly polyploid, so-named due to their relative sizes to one other. Two different types of nuclei existing in the cytoplasm are advised as "nuclear dimorphism", and it is a trait shared by most of the ciliates. Another property shared by most ciliates is the extensive genome rearrangements during their sexual development. Both the number of nuclei and how genomic rearrangements are controlled vary greatly amongst ciliate species. In my research material *P. tetraurelia* has one MAC and two MICs in each cell⁵.

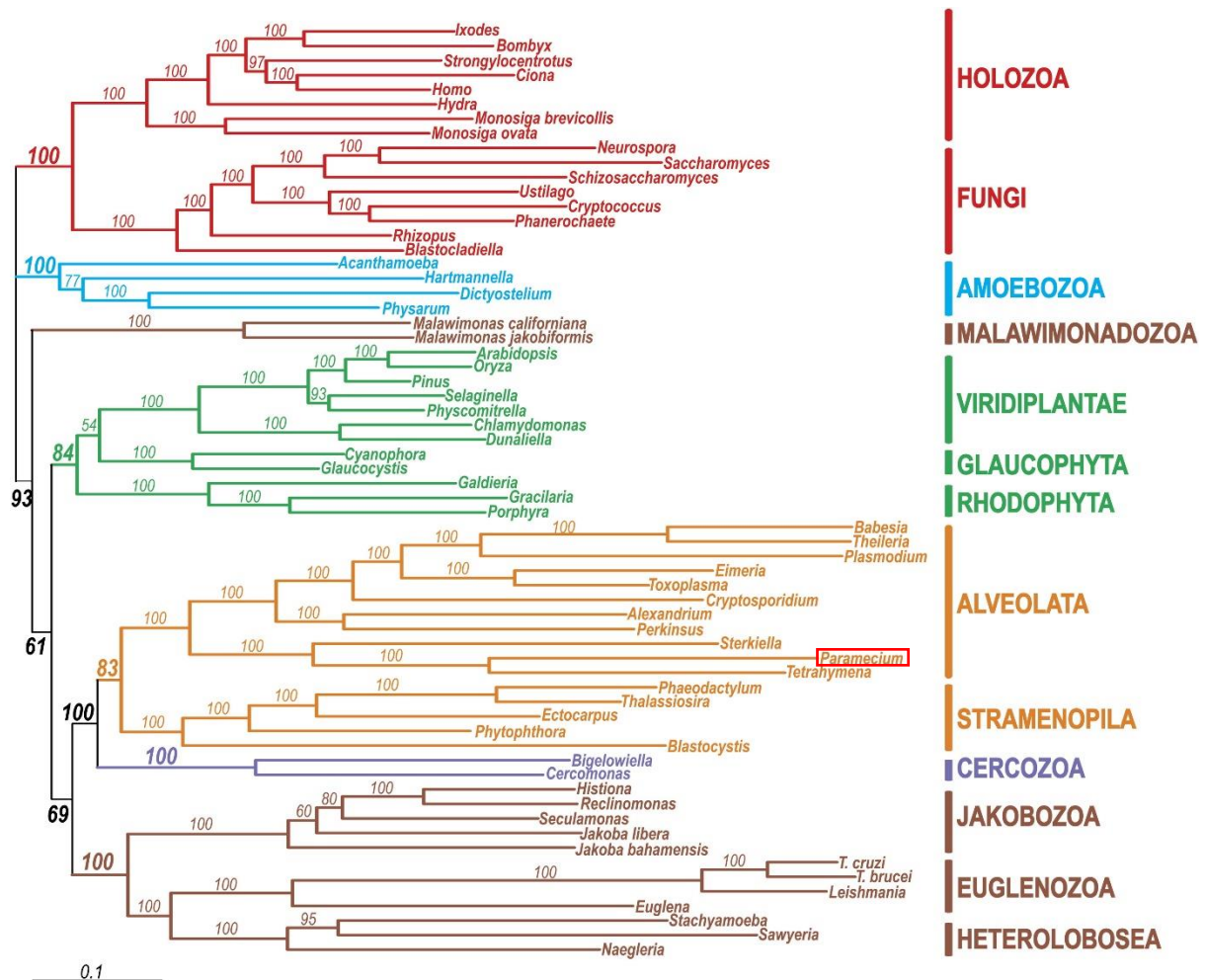


Figure 1. Phylogenetic tree of Eukaryotes. Adopted from ⁶. The tree, which contains 64 species, is built using 143 concatenated nucleus-encoded proteins (31,604 amino acid positions). The numbers represent RaxML analysis support values (100 repetitions) with the WAG + F + Γ model. For all branches, the posterior probability derived using Bayesian inference with MrBayes is 1.0. The number of amino acid substitutions per site is indicated by the scale bar. A gene fusion was used to root the tree. Ciliates are single-celled organisms that belong to the *Alveolata* superphylum. The tree includes the most widely researched families, *Paramecium*, *Oxytricha* (*Sterkiella*), and *Tetrahymena*. The *Alveolata* also includes parasitic protists such as *Plasmodium*. The ciliate families are further classified as *Oligohymenophora* (*Paramecium*) and *Stichotrichia*.

2.2. Life cycle and nuclear development in *Paramecium tetraurelia*

For the study of nuclear function and differentiation⁷, the process of meiosis, mitosis, autogamy, and conjugation in *P. tetraurelia* is quite useful. Also in studies of heredity, the ability of *Paramecium* achieving homozygosity of all loci at once with autogamy is particularly useful. The same is true for the production of heterokaryons by nuclear regeneration. Additionally, the investigator may readily regulate each of these steps. Two diploid MICs fulfil germline functions in one cell body, which is about 3µm in diameter, has around 50 chromosomes and a genome size of ~100 megabases⁸. The MIC is transcriptionally inactive during vegetative growth but can be a source of MAC generation and maturation during development. In addition to this, MIC can also maintain the genome information throughout sexual reproduction by meiosis and mitosis. Without the MAC, *P. tetraurelia* can only go through one or two cycles of fission, but without the MIC, the cells can endure more than one hundred fissions and can even mate⁹. The MAC genome looks like a simplified form of the MIC genome that primarily contains essential sequences for protein synthesis. The maternal MAC disappears during the sexual development of *P. tetraurelia*, and a new one from MIC takes its place¹⁰. The size of MAC is 35 µm in length and 12 µm in width with highly polyploid up to 800n copies¹¹. Due to the elimination of DNA occurring in sexual development, chromosomes in MAC are shredded into approximately 200 linear molecules, 50 kb to 1 Mb in size¹². The MAC is responsible for gene expression and considered a somatic nucleus. The existence of many nucleoli, which are absent from the MICs, and the fact that amacronucleate cells die without division, provide additional evidence for the gene expression activity in the MAC.

Like other ciliates, *P. tetraurelia* has the capacity for both vegetative growth and sexual development as shown in Figure 2. However, cells in immaturity cannot undergo sexual development like conjugation or autogamy. Additionally, cells can conjugate but cannot go through autogamy during a certain vegetative development phase following autogamy. This period is described as autogamous immaturity. Under normal conditions, like food-rich, less stressful, non-toxic etc., *P. tetraurelia* divides in a vegetative manner every 5 – 6 hours at 27 °C or 12 hours at 18 °C. Vegetative proliferation only occurs by binary fission, in which the MICs reproduce via mitosis. While the process of MAC division is called amitosis due to the absence of centromeres¹³, by which the MAC elongates and splits into two halves. The amitotic divisions does not ensure that two halves contain the same number of chromosomes.

After the vegetative division, each daughter cell will regulate its copy number to make it the same as their parental cells, although the mechanism behind is still an open question.

Besides the vegetative growth, *P. tetraurelia* cells must renew their somatic genome by sexual development since they can't divide vegetatively infinitely¹⁴. However, the presence of immortal ciliates that are incapable of sexual reproduction would imply that cells are essentially eternal and have evolved a mechanism to limit the ability for division when they develop the sexual process. The loss of such a mechanism can be shown by the emergence of strains in fatal species, such as *Tetrahymena pyriformis*, that can divide indefinitely¹⁵.

Conjugation and autogamy are two types of sexual reproduction of *P. tetraurelia* that are usually triggered by moderate starvation (the most employed strategy in the laboratory), environmental disturbance and ageing, which share very similar cytological steps¹⁶. The main distinction of the two processes is that during conjugation, the genetic material of two compatible mating type cells is exchanged, while autogamy, also referred to as self-fertilization, takes place within a single *P. tetraurelia* cell and forms homozygous cells. While autogamy happens in older cells, conjugation occurs in young cells. Generally, the sexual cycle begins with two meiotic divisions of both MICs in the cell, forming eight haploid nuclei, of which seven degrade quickly^{17,18}. The surviving one undergoes mitotic division, leading to two identical haploid nuclei. These two nuclei will be fused in autogamy or exchanged during one type of sexual development, conjugation, between *P. tetraurelia* have suitable mating types that form a zygotic nucleus. In the meantime, the parental MAC becomes fragmented but keeps the ability to transcribe as well as remain in the cells throughout the whole sexual development. The diploid zygote undergoes two further mitotic divisions very shortly after karyogamy. The sister nuclei are pushed to the opposite poles of the cell by the long spindles of the second postzygotic mitosis, with two in the front and two in the posterior area. Two of those nuclei will stay unchanged and generate new MICs in daughter cells. The other two nuclei (anlagen), on the other hand, will create new MACs. This polar localization is required for new MAC development, including enormous DNA synthesis, transcription, and chromosomal rearrangements. This is followed by a specific cell division known as karyonidal division, in which MICs are mitosis-separated into the progeny, whereas the two MACs do not divide and are merely segregated into two daughter cells. The old MAC gradually disappeared throughout the cycle. The fragments, on the other side, stay transcriptionally active for some reason and are processed by subsequent vegetative divisions¹⁸.

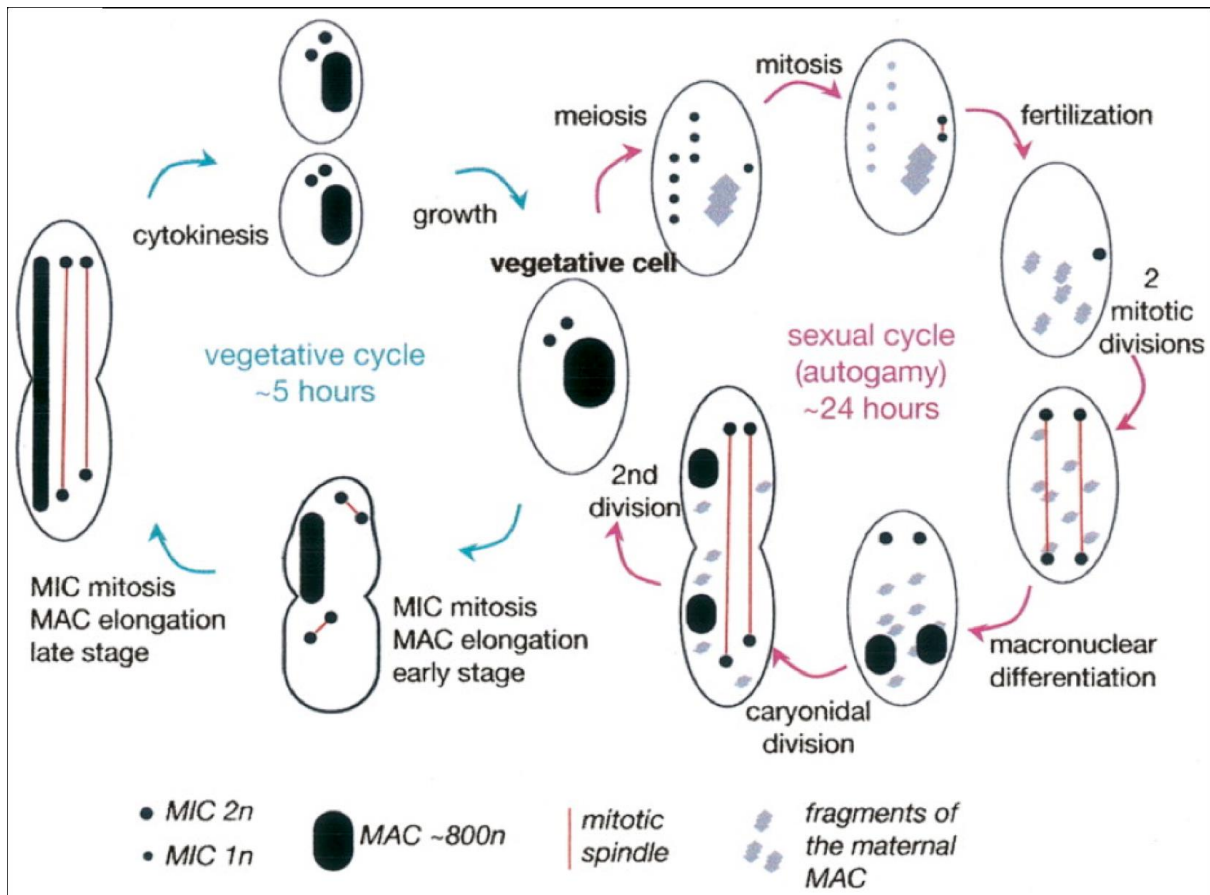


Figure 2. Vegetative (Left) and sexual (Right) phases of the *Paramecium* life cycle. Adapted from Beisson J⁴. The vegetative cell cycle (left part) starts from the MIC mitosis and MAC elongation under favourable conditions. The MAC divides amitotically into two daughter cells and the two daughter cells are separated by cytokinesis. The daughter MAC genomes will grow up to the same size as parental MAC in a poorly understood mechanism. Autogamy shown on the right side is one of the sexual cycles in *P. tetraurelia*. This event includes meiosis of each MIC, two parental diploid MICs become eight haploid MICs. In the meantime, old MAC started to fragment and seven out of eight monoploid MICs are degraded, the single surviving one goes through additional mitosis (two haploid MICs) and karyogamy resulting in a new diploid MIC. With two consecutive mitosis, one diploid MIC becomes four diploid MICs in the same cytoplasm. Two of them are chosen to develop into new developing MACs with progressively genome rearrangement, the other two MICs stay as MICs before another round of mitosis. The mechanism of this selection is still unclear. After that, the cell will be divided into two daughter cells with equal distribution of genetic material.

2.2.1. Progressive genome rearrangement

Even though the MAC is produced from the MIC, their genomic content and organisation differ significantly. The reason for the differences is that the MAC undergoes dramatic

genome rearrangement (Figure 3). The genome rearrangements include DNA amplification leading to high ploidy of MAC (up to 800 n) and the sequences eliminated often involve transposable elements and repeated sequences, like minisatellites. This causes chromosomal fragmentation via internal deletions or *de novo* telomere addition when left regions are reconnected and ligated¹². Internal eliminated sequences, or IESs, have to be removed precisely from the immature MAC since 80% of the IESs are located within protein-coding regions¹⁹. As a result, DNA elimination is critical for the formation of a functioning MAC genome. More than 45,000 single-copy, AT-rich IESs have been determined by knocking down the domesticated transposase PiggyMac (PGM), which is required for the removal of IESs during development²⁰.

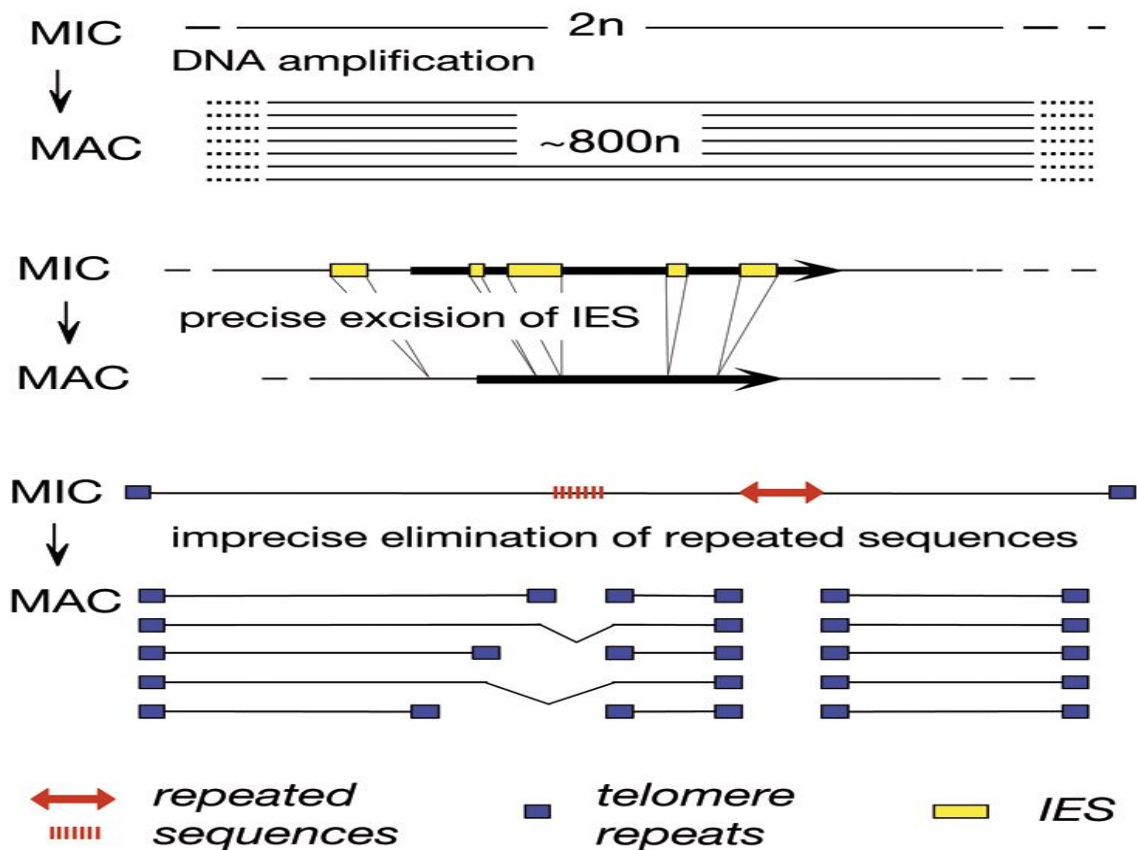


Figure 3. Genome rearrangement during the development of MAC⁴. Ploidy: In mature MICs, there are only two copies of chromosomes (2n); in mature MAC, the genome is amplified to highly polyploid (up to ~800n). Precise elimination of IESs: Around 45,000 single-copy, AT-rich IESs are eliminated in the MAC genome when developed from MIC. Imprecise elimination of repeated sequences: transposons and minisatellites, repeated sequences, are removed during the MAC's maturation. Fragmentation of chromosomes is formed by these imprecise eliminations and *de novo* telomerization stabilizes the newly formed free chromosome ends.

The length of an IES varies between 26 and 4838 bp, with one-third of IESs being 26-28 bp long. Furthermore, the short IESs found in *P. tetraurelia* have a size distribution (Figure 4) with a periodicity of 10.2bp, which corresponds to a double-stranded DNA helical repeat. While the second peak (expected at 35 bp) as seen in the profile only contains a few IESs, it is so-called the forbidden peak. This size range of IES may result from excision machinery restrictions and evolutionary pressure to IESs outside of certain size ranges²¹. IESs are hypothesised to be evolutionary remains of transposable elements that infiltrated the MIC genome, then degenerated over time by deletions and nucleotide substitutions²². Most IESs display lengths below 150 bp and are flanked with 5'-TA-3' repeats, one of them remains non-excised in the developed MAC genome after the IES has been eliminated²³. Every IES TA repeat is accompanied by the very weak consensus sequence TAYAGYNR, which is supposed to be decisive since any change in the conserved sequences can impede IES excision. The similarity of IES ends to *Tc1/mariner* transposons gives rise to the assumption that IES could be originated the insertion of these mobile elements followed by the missing coding capacity throughout evolution²⁴. Besides terminal IES sequences, sequences flanking IESs have been involved in excision in some cases. Excision was abolished in *Paramecium* by removing a piece of its flanking region from one end of the specific IES²⁵.

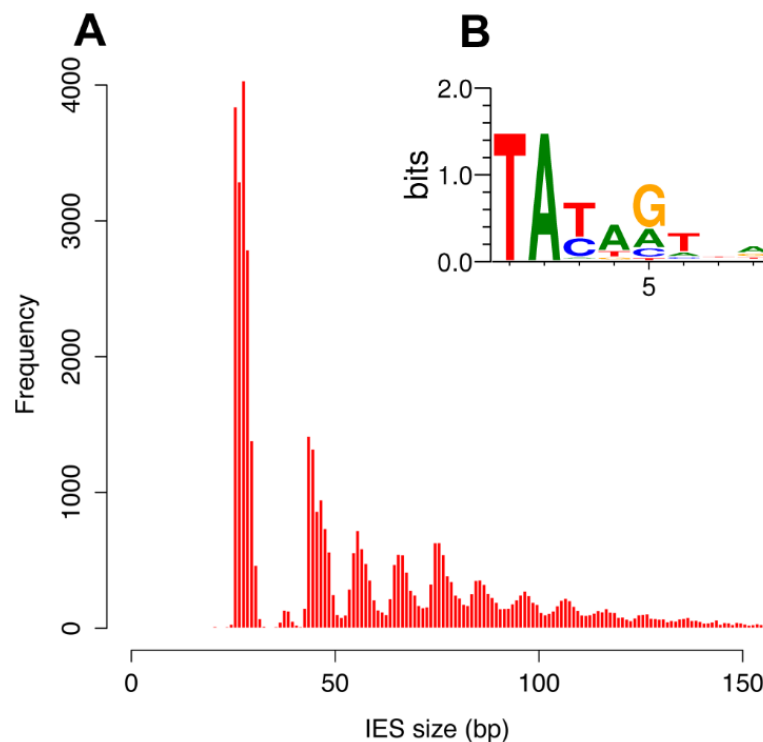


Figure 4. IES sequence distribution²¹. A) Histogram shows the genome-wide collection of IESs with lengths smaller than 150 bp. B) For the terminals of the genome-wide collection of IESs, a sequence logo depicting sequence preference at each place, was adjusted for a G+C content of 28%.

2.2.2. Scanning models in IES excision

The excision machinery's recognition of IESs is not well understood. Excision of these distinct sequences requires a precise match. The IESs' loosely conserved end consensus sequence is deficient in explaining their recognition pattern suggesting that there must be another mechanism behind the precise elimination. Several theories have outlined the presumed roles of small RNAs (sRNAs) in IES excision as well as their participation in epigenetic events²⁶⁻³⁰. This mechanism has been widely studied and accepted in IES excision as a model called “the scanning model” (Figure 5). This model, first proposed in *Tetrahymena thermophila*, outlines how sRNAs control the process of precise IES excision in a manner comparable to RNA interference (RNAi). In the example of *Paramecium*, two kinds of sRNAs have been found to mediate the cross talk between the MAC and MIC during autogamy: early expressed scan RNAs (scnRNAs) and late expressed IES RNAs (iesRNAs). At the onset of sexual development, in the meiosis of the MICs, the genome is bi-directionally transcribed to form longed double-stranded RNA transcripts³¹ which are processed by Dicer-like (Dcl) enzymes named Dcl2 and Dcl3²⁷. Recently, it has been reported these *Paramecium* enzymes had cleavage selectivity when generating scnRNA, with Dcl2 keeping a solid size preference for 25 nt and a terminal preference for 5' U and 5' AGA, and Dcl3 exhibiting a terminal preference for 5' UNG. Taken together, functional scnRNAs are 25nt in length and exhibit a 5' UNG preference³².

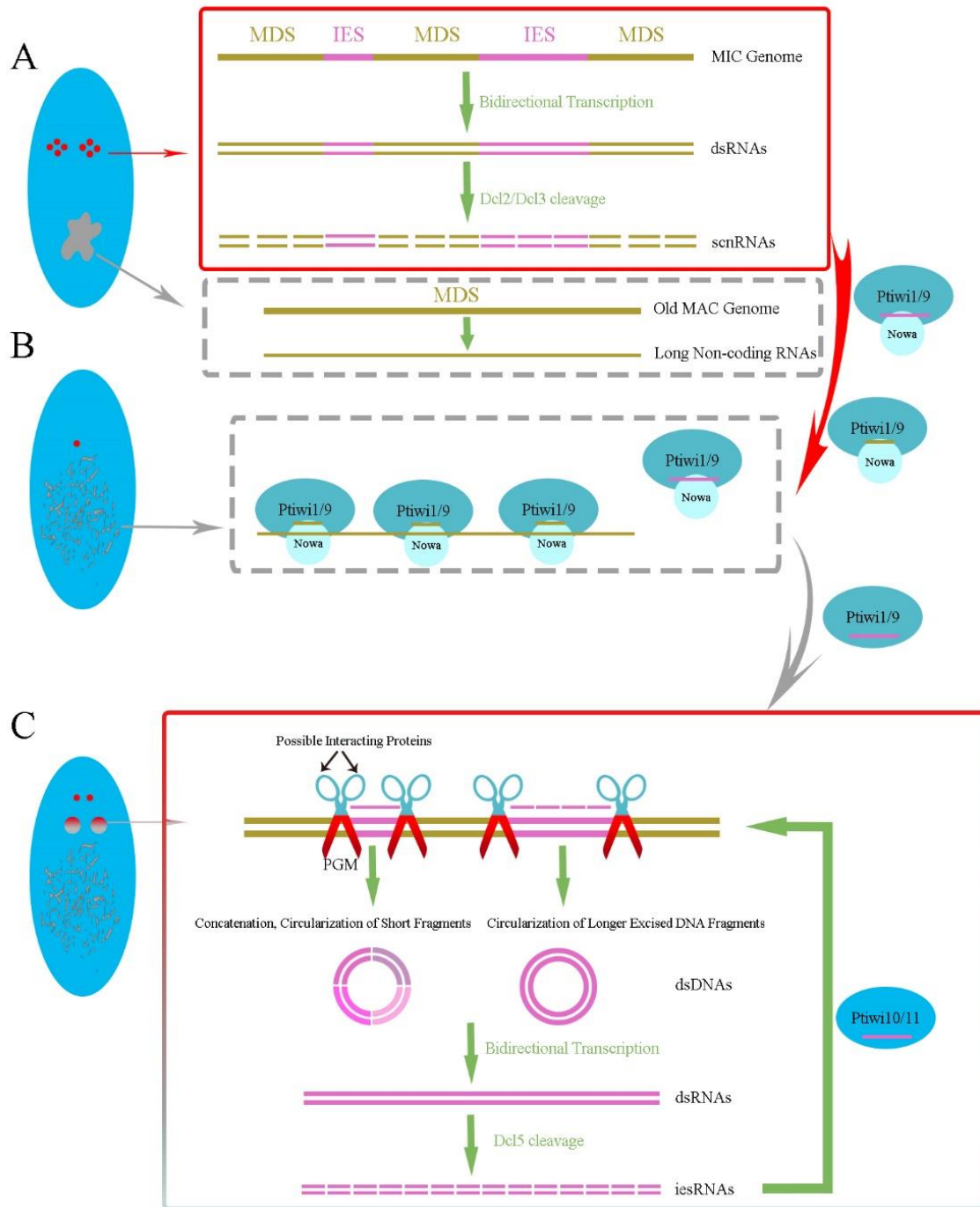


Figure 5. Scheme elucidating the scanning model in *Paramecium*. A) The meiosis of MIC initiates genome rearrangement. The MIC genome is transcribed bidirectionally, and the dsRNAs are processed into the scnRNAs, which consist of MDS (khaki) and IES (pink) dsRNA, by the Dcl2/3 cleavage. Ptiwi1/9 choose and carry one strand of the scnRNAs, and transport them into the fragmenting maternal MAC. B) This nuclear crosstalk might be mediated by Nowa proteins. The scnRNAs that are unable to match with MAC transcripts are transferred into new developing MACs by Ptiwi1/9. C) The new MACs, being clones of the MICs, include MIC-specific IES sequences, that

must be removed to generate a functioning somatic genome. The DNA regions marked by MIC-specific scnRNAs are supposed to be removed by PGM and co-factors. Shorter excised IESs concatenate then circularise, while longer excised IES circularises directly. The dsRNAs are transcribed from IES circles with a rolling-circle transcription method. Another Dicer-like enzyme, Dcl5, converts these transcripts into the second type of sRNAs: iesRNAs. As the name implies, iesRNAs only map IESs. The iesRNAs are targeted by additional Ptiwi proteins, Ptiwi10/11, as well as anchor more IESs for excision. This procedure is supposed to be a positive feedback loop to ensure all copies of each IES are completely removed.

After being produced in the MICs, scnRNAs are loaded onto specific Piwi proteins, Ptiwi1/9, which remove the matching passenger strand after selecting a guide strand³³ and immigrated into the old MAC. At this time, the old MAC is slowly fragmenting and its genome is transcribed into long non-coding RNAs³⁴. The Piwi proteins that transport the scnRNAs are believed to scan those prolonged RNA transcripts with the assistance of Nowa³⁵. The scnRNAs that match MDS bind to the transcripts and are inactivated selectively. The scnRNAs only containing germline-specific sequences, on the other hand, cannot match to any sequences from the MAC genome, are those desired scnRNAs. These sets of scnRNAs are carried into the new developing MAC by Ptiwi1/9. This kind of targeting is supposed to be a scan for complementary sequences again. Given that the new developing MAC is derived from MICs, the regions complementary to scnRNAs are IESs and are removed by PGM.

Another kind of short RNA is produced late in the new MAC development from IESs that are going to be removed. These small RNAs, known as iesRNAs, only map IES sequences. They range in size from 26 to 30 nucleotides and have a 5'UAG and 3'CNAU signature, with the characteristic 2nt 3' overhang signature of Dicer/Dicer-like protein activity. Dcl5 is in charge of iesRNA production from a double-stranded RNA precursor, and *DCL5* knockdown entirely prevents its occurrence. Inhibiting IES excision, as with Dcl2/3 co-silencing, significantly reduces iesRNA levels. Thus, iesRNAs are produced from eliminated IESs and function in the positive feedback loop to ensure all copies of each IES removed from the developmental MAC genome^{26,32}. Briefly, following excision, these IESs are either joined by alignment of TA overhang when they are longer than 200 bp³⁶ or similarly ligated with other IESs as long IESs when they are too short for circularisation. These extrachromosomal circles would be the source of the template for iesRNA precursor production. Theoretically, RNA polymerase complexes could interact with IES concatemers, this interaction provides a good

chance to generate enough copies of all IESs transcripts in it. As mentioned before, Dcl5 is in charge of iesRNAs production from double-strand iesRNA precursors. This sequence preference, interestingly, matches the ligated IES end conserved sequences of two IESs, or junctions between IESs. According to *in vitro* cleavage experiments, Dcl5 particularly detects these junctions and truncates sRNAs according to the distance between the junction motifs. The elimination would be blocked by mutations in these motifs. Consequently, iesRNA precursors are disassembled back into sRNAs that correspond to individual IESs²⁷. Like the chosen scnRNAs, double-strand iesRNA is loaded onto Ptiwi10/11, the second pair of Piwi proteins, which pick a specific strand and carry it to further IES copies in the genome³⁷. As IESs are mainly located in the coding regions in the genome, IES excision may be essential for iesRNA generation, as well as for the expression of genes implicated in the pathway. The IES excision in the developmental MAC might be a fundamental method for unblocking genes at the optimal time³⁷.

There are still several questions that should be asked in the scanning model. One of them is whether scanning occurs through a DNA: RNA based or RNA: RNA based mechanism. Because both hybrids are found in ciliates by direct and indirect evidence before, a previous member of our lab used Chromatin Associated RNA sequencing (ChAR-seq) to answer the question about DNA: RNA hybrid's existence in *P. tetraurelia*. Unfortunately, no evidence has been indicated that the sRNA: DNA hybrid presents in the scanning model in our lab. Actually, before answering this question, a prerequisite has to be confirmed whether helicase or similar proteins are included in the RNA-guided IES excision or not. If yes, could it be possible that the IES excision to be coupled with the massive genome amplification in the developmental MAC? If not, then how do the sRNAs recognize double-stranded, highly dense DNA in new MAC? Another question comes from the "cut and repair" mechanism. Following the excision, the ends of the flanking regions are subsequently ligated together in a way similar to the non-homologous end joining DNA repair mechanism. Ligase IV and Ku70/Ku80 have been identified as players to catalyse this repair^{19,38}. While the removal of IESs shortens the length of the chromosome when several shorter IESs or one longer IES (even 4 kb sometime) get truncated. In whatever way of repairing the lesion after excision, the ligation of ends pulls two pieces of chromosome nearer which should be impossible unless there was a mechanism that can close the spatial distance before or during the repairing.

2.3. Structural maintenance of chromosomes (SMC)

The genome compaction controls the organization of chromatin and its activity in the nucleus. As shown in Figure 6, in a typical metazoan cell, DNA is condensed up to 10,000 times in length to construct a metaphase chromosome compared to chromatin³⁹, which means the operating space for functional proteins has been reduced a lot. Since Walther Fleming⁴⁰ first defined the dynamic activity of chromosomes during cell division, its duplication and division into two daughter cells are the two essential processes. Chromosomes undergo incremental structural changes that guarantee their segregation with high fidelity, making them more than just passive cargo or information carriers⁴¹. How this astonishing feat of packing is accomplished and how the chromosomes are reliably segregated into the daughter cells have been central concerns. The SMCs is an abbreviation of structural maintenance of chromosome proteins which have been studied during the last decades. As critical participants in both chromosomal condensation and segregation, the convergence of evidence from genetic and biochemical techniques has been reported⁴². Nearly all investigated living things encompass SMC proteins. They are crucial for mitotic chromosomal dynamics, gene expression regulation, and DNA repair. Their activities in several dimensions of chromosomal activity are conserved in these species⁴³.

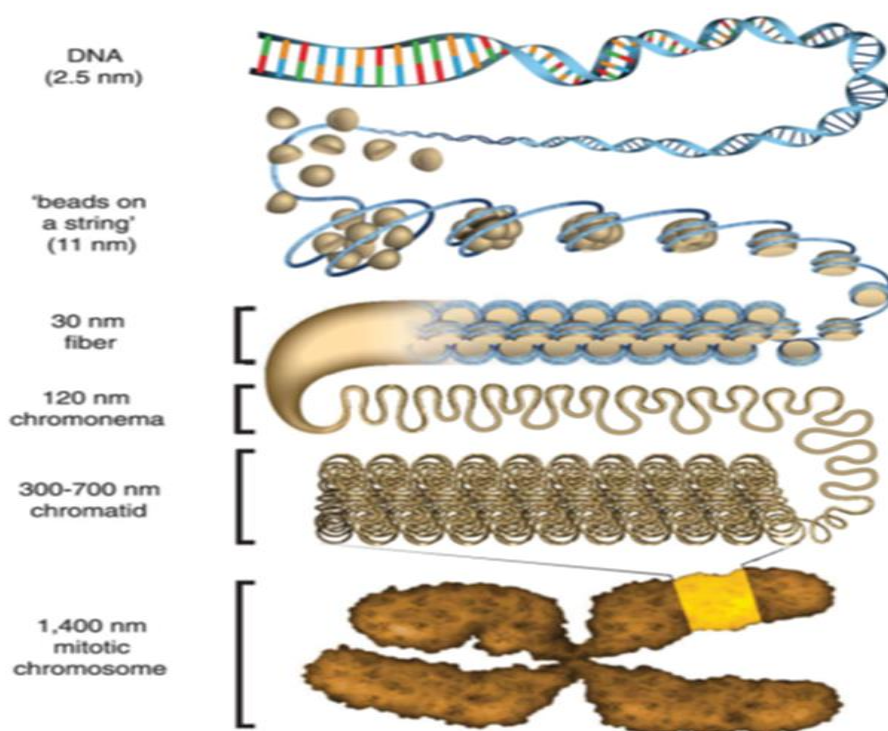


Figure 6. Hierarchical chromatin-folding model. Adopted from⁴⁴. DNA is organised into chromatin structures in the nucleus, which controls the activity and inheritance of human genomic DNA. A 147 bp long DNA strand is wrapped around an octamer of histones H2A, H2B, H3, and H4 to form an 11-nm DNA-core nucleosome particle. Each DNA-nucleosome particle is separated by 20 to 75 bp of histone H1-binding DNA. This primary nucleosome polymers further fold into secondary 30 nm fibres. There are two different structural models of the 30 nm fibres which refer to as the zigzag and solenoid fibre models. The solenoid fibre structure is 33 nm in diameter and includes six nucleosomes every 11 nm along the fibre axis. The diameter of the two-start zigzag fibre is 27.2 to 29.9 nm, with five to six nucleosomes per 11 nm. It is assumed that the 30 nm fibre assembles into helically folded 120-nm chromonema, 300 and 700 nm chromatids, and mitotic chromosomes.

Most DNA-based activities are influenced by SMC complexes. Each 1,000–1,300 amino acids long, 110 KDa to 170 KDa SMC protein comprises a core globular hinge domain. Recent research has revealed that the hinge domain is the primary place where these molecules dimerize^{45,46}. The hinge interface preferentially binds short single-strand DNA (ssDNA)⁴⁷ and can spread structural changes to the head domains via the coiled-coil regions^{48,49}. A globular domain containing a Walker A (GxxGxGKS/T) or Walker B motif (XXXXD, where X is any hydrophobic residue) (amino acid consensus sequences present in NTP-binding proteins named after J. E. Walker and co-workers, who initially discovered these motifs⁵⁰) flanks this domain and is bridged by two extended coiled-coils domains. The coiled-coil regions can transmit conformational changes induced by ssDNA interaction of the hinge domain to the head domains which triggers ssDNA-stimulated ATP hydrolysis, involving head-to-head disengagement⁵¹. The protein is folded at the hinge, allowing the coiled domains to interact in an anti-parallel manner⁵². As a consequence, a functional ATPase domain that resembles an ATP-binding cassette (ABC) domain structurally is formed by joining the amino and carboxyl termini^{53,54}. In such a complex, two SMC proteins bind at the hinge region to create long-armed V-shaped dimers^{45,55}, which are then attached to non-SMC subunits that are distinctive to the complex⁵⁶⁻⁵⁸. A member of the kleisin protein family brings together two head domains of the V-shaped SMC protein dimers, allowing SMC complexes to carry on ring-like shapes^{59,60}.

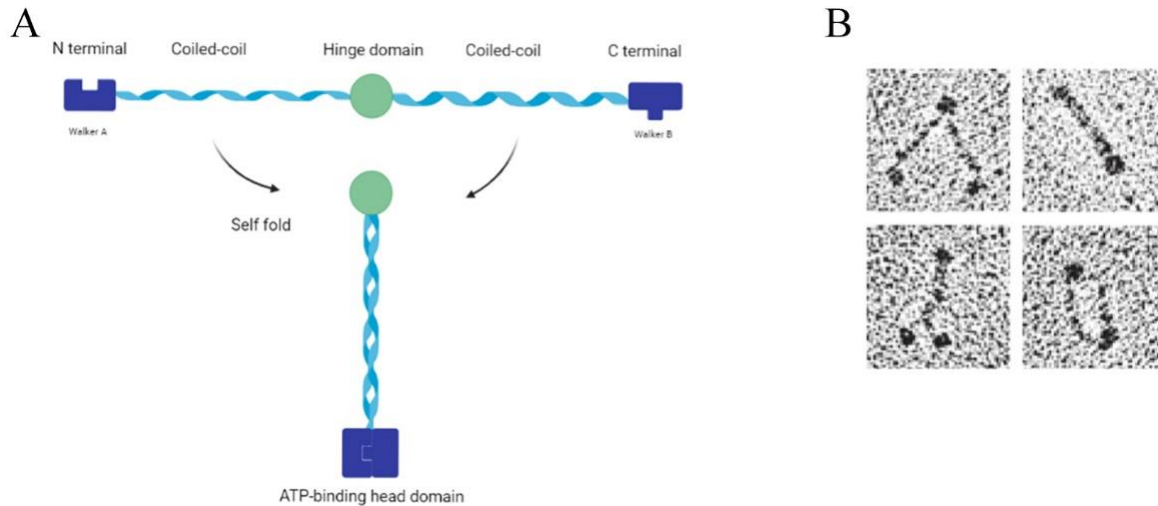


Figure 7. The architecture of SMC protein and SMC homodimers. A) A SMC protein's fundamental structure. The SMC self-folds through antiparallel coiled-coil interactions to create a hinge domain end and an ATP-binding head domain end. B) Dimerization is mediated by a hinge-hinge connection between two subunits, which results in a V-shaped molecule. The SMC homodimers display a wide range of conformations⁶¹.

Only one gene of each SMCs has been discovered in each of the prokaryotes examined, and it appears to form homodimers. Based on the sequence homologies, this family can be classified into six subfamilies in eukaryotes⁶² as in Figure 8. And the protein appears to form at least three types of heterodimers. These heterodimers involve the SMC1/SMC3 in the cohesin complex, the SMC2/SMC4 in the condensin complex, and the SMC5/SMC6 heterodimer, which forms a core part of a complex participating in DNA repair⁶³.

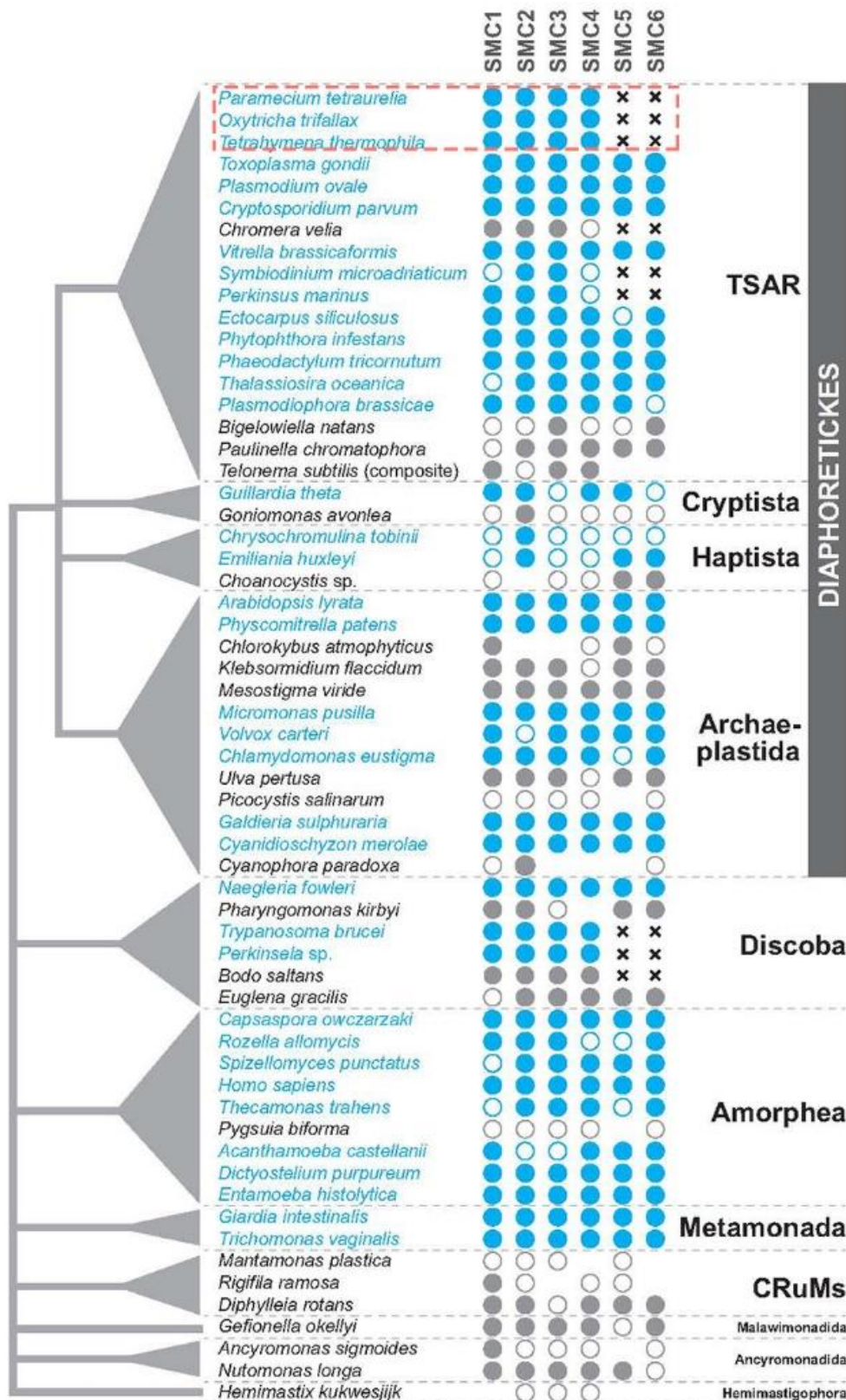


Figure 8. Exhibition of six SMC subfamilies in eukaryotes. Adopted from⁶⁴. SMC sequences were found in 59 species, which represent the main taxonomic assemblages in the eukaryotic tree. On the right, symbols of each species present the presence or absence of all these SMCs. The SMC5/SMC6

absent in those eukaryotes (x-marks) were indicated. When a subfamily was not discovered in the relative transcriptome database, no symbol in the relevant column was used to show undetermined.

2.3.1. The structure and function of condensin

Observations of mitotic chromosome kinematics in cytology first suggested the presence of molecules that compact chromatids or maintain sister chromatids together. The recovery of mutants deficient in these processes, together with the biochemical identification of mitotic chromosome-associated components, gave rise to the finding of condensin and cohesin⁶⁵. Condensin and cohesin both include the SMC family proteins at their cores, but the two complexes are structurally and functionally distinctive^{42,63}. Cohesin holds sister chromatids together until anaphase, before they separate, whereas condensin restructures chromosomes into their compact mitotic configuration⁶⁶.

As shown in Figure 9, five subunits comprise the highly conserved condensin that utilises ATP to drive conformational changes in DNA, allowing it to address DNA compaction, architecture, and segregation from bacteria to humans. Higher eukaryotes generally have two condensin complexes (I and II), both of which consist of SMC2 and SMC4 heterodimers as the core part. The main differences between the two condensins are their non-SMC subunits, CAP-D2, CAP-H and CAP-G present in condensin I, while CAP-D3, CAP-H2 and CAP-G2 consist of condensin II^{67,68}. Different species have different condensin I/II ratio. The condensin I/II ratio in human HeLa cells is 1:1, but 5:1 in the *Xenopus* egg, and 10:1 in isolated mitotic chromosomes from chicken DT40 cells⁶⁹. Interestingly, *Caenorhabditis elegans* (*C. elegans*) contains three distinct condensin complexes, condensin I and II, as well as a third one, condensin I^{DC}, which exclusively acts in dose compensation⁷⁰. In *T. thermophila*, a specialized condensin (condensin D) that does not appear to function in chromosome segregation has been identified by Howard-Till and co-workers⁷¹. It is essential for the completion of sexual reproduction and the developmental program of the somatic nucleus including DNA elimination. Condensins I and II also show distinct temporal and spatial localization profiles in higher eukaryotes. Condensin I is predominantly located in the cytoplasm in interphase and engages chromosomes just following the breakdown of the nuclear envelope in prometaphase, on the other hand, condensin II is mostly nuclear localization and attaches chromosomes when condensation occurs in prophase^{72,73}. A combination of two functional assays revealed that condensin II interacts with duplicated

regions of chromosomes⁷⁴. Mutation or removal of condensin subunits in a diversity of species disturbs appropriate chromosome condensation, resulting in chromosome segregation errors and cell death. Even though the two mitotic condensins are highly comparable, their pattern of localization implies that they may perform unique functions in the chromosomal organisation. Consistent with this assumption, depletion of either condensin I or II results in unique chromosomal defects, whereas depletion of both condensins results in more severe defects^{68,75}.

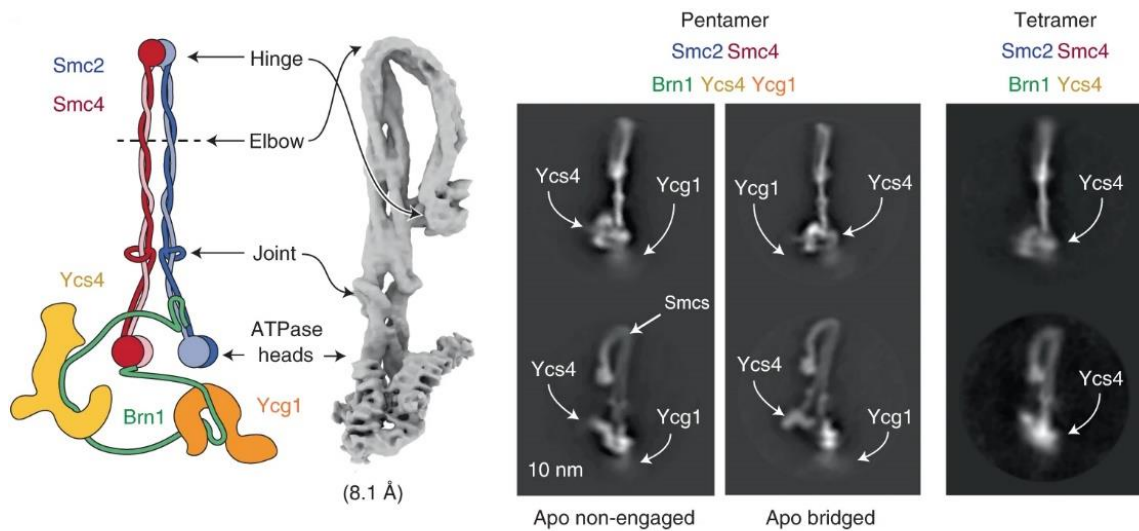


Figure 9. Cryo-EM structures of the yeast condensin holo complex in the nucleotide-free apo form. Adopted from⁷⁶. The left part is the schematic model of condensin, and the right part shows the 8.1-Å-resolution 3D map that shows its overall architecture.

Condensin has functional differences across species. Although it was previously thought that, in most organisms, condensin only interacts with chromosomes during the cell cycle when they are condensed (prophase to anaphase), an increasing amount of data have revealed that condensin also plays important functions in controlling the interphase genome⁷⁷. Even though they are widely distributed across the genome, genes that act in comparable processes frequently inhabit similar areas of the nucleus⁷⁸. Condensin associates with DNA replication termination and genome integrity maintenance in the nucleolar organiser territory, which contains ribosomal DNA repeats^{79,80}. Condensin both promotes the clustering of distributed loci into subnuclear regions and inhibits homologous connections^{81,82}. Condensin II dissolved synapsed chromosomes into individual homologous chromosomes in *Drosophila* ovarian nurse cells⁸³. This unpairing activity causes chromosomal compaction during interphase⁸⁴. It has been demonstrated that yeast condensin has a function in interphase chromatin

architecture and RNA polymerase III transcribed gene clustering too. Condensin-mediated localization of these genes in the nucleus aids in the three-dimensional organisation of the genome in budding and fission yeast⁸⁵. Mutations in yeast condensin subunits result in tRNA gene stationing deficiencies and partially block tRNA gene-mediated silencing⁸⁶, revealing another association between genome organization regulated by condensin and gene expression⁸⁷.

As cells advance through the cell cycle, chromosomes undergo substantial changes in structure. During mitosis, chromosomes are compressed into dense arrays of arbitrarily positioned sequential chromatin loops. There is growing evidence that the establishment and extension of DNA loops, also known as loop extrusion⁸⁸, is the fundamental mechanism behind SMC complexes' ability to organise DNA. Several putative models for loop extrusion by SMC complexes have been proposed. These models are exhibited in Figure 10. In DNA damage repair, the initial loading of condensin to DNA was thought to occur via the SMC hinge-DNA interactions at the ssDNA region which is generated behind the replicative helicase⁸⁹. Chromosome-conformation capture (Hi-C) on topological domains^{90,91} and polymer simulations⁹² suggested the formation of such DNA loops, whereas recent *in vitro* single-molecule studies provided experimental evidence of condensin's DNA translocase activity and ability to extrude DNA loops⁹³. Also, evidence of loop extrusion by real-time imaging of the formation and processive extension of DNA loops by yeast condensin has been reported in 2019⁹⁴. A direct DNA-binding site in the eukaryotic condensin complex formed by Ycg1^{Cnd3} HEAT-repeat and Brn^{Cnd2} kleisin subunit has been identified which serves as a safety belt that prevents DNA dissociation from the groove⁹⁵. The extrusion can be formed in an ATP hydrolysis-dependent, strictly asymmetric manner by condensin. Recent research results indicate that the active condensin complex transiently entraps the bases of a DNA loop in two distinct chambers. Single-molecule imaging and cryo-electron microscopy point to a possible power-stroke movement at the first chamber, which feeds DNA into the SMC-kleisin ring in response to ATP binding, whereas the second chamber remains upstream of the identical DNA double helix. By removing the stringent separation of the "motor" and "anchor" chambers, condensin is transformed from a one-sided to a bidirectional DNA loop extruder. It is inferred that the directionality of DNA loop extrusion is determined by the direction of two topologically coupled DNA segments during the SMC reaction cycle⁹⁶. These properties mainly mean that condensin makes stable contact with DNA at a binding site of non-SMC subunits and then reels the DNA from only one side.

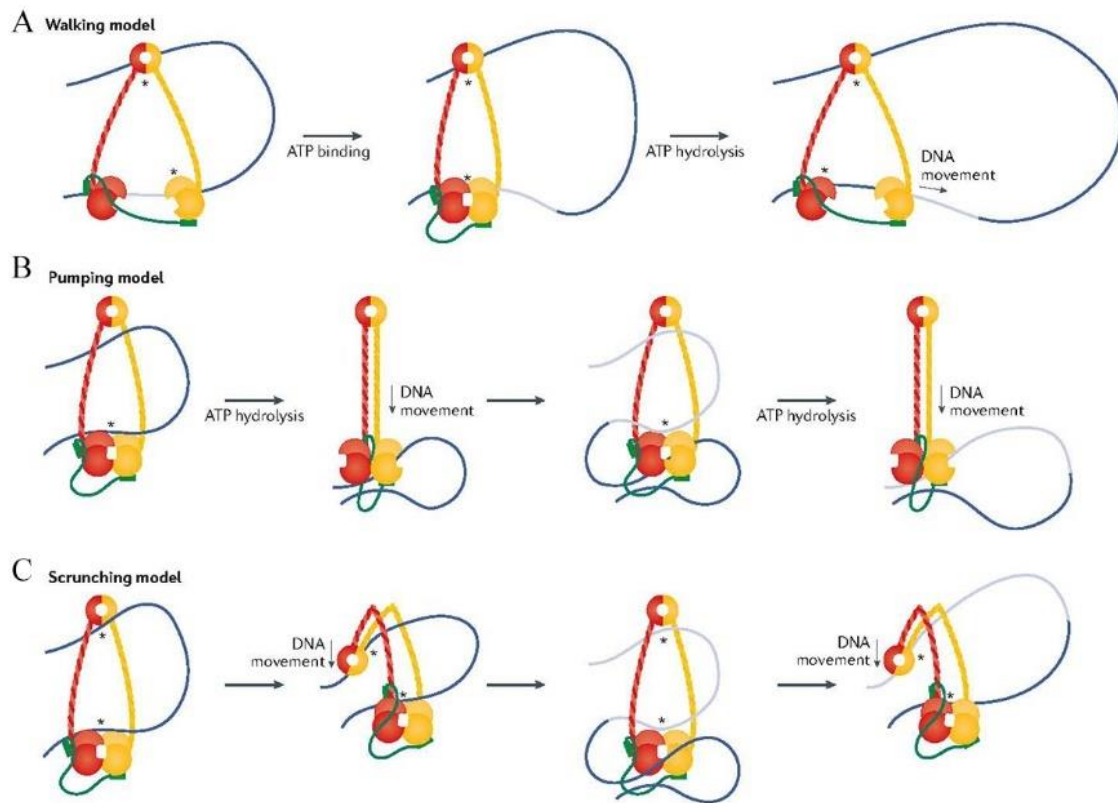


Figure 10. Putative models of loop extrusion. Adopted from⁹⁷. A) The walking model. During the SMC ATPase cycle, DNA segments (blue) are passed across SMC ATPase domains. If the hinge domain connects with a distal DNA segment during this process, loop extrusion may occur. If the hinge has a poor affinity for DNA and glides along it, symmetrical loop extrusion may occur. B) The pumping model. The SMC complex encircles a DNA loop and binds to it via the ATPase head domains. ATP hydrolysis causes the SMC coiled coils to align and pushes the DNA loop towards the ATPase heads. If the SMC complex encircles a second DNA loop (grey) after the head engagement, loop extrusion might occur. C) The scrunching model. At the ATPase heads and the hinge, the SMC complex attaches to DNA. If these transitions are connected to the SMC ATPase cycle, a folded conformation may facilitate the handover of a DNA segment from the hinge to the heads or vice versa, resulting in DNA translocation. If one DNA segment is constantly attached throughout this process, asymmetrical loop extrusion may ensue. If DNA binding shifts between the loop's two arms, symmetrical loop extrusion may occur.

Mitotic chromosomes fold as compact arrays of chromatin loops. An emerging model of prometaphase chromosomes is shown in Figure 11. As in chicken cells, the chromatin loops nested in a way of ~400 kb outer loops generated by condensin II split up by ~80 kb inner loops formed by condensin I. Chromosomes shrink as prometaphase progresses due to

increased helical winding, with the number of loops per turn rising. Consequently, the size of a helical turn ranges from ~3 Mb (~40 loops) to ~12 Mb (~150 loops)⁹¹.

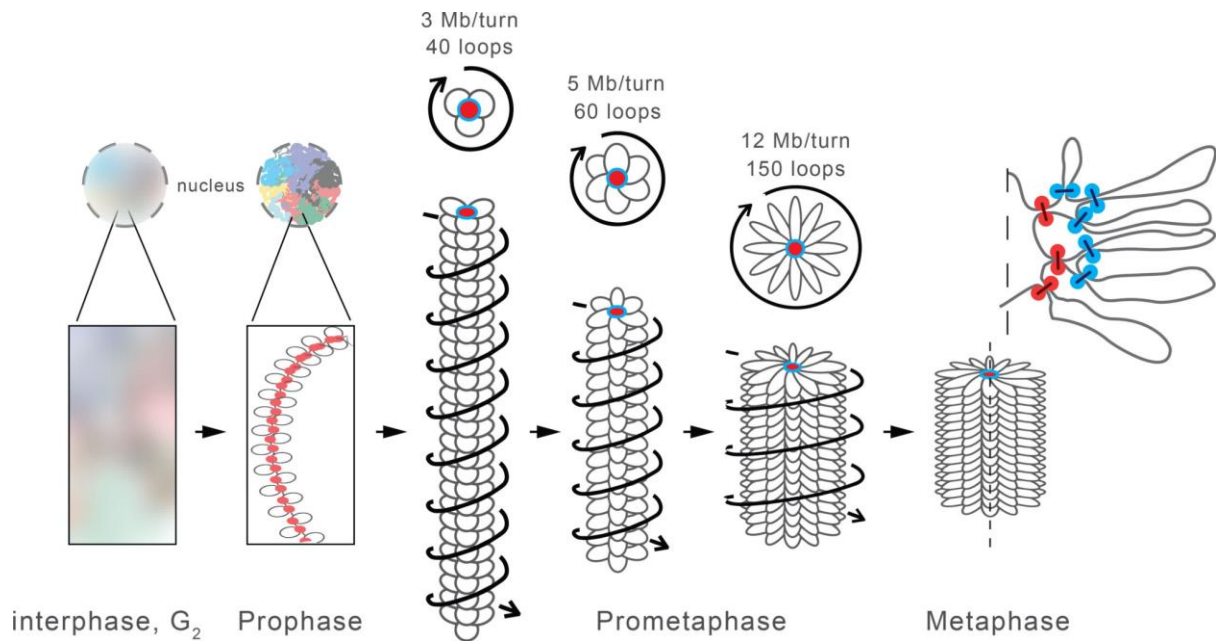


Figure 11. Schematic model of mitotic chromosome morphogenesis pathway. Adopted from⁹¹.

Condensin II compacts chromosomes into arrays of successive loops and sister chromatids divide along their length during prophase. In red is the scaffold of condensin II-mediated loop bases.

Condensin II-mediated loops become more enormous when the nuclear envelope breaking and the cell enters prometaphase, splitting into smaller 80 kb loops via condensin I. Chromosomes are depicted as loop arrays. The nested configurations of condensin II-mediated loop bases in the centre and condensin I-mediated loop bases in the periphery are depicted in red and blue, respectively. The core scaffold develops a helical configuration during prometaphase, with loops spinning around the scaffold as steps in a "spiral staircase" (the helical path of loops is indicated by arrows). Outer loops develop and the number of loops per turn grows as prometaphase advances, and chromosomes shrink to become the mature mitotic chromosome.

In addition to the loop extrusion, a new evidence shows that condensin might interact with the RNA-DNA hybrid and remove the RNA, followed by the annealing of ssDNA to form dsDNA⁸⁹. Before mitosis, condensin competes with other DNA-bound components and unloads them from the chromosomal region to generate a clean chromosome. The promotion of ssDNA annealing could be required to facilitate their faithful segregation⁹⁸. Studies in *S. pombe* also suggested the involvement of condensin I in DNA repair, which indicates that condensin I is recruited at damage sites of single strand break (SSB) through poly (ADP-ribose) polymerase 1 (PARP-1)⁹⁹. A single condensin molecular moving along DNA can

explain the introduction of positive supercoils into closed circular plasmids in the presence of ATP¹⁰⁰⁻¹⁰².

2.3.2. The SMCs in ciliates

As in Fig. 8, SMC1/2/3/4 are present in the genome while SMC5/6 is absent from ciliates. Only a few papers reported some functional analysis of condensin in *Tetrahymena*, and the functions of condensin in *Paramecium*, another ciliate also in the class Oligohymenophorea, have not been investigated till now. At any point throughout the cell cycle, there is no apparent chromosomal condensation in the MAC in *Tetrahymena*. The techniques needed to identify chromosomal condensation in *Saccharomyces cerevisiae*¹⁰³, which has chromosomes equivalent in size to *Tetrahymena* MAC chromosomes, are challenging to apply to *Tetrahymena*'s polyploid macronucleus. As mentioned before, the chromosome size in MAC ranges from 50kb to 1Mb, while the loop extrusion makes nested loops with 80kb inner loops from 400kb outer loops in DT40 cells. In extreme cases, condensin could not even extrude even one loop in MAC if the loop size was conserved in all organisms. We have to be careful about imitating those conclusions, especially the loop extrusion, from other organisms to *P. tetraurelia*. Corresponding to the concern, some surprising roles for condensin in *Tetrahymena* amitosis have been reported. First of all, SMC4 was found in both MIC and MAC during the vegetative growth, while the knockout of SMC4 (SMC4 KO) generates an apparent MAC segregation defect. In contrast to condensin depletion in other organisms, SMC4 KO in *Tetrahymena* did not affect the segregation of bulk DNA during the mitosis which could be because of the lack of microtubule elongation inside the MAC¹⁰⁴. Another study has indicated that condensin works in distinct ways on segregating chromosomes in the MIC and MAC of *Tetrahymena*. Condensin facilitates the condensation and resolution of MIC chromosomes and promotes the spatial distribution and segregation of shorter chromosomes in MAC. They also believed that the loop extrusion could be responsible to separate copied shorter chromosomes in MAC¹⁰⁵. A development-specific condensin complex, condensin D, has been identified in *Tetrahymena*. Unlike canonical condensin, condensin D is crucial to the completion of sexual reproduction and the development of MAC. This is the first report mentioning that the condensin complex is supposed to promote genome organization in DNA elimination by an indirect way⁷¹.

2.4. PiggyMac, a key protein in IES excisions

PiggyMac (PGM) is a domesticated transposase identified in *P. tetraurelia*. Although IES sequences resemble Tc/mariner transposable elements, the excision process is more akin to that seen in PiggyBac Transposons (Figure 12A). Tc/mariner transposons perform a cut and paste transposing which results in a 3 bp overhang. In contrast, the transposition of PiggyBac transposons induces double strand breaks (DSB) that creates 4 bp 5' overhangs, as seen in Paramecium's IESs^{24,106}. The PGM is a probable candidate which participates in IES excision since it has high homology with PiggyBac transposase and was shown to possess the catalytic triad, three conserved aspartic acids (D401D491D609). A downstream cysteine-rich (CR) domain and a C-terminal extension are predicted to adopt a coiled-coil (CC) structure which is required for the normal function of an active IES excision complex¹⁰⁷. The CR domain has been considered to be crucial for PGM's activity *in vivo*. It can bind two Zn²⁺ and form a cross-brace zinc finger. Additionally, the CR domain can connect with the N-terminal residues of histone H3 *in vitro*¹⁰⁸. Experiments revealed that the knockdown of PGM resulted in a fatal phenotype and impaired the excision of most IESs. Using a GFP-tagged PGM protein, they also demonstrated that PGM locates in the developmental MAC during the IES excision. As a result, it was suggested that PGM is the endonuclease responsible both for the accurate elimination of IESs and for the imprecise removal of repetitive sequences in the germline²⁰.

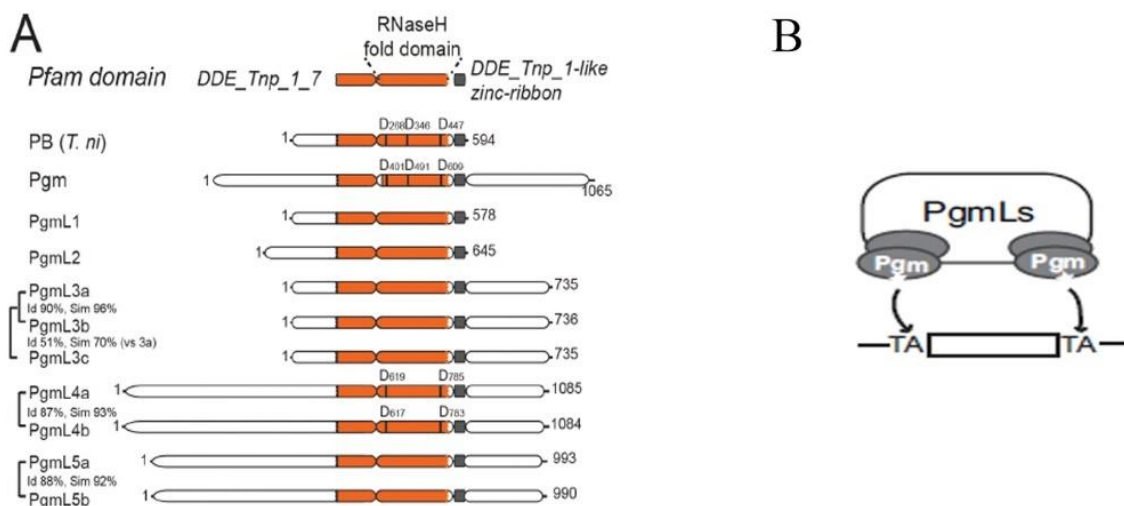


Figure 12. Domain structure of the PiggyBac transposase (PB) and model of IES excision by PGM/PGMLs complex. Adopted from¹⁰⁹. A) The Pfam domain DDE_Tnp_1_7 is shown in the orange domain, at its right side is the RNase H fold (conserved catalytic D residues are indicated by

vertical bars). Id indicates the percentage of sequence identity; Sim presents the percentage of similarity. B) this model is summarized according to previously published data. The active form of PGM is supposed to be a dimer. In the lack of knowledge of the complex's composition, one PGM homodimer is represented at each IES border, with all PGMLs forming a huge bridge structure. PGML subunits are postulated to drive the precise alignment of the PGM active site to those TA cleavage sites in a fully formed complex.

Besides PGM, five groups of distant PGM-like proteins (PgmLs, Figure 12) that are all able to interact with PGM and are essential for its localization and IES excision have been identified in *P. tetraurelia*¹⁰⁹. A co-factor of PGM in DNA elimination, Spt16-1, a subunit of histone chaperone FACT which is the key to reorganising nucleosomes and ensuring chromatin integrity, facilitating the localization of PGM¹¹⁰. The protein Ku80c has also been shown the unique property to license PGM-dependent DNA elimination¹¹¹. The DSB repair at those excised spots is accurate and efficient, ensuring that MAC chromosomes are rebuilt in the correct sequence and open reading frames are regenerated with accuracy¹³. The ligase IV-Xrcc4 complex, an important player of the C-NHEJ pathway¹¹², was demonstrated to repair DSBs at chromosomal IES elimination positions and during the circularization of eliminated IESs using RNAi-mediated functional investigation of candidate genes¹⁹.

3. Aim of the thesis

Aim I:

The first aim of this research was to explore the roles of condensin components in the IES processing in *P. tetraurelia*. So far, no such information has been reported and it is worth noticing that the chromosome structure, especially constructed by condensin, should be an important aspect for the processing of some or all IESs *in vivo*. Hence, to gain a more in-depth look at the relationship between condensin and IES excision, we first analysed the possibility of condensin components participating in IES removal by RNAi. When it was confirmed, additional functional analysis was included to elucidate the roles of condensin in IES excision. The expected results may contribute to supplementing the mechanism of genome rearrangement in *P. tetraurelia*, and provide a new vision into the activity of condensin in other organisms.

Aim II:

In addition to the research work on condensin, we set out to investigate the members of excision machinery in two different ways. The excision machinery is the most interesting complex for people who focus on the mechanism behind the IES excision. Until now, nobody has succeeded in isolating this machinery *in vivo*. So, for the first time, we used biotin-labelled IES complementary oligos to pull down the DNA excision machinery in IES excision. Mass spectrometry was used to analyse the elution to identify the components interacting with IESs. The second way to purify the eliminating complex is mutant PGM Co-immunoprecipitation. Since the PGM is supposed to be the core component of excision machinery according to its functional analysis, mutated PGM with tag in theory should be purified with the IES excision machinery. Also, mass spectrometry analysis is included.

4. Results

4.1.Part I: Research article: Functional analysis of structural maintenance of chromosomes (SMCs) in internal eliminated sequences (IESs) elimination in *Paramecium tetraurelia*

Author Contributions:

I conducted the design of the experiments, carried out all experiments, wrote the manuscript, produced and formatted the figures.

Sebastian Bechara performed all bioinformatics analysis and create the original version of Figure 2, Figure 4 and Figure 5.

**Functional analysis of structural maintenance of chromosomes (SMCs) in
internal eliminated sequences (IESs) elimination in *Paramecium tetraurelia***

Fukai Zhang¹, Sebastian Bechara¹, Mariusz Nowacki^{1*}

¹ Institute of Cell Biology, University of Bern, Bern 3012, Switzerland

* Corresponding author: Mariusz.nowacki@unibe.ch

Abstract

The structural maintenance of chromosomes (SMCs) is a large family of ATPases that play a variety of roles in the organisation and dynamics of higher-order chromosomes. They are central regulators of chromosome dynamics and the core component of condensin and cohesin. The internal eliminated sequences (IESs) excision is controlled by a lot of different factors that occur between two forms of nuclei in *Paramecium tetraurelia*. During this process, massive genome condensation and dissolution happen with several rounds of meiosis and mitosis where the SMCs play vital roles in organizing chromosomes. While the relationship between IES elimination and SMCs function has not been discovered in *Paramecium tetraurelia* until now. Here we applied RNA interference, genome sequencing, mRNA sequencing, immunofluorescence and mass spectrometry to investigate the roles of SMCs in IES elimination in *Paramecium tetraurelia*. The results indicate that SMC4-2 is a novel factor of IESs excision in *Paramecium tetraurelia*, while SMC4-1 is not. The localization of SMC4s also suggests that SMC4-1 seems like the canonical SMC4 in other organisms, while SMC4-2 is more like an IES-specific SMC4 which only exists in *Paramecium tetraurelia*. Loss of SMC4-1-GFP in old MAC brings up the possibility that decompacted chromosomes help the scanning of scnRNAs. The genesis of iesRNAs is strongly inhibited by the knockdown of SMC4-2. Silencing SMC4-2 with SMC2-1, SMC2-2 or SMC4-1 abolished the retention phenotype is a new finding too. The enrichment of different proteins from SMC4-1 and SMC4-2 suggests a possibility of a competitive relationship between them. These innovations highlight the potential of SMCs participating in IES processing and which in end will lead to a new mechanistic discovery.

Introduction

Paramecium tetraurelia is a widely distributed unicellular eukaryote in fresh water in the highly diverse ciliate phylum. Similar to other ciliates, the nuclear dimorphism makes them a talent model to explore genome dynamics and RNA mediated epigenetic regulation between their two diverse forms of nuclei. The germline micronucleus (MIC) serves as the genetic information stock next generation. The somatic macronucleus (MAC) is responsible for gene expression. Genetic information comparison between MAC and MIC results in large-scale and precise elimination of specified DNA regions from the developmental MAC genome. The packing of meters of linear DNA molecules into compact metaphase chromosomes is an inevitable step in meiosis and mitosis which makes condensin could be important to the genome rearrangement.

This sexual cycle can be triggered by food stress and conjugation which can induce MAC fragmentation and MIC meiosis. The two new developing MACs are derived from two copies of MIC during the sexual cycle after one mitosis and two mitotic divisions of MICs. Endoreplication in the new MAC increases the ploidy from $2n$ to $800n$. During this time, massive genome rearrangements occur which reproducibly remove the internal eliminated sequences (IESs). There are almost 45,000 annotated IESs within the new developing MAC. Precise excision is required for the functional maturation of genes containing IESs. No obvious feature has been found to clarify the precise removal of IESs except that most are flanked by TA¹. Two sets of small RNA defined as scnRNAs ('scan' RNAs)² and iesRNAs³ are supposed to be included in IES excision in early and late *P. tetraurelia* development respectively. In brief, during meiosis, the MIC is bi-directionally transcribed, yielding long transcripts that are then processed to yield scnRNAs. "Scanning" for comparable sequences in the parental MAC removes MAC genome-matching scnRNAs while enriching MIC genome-matching ones². Later in the development of the MAC, excised IESs circularize or concatenate to serve as a template for iesRNA precursors. Following that, generated iesRNAs assure the eradication of the majority of IESs^{3,4}. While mitotic and meiosis chromosomes are compacted with condensin, how the scanning model works under a compacted chromosome is still unknown.

Condensin is a large protein complex and plays critical roles in chromosome structure and segregation in cells⁵. Most of eukaryotes have two different types of condensin, condensin I and II. Condensin has a conserved dimer structure of two large proteins structural maintenance of chromosomes (SMC), SMC2 and SMC4, involved in organizing the genome by using the energy from ATP hydrolysis⁶. Both SMC2 and SMC4 self-fold to a head-to-end shape by the two ATPase domains. The hinge domain is situated in the heart of this V shape structure, the anti-parallel coiled-coil domains connect ATPase domains and the hinge domain. Dimerized by the hinge domains from SMC2 and SMC4, the core of the condensin forms⁷. In human⁸ or other eukaryotes^{9,10}, condensin I and II regulate chromosome assembly and segregation differently in both meiosis¹¹ and mitosis¹². The condensin complex connects to chromatin and progressively extrudes a DNA loop by binding DNA on one side and reeling from another side. Furthermore, chromosomes organized as nested loop arrays winding around a helical ‘spiral staircase’ within a cylindrical chromatid by condensin I and II reveals the conformation of mitotic chromosomes¹³. In addition to condensing chromatin into organized structures, condensin has been indicated such as single strand DNA (ssDNA) binding preference¹⁴, reannealing complementary ssDNA¹⁵, remove ssDNA binding proteins¹⁶ since condensin was first reported.

The relationships between SMCs function and IES elimination in *P. tetraurelia* are supposed to be important. Because we assume that the compacted DNA structure should transiently loosen when an IES inside the DNA loop is being excised. It has been declared that the steric hindrance generated by condensin could impact or inhibit transcription¹⁷. As mentioned above, massive transcriptions are needed for the IES excision, the hypothesis that IESs cannot be eliminated if the corresponding DNA region was compacted into dense chromosomes could be reasonable. In the present research, we assessed the effects of two homologs of SMC4 (SMC4-1, SMC4-2), and SMC2 (SMC2-1, SMC2-2) in *P. tetraurelia*. Strong IESs elimination failure is observed after RNA interference (RNAi) of SMC4-2. It indicates a direct/indirect effect of condensin proteins on IES excision. SMC location indicates that SMC4-1 participates in the whole development of *P. tetraurelia*, while SMC4-2 mainly exhibits in the late stage. Interacting proteins of SMC4-1 or SMC4-2 have also been investigated to shed the light on the functional complex of SMC4s in *P. tetraurelia*. Therefore, this study contributes to research on SMC4s in *P. tetraurelia* by demonstrating the functional difference between them in IES excision.

Methods

Paramecium cultivation

All experiments were performed with mating-type 7 of strain 51 of *P. tetraurelia*. *Klebsiella pneumoniae*-infected wheat grass powder medium (WGP; Pines International, Lawrence, KS) with 0.8 mg/L of β -sitosterol was treated to cultivate the cells (Merck). As previously mentioned, cultivation took place at a temperature of 27 °C^{18,19}.

Sequence alignment, domain prediction and phylogenetic trees generation

The *Paramecium* SMC4-1 (PTET.51.1.P0410063) and SMC4-2 (PTET.51.1.P0590135) sequences extracted from ParameciumDB (<https://paramecium.i2bc.paris-saclay.fr/>). Other SMC4 protein sequences were collected from previous reports^{20,21}. Multiple sequence alignment was carried out in MAFFT²² and BLAST tool in ParameciumDB. Conserved domains prediction of SMC4-1 and SMC4-2 were performed with Pfam²³. Expression pattern builds according to previous report²⁴. The phylogenetic tree was generated by using the W-IQ-TREE with the default setting²⁵.

Gene silencing of SMC2s and SMC4s

As a subunit of SMC part in condensin, the role of SMC2 in *P. tetraurelia* development needs to be explored at the same time. Similar to SMC4s in *P. tetraurelia*, SMC2-1 (PTET.51.1.G0330075) and SMC2-2 (PTET.51.1.G0450077) are annotated in the database. Knock-down (KD) of SMC2s and SMC4s were reached using RNAi by feeding double-strand RNAs as described before²⁶. Candidates' sequences were magnified from wild type MT7 genomic DNA with the primers in Supplementary Table S1. Next, either single or dual sequences were inserted inside of the two reversed T7 promoters in the L4440 vector²⁷. The plasmids were expanded in the feeding cells: HT115 (DE3) *Escherichia coli*. An empty L4440 vector without insertion was the negative control. Additionally, a PiggyMac (PGM)

RNAi plasmid from our lab was chosen as a positive control²⁸. Cross-silencing of other *P. tetraurelia* genes, according to RNAi off-target tests performed using the ParameciumDB²⁹ tool (https://paramecium.i2bc.paris-saclay.fr/cgi/tool/rnai_off_target), is unlikely. Around 200 cells/ml of *P. tetraurelia* cells were transplanted into the silencing medium. A total of 14 single cells that had completed sexual reproduction in the silencing media were then isolated and added to a freshly bacterized medium to assess the survival of the progeny following autogamy. Three days following their separation, cells were checked and recorded into three groups based on the observed phenotype (healthy, weak and death).

DNA extraction, IES PCR and Illumina Sequencing

Total DNA from 100 mL of each postautogamous culture was extracted with the GenElute Mammalian Genomic DNA Miniprep Kit (G1N70-1KT, Sigma-Aldrich). IES retention PCR was analyzed with genomic DNA and certain primers as previously described³. For deep sequencing, DNA of developmental MAC from 400 mL cells was extracted as previously described³⁰. According to established Illumina techniques, a 150-cycle paired-end Illumina TruSeq DNA library was created and sequenced at the University of Bern's NGS platform.

Calculation of IES retention scores (IRSs) in genome-wide and correlation matrix

The IRSs were estimated using ParTIES³¹. The number of reads associated with the eliminated IESs with just the MAC IES junction is denoted as IES, whereas the number of reads which accommodates the IES region is denoted as IES⁺. Only read pairs that were mapped were counted. Each read was tallied just once to prevent excessive counting brought on by paralogous matches. To prevent length biases brought on by IES length variance, reads were exclusively counted at IES ends. Then, an IRS is determined as follows: $IRS = IES^+ / (IES^+ + IES^-)$. Correlations were estimated with the Pearson method.

Total RNA extraction, mRNA sequencing and small RNA (sRNA) analysis

Total RNA was obtained from 200 mL of *P. tetraurelia* at 4 hours after 100% fragmentation. This timing is determined according to the strong GFP signal of SMC4-2 on the western blot. TRI reagent (Sigma-Aldrich) extraction was done following the suggested protocol. The mRNA library was produced based on standard Illumina protocols and sequenced at the NGS platform at the University of Bern. For sRNA sequencing, total RNA was sequenced by Fasteris SA (Geneva, Switzerland). The sRNAs were categorized into several size sets (15 – 35 nts), then aligned with HiSat2 (version 2.1.0) using default parameters³². Those reads mapped were sorted to OES, IES and MAC sequences, the mitochondrial, DNA from *Klebsiella pneumoniae* and the vector backbone.

The GFP and mCherry fusion constructs, microinjection and localization

The SMC4-1 or SMC4-2-GFP fusion construct under the endogenous regulatory sequences respectively contained MAC sequences upstream of the ATG and downstream of the TGA. The optimized GFP coding sequence³⁴ was inserted ahead of the stop codon. Before performing the microinjection, all plasmids containing the fusion transgene were digested with the AhdI (R0584, New England BioLabs) or SapI (R0569L New England BioLabs) to linearize them. The products were filtered through 0.22 µm Ultrafree® MC GV filter (UFC30GV0S, Millipore), and enriched with pure ethanol. DNA was dissolved using DNase-free ddH₂O to a final concentration of ~ 5.5 µg/uL. Finally, linearized DNA was microinjected into vegetative cell MACs³⁵. SMC4-1-mCherry constructs as described above. Positive injections were picked up by checking green and red signals under a microscope. A positive single clone was expanded to high density (3000 cells/ml). At various life cycle phases, small samples were taken and counterstained with 4',6-diamidino-2-phenylindole (DAPI). Fluorescence microscopy was used to detect GFP localization (Leica AF6000 system).

Flag-HA fusion construct, microinjection, immunoprecipitation, mass spectrometry

Fusion construct and microinjection were performed as described above. The positive injection was confirmed by Dot Blot^{33,36}. Immunoprecipitation was conducted as described before^{37,38}. Non-crosslinking was performed because the IP of SMC4-2 under crosslinking did not work at a pH below 10.4. In detail, 400 mL cells were harvested at 4 hours after 100% fragmentation, pellets were resuspended in 2 mL fresh lysis buffer (50 mM Tris pH 8.8, 150 mM NaCl, 5 mM MgCl₂, 1 mM DTT, 1% Triton X-100, 1× protease inhibitor complete tablet (Roche), and 10% glycerol) and sonicated until complete lysis. Lysates were spin down at 13,000× g, 4 °C for 30 min. Beads were washed with 1 mL IP buffer (10 mM Tris pH 8.8, 150 mM NaCl, 0.01% NP-40, 1 mM MgCl₂, 1× protease inhibitor and 5% glycerol) for three times before incubation. A total of 1 mL of the supernatant was mixed with 50 μL of Anti-HA affinity resin (Roche) at 4 °C while rotating O/N. Another 1 mL supernatant was frozen in liquid nitrogen and then store at -80 °C before use. After incubation, beads were washed using 1 mL IP buffer five times. Washed beads were resuspended in 50 μL IP buffer, boiled with 25 μL 5× SDS loading buffer at 95 °C, after cooling down on the ice, and immediately used for western blot and mass spectrometry analysis at the University of Bern.

Results

Identification of the *P. tetraurelia* SMC4s homolog

In Fig. 1a, the domain organization of SMC4s in *P. tetraurelia* is shown. A Pfam domain search predicted that domains are conserved in these two SMC4s while the sequence blast indicates only 37.36% identity between them. It highlights the question that why *P. tetraurelia* needs two SMC4s. In Figure 1b, we showed the phylogenetic tree of SMC4s from 22 species with maximum likelihood analysis, SMC4-1 in *P. tetraurelia* locates in an independent branch of ciliate SMC4, while SMC4-2 has a closer localization with *Tetrahymena*, a close relative with *Paramecium*. To compare the difference between SMC4-1 and SMC4-2, authors made an expression curve according to the ParameciumDB as shown in Fig. 1c. It is indicated that SMC4-1 has a long-term expression in the whole development stage of *P. tetraurelia*, while SMC4-2 starts expression after MIC meiosis which makes it a potential candidate of IES excision related proteins. Fig. 1c also presents a cross of expression and alterations in the expression's prominent position between SMC4s which gives the idea that specific SMC4 is needed in the distinct development stages and SMC4s may posse different functions referred to the given stage.

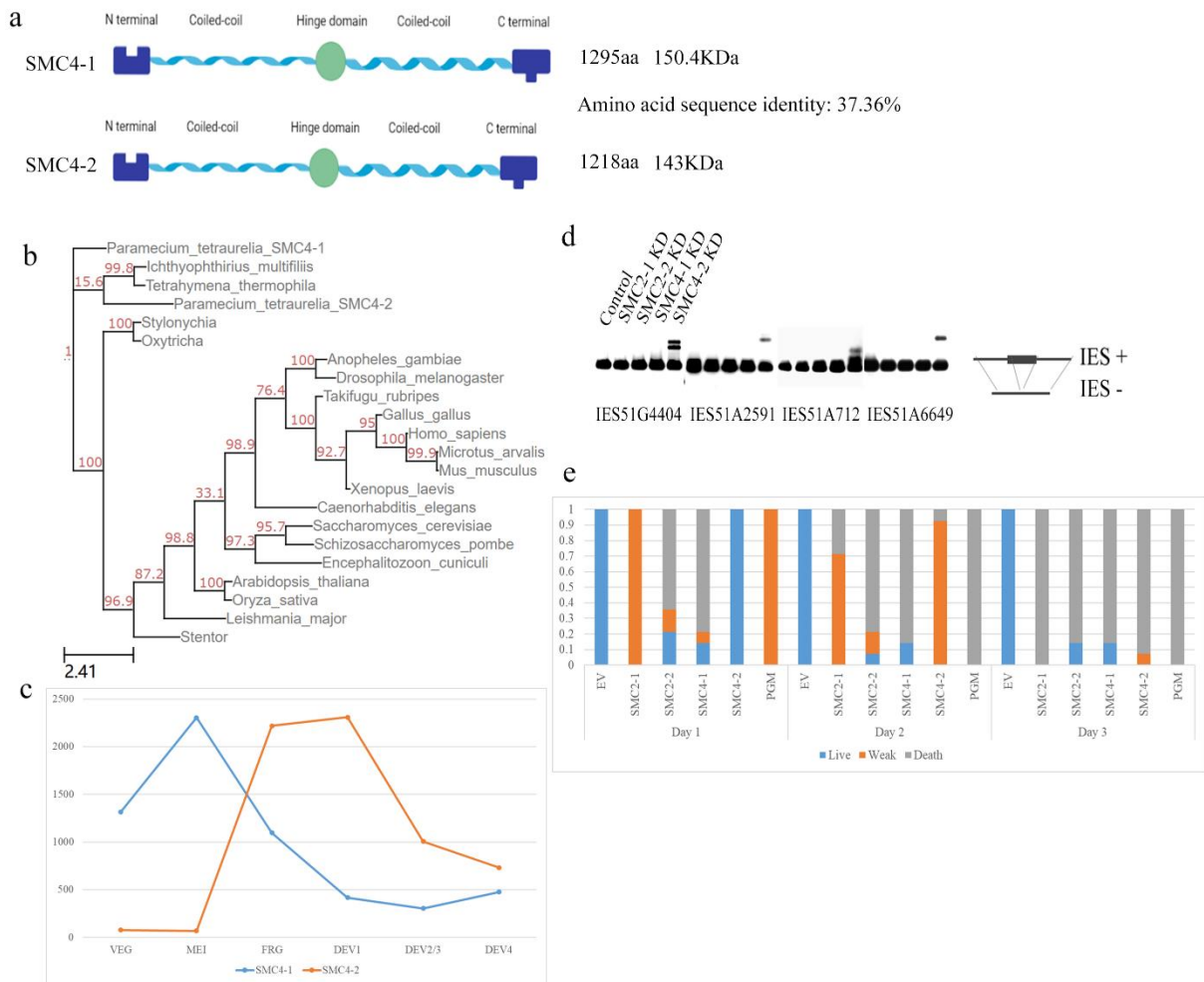


Figure 1. Structure and function comparison between SMC4-1 and SMC4-2 in *P. tetraurelia*. (a) Similarity and differences between SMC4-1 and SMC4-2 in *P. tetraurelia*. All information obtains from ParameciumDB, amino acid sequence identity gains from the BLAST tool on the website. Conserved domain/motifs in different colours. (b) Maximum Likelihood tree of SMC4s in ciliates and randomly selected organisms. (c) Time-course of gene expression for *P. tetraurelia* SMC4-1 and SMC4-2. The curve in blue represents the expression of SMC4-1, and the orange one indicates the expression of SMC4-2. The Y axis means the mean expression level. VEG: vegetative cells; MEI: beginning of MAC fragmentation and MIC meiosis; FRG: population when ~50% of cells have fragmented MACs; DEV1: earliest stage when a significant proportion of cells has visible MAC anlagen; DEV2/3: majority of cells with MAC anlagen; DEV4: majority of cells with MAC anlage. (d) Effect of EV, SMC2-1, SMC2-2, SMC4-1, SMC4-2 knockdowns on IES excision by IES PCRs. The excised form is shown as (IES-) and the unexcised form is shown as (IES+). The IES- form is always detectable due to the presence of the parental MAC in the sample. The IES+ is only present in IES retention in the newly developing MAC. (e) Effect of EV, SMC2-1, SMC2-2, SMC4-1, SMC4-2 and PGM KD on cell survival. The healthy, weak and death cells are shown in different colours. Blue: percentage of healthy cells (cell growing at a normal rate); orange: percentage of sick cells (altered

number of divisions or behaviour); grey: death cells. PGM KD was the positive control. The empty L4440 vector as the negative control. For each bar n = 14 cells.

SMC4-2 is essential for IES excisions in *Paramecium*

To figure out what the functions of SMC4s are in IES excision, RNAi was used to make a knockdown (KD) of SMC4s expressions at the mRNA level. The IES PCR results obtained from the preliminary analysis of KD are shown in Fig. 1d where the retention of IES excision is shown by two bands, the upper one is the DNA region that contains IES when elimination fails, and the lower bands are regions that succeed in IES excisions. From here we can tell that SMC4-2 KD provokes all tested IESs retention while there was no evidence that SMC4-1 KD influences that. As another core part of condensin, SMC2-1 and SMC2-2 KD IES PCR had been shown here too. Same with SMC4-1 KD, no IES retention was found. A survival test is a common way to determine the influence on the next generation after KD and whether all cells are under RNAi in *P. tetraurelia*. As shown in Fig. 1e, over 80% death rate has been shown in all SMCs KD which means SMCs play important roles in *P. tetraurelia*.

To gain a genome-wide perspective on how IESs are affected by SMC4-2 KD, developing MAC was isolated from the autogamy cells after RNAi and starvation, high-throughput sequencing analysis was performed, the IES retention score (IRS) distribution result shown in Fig. 2a. The most striking result to emerge from the data is that 99% (43889 out of 43900) IESs excision are affected by SMC4-2 KD, the peak of retention score is around 0.4 which indicates that SMC4-2 may participate in IES excision in an unknown way. This result is beyond our expectations and only PGM KD shows a similar but stronger right-skewed distribution (Fig. 2b) compare to all other previously examined factors of excision machinery. The results of the correlational analysis are summarized in Fig. 2c which illustrates some of the main characteristics of retention pattern after these factors' KD. It is apparent from this table that very few correlations between SMC4-2 KD and any other KD. More efforts are needed before we can confirm that SMC4-2 engage in IES processing in a new way.

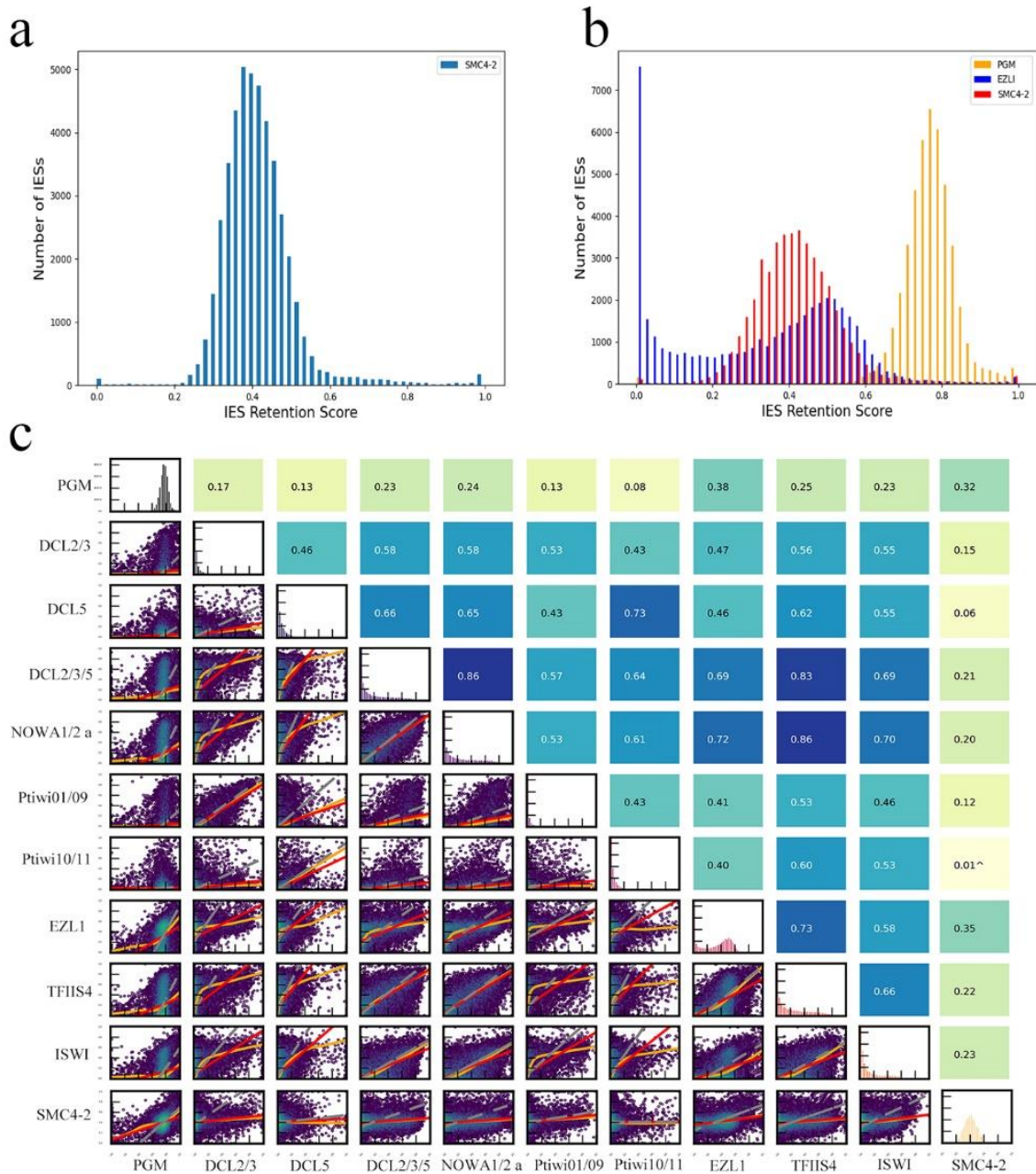


Figure 2. IES retention pattern analysis. (a) Retention score distribution was determined by sequencing DNA extracted from a cell fraction enriched in new MACs after SMC4-2 KD. Y axis means the number of IESs. X axis means the percentage of single unexcised IES among its copies. (b) Integrated IES retention distribution of PGM (in orange), EZL1 (in blue) and SMC4-2 (in red) KDs. (c) Correlation in IES retention. The retention score of PGM, DCL2/3, DCL5, DCL2/3/5, NOWA1/2a, Ptiwi01/09, Ptiwi10/11, EZL1, TFIIIS4, ISWI are from our lab, SMC4-2 retention score is from this study. The correlation coefficients of Pearson are given at the right part of the graph correspondingly.

Two SMC4s localization shows diverse patterns in the cell cycle

The next section of the survey was concerned with why SMC4-2 are such important to IES excision. Authors first constructed an SMC4-2-GFP vector with 300bp up- and downstream of the SMC4-2 coding sequence then linearized the vector and microinjected it into vegetative MAC. The localization of SMC4-2 in Fig. 3a highlights that SMC4-2 uniquely locates in newly developing MACs although the green signal loses in the post autogamy stage. Here we speculate that SMC4-2 exhibits the possibility to process IESs excision spatially and temporally. While another problem rises from here, if SMC4-2 was also a component of condensin, its absence in vegetative, early and post-autogamy is unacceptable to chromosome structure. As we know from the expression pattern, there is still another SMC4—SMC4-1 in *P. tetraurelia* and it has a long-term expression throughout the whole life cycle. So, it's reasonable that SMC4-1 serve as the “condensin SMC4” in *P. tetraurelia*. To figure out how the localization of SMC4-1 in the development of the *P. tetraurelia* looks, a linearized SMC4-1-GFP vector was injected into vegetative MAC in the same way as SMC4-2-GFP did. In Fig. 3b, the green signal represents SMC4-1 exclusively locates in nuclei including MICs through life, MACs except for the one that is going to be, as well as already fragmented MACs (old MACs). Considering the roles of condensin SMC4 in the dynamics of chromosomes and the scnRNA and iesRNA model, authors hypothesise that the dissociation of SMC4-1 in old MACs may be the premise of small RNAs from MICs matching to the long non-coding transcripts in old MAC genome. In Supplementary Figure S1, authors made a double injection by mixing equal amounts of SMC4-1-mCherry (red) and SMC4-2-GFP (green) into the vegetative MACs to check the co-localization of SMC4s in the development of *P. tetraurelia*. There was a significant positive correlation between them, the red and green signals can be visualized in newly developing MAC at a late time point. The single most interesting doubt to emerge from the localization was why two SMC4s are needed in the newly developing MACs if SMC4-1 and SMC4-2 served the same. If not, then what different functions they had on chromosome structure and IES excision.

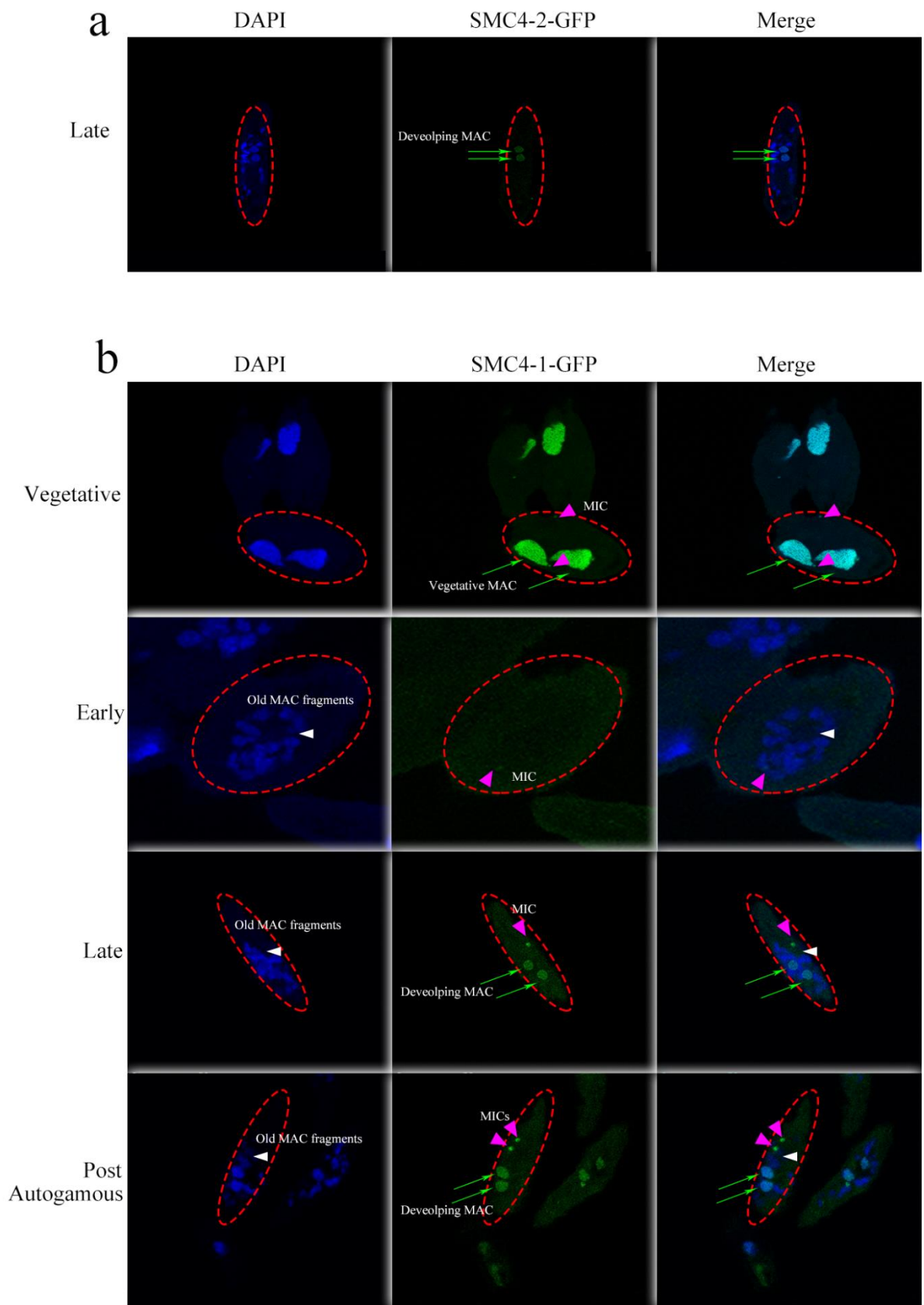


Figure 3. Localization of SMC4-1 and SMC4-2 tagged with GFP. (a) SMC4-2 tagged with GFP was exclusively localized in the macronuclear. (b) SMC4-1 tagged with GFP has a wide distribution

including vegetative macronuclear and micronuclear, new developing macronuclear and micronuclear, not in macronuclear which is going to be fragmented and old macronuclear fragments. The red dotted line represents the *P. tetraurelia* cell body. DAPI staining in blue represents DNA. Green signals represent SMC4-2 in a and SMC4-1 in b. Green arrows represent developing MAC. Pink arrowheads point to MICs, and arrowheads in white represent old MAC fragments.

Knockdown of SMC4-2 disrupts genes expression at a late time point in *P. tetraurelia*

To know how SMC4-2 KD affect the IES excision and what kind of process SMC4-2 participate in *P. tetraurelia*, we performed mRNA sequencing of RNA samples from the late time of EV control and SMC4-2 KD. From Fig. 4a we can tell, SMC4-2 KD disrupts the expression of quite a long of genes. The downregulation of PTIWI06, PTIWI07, PTIWI10 and PTIWI11 highlighted on the plot could be because IESs exist in their promoters and coding regions. When we narrow to the top 50 most differentially expressed genes (DEGs, where the variance is the highest between samples) in Fig. 4b, it is significant that SMC4-2 KD can upregulate gene expression in a late time point including PGML5 and other PGMLs (not in the top 50, but still significant), the co-factor of PGM in IES excision³⁹. In Fig. 4c, we provide a GO enrichment map. Enriched RNA-related GO terms indicate SMC4-2 could participate in RNA processing pathway. For the first time, SMC4-2 was reported to regulate the gene expression in *P. tetraurelia*. It is supposed that SMC4-2 plays downregulating roles in the development of *P. tetraurelia*, when disrupts the expression of SMC4-2, the depression from it would be released, and then a large number of genes could be expressed.

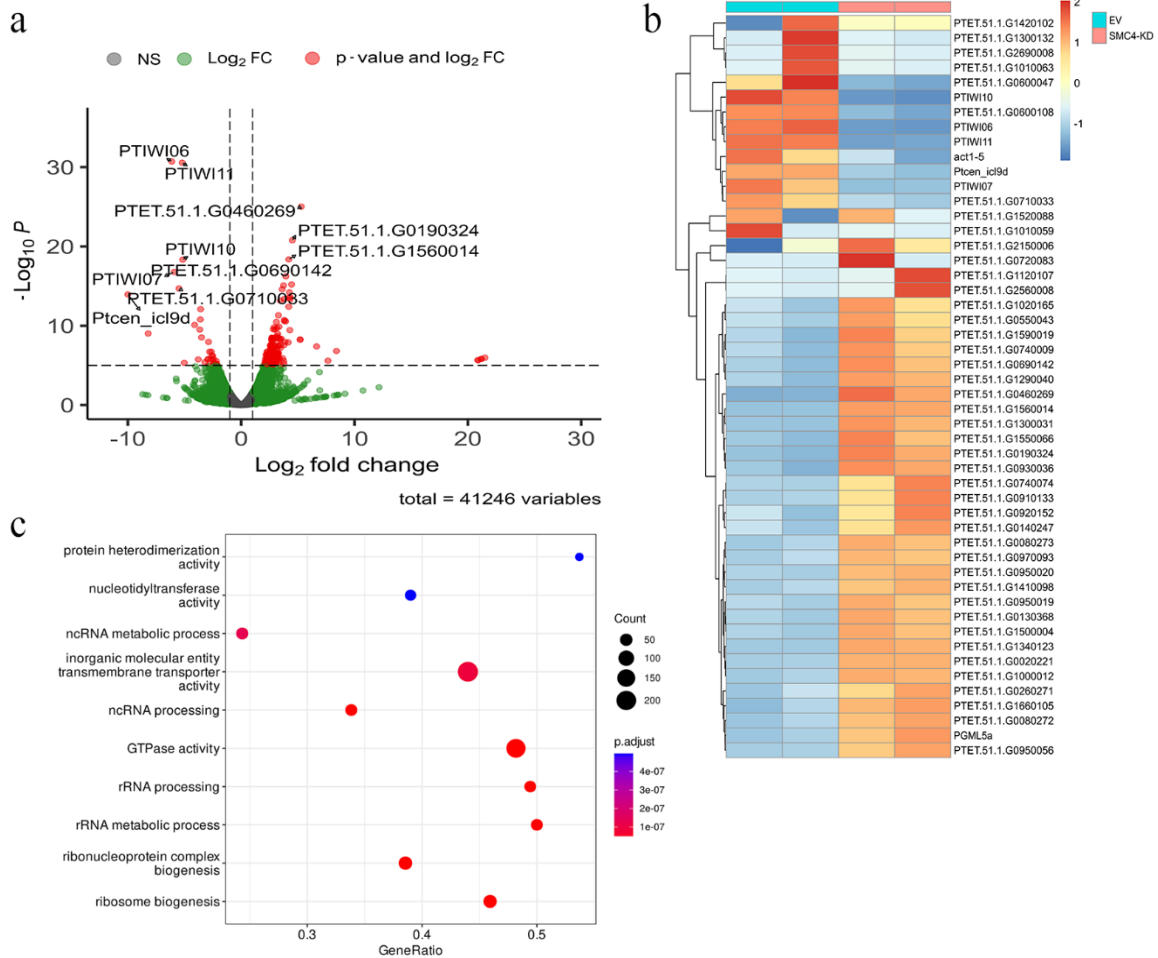


Figure 4. Differential expression and GO enrichment in SMC4-2 KD compared to EV. (a) Volcano plots showing the differentially expressed genes detected in SMC4-2 KD compare to the control. The most statistically significant genes are shown toward the top, with upregulated genes on right and downregulated proteins on left. Grey dots mean no significant difference, and green dots represent significance only in fold change. The X-axis represents log₂ (fold change) values and Y-axis represents $-\log_{10}$ (pval) values. (b) The top 50 most differentially expressed genes in SMC4-2 KD compare to the control. Light blue on the top represents two replicates of EV, the orange means two replicates of SMC4-2 KD. The red (upregulated) and blue (downregulated) colour and intensity of the boxes represent changes in gene expression. (c) GO terms enrichment map. The x-axis shows the Gene ratio, the percentage of total DEGs in the given GO term; the y-axis corresponds to GO terms. Count represents the number of genes enriched in a GO term. The colour of the dot represents the p adjust value.

SMC4-2 knockdown wipes out the production of iesRNAs at a late time point

To know how SMC4-2 engages in most IESs excision, a small RNA analysis was performed to detect whether scnRNA or iesRNA are affected by the RNAi of SMC4-2. Since we already know that SMC4-2 exclusively locates in newly developing MAC and scnRNA is produced during the early meiosis in *P. tetraurelia*^{2,3}, it's unlikely the RNAi of SMC4-2 can disrupt the production of scnRNA. So, authors only focused on the genesis of iesRNAs which are 26-30 nts long and generated in the newly developing MAC^{3,4,37}. To assess the production of iesRNA in a high resolution, small RNA sequencing was performed and the detailed information of detected small RNAs are clustered into several groups. All these RNAs are shown in the bar chart (Fig. 5a, b) with a size strategy. Compared with EV, it is apparent from here that extremely few iesRNAs can be recognized from 26-30 nts. In general, SMC4-2 KD disrupts IES excision may be partly because of abolishing the genesis of iesRNAs.

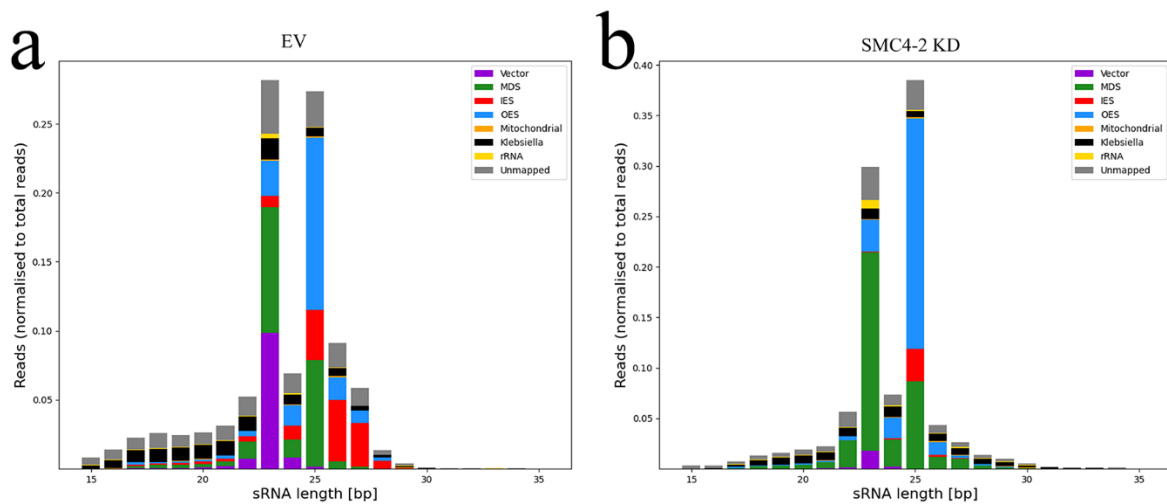


Figure 5. Small RNA sequencing in EV and SMC4-2 KD. (a, b) Histograms of small RNAs classified by length. Both panels show the distribution at a late time point (specifically 4 hours after 100% fragments). The reads map to MDS is shown in green or IESs in red. A significant absence of 26-30 bp, in which the iesRNAs are, is observed in SMC4-2 KD.

Knockdown of SMC2-1/SMC2-1/SMC4-1 getting rid of the IES retention after SMC4-2 KD

In theory, SMC4 functions in cells in proteins complex way like condensin. So, if SMC4-2 manipulated IES excision in condensin form, the disruption of the remaining part of condensin should be robust or at least retain the IES retention phenotype under SMC4-2 KD. Therefore, the authors conducted double silencing of SMC4-2 with SMC2-1, SMC2-2 or SMC4-1. Surprisingly, as in Fig. 6a, the IES retention phenotype has disappeared in all these

double silencings. The survival test in Fig. 6b represents that at least 80% of cells have been affected after feeding with a double silencing medium. To get a convincing result, in addition to mixing two cultures of a single RNAi medium, the authors also constructed 3 silencing vectors which contain corresponding regions to double silencing, by this way, differential production of double strand RNA (dsRNA) to each gene should be excluded. Still, the IES retention phenotype induced by SMC4-2 silencing is no longer detectable.

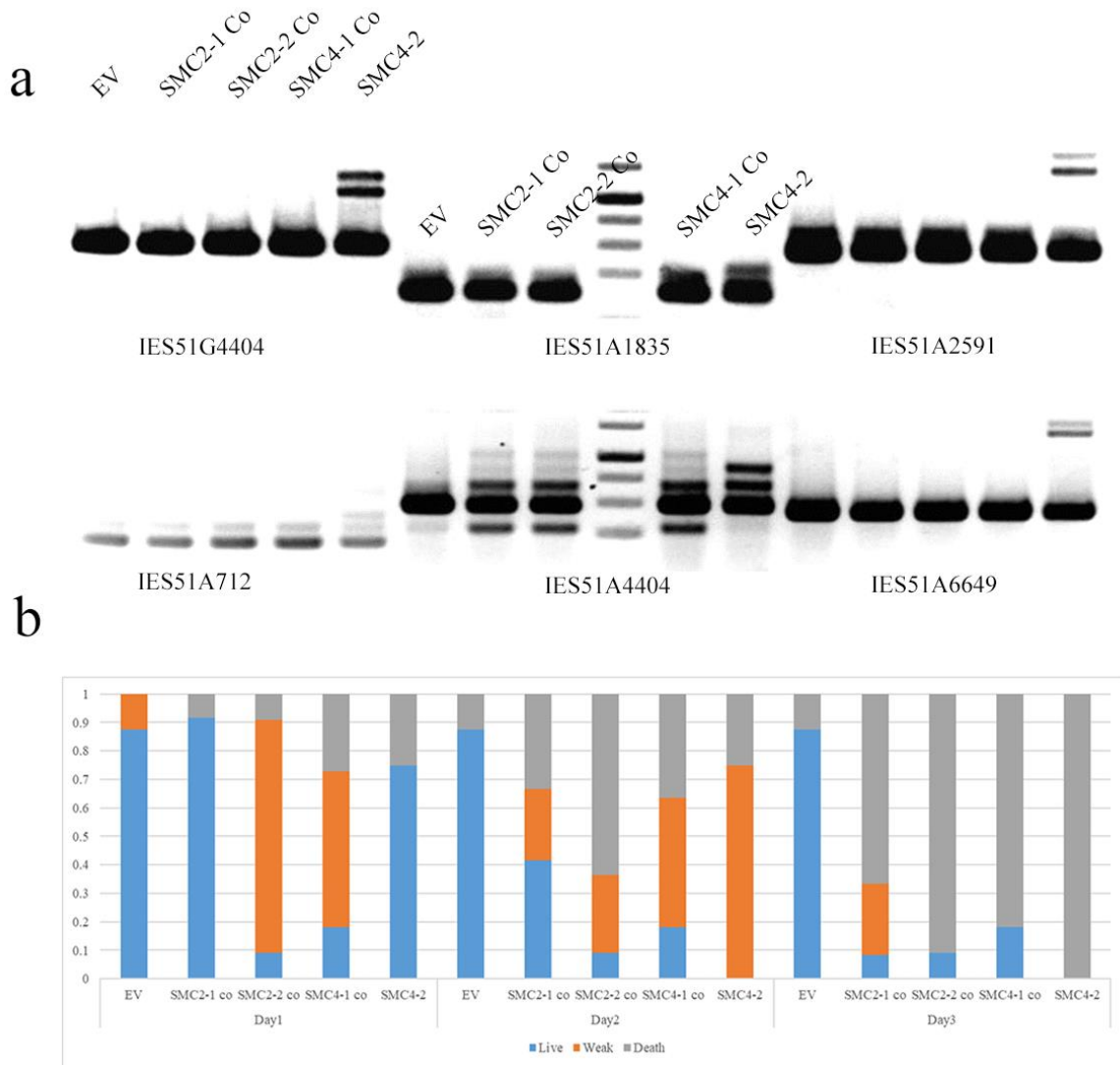


Figure 6. Co-silencing of SMC4-2 with SMC2-1, SMC2-2 or SMC4-1. (a) IES PCR of co-silencing. IES retention was tested by PCR using primers flanking IESs sequences. (b) Survival test of co-silencing.

Co-immunoprecipitation identify distinct interacting proteins between SMC4-1 and SMC4-2

To compare the difference between SMC4-1 and SMC4-2, authors applied co-immunoprecipitation coupling mass spectrometry to analyse the interacting proteins of Flag-HA tagged SMC4s at the same time point. As shown in Fig. 7a, SMC4-2-Flag-HA and SMC4-1-Flag-HA have been detected by anti-HA primary antibodies in cell lysate and bound solution. After analysed by Shotgun Liquid Chromatography Tandem Mass spectrometry (LC-MS/MS) with non-labelled samples, PGM or other IES critical proteins are undetectable in any of these interacting proteins is beyond our expectation. While the more surprising observation is the enrichment difference of SMC2s in these two SMC4s. the Venn diagrams (Fig. 7b and Fig. 7c) illustrate the relationships of differential enrichment and unique proteins among SMC4-1, SMC4-2 and WT interactions. In Fig. 7b, the grey arrow points to the SMC2-1 means it highly accumulated in both SMC4-1 and SMC4-2 enrichment compared to WT, but there is no different enrichment between SMC4-1 and SMC4-2 which indicates SMC4-1 and SMC4-2 may bind the same amount of SMC2-1 in this time point. The red arrow point to SMC4-2 and SMC2-2 means these two proteins not only upregulated in SMC4-1 and SMC4-2 compared to WT but also enriched in SMC4-2 compared to SMC4-1. The blue arrow pointing to SMC4-1 in Fig. 7c indicates that SMC4-1 is a unique protein which can only be detected in the SMC4-1 interacting dataset. Taken together, these results provide completely new insights into the diverse elements of SMC4s interactions in the development of *P. tetraurelia*.

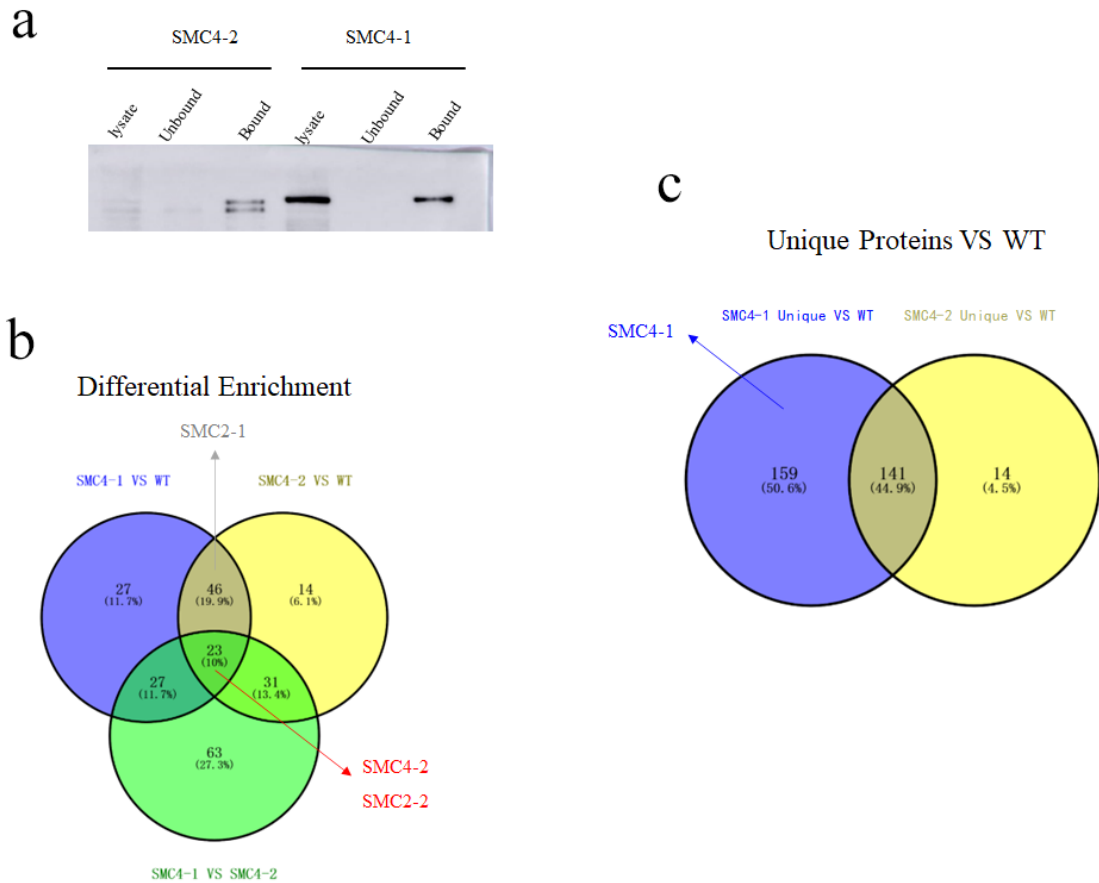


Figure 7. Co-immunoprecipitation of Flag-HA tagged SMC4-1 and SMC4-2 at a late time point.

(a) Western blot of Flag-HA tagged SMC4-2 and SMC4-1 pulled down with anti-HA antibodies.

Lysate: cell lysate; Unbound: supernatant by spinning down anti-HA beads-lysate mixture after overnight incubation; Bound: enriched target proteins on beads after five times washing. The

molecular weight of SMC4-1 ~150KD, molecular weight of SMC4-2 ~143KD. (b, c) Venn diagram of differential enrichment and unique proteins vs wild type. (b) Venn diagrams showing the overlap in differential enrichment of SMC4-1 vs WT, SMC4-2 vs WT and SMC4-1 vs SMC4-2. The grey arrow represents non-regulated in SMC4-1 vs SMC4-2. The red arrow means upregulated in SMC4-2 compared to SMC4-1. (c) Venn diagram shows the overlap in unique proteins of SMC4-1 vs WT and SMC4-2 vs WT. The blue arrow indicates unique protein only can be seen in SMC4-1 enrichment.

Discussion

Structural maintenance of chromosomes (SMC) complexes are the primary chromosome organizers in all living organisms^{5,40}. These protein complexes play central roles in DNA

replication⁴¹, chromosome condensation and segregation⁴², gene expression⁶, and DNA damage repair⁴³. In reviewing the literature, no data was found on the association between SMC4 and IES excision in *P. tetraurelia* even expand to ciliates. This is the first report that discovered and explored the relationship between SMC4-2 and IES processing. The important finding here is SMC4-2 KD shows a very strong IES retention phenotype, while other members of the *P. tetraurelia* SMC family including SMC2s and SMC4-1 don't. From here, authors suspect that SMC4-2 must have some unique function in addition to serving as the potential condensin component. Because if not, the knockdown of SMC2s and SMC4-1 should have similar results on IES excision. But the mechanism behind SMC4-2 regulating IES excision is still unknown, and from the structural prediction of SMC4-2, nothing significant characteristics can be presumed as the possible reason for this regulation. So, more indirect regulations have been taken into consideration.

The second interesting result from this work is the dynamic changes of SMC4s localization in the life cycle. As mentioned in the results part, SMC4-2 is localized specifically in newly developing MACs while SMC4-1 shows a more complex and remarkable positing strategy in both MICs and MACs. The observed green signal in newly developing MAC of SMC4-2-GFP injected cells could be attributed to the possibility that SMC4-2 processes IES excision or is involved in that at least. This study did not find a significant SMC4-2 localization in any other nucleus. This finding suggests that SMC4-2 is not the fully functional condensin-SMC4 in *P. tetraurelia*. Hence, SMC4-1-GFP injection was performed in vegetative cells and the GFP signal was observed from the vegetative stage to the post-autogamy cells. Interestingly, SMC4-1 has localization in all nuclei including MICs and vegetative and newly developing MACs. These results are consistent with data obtained in *Tetrahymena* which suggests that Smc4p may be involved in amitotic, mitotic and nuclear division²¹. One unanticipated finding was that the SMC4-1 signal was not seen in early MACs and old MAC fragments which suggests a dynamic dissociation of SMC4-1 from the genome as cells into autogamy. It's still unknown what would happen after SMC4 released from the chromosome and what the chromosome looks like in *P. tetraurelia*. The most significant progress here is scnRNAs produced from MICs and matured in old MAC before guiding IES excision⁴⁴. Hence, it conceivably we hypothesized that the dissociation of SMC4-1 in old MAC exposes a highly accessible DNA structure to DNA binding proteins⁴⁵, this would be a good opportunity for scnRNAs to scan their target DNA regions. The co-localization results confirm the temporal

and spatial association between SMC4-1 and SMC4-2 at a late time point. Either SMC4-1 and SMC4-2 have some overlap in function or it's just a coincidence needs further study.

The mRNA sequencing results indicate that only several PTIWI proteins were affected by SMC4-2 KD while other important proteins like PGM and Dcls (except upregulated Dcl5) were not included in the DEGs. The downregulation of PTIWI6/7/10/11 could be because of IESs' insertion in their promoter and coding regions. The IESs retention introduced by SMC4-2 KD disrupts the transcription and translation of these genes. This result reminds us of the possibility that IESs retention under SMC4-2 KD is not because of the downregulation of DNA excision machinery. Another interesting result under SMC4-2 KD is the upregulation of such amount of genes which reminds us that SMC4-2 could be a repressor of gene expression in the development of *P. tetraurelia*. Further study needs to be done to explore the real role of SMC4-2 in *P. tetraurelia*.

Another interesting result from the sRNA sequencing is that the population of the iesRNA was markedly depressed. For the first time, SMC4-2 was supposed to potentially manipulates the yield of specific sRNAs in ciliate. Here we assume that the possibility of SMC4-2 KD clearing away iesRNAs could be because SMC4-2 inhibits the early IES excision which is the template of iesRNA transcription. Further study is needed to explore the detailed mechanism behind SMC4-2 affect iesRNA production in *P. tetraurelia*.

The co-silencing results here indicate an outcome regard of restoring IES elimination under SMC4-2 KD by introducing a knockdown of SMC2-1, SMC2-2 or SMC4-1. The double silencing should robust the IES retention phenotype or retain it if SMC4-2 formed condensin with SMC2s in *P. tetraurelia*. If SMC4-2 had nothing to do with SMC4-1 and SMC2s, these double silencing should exhibit combing phenotypes of single silencing such as IES retention. In this study, no IES retention can be observed under double silencing. This is the first report that mention the IES retention phenotype can be restored when introducing another knockdown. No related report can be learned from to explain this phenotype. The LC-MS/MS results give us detailed information about how SMC4s interact with other proteins at the late time point. It is somewhat surprising that no PGM or other IES-related proteins were noted in the SMC4-2 interacting dataset. Not surprisingly, no such proteins

were found in SMC4-1 interactions. Although there is no direct evidence to prove that SMC4-2 processes IES excision, the truth that SMC4-2 KD affect IES excision and iesRNA production is still clear. In addition to these results, more interactions were found in differential expression and unique datasets in these two analyses. As mentioned before, when performing Co-IP by SMC4-1-Flag-HA as bait, all SMC4s and SMC2s can be captured at this time point, while only SMC2s were exhibited when using SMC4-2-Flag-HA as bait, SMC4-1 was not presented. The relationship between SMC4-1 and SMC4-2 has to be reconsidered. If they interacted with each other, the absence of SMC4-1 in the SMC4-2 pull-down is unacceptable since SMC4-2 can be enriched by SMC4-1. In these two experiments, the only thing that changed was the concentration of them because of the injection which introduced exceeding protein compared to their endogenous amount. Under this circumstance, the ratio between SMC4-1 and SMC4-2 at a late time point has been either flipped or enhanced which could be the reason why the SMC4-1 and SMC4-2 interaction was lost. This observation may support the hypothesis that SMC4-2 may potentially replace the position of SMC4-1 in condensin that interacts with SMC2s in a competitive binding way. This assumption is based on the fact that SMC4-1 and SMC4-2 share conserved domains and the potential to form condensin complexes with SMC2. Similar to the endogenous ratio, when introducing a large amount of SMC4-2 into a late time point, it may compete with endogenous SMC4-1 on binding with SMC2s, the SMC4-1 dissociated from chromosomes but not degraded according to the continuous fluorescence. The ‘SMC4-2 plus SMC2s’ condensin complex could be the late condensin form that may participate in IESs excision as SMC4-2 was supposed to be the important co-factor of this process but SMC2s are not in this study. Contrary to the native ratio, as injecting SMC4-1 into MACs, the ratio at the late time point between SMC4-1 and SMC4-2 was flipped, SMC4-2 was still able to occupy SMC4-1’s position while a high amount of SMC4-1 could inhibit this process that may stable the interaction with SMC4-2. For sure, this assumption needs to be interpreted with caution. Here we just bring up one possibility which can fit all results got from the study. Readers should judge the model carefully.

Conclusion

This research aimed to study the effect of SMCs in processing IES excision in *P. tetraurelia*. The most interesting finding here is that SMC4-2 play important role in manipulating IESs and iesRNAs production. To our knowledge, this is the first report of the interaction between SMC4-2 and IES excision in *P. tetraurelia*. The second major finding was that SMC4-1 degraded in old MAC potential to be the initial step of IES processing which is also the first report of SMC4-1 dissociation at an early time point. The research has also shown that it's very likely that SMC2s and SMC4-1 take participate in SMC4-2 handling IES excision which has not been explored before. The last but not the least finding is that we described the interactions between SMC2s and SMC4s and the absence of SMC4-1 was reported in the SMC4-2 Co-IP results. Combining all results in this study, the authors proposed a competitive model which makes an explanation for each part of these findings. The current data highlight the importance of SMC4-2 in the genome rearrangement in *P. tetraurelia* beyond the classic definition of SMC4 in the maintenance of chromosomes in other organisms^{46,47}. This project is the first comprehensive investigation of condensin SMCs' independent or dependent influences on IES excision which should contribute to existing knowledge of IES processing by providing newly potential co-factors from a completely new direction. The generalizability of these results is subject to certain limitations. Despite this, the study certainly adds a novel angle at which to look at this process. The precise mechanism of SMC4-2 in this progress remains to be elucidated. Further work is still needed to establish whether the competitive model is true or not. In general, this study provides a new foundation for additional investigation which may in the end lead to an exciting mechanistic discovery.

Reference

- 1 Bhullar, S. *et al.* A mating-type mutagenesis screen identifies a zinc-finger protein required for specific DNA excision events in *Paramecium*. *Nucleic acids research* **46**, 9550-9562, doi:10.1093/nar/gky772 (2018).
- 2 Lepere, G. *et al.* Silencing-associated and meiosis-specific small RNA pathways in *Paramecium tetraurelia*. *Nucleic acids research* **37**, 903-915, doi:10.1093/nar/gkn1018 (2009).
- 3 Sandoval, P. Y., Swart, E. C., Arambasic, M. & Nowacki, M. Functional diversification of Dicer-like proteins and small RNAs required for genome sculpting. *Developmental cell* **28**, 174-188, doi:10.1016/j.devcel.2013.12.010 (2014).
- 4 Allen, S. E. *et al.* Circular Concatemers of Ultra-Short DNA Segments Produce Regulatory RNAs. *Cell* **168**, 990-999 e997, doi:10.1016/j.cell.2017.02.020 (2017).
- 5 Hirano, T. Condensin-Based Chromosome Organization from Bacteria to Vertebrates. *Cell* **164**, 847-857, doi:10.1016/j.cell.2016.01.033 (2016).
- 6 Wood, A. J., Severson, A. F. & Meyer, B. J. Condensin and cohesin complexity: the expanding repertoire of functions. *Nature reviews. Genetics* **11**, 391-404, doi:10.1038/nrg2794 (2010).
- 7 Anderson, D. E., Losada, A., Erickson, H. P. & Hirano, T. Condensin and cohesin display different arm conformations with characteristic hinge angles. *The Journal of cell biology* **156**, 419-424, doi:10.1083/jcb.200111002 (2002).
- 8 Ono, T., Fang, Y., Spector, D. L. & Hirano, T. Spatial and temporal regulation of Condensins I and II in mitotic chromosome assembly in human cells. *Molecular biology of the cell* **15**, 3296-3308, doi:10.1091/mbc.e04-03-0242 (2004).
- 9 Shintomi, K. & Hirano, T. The relative ratio of condensin I to II determines chromosome shapes. *Genes & development* **25**, 1464-1469, doi:10.1101/gad.2060311 (2011).
- 10 Chan, R. C., Severson, A. F. & Meyer, B. J. Condensin restructures chromosomes in preparation for meiotic divisions. *The Journal of cell biology* **167**, 613-625, doi:10.1083/jcb.200408061 (2004).
- 11 Nishide, K. & Hirano, T. Overlapping and non-overlapping functions of condensins I and II in neural stem cell divisions. *PLoS genetics* **10**, e1004847, doi:10.1371/journal.pgen.1004847 (2014).
- 12 Green, L. C. *et al.* Contrasting roles of condensin I and condensin II in mitotic chromosome formation. *Journal of cell science* **125**, 1591-1604, doi:10.1242/jcs.097790 (2012).
- 13 Gibcus, J. H. *et al.* A pathway for mitotic chromosome formation. *Science* **359**, doi:10.1126/science.aao6135 (2018).
- 14 Sakai, A., Hizume, K., Sutani, T., Takeyasu, K. & Yanagida, M. Condensin but not cohesin SMC heterodimer induces DNA reannealing through protein-protein assembly. *The EMBO journal* **22**, 2764-2775, doi:10.1093/emboj/cdg247 (2003).
- 15 Sutani, T. & Yanagida, M. DNA renaturation activity of the SMC complex implicated in chromosome condensation. *Nature* **388**, 798-801, doi:10.1038/42062 (1997).
- 16 Akai, Y. *et al.* Opposing role of condensin hinge against replication protein A in mitosis and interphase through promoting DNA annealing. *Open biology* **1**, 110023, doi:10.1098/rsob.110023 (2011).

-
- 17 Festuccia, N., Gonzalez, I., Owens, N. & Navarro, P. Mitotic bookmarking in development and stem cells. *Development* **144**, 3633-3645, doi:10.1242/dev.146522 (2017).
- 18 Beisson, J. *et al.* Mass culture of Paramecium tetraurelia. *Cold Spring Harbor protocols* **2010**, pdb prot5362, doi:10.1101/pdb.prot5362 (2010).
- 19 Beisson, J. *et al.* Maintaining clonal Paramecium tetraurelia cell lines of controlled age through daily reisolation. *Cold Spring Harbor protocols* **2010**, pdb prot5361, doi:10.1101/pdb.prot5361 (2010).
- 20 Cobbe, N. & Heck, M. M. The evolution of SMC proteins: phylogenetic analysis and structural implications. *Molecular biology and evolution* **21**, 332-347, doi:10.1093/molbev/msh023 (2004).
- 21 Cervantes, M. D., Coyne, R. S., Xi, X. & Yao, M. C. The condensin complex is essential for amitotic segregation of bulk chromosomes, but not nucleoli, in the ciliate Tetrahymena thermophila. *Molecular and cellular biology* **26**, 4690-4700, doi:10.1128/MCB.02315-05 (2006).
- 22 Katoh, K., Rozewicki, J. & Yamada, K. D. MAFFT online service: multiple sequence alignment, interactive sequence choice and visualization. *Briefings in bioinformatics* **20**, 1160-1166, doi:10.1093/bib/bbx108 (2019).
- 23 J. Mistry, S. Chuguransky, L. Williams, M. Qureshi, G.A. Salazar, E.L.L. Sonnhammer, S.C.E. Tosatto, L. Paladin, S. Raj, L.J. Richardson, R.D. Finn, A. Bateman. *Nucleic Acids Research* doi: 10.1093/nar/gkaa913 (2020).
- 24 Arnaiz, O. *et al.* Improved methods and resources for paramecium genomics: transcription units, gene annotation and gene expression. *BMC genomics* **18**, 483, doi:10.1186/s12864-017-3887-z (2017).
- 25 Trifinopoulos, J., Nguyen, L. T., von Haeseler, A. & Minh, B. Q. W-IQ-TREE: a fast online phylogenetic tool for maximum likelihood analysis. *Nucleic acids research* **44**, W232-235, doi:10.1093/nar/gkw256 (2016).
- 26 Beisson, J. *et al.* Paramecium tetraurelia: the renaissance of an early unicellular model. *Cold Spring Harbor protocols* **2010**, pdb emo140, doi:10.1101/pdb.emo140 (2010).
- 27 Fire, A. *et al.* Potent and specific genetic interference by double-stranded RNA in Caenorhabditis elegans. *Nature* **391**, 806-811, doi:10.1038/35888 (1998).
- 28 Baudry, C. *et al.* PiggyMac, a domesticated piggyBac transposase involved in programmed genome rearrangements in the ciliate Paramecium tetraurelia. *Genes & development* **23**, 2478-2483, doi:10.1101/gad.547309 (2009).
- 29 Arnaiz, O. & Sperling, L. ParameciumDB in 2011: new tools and new data for functional and comparative genomics of the model ciliate Paramecium tetraurelia. *Nucleic acids research* **39**, D632-636, doi:10.1093/nar/gkq918 (2011).
- 30 Arnaiz, O. *et al.* The Paramecium germline genome provides a niche for intragenic parasitic DNA: evolutionary dynamics of internal eliminated sequences. *PLoS genetics* **8**, e1002984, doi:10.1371/journal.pgen.1002984 (2012).
- 31 Denby Wilkes, C., Arnaiz, O. & Sperling, L. ParTIES: a toolbox for Paramecium interspersed DNA elimination studies. *Bioinformatics* **32**, 599-601, doi:10.1093/bioinformatics/btv691 (2016).
- 32 Bechara, S., Kabbani, L., Maurer Alcalá, X. & Nowacki, M. Identification of novel, functional long non-coding RNAs involved in programmed, large scale genome rearrangements. *Rna*, doi:10.1261/rna.079134.122 (2022).
- 33 Kim, D., Paggi, J. M., Park, C., Bennett, C., & Salzberg, S. L. Graph-based genome alignment and genotyping with HISAT2 and HISAT-genotype. *Nature biotechnology*, **37**(8), 907–915. doi.org:10.1038/s41587-019-0201-4 (2019).

-
- 34 Nowacki, M., Zagorski-Ostojka, W. & Meyer, E. Nowa1p and Nowa2p: novel putative RNA binding proteins involved in trans-nuclear crosstalk in *Paramecium tetraurelia*. *Current biology : CB* **15**, 1616-1628, doi:10.1016/j.cub.2005.07.033 (2005).
- 35 Beisson, J. *et al.* DNA microinjection into the macronucleus of paramecium. *Cold Spring Harbor protocols* **2010**, pdb prot5364, doi:10.1101/pdb.prot5364 (2010).
- 36 Furrer, D. I., Swart, E. C., Kraft, M. F., Sandoval, P. Y. & Nowacki, M. Two Sets of Piwi Proteins Are Involved in Distinct sRNA Pathways Leading to Elimination of Germline-Specific DNA. *Cell reports* **20**, 505-520, doi:10.1016/j.celrep.2017.06.050 (2017).
- 37 Hoehener, C., Hug, I. & Nowacki, M. Dicer-like Enzymes with Sequence Cleavage Preferences. *Cell* **173**, 234-247 e237, doi:10.1016/j.cell.2018.02.029 (2018).
- 38 Reuter, M. *et al.* Loss of the Mili-interacting Tudor domain-containing protein-1 activates transposons and alters the Mili-associated small RNA profile. *Nature structural & molecular biology* **16**, 639-646, doi:10.1038/nsmb.1615 (2009).
- 39 Bischerour, J. *et al.* Six domesticated PiggyBac transposases together carry out programmed DNA elimination in *Paramecium*. *eLife* **7**, doi:10.7554/eLife.37927 (2018).
- 40 Uhlmann, F. SMC complexes: from DNA to chromosomes. *Nature reviews. Molecular cell biology* **17**, 399-412, doi:10.1038/nrm.2016.30 (2016).
- 41 Terakawa, T. *et al.* The condensin complex is a mechanochemical motor that translocates along DNA. *Science* **358**, 672-676, doi:10.1126/science.aan6516 (2017).
- 42 Hirano, T., Kobayashi, R. & Hirano, M. Condensins, chromosome condensation protein complexes containing XCAP-C, XCAP-E and a *Xenopus* homolog of the *Drosophila* Barren protein. *Cell* **89**, 511-521, doi:10.1016/s0092-8674(00)80233-0 (1997).
- 43 De Piccoli, G., Torres-Rosell, J. & Aragon, L. The unnamed complex: what do we know about Smc5-Smc6? *Chromosome research : an international journal on the molecular, supramolecular and evolutionary aspects of chromosome biology* **17**, 251-263, doi:10.1007/s10577-008-9016-8 (2009).
- 44 Michelini, F. *et al.* From "Cellular" RNA to "Smart" RNA: Multiple Roles of RNA in Genome Stability and Beyond. *Chemical reviews* **118**, 4365-4403, doi:10.1021/acs.chemrev.7b00487 (2018).
- 45 Thattikota, Y. *et al.* Cdc48/VCP Promotes Chromosome Morphogenesis by Releasing Condensin from Self-Entrapment in Chromatin. *Molecular cell* **69**, 664-676 e665, doi:10.1016/j.molcel.2018.01.030 (2018).
- 46 Hirano, T. At the heart of the chromosome: SMC proteins in action. *Nature reviews. Molecular cell biology* **7**, 311-322, doi:10.1038/nrm1909 (2006).
- 47 Burmann, F. *et al.* An asymmetric SMC-kleisin bridge in prokaryotic condensin. *Nature structural & molecular biology* **20**, 371-379, doi:10.1038/nsmb.2488 (2013).

Late

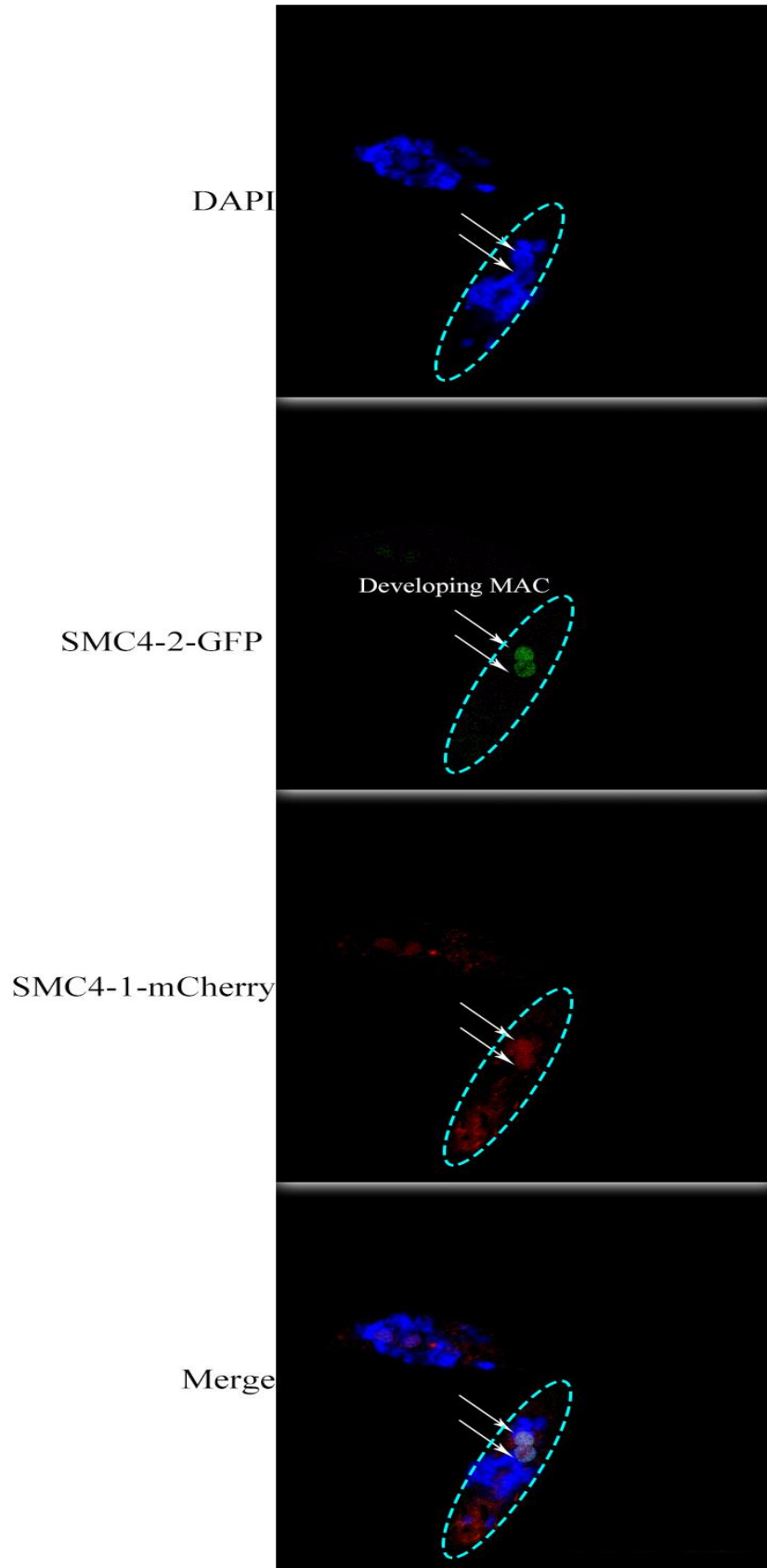


Figure S1. Co-localization of SMC4-1 tagged with mCherry and SMC4-2 tagged with GFP at late time point. DAPI represents DNA in blue, green signal represents SMC4-2 tagged with GFP, red signal represents SMC4-1 tagged with mCherry.

Oligo name	Sequence 5'-3'
SMC4-1 +f R	TCAACATGAATAATTAATTTTAAATTCTTCATTCTT
SMC4-1 +f F	AAAGAATTAAGTAGTATTTTGCAGAAAAAATATTAAG
SMC4-1 +fv 3 F	TGAAATGATTTTAAAATATTCATATTCCATTATTG
SMC4-1 +fv 3 R	TCTATTTTAATTAACGTTTTTCATTGTTTTTC
SMC4-1 +fv F	CAGACTGAAAGTGAAGAGCCAT
SMC4-1 +fv R	CATTTTATGTAAATATATTTAATATTTTAAATTAACTTTTGG
SMC4-2 +F R	GAATTAATTCAAGATCTAAATATTCGTAACA
SMC4-2 +F F	ATGCGCAATTTAATTTGAGCAATATT
SMC4-2 +fv 3 F	TGAAATTTATATTAAATTATAATCAATTAATTTTATC
SMC4-2 +fv 3 R	AACTTCTAATTAGATGACTTCTGTTGAA
SMC4-2 +fv F	ATTAAGGAAGTTATTTTGGAGAATTTTAAATC
SMC4-2 +fv R	CATATTTTCTATCATTTAATTTTCTACTCAAA
SMC2-1 sil F	ATATGAGCTCATGTGGATCAAAGAAATCATTATCGA
SMC2-1 sil R	TACCAGGAGACAAAAAGAACTATAGACTCGAGTAAA
SMC2-2 sil F	ATATGAGCTCAGAACAACCTGAATAGAGAGATTACACA
SMC2-2 sil R	AAAAGAATTCTAATCATTAAAAGACAAAAAGTTGCTCGAGTAAA
SMC4-1 sil F	ATATGAGCTCATGCAGACTGAAAGTGAAGAGC
SMC4-1 sil R	TTTACTCGAGTGTTTTGTTATGATGTCAGATTGTTCACT
SMC4-2 sil F	ATATGAGCTCATGATTAAGGAAGTTATTTTGGAGAATTTT
SMC4-2 sil R	TTTACTCGAGTATCTACCTTATTTTATTTTCTGGAATCA
SMC2-1 Co-sil F	ATATCCCGGGATGTGGATCAAAGAAATCATTATCGA
SMC2-2 Co-sil F	ATATCCCGGGAGAACAACCTGAATAGAGAGATTACACA
SMC4-1 Co-sil F	ATATCCCGGGATGCAGACTGAAAGTGAAGAGC
SMC4-2 Co-sil-R	TTTACCCGGGTATCTACCTTATTTTATTTTCTGGAATCA

Table S1. Oligo sequences used for the study.

4.2.Part II: Purification of IES excision machinery by affinity capture and mass spectrometry from *Paramecium tetraurelia*.

The elimination of IESs can be regulated at many different levels, such as sequence preference on DNA, and the interaction with small RNAs and proteins. Protein is the main executor of life activity, proteins bind to distinct sites on the DNA, which recognize and cleavage the corresponding IESs. From previous studies, PGM, a domesticated transposase, has been supposed to cleavage IESs during development²⁰. Despite being such an important protein in this process, nobody succeeds in identifying the protein complexes that interact within/around the IES regions *in vivo* which makes the mechanism behind the IES excision still unclear. Here, we propose an *in vivo* method, adopted from Pooja Murarka¹⁴⁰, for the identification of IES binding excision machinery complexes in *P. tetraurelia* where the 3 tandem IESs-protein complexes formed *in vivo* are crosslinked by formaldehyde. In the autogamy or conjugation of *P. tetraurelia*, the development of new MAC is always accompanied by fragmented old MAC which makes any attempt to purify new MAC-specific stuff like the excision machinery always heavily contaminated by nonspecific fractions. The highlight point of this method is the idea that we use IES regions as the hot point to purify the excision machinery which is only present in new developing MAC. So, we can exclude the old MAC contamination. These complexes are further purified and the DNA is sequenced, bound proteins are identified, and potential binding RNA is kept for analysis. The method is schematically described in Figure 13. This method provides a new way to isolate *in situ* excision machinery based on complementary oligos purification and mass spectrometry analysis in the development of *Paramecium*.

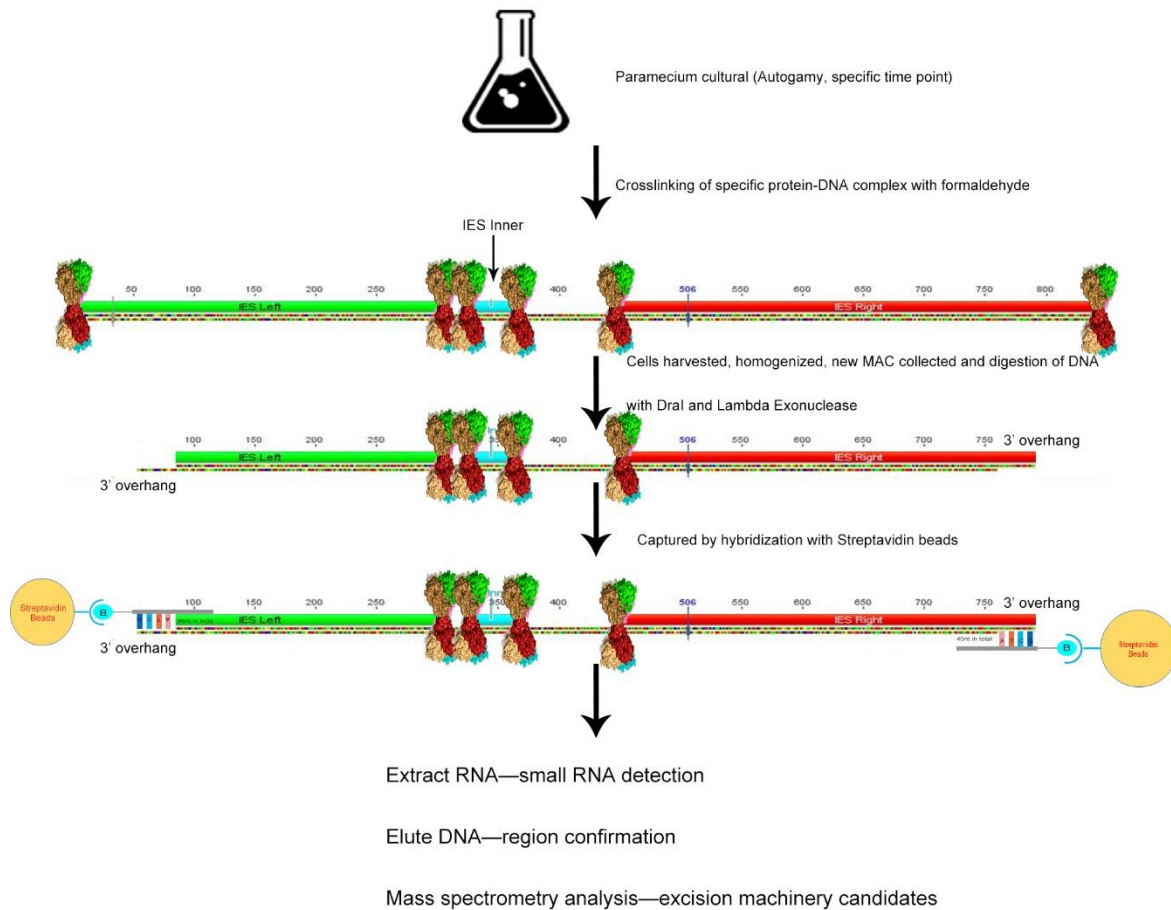


Figure 13. Schematic diagram presenting the experimental procedure followed. A method for isolation and identification of excision machinery (protein complex supposed to be attached at the end of each IES when cutting). By cross-linking the excision machinery to IESs with formaldehyde when cells are in the timing of IESs elimination, such protein-DNA complexes are fixed in vivo. The new MAC is then subjected to digestion with restriction enzymes to generate overhangs, which further binds to corresponding biotinylated oligos attached to streptavidin beads. The purified complex then proceeds accordingly.

A major problem in isolating the excision machinery from paramecium is that nobody for sure knows what protein is in the complex. Even the PGM is putative to be the executor of IES cleavage just because of some indirect evidences^{20,107-109}. The chromatin immunoprecipitation (ChIP) assay is another extensively used approach for detecting DNA binding protein¹⁴¹. The ChIP assay is used to profile DNA-binding proteins throughout the whole genome. Aside from cost and availability, ChIP has technological limitations. Because this approach requires specific antibodies, it cannot be utilised when the target proteins are unknown¹⁴². Therefore, to gain a more comprehensive and precise insight into the intact excision machinery, accurately capturing the moment of IESs elimination by the complex has

to be performed from DNA or RNA level. In this method, we decided to achieve the goal by performing on the DNA level since RNA is relatively unstable compared to DNA.

The first step of this experiment is to determine the target region in the genome which contains 3 tandem IESs regions and the length should be limited. There are several concerns with these specific requirements. Firstly, these 3 tandem IESs should include two longer IESs at the outside of the inner one (less than 100 bp) because this method needs restriction enzyme digestion on the outer IESs. The two outer IESs need a restriction site >100 bp from the innermost IES end (restriction sites should not cut inside of the outer restriction cut sites). This treatment shortens the IES and the excision machinery out of the restriction sites will be lost. Hence, longer IESs are needed to be sure there is enough IES residual left. Secondly, the possibility that short IES (26-28bp) employ different mechanisms of elimination compared to longer one reminds us that involving different length IESs would be a better way to have a comprehensive insight into the components of excision machinery. Thirdly, the priming site should be specific to these two outer IES ends (priming sites exposed by exonuclease digestion). Fourthly, since various proteins can bind with DNA in a bunch of biology progress, a negative control has to be included to exclude the IES-unspecific binding proteins. This negative control is picked up according to several principles like similar total length, same restriction sites, and close existence time with the target region (3 tandem IESs). Bioinformatic analysis was conducted by Victor Mason, detailed information regarding all candidates can be found in the appendix. To determine when the target region and negative control are present in new developing MAC of *Paramecium*, genomic DNA from different time point (100% fragments to 10 hours after 100% fragments, 2 hours interval) has been extracted and PCRs with specific primers were performed respectively as shown in Figure 14. The negative control refers to IESPGM.PTET51.1.23.362798 (798-, if not specified) and target region referring to IESPGM.PTET51.1.18.134377 (377+, if not specified) were chosen because both of them can be detected at the same time point. In addition to this, they have the same restriction site as Dra I which generate similar length of products. After sequencing the PCR products, we confirmed that 10 hours after 100% fragments is a reasonable time point for the experiment.

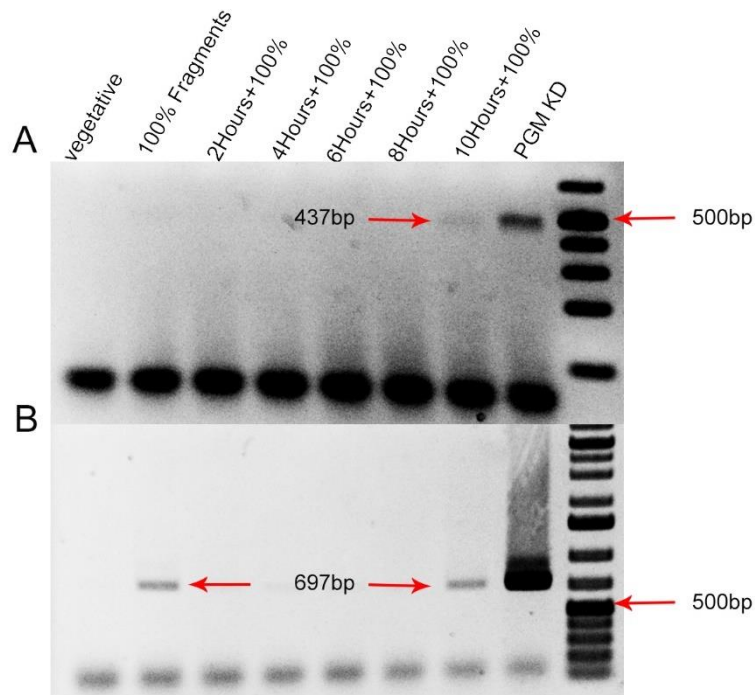


Figure 14. PCR determines the presence of the 798- (697bp) and 377+ (437bp) target regions.

Genomic DNA of different time points were taken from vegetative (negative) to 10 hours + 100% fragments, as well as genomic DNA from PGM knock down as a positive control. Oligos which were used to pull down target regions were taken as primers without biotin modification. A) The 377+ region can only be detected at 10 hours + 100% fragments and positive control. B) The 798- region presented at 100% fragments, 10 hours + 100% fragments and positive control. The overlap timing of 377+ and 798- is 10 hours + 100% fragments.

The second step is the purification of new developing MAC without breaking the nuclear envelope. Since the MIC genome contains the IES sequence, it would be contamination to the specific binding of primer. So, we have to exclude the MIC genome from the purifying step. Due to the IES elimination is being believed to happen in developmental MAC, and we need the DNA-protein interactions not dissolved before elution, any intensive treatment that would potentially disrupt the interactions are forbidden including heating and a high amount of detergent. We modified a purification of the developing MAC method from O. Arnaiz²¹ to isolate the intact developing MAC. This modification gives us the opportunity to keep the interactions in nuclei stable after ultracentrifuge.

The third step is nuclear membrane lysis and chromatin release. A high-quality chromatin preparation is very important to DNA-protein interaction capture. This step is critical to the successful enriching of the target region with binding proteins, since we need to lysis the

nuclei membrane but not disrupt the DNA-protein interactions in nuclei. Commonly, 0.1% sodium dodecyl sulfate (SDS) is the concentration used in nuclear lysis, and luckily, according to H. Belaghzal's report¹⁴³, nuclear proteins that are not cross-linked to DNA can be eliminated, and the chromatin would be opened for better and more homogenous digestion treated with 0.1% SDS which means cross-linked DNA-proteins will not be disrupted when treated with 0.1% SDS. An additional step to open the chromatin by incubating at 65°C for 10 minutes was included.

Detail operations including restriction enzyme digestion, Biotin labelled oligo incubation, Dynabeads™ MyOne™ magnetic beads purification and separation of different components are presented in the 'Method' part.

Methods

1. *Paramecium* strain 51, mating type 7 were used. Cultivation and autogamy were performed as previously described¹²².
2. 100 mL of cells was used to extract DNA at each time point (100% fragments to 10 hours after 100% fragments, 2 hours intervals). PCR confirmation of 377+ and 798- were done with GoTaq polymerase (M3001, Promega) using primers without Biotin.
3. Collect cells at 10 hours + 100% in 15ml tubes with 20ul 50X protease inhibitor. Aliquots all into eight 15ml tubes, 4 for non-cross linking with two replicates for 798- and 377+, and 4 for the cross-linking group.
4. For cross-linking: 1 ml/sample formaldehyde added into the cell, shaking at room temperature (RT) 10min, gently invert the tube every 1-2 min.

For non-cross linking, to step 6

5. Quench the cross-link with 100ul 1.25M Glycine, mix gently and incubate at RT 5min.
6. Fill up a few ml pre-cold PBS, gently resuspend, then fill the rest of the tube with PBS and invert the tube to mix, 4°C, 279rcf for 2min twice. Remove as much supernatant as possible.
7. Resuspend in 2.5 volumes of Lysis Buffer 1 and transfer half of them to the middle size homogenizer; incubate 5min on ice. In the meantime, pre-cool the centrifuge
8. Homogenise cells and check with DAPI staining frequently until no intact cell can be found.

-
9. Transfer lysate to a 15 mL tube, fill up with Wash Buffer, mix by inverting, centrifuge at 1000 RCF, 4 °C for 3 min, and remove supernatant.
 10. Resuspend the pellet with 2 mL Wash Buffer, fill up to 15 mL, invert mixing, and spin down as in step 9.

Using a cut tip to avoid breaking MACs.

11. Resuspend lysate in 3 volumes of Sucrose Buffer.
12. Transfer 3 mL of Sucrose Buffer to an ultracentrifuge tube (Beckman Coulter 344060 14×95 mm). Slowly add the cell lysate on top, then fill up with Wash Buffer (gently, avoid disrupting the layer formation).
13. Balance the samples and spin down for 1 h, 4 °C, 35,000 RPM with rotor: SW40Ti
14. Discard the supernatant with a Pasteur pipette, and then wash the pellet twice by resuspending it in 500 µL of ice-cold 1× ThermoPol® Reaction Buffer (10× attached, diluted to 1X). Then transfer all to a 1.5 mL RNase-free tube, centrifuging for 5 min at 2,500 ×g, 4 °C.
15. Remove the supernatant, resuspend in 1× ThermoPol® Reaction Buffer, and check the MACs under a microscope by DAPI staining.

Save 18 µL of lysate for the chromatin integrity control:

Take 18 µL of lysate and add 32µL with 1x ThermoPol® Reaction Buffer and 10µL of Proteinase K (10 mg/mL). Incubate at 65 °C for 30 min. Purify DNA by single phenol-chloroform extraction without ethanol precipitation. Check the quality of the sample by running it on 0.75% agarose gel. The sample is good if DNA is either stuck in the well or runs as a single high band (>23 kb) (2ul DNA+8ul H₂O+2ul Loading Dye).

16. Add 40 µL of 1% SDS to each sample and mix carefully by pipetting until MAC staining becomes transparent. Avoid making bubbles.
17. Metal bath for 10 min at 65 °C to dissolve chromatin. Then put tubes on ice immediately.
18. Quench the SDS with 44.4 µL of 10% Triton X-100. Mix gently by pipetting and avoid making bubbles.
19. Add 9.4 µL of 10× ThermoPol® Reaction Buffer to have a final 1× ThermoPol® Reaction Buffer).
20. Add 50 U Dra I, mix gently, and incubate at 37 °C for 5 - 15 min. Add 50 U Lambda exonuclease to the mixture and incubate for 15 s at 37 °C. Incubate at 75 °C for 10 min to inactivate.

(Optional) ASSESS THE DIGESTION

Mix 10 µL products with 40 µL of 1x ThermoPol® Reaction Buffer and 10 µL of Proteinase K (10 mg/ml). incubate at 65 °C, 30 min, purify DNA by phenol-chloroform extraction like mentioned before and run 0.75% gel electrophoresis.

21. During the incubation, resuspend the Dynabeads™ MyOne™ magnetic beads in the vial by vortex for >30 sec.
22. Transfer 100ul beads to an RNase-free tube.
23. Add 1 mL of 1X Binding & Washing Buffer and resuspend.
24. Keep the tube on a magnet for 1 min and remove the supernatant.
25. Remove the tube from the magnet and resuspend the washed beads in 1ml W&B buffer.
26. Repeat steps 24-25 twice, for total of 3 washes.
27. Resuspend washed beads in 100 µL 2× Binding & Washing Buffer to a final concentration of beads at 5 µg/µL.
28. After inactivation, immediately add 5.52 µL of each Biotin-labelled primer (primer concentration at 1 µM) into the sample, mix well and incubate at 49°C for 10 min.
29. Mix incubation and resuspended beads, and add 94.25 µL 5M NaCl to adjust NaCl concentration to 1 M. Incubate at 4°C O/N on rotation.
30. Separate the coated beads with a magnet for 2 min, and keep the supernatant in a new RNase-free tube.

Optional (check the pull-down efficiency):

Aliquots 50 µL mix with 10ul SDS loading dye and boil at 95 °C for 15-20 min and store at -20 °C.

Another 50 µL store at -20 °C for 377+ PCR detection.

Freeze left in liquid nitrogen, and store at -80 °C

31. Resuspend beads with 1 mL 1X Binding & Washing Buffer and separate the beads with a magnet for 2 min, discard the supernatant.
32. Repeat step 31 twice.
33. Resuspend in 150 µL RNase free water and transfer 50 µL into a new 1.5 mL tube, add 12.5 µL 5× SDS loading buffer, boil at 95 °C for 15-20 min; Add another 100 µL

RNase free water to the leftover and transfer 100 μ L in another new RNase-free tube, freeze in liquid nitrogen for RNA extraction later.

DNA Extraction from the beads

34. Wash the DNA-coated Dynabeads in 50 μ L 1 \times SSC with magnet separation.
35. Resuspend the beads in another 50 μ L of 1 \times SSC, and incubate at 95 $^{\circ}$ C for 5 minutes.
36. Immediately put the tube on the magnet, stand for 1 – 2 minutes, and transfer the supernatant to a nuclease-free tube, the supernatant contains a non-biotinylated DNA strand.
37. Performing PCR to check the existence of the 377+ regions.

RNA extraction from the beads

38. Add 1 mL TRI Reagent[®] to the frozen sample and vortex thoroughly, transfer all solution into a 15 mL tube and add another 2 mL TRI into the 15 mL tube.
39. Put 15mL tube on rotation at RT for 5min.
40. Add 0.6 mL chloroform into the sample, vortex for at least 15 sec, then let the sample stand for 5 min at RT.
41. Spin down at max. speed for 15 min at 4 $^{\circ}$ C.
42. Carefully transfer the upper colourless phase into a 15 mL tube and aliquots 750 μ L to each 1.5 mL tube.
43. Add 500 μ L isopropanol to each tube, mix by inverting and stand at RT for 10 min.
44. Spin down at 1,200 RCF for 10 min at 4 $^{\circ}$ C.
45. Discard the supernatant, and wash the pellet with 1 mL of 75% ethanol.
46. Spin down at 7,500 RCF for 5 min at 4 $^{\circ}$ C.
47. Discard supernatant, and wash with 1 mL 75% ethanol once.
48. Discard supernatant, centrifuge for 30 sec, and discard the supernatant.
49. Make a tent with RNase Zap cleaned alumina, leave the lid opening, and air dry the pellet under 37 $^{\circ}$ C for 30 min.

-
50. Resuspend with 30 μ L nuclease-free ddH₂O, and incubate at 60 °C for 15 min to dissolve the pellet.

Silver staining to check the enriched proteins

51. A 10% sodium dodecyl sulfate–polyacrylamide gel electrophoresis (SDS-PAGE) gel run as usual.
52. Fix gel in 100 mL fixative solution overnight at RT with shaking.
53. Wash the gel 20 min with 50% Ethanol on shaking at RT, twice.
54. Treat the gel exactly for 1 min with 98ml Sodium thiosulphate (3-4 flakes in 100ml MilliQ water).
55. Wash the gel 20 seconds with MilliQ water three times.
56. Treat the gel with AgNO₃ for 30 min.
57. Wash the gel 20 seconds with MilliQ water for three times.
58. Develop the gel with 100ml developing solution until the bands reached the desired intensity.
59. Stop the reaction with 100ml Stop Solution
60. Scan the gel warped with glossy film.

Mass spectrometry preparation and analysis

Two replicates of each group were sent for mass spectrometry at the Mass Spectrometry and Proteomics facility (PMSCF, Bern, Switzerland). A 12 % SDS-PAGE gel was prepared and run 0.6cm into the resolving gel, the apparatus was disassembled and the stacking gel was removed. The gel was stained with InstantBlue (Expedeon) until the bands became visible and the band of interest was then cut out and cut into 6 small cubes of about 1 mm² and the cubes were put in an Eppendorf tube. The cubes were covered with 100 μ L of 20% ethanol, and stored at 4 °C before sending.

Protein identification and statistics were performed by Manfred Heller at the PMSCF. Shotgun Liquid Chromatography Tandem Mass spectrometry (LC-MS/MS) with non-labelled samples was performed and the peptide identification was made with EasyProt software and

processed with MaxQuant software for estimation of protein abundances^{144,145}. For the analysis, the LFQ and Top3 algorithms built into MaxQuant software were used for the label-free protein quantification.

Only proteins exclusively present in the 377+ group and not 798- samples, as well as deemed significant in both Top3 and LFQ were analysed. To filter the results, the IDs were converted into UniProt Accession numbers and entered into the PANTHER and AgBase databases to retrieve Gene Ontology terms and protein names¹⁴⁶⁻¹⁴⁸. Known contaminants such as ribosomal proteins and proteins not present in the same cellular compartment as the bait was excluded. The remaining proteins were manually searched for in the ParameciumDB to find out potentially interested proteins.

Recipes

Lysis buffer 1

	Amount	Final concentration
H ₂ O	4.915ml	
Sucrose	0.43g	0.25M
2M MgCl ₂	25ul	10mM
1M Tris pH6.8	50ul	10mM
NP-40	10ul	0.2%
Roche protease inhibitor	100ul	1X

Wash buffer

	Amount	Final concentration
H ₂ O	197ml	
Sucrose	17.2g	0.25M
2M MgCl ₂	1ml	10mM
1mM Tris pH7.4	2ml	10mM

Sucrose buffer

	Amount	Final concentration
H ₂ O	14.775ml	
Sucrose	10.77g (little by little)	2.1M
2M MgCl ₂	75ul	10mM
1M Tris pH7.4	150ul	10mM

2X Binding & Washing Buffer

	Amount	Final concentration
1M Tris-HCl pH 9	100ul	10mM
0.5M EDTA	20ul	1mM
2M NaCl	9.88ml	2M

Fixative Solution

	Amount	Final concentration
MilliQ water	39.95ml	
Methanol	50ml	50%
Acetic Acid	10ml	10%
Formaldehyde	50ul	50ul

Developing Solution

	Amount
MilliQ water	Up to 100ml
Na ₂ CO ₃	6g
Sodium Thiosulphate	2ml
Formaldehyde	50ul

Stop Solution

	Amount
MilliQ water	95ml
Acetic Acid	5ml

Results

To assess the potential timing for the purification, PCR using 377+ and 798- primers without Biotin were conducted at each time point separately. The results were shown in Figure 14. As shown, only at 10 hours +100% fragments can both 377+ and 798- be seen which means it's a possible time window for pulling down interacting proteins *in vivo*. To confirm the corresponding bands are the desired region we expected, the PCR products were analysed and confirmed by sanger sequencing in Microsynth company (Switzerland) using corresponding primers.

To assure the time point was also correct when performing the pull-down assay. Total DNA was extracted from the aliquot of culture and checked the presence of the target region with PCR. As seen in Figure 15, both target regions can be observed in the harvested cells. To confirm the target DNA was enriched on the beads, another PCR was done with the eluted DNA and the results were shown in Figure 15. Taken together, it can be assured that desired DNA regions were enriched on beads.

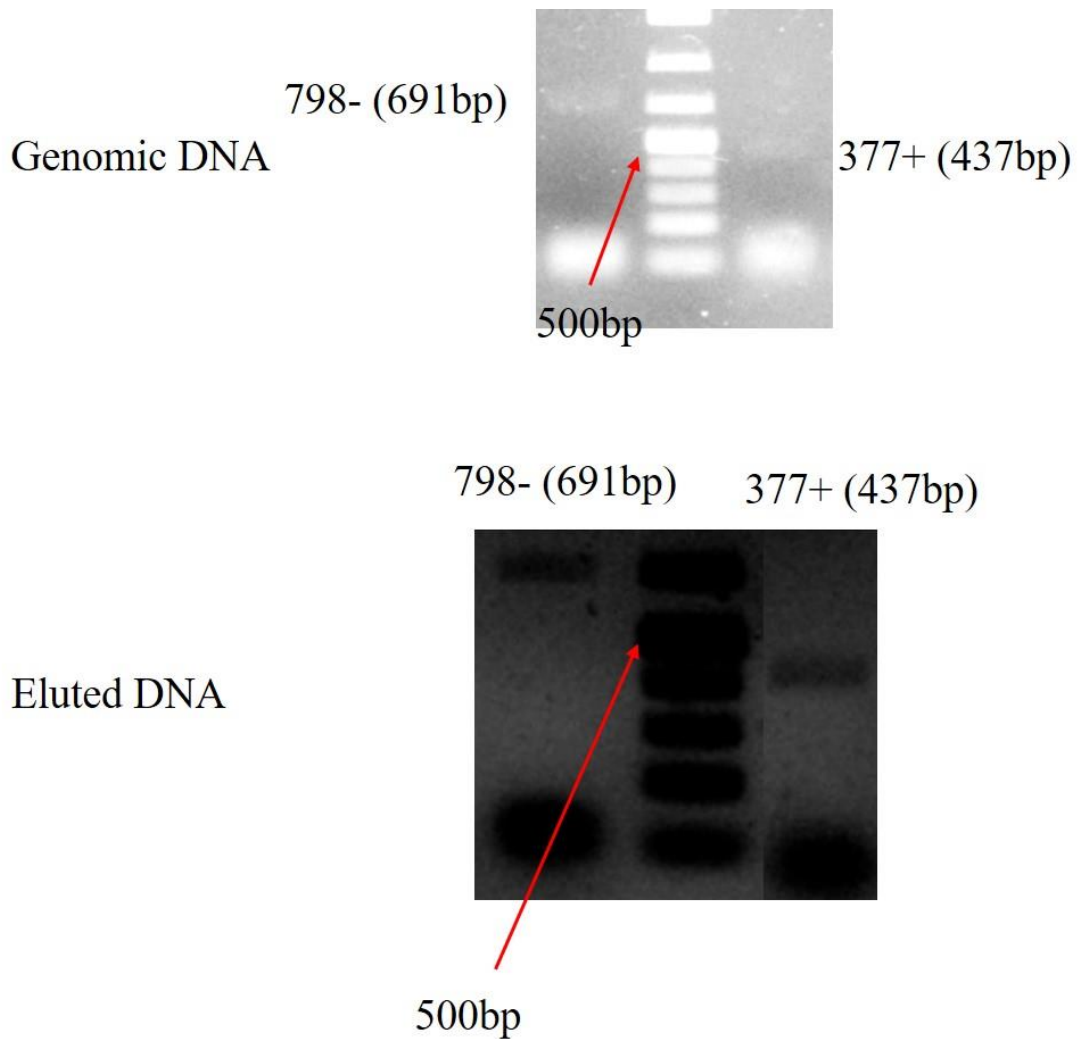


Figure 15. PCR determines the presence of the 798- (697bp) and 377+ (437bp) from genomic DNA and elution. DNA from cells and elution of 10 hours + 100% fragments were extracted.

To normalize the loading amount of each sample for mass spectrometry, we assumed that the number of proteins should be the same within the group if we could balance the concentration of DNA on beads. After eluting the DNA from the beads and measuring the concentration of each sample, samples corresponding to the same amount of DNA were loaded onto the SDS gel to check the enriched proteins (as shown in Figure 16) and prepare for mass spectrometry analysis.

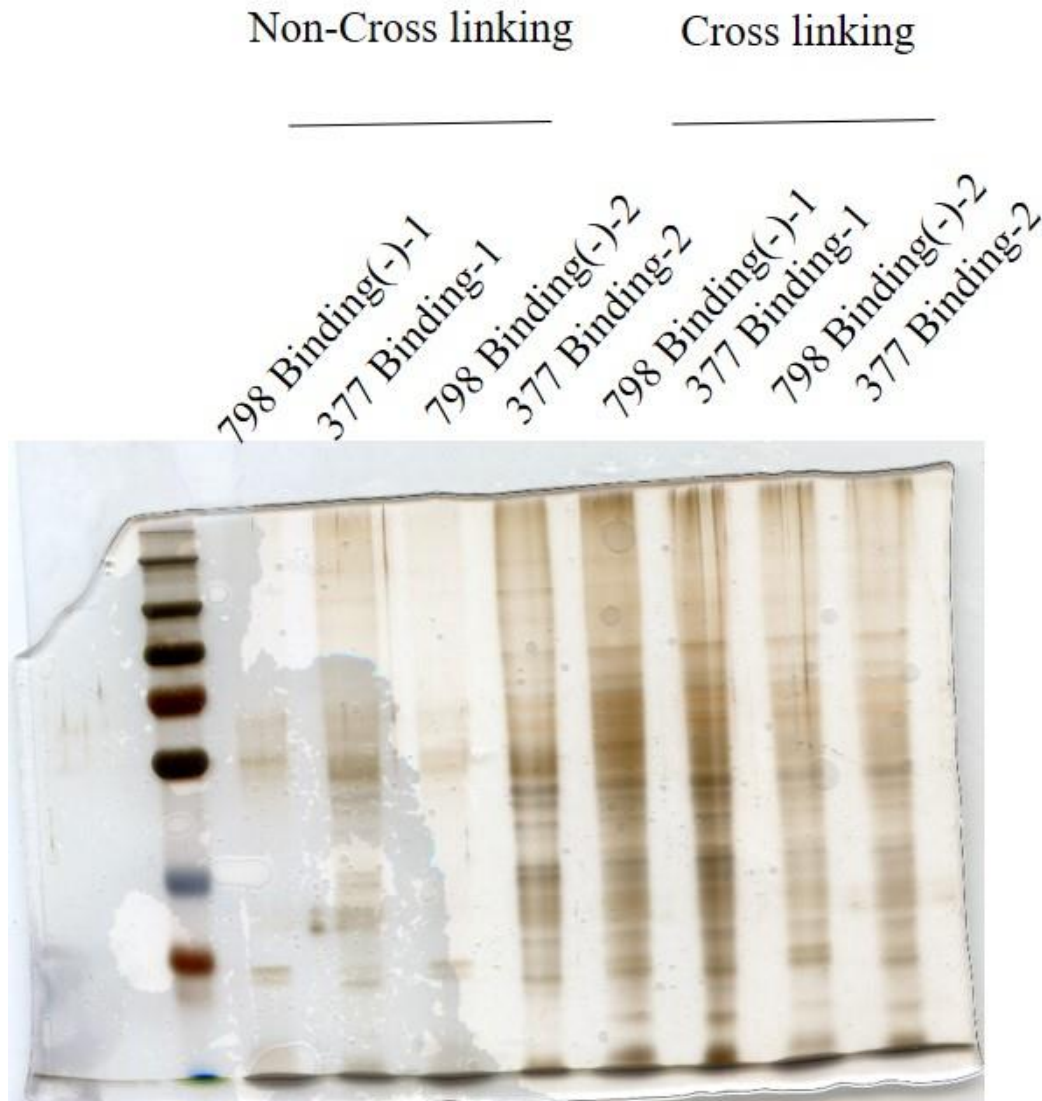


Figure 16. Silver staining of the enriched complex. All loading samples were normalized according to the eluted DNA amount. Both non-cross-linking and cross-linking are included. A 10% SDS-PAGE gel was used. Silver staining was performed.

All enriched proteins that were only presented in 377+ groups were shown in Table 1. However, none of the known key players of *P. tetraurelia* genome rearrangements, like the PTIWI proteins, PGM, NOWA proteins, EZL1, etc. was found by mass spectrometry. Several assumptions can explain this phenomenon. The first one is that the excision machinery which may contain PGM transiently binds on its target region and detach immediately after introducing cleavage on the IES boundary. This potential ‘cut and go’ mechanism indicates the chance of the excision machinery enrichment is extremely low which means it’s possible that we only pull down the DNA region without the excision machinery. Although we have already confirmed the time point, we took is a good one on the DNA level, it's still possible

that 10 hours + 100% fragments is too late for IES elimination. In general, key players of IES elimination have relatively early expression profiles, like PGM, PTIWIs, DCLs, NOWAs, etc. are highly expressed from MEI to DEV1 which are all earlier than 10 hours + 100% fragments. In the meantime, M. Bétermier etc. has already reported that excision was shown to start 12 to 14 h after conjugation and was essentially completed at 16 h, while conjugation and autogamy share very similar cytological steps¹⁶. We did not compare the 16 hours after conjugation with 10 hours + 100% fragments experimentally, but according to our experiences, 16 hours after conjugation is much earlier than 10 hours + 100% fragments which means by that time, IES excision should have been finished and the excision machinery should not work anymore. The above possibilities remind us that other time points should be taken into consideration for enriching the excision machinery.

Table 1. List of unique peptides found in 377+, not 798- mass spectrometry.

	Synonyms	Description	iTop3 log2FC 377NC - 798NC
PTET.51.1.P0010534	TMP2d, TMP2D, TMP_T2d,	Coiled coil domain	2.534444058
PTET.51.1.P0030180		Ammonium transporter AmtB-like domain	3.166234709
PTET.51.1.P0040316		Coiled coil domain	3.517747077
PTET.51.1.P0060088	EPI31	Protein of unknown function DUF2816	5.789938319
PTET.51.1.P0070055		Coiled coil domain	4.692241051
PTET.51.1.P0070167		Ammonium transporter AmtB-like domain	3.11997365
PTET.51.1.P0090210	TMP21j, PTETG900001001	Coiled coil domain	5.785905363
PTET.51.1.P0110059		Coiled coil domain	5.277202169
PTET.51.1.P0110160		Ammonium transporter AmtB-like domain	3.155710977
PTET.51.1.P0110226	PTETG1100007001, SFA12d	Coiled coil domain	4.091869323
PTET.51.1.P0110247		Coiled coil domain	4.184921652
PTET.51.1.P0130214	EPI21	Protein of unknown function DUF2816	3.40344546
PTET.51.1.P0130289		Coiled coil domain	2.254467887
PTET.51.1.P0130338	EPI17	Protein of unknown function DUF2816	5.822698301
PTET.51.1.P0160035	EPI26	Protein of unknown function DUF2816	6.81661733
PTET.51.1.P0170089	EPI36, KdA2	Protein of unknown function DUF2816	5.370628316
PTET.51.1.P0170267	EPI45	Protein of unknown function DUF2816	5.733245774
PTET.51.1.P0180254			3.938814947
PTET.51.1.P0180262	TMP1f, T1f, TMP_T1f,	Coiled coil domain	4.015563305
PTET.51.1.P0190295	EPI16	Protein of unknown function DUF2816	2.254481094

PTET.51.1.P0200169	EPI19	Protein of unknown function DUF2816	2.106901089
PTET.51.1.P0210006		Coiled coil domain	3.343525572
PTET.51.1.P0230038			3.963123772
PTET.51.1.P0230185	TMP21c, PTETG2300009001	Coiled coil domain	3.503985457
PTET.51.1.P0260023		Coiled coil domain	3.296661406
PTET.51.1.P0260169	TMP21h, PTETG2600001001	Coiled coil domain	2.927813739
PTET.51.1.P0270102	EPI46, KdA10	Protein of unknown function DUF2816	8.374352378
PTET.51.1.P0310127		Histone-fold	1.129961656
PTET.51.1.P0330153	EPI13	Protein of unknown function DUF2816	6.145864103
PTET.51.1.P0350305	PTETG3500005001	Coiled coil domain	2.804309603
PTET.51.1.P0360200	TMP42f, PTETG3600005001	Coiled coil domain	2.748648714
PTET.51.1.P0380195		Glyceraldehyde/Erythrose phosphate dehydrogenase family	3.236344749
PTET.51.1.P0390135	TMP1i	Coiled coil domain	3.683297633
PTET.51.1.P0440082	TMP31e	Coiled coil domain	4.324150318
PTET.51.1.P0460182	TMP1d, T1d, TMP_T1d	Coiled coil domain	4.696906944
PTET.51.1.P0500133	EPI29	Protein of unknown function DUF2816	6.840888567
PTET.51.1.P0510026	PTETG5100005001	Coiled coil domain	1.542966515
PTET.51.1.P0520250	EPI34	Protein of unknown function DUF2816	6.095102095
PTET.51.1.P0540235		Coiled coil domain	3.349462273
PTET.51.1.P0580083		Fibrillarin	1.736609963
PTET.51.1.P0590095		Coiled coil domain	3.994218106
PTET.51.1.P0590139		Coiled coil domain	0.83176968
PTET.51.1.P0600043	EPI35	Protein of unknown function DUF2816	3.149456236
PTET.51.1.P0620035		Coiled coil domain	4.04062303
PTET.51.1.P0660064			1.115913082
PTET.51.1.P0660264		Coiled coil domain	4.393618351
PTET.51.1.P0710131	alphaPT4, tub_alphaPT4,	Tubulin	1.598686896
PTET.51.1.P0710219	EPI39	Protein of unknown function DUF2816	3.248001092
PTET.51.1.P0720201		Coiled coil domain	3.82938176
PTET.51.1.P0760096	EPI2	Protein of unknown function DUF2816	4.194158052
PTET.51.1.P0790177		Coiled coil domain	2.738097151
PTET.51.1.P0870174		Histone H2B	3.361690641
PTET.51.1.P0890143	EPI32	Protein of unknown function DUF2816	2.76999129
PTET.51.1.P0900049	EPI41	Protein of unknown function DUF2816	5.405962689
PTET.51.1.P0940194		Ammonium transporter	4.716764313
PTET.51.1.P0980135	T1-b, TMP1b	Coiled coil domain	2.802661429

PTET.51.1.P0980151	TMP42q, PTETG9800005001	Coiled coil domain	4.046552875
PTET.51.1.P0990148	EPI49	Protein of unknown function DUF2816	3.926971376
PTET.51.1.P1120164		Coiled coil domain	2.988272234
PTET.51.1.P1170022		Histone-fold	3.085289639
PTET.51.1.P1190042		Ammonium transporter AmtB-like domain	4.363070913
PTET.51.1.P1190122	EPI33	Protein of unknown function DUF2816	3.312833769
PTET.51.1.P1210094	TMP4b, T4c, TMP_T4c,	Coiled coil domain	3.043418246
PTET.51.1.P1210124	TMP32b	Coiled coil domain	2.059115894
PTET.51.1.P1370064	H3P3	Histone H3/CENP-A	2.870751576
PTET.51.1.P1370127	PtRPB1, RPB1	RNA polymerase Rpb1, domain 5	1.463019759
PTET.51.1.P1400098	EPI51	Protein of unknown function DUF2816	3.338539768
PTET.51.1.P1470130	TMP21e	Coiled coil domain	2.883304001
PTET.51.1.P1470169	PTETG14700002001	Coiled coil domain	3.910248714
PTET.51.1.P1500107	PTETG15000003001	Coiled coil domain	2.566474837
PTET.51.1.P1630088	beta-PT2, bPT2, SU3, tub_betaPT2	Tubulin	3.837856426
PTET.51.1.P1710041	EPI6	Protein of unknown function DUF2816	7.081169883
PTET.51.1.P1730070		EF-hand domain pair	6.162553257
PTET.51.1.P1770034			5.329433056
PTET.51.1.P5560009		Histone H2A	5.877785018

4.3.Part III: Expression of dominant negative form of PiggyMac in *Paramecium tetraurelia*

Nobody has succeeded in enriching PGM interacting proteins in *P. tetraurelia*. As mentioned above, the excision machinery potentially works in a ‘cut and go’ way in *P. tetraurelia* which indicates the interaction between excision machinery and the IES regions is transient. Our previous method does not have the potential to capture such short-time interaction. Hence, we conducted an expression of dominant negative PGM¹⁰⁷ (PGM 3A) tagged with Flag-HA in *P. tetraurelia* and performed Co-immunoprecipitation at the late time point. Since the three conserved aspartic acids are supposed to constitute a functional catalytic triad²⁰, the PGM 3A harbours D to A substitution at these positions has a dominant-negative effect in *P. tetraurelia*. Using this mutant, we assumed that the presumed ‘cut and go’ way would be switched to ‘bind but stay’, which gives us a great chance to purify the PGM interacting proteins without considering the transient binding. By this method, we were trying to answer the question that why this purification is still not reported and it should fill the gap if we could succeed.

First of all, the PGM coding gene was amplified from the genomic DNA and inserted into the pGEM-T easy vector by TA cloning. After that, the Flag-HA-coding fragment which recoded according to the codon preference of *Paramecium* was inserted before the stop codon of the PGM 3A gene. In this construct, the PGM 3A-Flag-HA coding sequence joints upstream and downstream non-coding sequences for its expression and regulation. Then, the positive plasmid was extracted and linearized by Ahd I (New England Biolabs). The purified fragment was microinjected into the vegetative MAC and positive injection strains were confirmed by doing Dot Blot. The last step is enrichment. Different time points were taken for detecting the HA signal by western blot as shown in Figure 17. In the meantime, we performed IES PCR and survival test to check the influence of PGM 3A mutation on the IES elimination and survival of its progeny. From Figure 18 A and B, we can tell all chosen IESs’ excision were inhibited which is consistent with the dominant-negative effect on sexual progeny survival. It supports the idea that dominant-negative protein not only coexists with endogenous protein but also exhibits an impaired function out of the normal one.

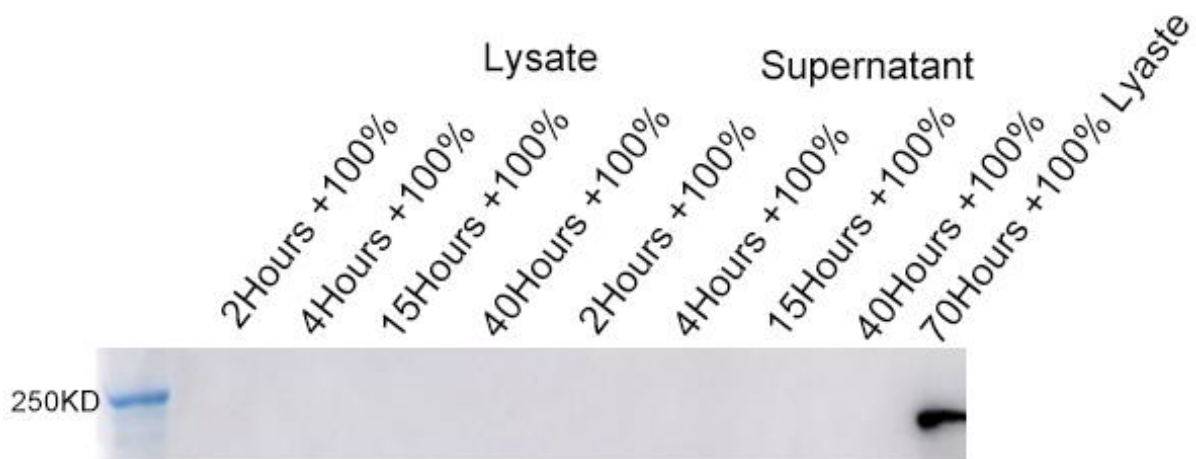


Figure 17. Western blot analysis with the anti-HA antibody of PGM-3A-Flag-HA injected cells from different time points. Transformed cells were cultured to corresponding time points, and cell lysate and supernatant were taken equally to prepare the samples for western blot. At the 70hours + 100% fragments, only cell lysate was taken.

There are several points that should be looked at carefully. We tried a lot of different conditions before the band observed on the membrane although it is a bit too late for IES excision. Therefore, we concluded some hints for future study. The first one we want to emphasize is the pre-treatment with 5% SDS under 100 °C for 3 min before boiled with 5X SDS loading buffer as previously described¹⁰⁹. Western blot never returns a positive band in PGM 3A-Flag-HA without this pre-treatment. An additional 5% SDS (final concentration) supply reminds us the possibility of why there is no report regarding the *in vivo* purification using PGM as bait. It looks like the PGM is not disrupted even boiled with 2% SDS at 95 °C. We assumed that the HA tag may be folded inside of the PGM structure which makes the Anti-HA primary antibody fail on binding. If our assumption was true, then the Co-IP using Anti-HA beads would not enrich the PGM 3A-Flag-HA from the lysate either. To test this possibility, we introduced a codon optimized GFP sequence between PGM and Flag-HA in the pGEM-T easy vector. This insertion could in theory increase the spatial distance between PGM and Flag-HA after being expressed in *P. tetraurelia* MAC, which could make the HA tag detectable. Another benefit of introducing GFP is the determination of timing and localization¹⁰⁷ of PGM 3A in the development of *P. tetraurelia*. In Figure 19, PGM 3A-GFP-Flag-HA displayed a homogeneous pattern without significant foci suggesting that PGM foci

are associated with its normal function, especially with IES elimination as shown in Figure 18 A and B.

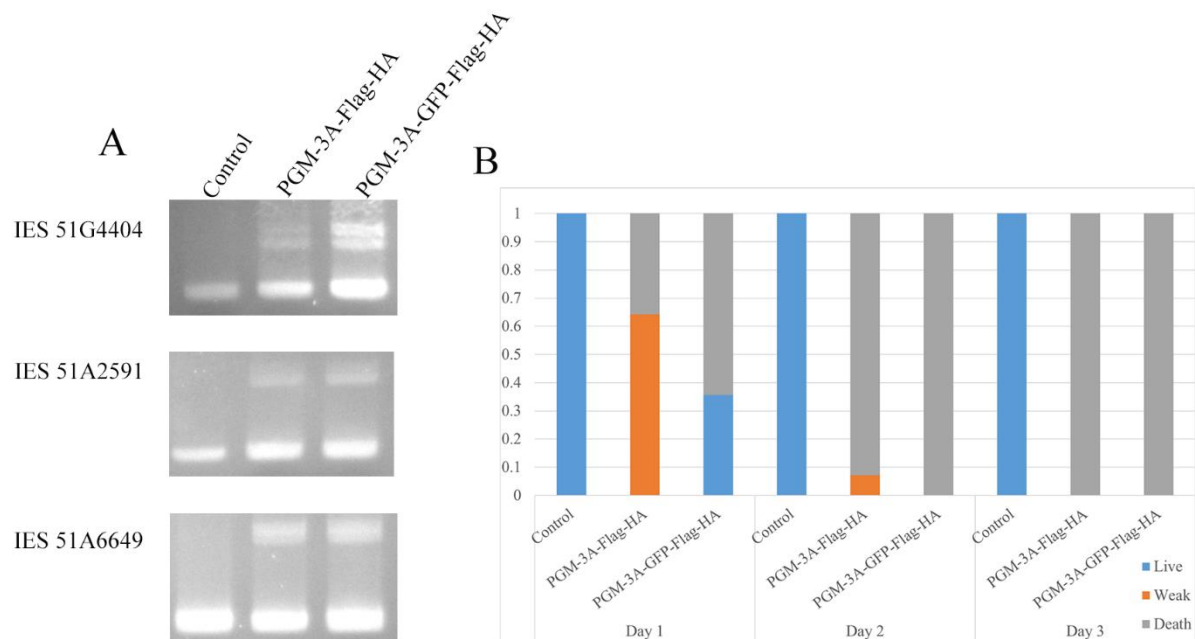


Figure 18. Effect of PGM-3A-Flag-HA and PGM-3A-GFP-Flag-HA injection on IES excision and progeny survival.

A) The IES retention PCR results. Genomic DNA was extracted from vegetative cells, PGM-3A-Flag-HA and PGM-3A-GFP-Flag-HA injected cells at the post autogamy stage. The retention was indicated by upper bands. B) The survival test. A total of 14 cells were taken from each group. Y axis presents the percentage of live, weak or death cells. X axis presents each group in 3 days.

The second one is the time point. According to the expression pattern of PGM in *P. tetraurelia*, there should be a large amount of PGM expressed in each time point we took for the western blot and Co-IP. According to the results, the PGM 3A-Flag-HA signal can only be seen at a postautogamous time point (around 70 hours + 100% fragments). As we mentioned above, 10 hours +100% fragmentation is too late to purify the excision machinery, the signal we got at such a late time point (70 hours +100% fragmentation) could just be because of the accumulation same as the previous report¹⁰⁷. This accumulation could be useless because of the possibility that interacting proteins disassembled either excision happened or not.

PGM-3A-GFP-Flag-HA Late

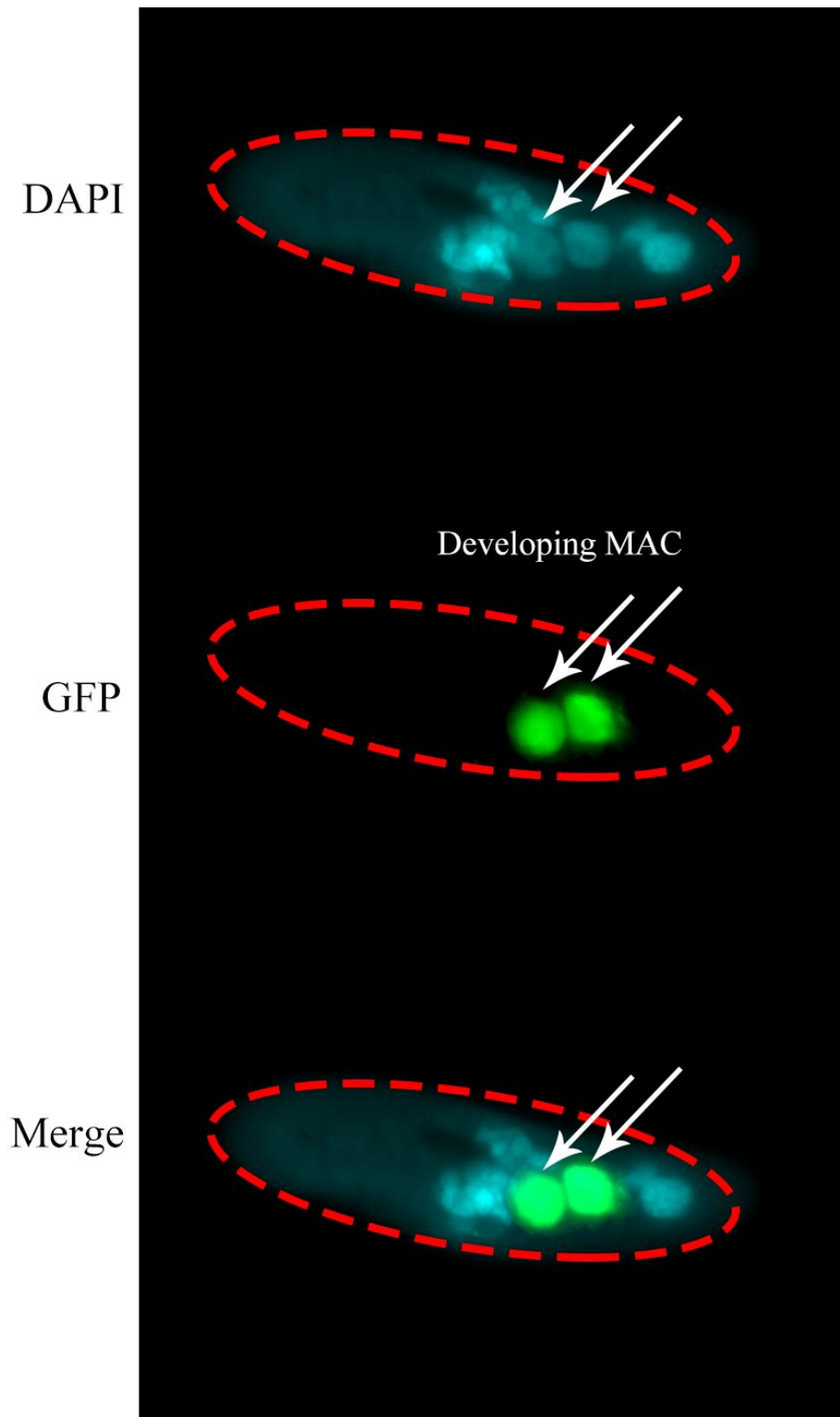


Figure 19. PGM-3A-GFP-Flag-HA localization in *Paramecium tetraurelia*. Localization of PGM-3A-GFP-Flag-HA in the developing MAC. The top panel indicates DAPI staining in blue, which

indicates DNA. The panel in middle shows the GFP signal in green. The panel at the bottom represents a merge of GFP and DAPI. White arrows point new developing MACs.

Another hint is about the transferring condition. Although we did not test other transferring conditions on 70 hours +100% fragments sample, we do try different transferring time on other time points and none of them succeeded in imaging the HA signal if we ignored the time point issue. So, the only condition that returns a clear HA signal on the membrane after western blot is 4 hours of transferring under constant 110V on ice. Be careful, with long time transferring, keeping the solution at a low temperature is crucial.

5. Conclusions and perspective

Paramecium tetraurelia is characterized by the co-existence of two types of nuclei in one cytoplasm: a diploid micronucleus (MIC) and a highly polyploid macronucleus (MAC). The development of the MAC raising from the MIC and the genome rearrangement in this progress is an excellent model to understand the mechanism behind DNA elimination and recombination in other organisms. The mechanism of genome rearrangement in *P. tetraurelia* has been thoroughly investigated in recent years, and numerous novel components involved in IES elimination have been found. With processing IESs, new developing MAC generated from MIC go through several rounds of meiosis and mitosis where condensin is supposed to be essential to the faithful genome structure and separation. However, whether condensin participated in IES elimination or not is still unclear.

In all species, structural maintenance of chromosomes (SMCs) proteins are essential for effective chromosomal transmission during replication and genomic segregation. Condensin core subunits (SMCs) are conserved across all eukaryotic species investigated so far. In addition to the SMC subunits, condensin also contains a distinct set of non-SMC subunits. Although SMCs in ciliates are close relatives to those in other organisms, little is known of their detailed functions in *P. tetraurelia*. Furthermore, the investigation of *P. tetraurelia* SMCs may reveal a new aspect of the function of SMCs. To explore whether condensin participated in IES processing, we focused on the behaviour of SMC subunits of condensin in IES elimination. In this study, we identified one of two SMC4s in *P. tetraurelia*, SMC4-2, is necessary for proper genome rearrangement and progeny survival. The specific localization of SMC4-2 in new developing MAC provides the spatial possibility for participating in IESs elimination. The results from IES PCR, genome sequencing and survival test confirm that SMC4-2 is needed in the processing of IESs in the development of *P. tetraurelia* in some unknown mechanism. One potential explanation for this finding is that SMC4-2 can manipulate the production of iesRNAs, one group of small RNAs which are crucial to the positive feedback of IES elimination in scanning model, according to the small RNAs sequencing analysis. Distinct from the performance of SMC4-2 in *P. tetraurelia*, SMC4-1 expresses and behaves in a relatively early stage which seems like be able to get the genome ready for producing scnRNAs. This hypothesis comes from the localization of SMC4-1 in all

stage of nuclei except the MAC that is going to be fragments. Interestingly, although no IES retention phenotype has been found in the RNAi of SMC2-1, SMC2-2 and SMC4-1, co-silencing of these genes with SMC4-2 separately abolished the IES retention phenotype in single silencing of SMC4-2. These phenotypes remind us that SMC2s and SMC4-1 could participate in SMC4-2 processing IES elimination in unknown mechanisms. By performing *in vivo* Co-immunoprecipitation and mass spectrometry analysis, we found that the interactions between SMC4-1 and SMC4-2 changed accordingly. Using SMC4-1 as bait, SMC4-2 can be enriched as an interacting protein of SMC4-1, while SMC4-1 cannot be detected using SMC4-2 as bait *in vivo*. We proposed a competitive model in that the competitive binding of DNA by SMC4-1 and SMC4-2 changes according to the ratio of concentration between them. This competition blocks or unlocks the IES accessibility to the excision machinery. Due to time constraints, we did not do further research to test the model. Therefore, this hypothesis has to be looked at carefully.

Programmed DNA elimination is a significant developmental genome modification in which certain DNA sequences, up to 90% of the genome in some cases, are removed from somatic lineages. Programmed DNA elimination in animals has sparked a lot of discussion curiosity and speculation since its discovery in 1887. The single-cell ciliates including *P. tetraurelia* are the best-studied instances of programmed DNA elimination in eukaryotes. While the mechanism behind this massive genome rearrangement remains poorly understood. Although a scanning model has been widely accepted to explain how two sets of small RNAs guide the IES excisions, the real players (also refer to as an excision machinery) of IES elimination are still unclear. In this part of my study, we developed an improved method to purify the excision machinery by affinity capture and mass spectrometry. The main idea of this attempt is to capture potential DNA excision machinery binding on the IES region by oligos complementary to the IES. By using bioinformatic analysis, we picked up several candidates for both target region and negative control as well as confirmed the existence time of these regions. With the Biotin labelled oligos complementary to the target region or negative control, we successfully developed, optimized and practiced this 3-IESs capturing method on *P. tetraurelia*. We were able to collect enriched interacting data from specific DNA regions at a specific time point during genome rearrangement. However, no key players of this progress like PGM, PTIWI, NOWA, or even the SMC4-2 we identified above, have been found in the results. Although the target region and control DNA regions have been confirmed in both

input and output, the MS results still need to be looked at carefully. We provided several possibilities for these scenarios: I) the timing of IES elimination could be earlier than the time point we chose for the capturing. It has been reported before that IES excision was shown to start 12 to 14 h after conjugation and was essentially completed at 16 h which means the time point (10 hours + 100% fragments) we took could be too late to capture the DNA excision machinery since the IES excision has been done. II) it also could be because the excision machinery behaves in a ‘cut and go’ way, which means its binding on DNA is transient and the time window for capturing the excision machinery-DNA complex is too narrow.

The PGM is a crucial candidate in IES excision which has high homology with PiggyBac transposase. It should be a good candidate to study the mechanism behind IES excision in *P. tetraurelia*. By introducing Flag-HA tagged PGM with three mutants on its conserved aspartic acids, we try to do the *in vivo* co-immunoprecipitation to enrich the PGM complex during the development of *P. tetraurelia*. By introducing these mutants, those PGMs were supposed to be not able to cut the IES regions, hence the DNA excision machinery where PGM should be involved would not dissociate from the IES region. We assume it would provide a good chance to enrich the DNA excision machinery by the IES-specific pull down method we developed. Although we failed on detecting any HA signal from PGM-3A on anti-HA beads enrichment, we do provide some hints for further study. At least to PGM, *P. tetraurelia* can exhibit the impaired PGM effect even the endogenous PGM is there, which makes further functional research easier. Because researchers do not need to knock down or knock out the endogenous proteins before introducing the manipulated one.

6. Methods and Materials

6.1. *Paramecium* strain and cultivation

The strain 51, mating type 7 of *Paramecium tetraurelia*, was used. Cultivation and autogamy were performed at 27 °C as described⁴.

6.2. Ethanol fixation and staining for *Paramecium*

Collect and wash samples at specific time point as previously described, add 5 mL ice-cold 70 % ethanol to the cell pellet for fixation. Transfer all into a 15 ml tube. Store at 4 °C until further implementation.

Transfer 150 µL fixed cell on glass slide, air dry it at RT.

Wash with PBS pH 7.4 3 times in a chamber.

Air dry the slide.

Add one drop staining solution and cover with cover glass, keep in the dark.

6.3. Cloning

All gene fragments were amplified using primers listed and Phusion[®] High-Fidelity DNA Polymerase or Q5[®] High-Fidelity DNA Polymerase and cloned into pGEM T easy vector or L4440 vector.

PCR products purification was performed always.

Gibson assembly

	Volume
Vector	50-100 ng
Insert	5-fold molar excess of vector*
GA mix	5 μ L
H ₂ O	To 10 μ L

*: calculate with NEBioCalculator (<https://nebiocalculator.neb.com/#!/ligation>)

50 °C 30 min

65 °C 20 min

Immediately use or keep at 4 °C for short time.

Dialysis the ligation product for 20-40 min.

Mix with 50 μ L competent cell (10 μ L cell mix with 190 μ L ddH₂O), incubate on ice for 30 min.

Electroporation and resuspend in 500 μ L TB, shaking at 37 °C before plating on selective medium.

6.4.Silencing specific gene by dsRNAs feeding

Protocol adapted from^{4,149}.

Bacterial pre-culture: Incubate *E.coli* feeding bacteria (strain HT115) accommodating related DNA sequence in 5 mL LB selecting medium with 0.1 mg/mL ampicillin and 0.0125 mg/mL tetracycline O/N shaking at 37 °C.

Dilute the pre-culture ~1:100 in WGP (900ul pre-culture in 90ml WGP) containing 0.1mg/ml ampicillin and incubate O/N shaking at 37 °C until the OD₆₀₀ > 0.16.

Dilute the culture to OD₆₀₀= 0.04 with WGP containing 0.1mg/ml ampicillin to 200ml, shaking at 37 °C until OD₆₀₀> 0.07 (around 80min).

Add IPTG to a final concentration of 0.4 mM, incubate at least 4 hours or O/N shaking at 37 °C

Cooling the medium to 27 °C by water bath and supply 0.8 mg/l of β -sitosterol.

Add mature *P. tetraurelia* cells to the culture at a concentration of 200 cells/mL.

Keep the culture at 27 °C until specific time point.

6.5.Survival test

Prepare depression slides with 600 µL 0.2× WGP containing 0.8 mg/l β-sitosterol in each compartment.

Pick single cell into each compartment under microscope.

Monitor the growth of the cells with marked as healthy (normal dividing), weak (dividing slowly or not dividing) or dead for at least 3 days (27 °C).

6.6.Genomic DNA extraction of *P. tetraurelia* cells

100 mL of post-autogamous or vegetative cells was collected and washed as previously described. Genomic DNA was extracted using the GenElute Mammalian Genomic DNA MiniPrep Kit (Sigma).

6.7.IES retention PCR

Chosen IESs were checked for retention on knockdown of specific genes. GoTaq G2 DNA polymerase (Promega) and standard primers (primers list) were used. A total 12.5 ng of genomic DNA serve as input of each PCR.

6.8. Microinjection linearized DNA fragments into the Macronucleus

Protocol adapted from⁴.

DNA preparation:

Plasmid DNA from 100 mL culture was extracted using the QIAGEN Plasmid Plus Midi kit.

Linearize 100 µg of plasmid by AhdI or SapI.

Equal volume of Phenol : chloroform was added into the digestion product.

Vortex for 50sec, spin down at max. speed for 5min at 4 °C, DNA will be separated into the upper layer.

Carefully transfer only upper layer into the Ultra-free-MC-GV centrifugal filters (Millipore) and spin down at max. speed for 4 min.

Add 1/10 volume of 3 M NaOAc (pH 5.2) and 2.5 volume of ice-cold pure ethanol, flick to mix, incubate for at least 2 hours to O/N at -20 °C.

Centrifuge at max. speed for 10 min at 4 °C and wash DNA pellet with 1 mL ice-cold 75% ethanol.

Centrifuge at max. speed for 5min at 4 °C once more, discard ethanol as much as possible.

Cover the tube with tinfoil and air dry the pellet at 37 °C.

Resuspend in 5 µL nuclease free water, measure the concentration and adjust it to 5.5 µg/µL

Cells preparation

Young cells (6-8 generations) recovered from post autogamous wildtype cells were transferred into slides containing 600 µL 2mg/mL Volvic-BSA solution.

Washing cells by transferring them to another slide containing Volvic-BSA solution.

Make of Volvic-BSA droplets in immersion oil and pick one cell into each droplet under microscope.

Injection:

Remove the Volvic-BSA solution to immobilize the cell in the droplet.

Inject prepared DNA with injection needle into the MAC and add the Volvic-BSA solution back to the droplet.

Transfer all cells into 600 μL 0.2 \times WGP media to wash the DNA outside of the cells.

Transfer the injected cells back into slides containing 0.2 \times WGP media separately and culture at 27°C.

6.9. Dot Blot

For the positive control, add 10pg, 50pg, 100pg of injected plasmid into 400 μ L ddH₂O in 1.5 mL tubes.

Transfer 400 μ L of injected culture (cell density \sim 1,000 cells/mL) into 1.5mL Eppendorf tube.

Add 50 μ L of 0.5 M EDTA (pH 8) and 50 μ L of 4 M NaOH to samples including control.

Cells can be stored at -80 °C after EDTA adding, in that case, mix NaOH before using.

Incubate all samples at 68 °C for 30min.

In this 30min, prepare the Dot Blot equipment, whatman paper and Hybond-XL membrane (GE Healthcare Life Science). Add 20 mL Church buffer into the incubating bottle.

Briefly soaking membrane and paper in 0.4M NaOH before using, set the equipment.

Spin down all samples at max. speed for 1 min, chill them on ice.

Run all samples through the membrane by vacuum.

Incubate the membrane in 0.4 M NaOH on shaker for 15 min.

Wash the membrane with 2 \times SSC buffer for 15 min by shaking.

Dry the membrane with whatman paper, put it into the bottle containing Church buffer, incubate at 60 °C for 2 hours.

Heat the radioactive probe at 100 °C for 10 min.

Discard the Church buffer and incubate the membrane with radioactive probe at 55 °C for O/N.

The radioactive probe can be re-used, wash the membrane twice with 2 \times SSC containing 0.1% SDS at 55 °C for 10-15 min.

Dry the membrane carefully, wrap in saran foil.

Expose the membrane on the IP screen for more than 2 hours.

Labeling radioactive probes by Klenow enzyme

Order [α -P³²] ATP, 2 Mbq = 5 μ L.

DNA preparation:

DNA fragments used for labelling with GoTag G2 DNA Polymerase (Promega) were amplified by PCR.

Purify the PCR products, dilute to 25 ng/ μ L.

Mix 25 ng DNA with 20 μ L ddH₂O, denature by boiling for 5 min.

Put samples on ice immediately.

Add: 1 μ L 500 μ M TTP

1 μ L 500 μ M CTP

1 μ L 500 μ M GTP

20 μ L 2.5X RadPrime buffer

Add 5 μ L (~2 MBq [α -P³²] ATP) and 1 μ L Klenow enzyme in C-lab.

Mix carefully and quick spin down 15-30 sec.

Incubate at 37 °C for 10 min.

Add 5 μ L Stop buffer to stop the reaction.

Add 10 mL Church buffer and store at -20 °C.

6.10. Macronuclear DNA isolation

Protocol adapted from²¹.

Day 1

Pre-cool the centrifuge, put all buffers on ice.

Collect and wash the cell as previously described.

Resuspend the pellet in 2.5 volumes of lysis buffer 1, transfer into pre-cold homogenizer on ice. Incubate 5 min.

Lyse mixture on ice by homogenizing. Check with DAPI frequently (10 μ L cells + 1 μ L DAPI). Stop cracking until only intact MACs are visible by DAPI staining.

Transfer all to a 15 mL tube. Mix with 14 mL of pre-cold wash buffer by inverting.

Spin down at 4 °C, 1000RCF for 3 min, discard supernatant.

Resuspend the pellet with 2 mL wash buffer using cut-tip pipette, repeat the wash step above.

Resuspend the pellet in 3 volumes of pre-cold sucrose buffer. The volume should not over 2mL. Avoid DNA shearing.

Transfer 3 mL sucrose buffer to ultracentrifugation tube. Add the lysate on top of sucrose buffer. Add wash buffer on the top of lysate.

Centrifuge for 1 hour at 4 °C, 35,000 RPM, rotor: SW40Ti.

Discard supernatant thoroughly.

Resuspend the MAC pellet in 500 μ L of 10 mM Tris pH 7.4, 10 mM MgCl₂.

Transfer all into a 15 mL tube, mix with 3 volumes of lysis Buffer 2.

Incubate O/N at 55°C.

Day 2:

Phenol extraction: add 1 volume phenol : chloroform : IAA (25:24:1) to the sample.

Shake the sample a few times and spin down at max. speed for 10 min at 4 °C.

Pre-soak the Slide-a-Lyzer Dialysis cassette in ice-cold dialysis buffer (10 mM Tris-HCl pH 8, 1 mM EDTA pH 8).

Transfer aqueous products into the cassette with a syringe through the cap.

Remove the excess air after loading the sample by pressing the membrane.

Dialysis at 4 °C in a large beaker by slowly rotating using a magnetic stirrer.

Replace buffer after 2 and 4 hours, then incubate O/N.

Day 3:

Recover the DNA from the cassette with a syringe.

Concentrate the DNA using the Amicon Ultra 2 mL filters.

Fill the device with sample and centrifuge at 4,000 RPM for 10 min.

Invert the device, centrifuge at 1,000 RPM for 2 min to harvest concentrated DNA.

Measure DNA concentration. Load 1 µg on gel to check the DNA integrity.

Buffers

Lysis buffer 1	Amount	Final concentration
H ₂ O	4.915 mL	
Sucrose	0.43 g	0.25 M
2 M MgCl ₂	25 µL	10 mM
1 M Tris pH 6.8	50 µL	10 mM
NP-40	10 µL	0.2%

Wash buffer	Amount	Final concentration
H ₂ O	59.1 mL	
Sucrose	5.16 g	0.25 M
2 M MgCl ₂	300 µL	10 mM
1 M Tris pH 7.4	600 µL	10 mM

Sucrose buffer	Amount	Final concentration
H ₂ O	9.85 mL	
Sucrose	7.18 g	2.1 M
2 M MgCl ₂	50 μL	10 mM
1 M Tris pH 7.4	100 μL	10 mM

Lysis buffer 2	Amount	Final concentration
0.5 M EDTA	4.25 mL	~0.5 M
10% SDS	500 μL	1%
N-lauryl sarcosine	0.05 g	1%
20 mg/mL proteinase K	250 μL	1 mg/mL

Dialysis buffer	Amount	Final concentration
1 M Tris pH 8	10 mL	10 mM
0.5 M EDTA	2 mL	1 mM
H ₂ O	To 1 L	

6.11. Total RNA extraction with TRI

Frozen collected cell pellet in liquid nitrogen immediately by drops and stored at -80 °C.

Add 6 mL of TRI to the frozen pellet on dry ice.

Vortex the pellet until completely dissolved one by one.

Incubate 5min at RT on rotator.

Add 1.2 mL chloroform and vortex for 15 sec.

Stand 5 min at RT.

Centrifuge at max. speed for 15 min at 4 °C.

Carefully transfer the top phase into a 15 mL falcon tube, make aliquots of 750 µL in RNase free Eppendorf tubes.

Add 500 µL isopropanol to each aliquot, mix by inverting and stand at RT for 10 min.

Centrifuge at 12,000 RCF, 4 °C for 10 min to pellet the RNA.

Remove the supernatant, resuspend with 1 mL 75% ethanol.

Centrifuge at 7,500 RCF, 4 °C for 5 min.

Repeat wash with another 1 mL 75% ethanol and centrifuge.

Remove supernatant thoroughly.

Air dry the RNA pellet at 37 °C covered with a tinfoil tent.

Add 30 µL nuclease free ddH₂O into the RNA pellet, incubate at 60 °C for 15 min to dissolve RNA.

6.12. Analysis of sRNA in denaturing gel

Gel preparation

Add 5 mL of autoclaved water into an autoclaved 100 ml screw cap bottle (Type A is best for stirring)

Add 16 ml Acrylamide (30% Acrylamide/ Bis Solution 19:1) with sterile pipette

Add 12.6 g Urea (pellet not powder)

Add 3 mL 10× TBE

Dissolve it with a magnetic stir bar (approx. 1 h)

16% polyacrylamide-7M Urea gel

30% Acrylamide/ Bis Solution 19:1	16 mL
Urea-7M (60.1 g/ mol)	12.6 g
10× TBE	3 ml
ddH ₂ O autoclaved	Up to 30 mL

Chamber preparation

Wash entire equipment with hot water, ddH₂O and 100% ethanol carefully.

Air dry all parts before assemble the system.

Pour the gel

Pass gel solution through a 0.22 µm filter into a autoclaved 100 ml screw cap bottle with a 50 mL syringe.

Chill on ice over 5 min.

Add 150 µL 10% APS and 30 µL TEMED, mix gently.

Chill on ice over 5 min.

Pour the gel with 50 mL syringe, avoid bubbles, insert the comb in immediately.

Let the gel polymerize for 1-2 hours.

RNA 5' end labelling

Master mix	1 reaction
10× Buffer B (exchange buffer)	0.6 µL
PEG 6000 (24%)	1.2 µL
RNase inhibitor	0.6 µL
γ-P ³² -ATP (0.4 Mbq, add in C-lab)	1 µL
PNK	0.6 µL

Add 4 µL of master mix to each 2 µL RNA sample in C-lab.

Incubate at 37 °C for 30 min.

Mix 12 µL RNA loading dye (100 µL 6× DNA loading dye + 900 µL formamide) with each sample.

Heat samples to 80 °C for 10 min, put on ice afterwards.

Add 0.5× TBE buffer to the assembled chamber.

Remove combs and clean slots with 0.5× TBE buffer (use syringe).

Pre-run for more than 30 min at 25 mA (fix).

Wash slots again before loading.

Load the samples and ladder, better separate samples by loading dye. Fill empty slots with loading dye.

Run the gel at 25 mA (fix) until the blue is at half of the gel (30-40 min).

Disassemble the frame and cover the gel (still attached to one of the plates) with saran foil.

Put phosphor screen on top and expose for 1-2 hours or O/N.

6.13. Co-immunoprecipitation

Adapted from¹⁵⁰.

Collect and wash the cells as previously described. Transfer the cell pellet (~0.5 mL) into 15 mL Falcon tubes.

Non-crosslinking: go the wash step or put samples at 4 °C before washing.

Cross linking:

Add 1 mL of 1% PFA and shake for 10 minutes at RT.

Add 100 µL of 1.25 M Glycine, incubate for 5 min to quench on shaker at RT.

Wash samples twice with PBS (pH 7) at 279 RCF, 4 °C for 2 min.

Gently resuspend with a few mL of PBS, then fill it up and invert the tube to mix.

Discard supernatant. Add 2 mL of ice-cold lysis buffer to the pellet and resuspend thoroughly.

Sonicate with 30 % amplitude, 10 sec on, 1min rest, 15 cycles.

Stain 10 µL product with DAPI, check under microscope to make sure the sonication is efficient.

Transfer the sample to 2 ml tubes and centrifuge at 13, 000 RCF, 4 °C for 30 min.

Transfer the supernatant to two new RNase free 1.5 ml Eppendorf tubes (1 ml to each).

Freeze all components in liquid nitrogen, store at -80 °C. Keep one tube on ice when perform further enrichment immediately.

Transfer 50 µL beads mixture of each IP sample into nuclease free tubes.

Add 1 mL IP buffer to the beads, mix gently by inverting.

Centrifuge at 500 RCF, 4 °C for 2 min.

Remove supernatant gently. Repeat wash twice.

Add 1 mL of the lysate to cleaned beads, incubate at 4 °C O/N on rotating.

Centrifuge at 500 RCF, 4 °C for 2 min.

Transfer the supernatant as unbound in a nuclease free tube on ice for further analysis.

Mix gently with 1 ml of IP buffer by inverting, do not pipetting.

Repeat this wash for another 4 times.

Resuspend beads gently in 1 mL of ice-cold IP buffer, transfer all to another nuclease free tube.

Centrifuge at 500 RCF, 4 °C for 2 min, discard supernatant (leave about 50 µl).

For PGM included samples, first add equal volume of 10% SDS and boil at 100 °C for 3 min. Add 12.5 µL 5× loading dye and boil at 95 °C for 10-20 min. store at -20 °C.

Buffers

Lysis buffer	10 mL	Final concentration
1 M Tris HCl pH 8.8 (<i>modify accordingly</i>)	500 µL	50 mM
2 M NaCl	750 µL	150 mM
2 M MgCl ₂	25 µL	5 mM
100% Triton X-100	100 µL	1%
50× protease inhibitor (<i>EDTA free</i>)	200 µL	1×
80% Glycerol	1.25 mL	10%
DTT	10 µL	1 mM
Milli-Q water	7.165 mL	

IP buffer (W/O NP-40)	200 mL	Final concentration
1 M Tris HCl pH 8.8 (<i>modify accordingly</i>)	2 mL	10 mM
2 M NaCl	15 mL	150 mM
2 M MgCl ₂	100 µL	1 mM
80% Glycerol	12.5 mL	5%
Milli-Q water	170.4 mL	

Store at RT.

Add 1 μ L NP-40 to 10 mL IP buffer to make the complete IP buffer before usage.

6.14. SDS-PAGE

Gel preparation:

Clean glass plates with hot water and pure ethanol, air dry on tissue paper.

Prepare the gel according to the Protocol (Modified from Harlow and Lane 1988).

TABLE A8-9 Solutions for Preparing Resolving Gels for Tris-glycine SDS-Polyacrylamide Gel Electrophoresis

↓ COMPONENTS / GEL VOLUME ⇒	VOLUME (ml) OF COMPONENTS REQUIRED TO CAST GELS OF INDICATED VOLUMES AND CONCENTRATIONS								
	5 ml	10 ml	15 ml	20 ml	25 ml	30 ml	40 ml	50 ml	
6% gel									
H ₂ O	2.6	5.3	7.9	10.6	13.2	15.9	21.2	26.5	
30% acrylamide mix <!>	1.0	2.0	3.0	4.0	5.0	6.0	8.0	10.0	
1.5 M Tris (pH 8.8)	1.3	2.5	3.8	5.0	6.3	7.5	10.0	12.5	
10% SDS	0.05	0.1	0.15	0.2	0.25	0.3	0.4	0.5	
10% ammonium persulfate <!>	0.05	0.1	0.15	0.2	0.25	0.3	0.4	0.5	
TEMED <!>	0.004	0.008	0.012	0.016	0.02	0.024	0.032	0.04	
8% gel									
H ₂ O	2.3	4.6	6.9	9.3	11.5	13.9	18.5	23.2	
30% acrylamide mix <!>	1.3	2.7	4.0	5.3	6.7	8.0	10.7	13.3	
1.5 M Tris (pH 8.8)	1.3	2.5	3.8	5.0	6.3	7.5	10.0	12.5	
10% SDS	0.05	0.1	0.15	0.2	0.25	0.3	0.4	0.5	
10% ammonium persulfate <!>	0.05	0.1	0.15	0.2	0.25	0.3	0.4	0.5	
TEMED <!>	0.003	0.006	0.009	0.012	0.015	0.018	0.024	0.03	
10% gel									
H ₂ O	1.9	4.0	5.9	7.9	9.9	11.9	15.9	19.8	
30% acrylamide mix <!>	1.7	3.3	5.0	6.7	8.3	10.0	13.3	16.7	
1.5 M Tris (pH 8.8)	1.3	2.5	3.8	5.0	6.3	7.5	10.0	12.5	
10% SDS	0.05	0.1	0.15	0.2	0.25	0.3	0.4	0.5	
10% ammonium persulfate <!>	0.05	0.1	0.15	0.2	0.25	0.3	0.4	0.5	
TEMED <!>	0.002	0.004	0.006	0.008	0.01	0.012	0.016	0.02	
12% gel									
H ₂ O	1.6	3.3	4.9	6.6	8.2	9.9	13.2	16.5	
30% acrylamide mix <!>	2.0	4.0	6.0	8.0	10.0	12.0	16.0	20.0	
1.5 M Tris (pH 8.8)	1.3	2.5	3.8	5.0	6.3	7.5	10.0	12.5	
10% SDS	0.05	0.1	0.15	0.2	0.25	0.3	0.4	0.5	
10% ammonium persulfate <!>	0.05	0.1	0.15	0.2	0.25	0.3	0.4	0.5	
TEMED <!>	0.002	0.004	0.006	0.008	0.01	0.012	0.016	0.02	
15% gel									
H ₂ O	1.1	2.3	3.4	4.6	5.7	6.9	9.2	11.5	
30% acrylamide mix <!>	2.5	5.0	7.5	10.0	12.5	15.0	20.0	25.0	
1.5 M Tris (pH 8.8)	1.3	2.5	3.8	5.0	6.3	7.5	10.0	12.5	
10% SDS	0.05	0.1	0.15	0.2	0.25	0.3	0.4	0.5	
10% ammonium persulfate <!>	0.05	0.1	0.15	0.2	0.25	0.3	0.4	0.5	
TEMED <!>	0.002	0.004	0.006	0.008	0.01	0.012	0.016	0.02	

Modified from Harlow and Lane (1988).

TABLE A8-10 Solutions for Preparing 5% Stacking Gels for Tris-glycine SDS-polyacrylamide Gel Electrophoresis

↓ COMPONENTS / GEL VOLUME ⇒	VOLUME (ml) OF COMPONENTS REQUIRED TO CAST GELS OF INDICATED VOLUMES								
	1 ml	2 ml	3 ml	4 ml	5 ml	6 ml	8 ml	10 ml	
H ₂ O	0.68	1.4	2.1	2.7	3.4	4.1	5.5	6.8	
30% acrylamide mix <!>	0.17	0.33	0.5	0.67	0.83	1.0	1.3	1.7	
1.0 M Tris (pH 6.8)	0.13	0.25	0.38	0.5	0.63	0.75	1.0	1.25	
10% SDS	0.01	0.02	0.03	0.04	0.05	0.06	0.08	0.1	
10% ammonium persulfate <!>	0.01	0.02	0.03	0.04	0.05	0.06	0.08	0.1	
TEMED <!>	0.001	0.002	0.003	0.004	0.005	0.006	0.008	0.01	

Modified from Harlow and Lane (1988).

Gel running:

Run at 80 V (~30 min), switch the voltage to 110V as soon as the dye reaches the resolving gel.

Buffers

10× SDS running buffer	1 L	Final concentration
Tris Base	30.2 g	0.25M
Glycine	144 g	1.92 M
SDS	10 g	1%
ddH ₂ O	To 1 L	

Dilute 1:10 before usage.

5× SDS loading buffer	10 mL
10% SDS	2 mL
0.5 M Tris-HCl pH 6.8	1.2 mL
50% Glycerol	4.8 mL
Bromphenol blue	Tiny
β-Mecaptoethanol	500 μL
ddH ₂ O	To 10 mL

Aliquot to 1 mL/tube, store at -20 °C.

6.15. Silver staining

Fix the gel from SDS-PAGE in 100 mL Fixative solution at RT O/N.

Wash with 50% ethanol 20 min twice.

Treat the gel for exactly 1 min with 98 mL Sodium Thiosulphate (3-4 flakes in 100 mL Milli-Q water).

Wash with ddH₂O 20 sec for 3 times.

Treat the gel with AgNO₃ solution for 30 min. (AgNO₃ can be reused)

Wash with ddH₂O 20 sec for 3 times.

Develop the gel with 100 mL Developing solution until bands clear.

Stop the reaction with 100 mL Stop solution and scan the gel.

Solutions

Fixative solution (<i>mix in order</i>)	100 mL	Final concentration
Milli-Q water	39.95 mL	
Methanol	50 mL	50%
Acetic Acid	10 mL	10%
Formaldehyde	50 µL	

Developing solution	100 mL
Na ₂ CO ₃	6 g
Sodium Thiosulphate solution	2 mL
Formaldehyde	50 µL
Milli-Q water	To 100 mL

Stop solution	100 mL
Milli-Q water	95 mL
Acetic acid	5 mL

6.16. Western blot

Run the SDS-PAGE as usual.

Wash gel, resins the gel, sponges, whatman paper and membrane in ice-cold working transfer buffer.

Assemble the cassette from the black side



Using 15 mL tube to remove the bubbles.

Setup the cassette in correct direction in the chamber.

Put an ice package into the chamber, fill it up with ice-cold working transfer buffer. Put the chamber in ice bath if necessary

Transfer for at least 2 hours under 110 V. Time and voltage can be adjusted according to different proteins.

Disassemble the equipment, block the membrane with PBST containing 5% milk for 30 min-1 h at RT.

Incubate with primary Antibody (HA-Tag (C29F4) Rabbit mAb #3724) 1:1000 in blocking solution 3 - 4 h at RT or O/N at 4 °C.

Wash 3× 5 min with PBST at RT.

Incubate secondary antibody (1 µL in 10 mL blocking solution).

Shaking at RT for 1 hour.

Wash 3× 5 min with PBST at RT.

Develop the membrane with Luminata Crescendo Western HRP Substrate (Millipore), expose membrane with Amersham Imager 600.

6.17. N-6× His-SUMO-PGM Expression

Cloning the N-6× His-SUMO-PGM plasmid into BL21 strain cells.

Pick up single positive clone into 15 mL LB culture containing 15 µL kanamycin, incubate at 37 °C, O/N.

Dilute the pre-cultural to 1 : 100 with LB, supplying with 1 : 1000 kanamycin.

Incubate the dilution at 37 °C on shaker until the OD₆₀₀ is 0.4.

Add IPTG to final concentration 0.2 mM, incubate over 6 hours.

Collect all culture by centrifuge at 4200 RPM, 4 °C for 1 hour.

Remove the supernatant, resuspend the pellet with 0.9% NaCl.

Centrifuge at max. speed, 4 °C for 15 min.

Frozen the pellet in liquid nitrogen, store in -80 °C freezer.

6.18. N-6× His-SUMO-PGM purification

Add 25 ml lysis buffer into the pellet from expression, keep on ice 30min, and dissolve by pipetting.

Sonication: 30% amplitude, 10 sec robust, 1 min rest, total robust 6 min until transparent.

Take 100 µL lysate mix with 100 µL 10% SDS, boil at 100 °C for 3 min.

Add 50 µL 5× loading buffer, boil at 95 °C for 10min (lysate).

Wash the glass tube with hot water, ddH₂O, and 100% ethanol before usage.

Transfer lysate after sonication into two 30ml glass tubes, 15ml each, balance by scale. Fit tube into rubber tube, spin down lysates at 11000 RPM (~14000 ×g), 4 °C for 45min.

Well mix the beads (50% of mixture), transfer 2 mL beads mixture into a 50 mL falcon tube.

Wash beads with 20 mL wash buffer and spin down 5min at 500 ×g, 4°C, 3times.

Take 100 µL supernatant and pellet which resuspended with same volume of input, mix with 100 µL 10% SDS, boil at 100 °C for 3 min separately.

Add 50 µL 5× loading buffer, boil at 95 °C for 10min (supernatant and pellet).

Add all supernatant (~30 mL) from above to gently resuspend beads, incubate in 4 °C room for 30 min-1 hour to bind PGM by rotating.

Transfer all mixture into a 20 mL Chromatography Columns, collect flow through as unbound.

Wash the column three times with 25 mL washing buffer, collect the first wash for western blot (Wash).

Aliquot SUMO protease 4ul/tube keep in -20 °C.

Resuspend beads in column with 1 mL working buffer (2 mL in total), transfer to 2 mL tube and incubate in 4 °C room on rotating for 40 min or O/N.

Wash the Chromatography Columns with 20 mL ddH₂O 10times, keep column filled with ddH₂O at 4 °C for reusing.

Collect the flow through which is the protein needed. Take 6 µL in PCR tube, measure concentration with Nanodrop Protein 280 (standard BSA control 1 mg/mL).

Take 100 µL protein and beads which diluted into same volume with input, mix with 100 µL 10% SDS, boil at 100 °C for 3 min separately.

Add 50 µL 5× loading buffer, boil at 95 °C for 10min (elution and beads).

Aliquot protein in 50-100 µL/PCR tube. Two tubes should be free of glycerol, frozen in liquid nitrogen immediately. Add equal 80% glycerol into other tubes, frozen in liquid nitrogen, store according further requirements.

Buffers

Lysis buffer	50 mL	Final concentration
1M Tris HCl pH 9	2.5 mL	50 mM
5M NaCl	1.5 mL	150 mM
80% Glycerol	6.25 mL	10%
β- mercaptoethanol	35 µL	10 mM
50× protease inhibitor EDTA-free	1 mL	1×
Lysozyme	50 mg	1 mg/mL
ddH ₂ O	38.715	

Wash buffer	300 mL	Final concentration
1M Tris HCl pH 9	15 mL	50 mM
5M NaCl	30 mL	500 mM
80% Glycerol	37.5 mL	10%
DTT	300 μ L	1 mM
Imidazole	408.48 mg	20 mM
ddH ₂ O	217.29 mL	

Working buffer	2 mL	Final concentration
1M Tris HCl pH 8	40 μ L	20 mM
5M NaCl	200 μ L	500 mM
SUMO protease	4 μ L	
ddH ₂ O	1756 μ L	

6.19. Denaturing urea polyacrylamide gel electrophoresis

Dissolve the gel solution at 37 °C water bath in a 50 mL tube, shake frequently until complete dissolve.

During this time, clean SDS-PAGE equipment with hot water, ddH₂O and 100% ethanol, ary dry them.

Filter the solution into a new 50 mL falcon tube through 0.22 µm.

Chill the solution on ice.

Add 75 µL 10% APS and 15 µL TEMED, mix gently.

Chill on ice for another 5min.

Pour solution into the gap and insert the comb, lay the equipment on a tip box and put a bottle on the top of cover glass to remove the gap between comb and gel.

Using 200 µL pipette to clean the hole.

Pre-running at 150 V, 20 min.

Mix 5 µL DNA or RNA with 10 µL loading dye.

Boil at 95 °C 2 min, immediately put them on ice for at least 5 min before loading.

Fill the equipment with 1× TBE solution.

Load all samples, fill the gap with dye, run at 150 V for about 1 hour.

Ethidium bromide (EB) staining and imaging.

Gel solution	15 mL
10 TBE	1.5 mL
40% acrylamide 19:1	3 mL
Urea	6.3 g
ddH ₂ O	3.5 mL

6.20. Primer List

Oligo name	Sequence 5'-3'
SMC4-1 +f R	TCAACATGAATAATTAATTTTAAATTCTTCATTCTT
SMC4-1 +f F	AAAGAATTAAGTAGTATTTTGCAGAAAAAATATTAAG
SMC4-1 +fv 3 F	TGAAATGATTTTAAAATATTCATATTCCATTATTG
SMC4-1 +fv 3 R	TCTATTTTAATTAACGTTTTTCATTGTTTTTC
SMC4-1 +fv F	CAGACTGAAAGTGAAGAGCCAT
SMC4-1 +fv R	CATTTTATGTAAATATATTTAATATTTTAAATTAACTTTTGG
SMC4-2 +F R	GAATTAATTCAAGATCTAAATATTCGTAACA
SMC4-2 +F F	ATGCGCAATTTAATTTGAGCAATATT
SMC4-2 +fv 3 F	TGAAATTTATATTAATTAATAATCAATTAATTTTATC
SMC4-2 +fv 3 R	AACTTCTAATTAGATGACTTCTGTTGAA
SMC4-2 +fv F	ATTAAGGAAGTTATTTTGGAGAATTTTAAATC
SMC4-2 +fv R	CATATTTTCTATCATTTAATTTTCTACTCAA
SMC2-1 sil F	ATATGAGCTCATGTGGATCAAAGAAATCATTATCGA
SMC2-1 sil R	TACCAGGAGACAAAAGAACTATAGACTCGAGTAAA
SMC2-2 sil F	ATATGAGCTCAGAACAACCTGAATAGAGAGATTACACA
SMC2-2 sil R	AAAAGAATTCTAATCATTAAAAGACAAAAGTTGCTCGAGTAAA
SMC4-1 sil F	ATATGAGCTCATGCAGACTGAAAGTGAAGAGC
SMC4-1 sil R	TTTACTCGAGTGTTTTGTTATGATGTCAGATTGTTCACT
SMC4-2 sil F	ATATGAGCTCATGATTAAGGAAGTTATTTTGGAGAATTTT
SMC4-2 sil R	TTTACTCGAGTATCTACCTTATTTTATTTTCTGGAATCA
SMC2-1 Co-sil F	ATATCCCGGGATGTGGATCAAAGAAATCATTATCGA
SMC2-2 Co-sil F	ATATCCCGGGAGAACAACTGAATAGAGAGATTACACA
SMC4-1 Co-sil F	ATATCCCGGGATGCAGACTGAAAGTGAAGAGC
SMC4-2 Co-sil-R	TTTACCCGGGTATCTACCTTATTTTATTTTCTGGAATCA
377 F	AAAGATAAATATGAAATTTGTTGGTGAATTTTAAT
377 R	AAATTAACCTTGGATTATGAATTCAAATATAAAT
798 F	AAAATTAAGTTTCTGGATAATATATGATATGGTTA
798 R	AAATAACCTATCCAAAATAACCTAACAGAA

IES		Retention score										
Classical IES name	IES name in reference MAC+ IES assembly	Maternal control score	EV	PGM-KD	CAF1-KD	SDCP-KD	NOWA1-KD	DCL2/3-KD	DCL5-KD	DCL2/3/5-KD	PT01/09-KD	PT10/11-KD
51G11	IESPGM.PTETS1.1.51.451201		0.03	0.80	0.5	0.44	0.53	0.05	0.20	0.56	0.02	0.20
51G1413	IESPGM.PTETS1.1.51.452624	0.00	0.01	0.78	0.35	0.12	0.1	0.01	0.02	0.04	0.00	0.00
51G1832	IESPGM.PTETS1.1.51.453043	0.00	0.00	0.73	0.04	0.04	0.02	0.00	0.00	0.02	0.01	0.01
51G2832	IESPGM.PTETS1.1.51.454043	0.87	0.00	0.77	0.6	0.2	0.59	0.23	0.00	0.71	0.41	0.00
51G4404	IESPGM.PTETS1.1.51.455615	0.97	0.00	0.84	0.57	0.48	0.81	0.60	0.01	0.75	0.77	0.01
51G6447	IESPGM.PTETS1.1.51.457658		0.00	0.78	0.05	0.09	0.05	0.04	0.00	0	0.01	0.01
51A1712	IESPGM.PTETS1.1.106.281631	0.34	0.00	0.78	0.44	0.64	0.75	0.07	0.06	0.71	0.18	0.08
51A1835	IESPGM.PTETS1.1.106.284157	0.00	0.00	0.80	0.02	0.08	0.03	0.00	0.00	0.04	0.00	0.00
51A2591	IESPGM.PTETS1.1.106.284913	0.99	0.00	0.91	0.63	0.48	0.81	0.54	0.00	0.81	0.66	0.00
51A4404	IESPGM.PTETS1.1.106.286750	0.00	0.00	0.83	0	0.23	0	0.00	0.00	0	0.00	0.00
51A4578	IESPGM.PTETS1.1.106.286924	0.00	0.00	0.78	0.41	0.24	0.20	0.05	0.00	0.08	0.03	0.00
51A6435	IESPGM.PTETS1.1.106.288781	0.00	0.00	0.77	0.01	0.04	0.01	0.00	0.00	0	0.00	0.00
51A6649	IESPGM.PTETS1.1.106.288995	0.58	0.00	0.81	0.53	0.60	0.57	0.56	0.01	0.74	0.48	0.00
Dcl5d-01	IESPGM.PTETS1.1.8.257314		0.02	0.75	0.39	0.23	0.77	0.03	0.50	0.73	0.07	0.25
Dcl5d-02	IESPGM.PTETS1.1.16.506105		0.00	0.95	0.61	0.65	0.47	0.02	0.38	0.73	0.05	0.51
Dcl5d-03	IESPGM.PTETS1.1.39.60104		0.00	0.74	0.13	0.09	0.31	0.00	0.37	0.6	0.00	0.25
Dcl5d-04	IESPGM.PTETS1.1.168.68297		0.00	0.69	0.04	0.03	0.46	0.05	0.37	0.81	0.06	0.22

Classical IES name	Primer		Position		Band Size		Annealing Temperature
	Forward Primer	Reverse Primer	Scaffold	Start	IES+	IES-	Tm
51G11	ATCATAAGATTGATATCTTCTCCCTCTCC	ACTTGCTACTAAGCAAGAAACATTGAGAG	51	478642	296	253	54
51G1413	GAAGCTGCTTGTTAAGAATCTACTGG	GCATCCAGCACTAGTTGAATTTACTGTAC	51	480108	220	168	62
51G1832	CTATAACTCTGAAGCTGCTGTAATATG	TTGTCAATGAGCCATTAAACAGTTGCTGGAT	51	480579	217	187	62
51G2832	GCTATAACTCTGAAGCTGCTGTAATATG	TTGTCAATGAGCCATTAAACAGTTGCTGGAT	51	481609	393	164	60
51G4404	CTGTGCTACACATTGTGCATATGTTACT	GCTGTAAGATTAACTTGAAGCATGATCAAG	51	483410	501	299	60
51G6447	AATGCATCAAATGATGTAATCTCTGCT	AATTTGTAAGATCCAGCGCAGGCAAG	51	485675	137	109	57
51A1712	TTTTGTCAAAAAGACATGTACAAAATGAG	TAGAATACTAAGAGATTCAATACAACAAC	106	196699	234	157	57
51A1835	TAATGTATTGATAAGCTTGCCTACAGCC	ATCTAACATCTTGAATGTTACTGATCC	106	299405	166	138	60
51A2591	ATGTGTTGGACTGGATGGCATGAGAAG	GATGTAGCATAACTTATCAACAATCCAT	106	300189	639	269	60
51A4404	TGGAATAGTCTGCATCCACAGCTGCTTGC	CCAGTTATTGAACTGCAACTTACTGCAATG	106	302396	355	278	57
51A4578	CCTGCAGTAAGTTCAGTTCAATAACTGG	TGTAGTCTTAAAATCTTAGCATGTTGTACC	106	302647	1007	125	57
51A6435	CAAATTGTGCTACTAGAGGTACATGTTTCC	GCGACATCAATAGTAACAGCTGAGCATGAG	106	305407	305	277	57
51A6649	ACTGCACCTCTAACTTTAACAAAGCGAAGCA	CAGCAGTACATCCAGCTCTAAGTTTAGC	106	305649	628	258	57
MT	GGTGTATTATCTTAATGTTGACCCCTCAC	CCATCTATACTCCATCTTTATCTTAATTCAT			460	265	55
Dcl5d-01	CCAGTCTTTATAACTCCAAATATACTAATGTTAATTGCC	CTTGTGTTGTAATATCAATGAAAATCTTGATG	8	269999	296	249	55
Dcl5d-02	TTTTCATACTCATCTCACCCTACTCCC	ATAATATAAACTTTGAAGCCCTGAAAGCCG	16	525921	520	424	55
Dcl5d-03	TTTCATCGTTCTCAAAATGGATGCC	ATCAATATGAATTTTATTTGTTTATAAAGCGTCTGG	39	64383	235	163	55
Dcl5d-04	TTAAGGTACTTCTCATCCATAGTCAGCC	AACAATATGAGTTAGAAATTTAAAATCTTGAGGGAATCC	168	70859	278	220	55

7. References

- 1 Prescott, D. M. The DNA of ciliated protozoa. *Microbiological reviews* **58**, 233-267, doi:10.1128/mr.58.2.233-267.1994 (1994).
- 2 Gao, F. *et al.* Systematic studies on ciliates (Alveolata, Ciliophora) in China: Progress and achievements based on molecular information. *European journal of protistology* **61**, 409-423, doi:10.1016/j.ejop.2017.04.009 (2017).
- 3 Philippe, H., Germot, A. & Moreira, D. The new phylogeny of eukaryotes. *Current opinion in genetics & development* **10**, 596-601, doi:10.1016/s0959-437x(00)00137-4 (2000).
- 4 Beisson, J. *et al.* Paramecium tetraurelia: the renaissance of an early unicellular model. *Cold Spring Harbor protocols* **2010**, pdb emo140, doi:10.1101/pdb.emo140 (2010).
- 5 Cummings, D. J. Studies on Macronuclear DNA from Paramecium aurelia. *Chromosoma* **53**, 191-208, doi:10.1007/BF00329171 (1975).
- 6 Rodriguez-Ezpeleta, N. *et al.* Toward resolving the eukaryotic tree: the phylogenetic positions of jakobids and cercozoans. *Current biology : CB* **17**, 1420-1425, doi:10.1016/j.cub.2007.07.036 (2007).
- 7 Betermier, M. & Duharcourt, S. Programmed Rearrangement in Ciliates: Paramecium. *Microbiology spectrum* **2**, doi:10.1128/microbiolspec.MDNA3-0035-2014 (2014).
- 8 Katz, L. A. Evolution of nuclear dualism in ciliates: a reanalysis in light of recent molecular data. *International journal of systematic and evolutionary microbiology* **51**, 1587-1592, doi:10.1099/00207713-51-4-1587 (2001).
- 9 Hedgpeth, J. W. The Biology of Paramecium. *Science* **118**, 727-727, doi:doi:10.1126/science.118.3076.727.b (1953).
- 10 Coyne, R. S., Lhuillier-Akakpo, M. & Duharcourt, S. RNA-guided DNA rearrangements in ciliates: is the best genome defence a good offence? *Biology of the cell* **104**, 309-325, doi:10.1111/boc.201100057 (2012).
- 11 Wagtendonk, W. J. v. A Ciliate: The Anatomy of Paramecium aurelia *Science* **170**, 155-156, doi:doi:10.1126/science.170.3954.155.b (1970).
- 12 Le Mouel, A., Butler, A., Caron, F. & Meyer, E. Developmentally regulated chromosome fragmentation linked to imprecise elimination of repeated sequences in paramecia. *Eukaryotic cell* **2**, 1076-1090, doi:10.1128/EC.2.5.1076-1090.2003 (2003).
- 13 Dubois, E. *et al.* Transposon Invasion of the Paramecium Germline Genome Countered by a Domesticated PiggyBac Transposase and the NHEJ Pathway. *International journal of evolutionary biology* **2012**, 436196, doi:10.1155/2012/436196 (2012).
- 14 Terue Harumoto, B. Paramecium: Genetics and Epigenetics. *The Quarterly Review of Biology* **84**, 201-202, doi:10.1086/603492 (2009).
- 15 Morgens, D. W. & Cavalcanti, A. R. Amitotic chromosome loss predicts distinct patterns of senescence and non-senescence in ciliates. *Protist* **166**, 224-233, doi:10.1016/j.protis.2015.03.002 (2015).
- 16 Chalker, D. L., Meyer, E. & Mochizuki, K. Epigenetics of ciliates. *Cold Spring Harbor perspectives in biology* **5**, a017764, doi:10.1101/cshperspect.a017764 (2013).
- 17 Betermier, M. Large-scale genome remodelling by the developmentally programmed elimination of germ line sequences in the ciliate Paramecium. *Research in microbiology* **155**, 399-408, doi:10.1016/j.resmic.2004.01.017 (2004).

-
- 18 Meyer, E. & Garnier, O. Non-Mendelian inheritance and homology-dependent effects in ciliates. *Advances in genetics* **46**, 305-337, doi:10.1016/s0065-2660(02)46011-7 (2002).
- 19 Kapusta, A. *et al.* Highly precise and developmentally programmed genome assembly in *Paramecium* requires ligase IV-dependent end joining. *PLoS genetics* **7**, e1002049, doi:10.1371/journal.pgen.1002049 (2011).
- 20 Baudry, C. *et al.* PiggyMac, a domesticated piggyBac transposase involved in programmed genome rearrangements in the ciliate *Paramecium tetraurelia*. *Genes & development* **23**, 2478-2483, doi:10.1101/gad.547309 (2009).
- 21 Arnaiz, O. *et al.* The *Paramecium* germline genome provides a niche for intragenic parasitic DNA: evolutionary dynamics of internal eliminated sequences. *PLoS genetics* **8**, e1002984, doi:10.1371/journal.pgen.1002984 (2012).
- 22 Klobutcher, L. A. & Herrick, G. Consensus inverted terminal repeat sequence of *Paramecium* IESs: resemblance to termini of Tc1-related and *Euplotes* Tec transposons. *Nucleic acids research* **23**, 2006-2013, doi:10.1093/nar/23.11.2006 (1995).
- 23 Steele, C J *et al.* "Developmentally excised sequences in micronuclear DNA of *Paramecium*." Proceedings of the National Academy of Sciences of the United States of America vol. 91,6: 2255-9. doi:10.1073/pnas.91.6.2255 (1994)
- 24 Plasterk, R. H., Izsvak, Z. & Ivics, Z. Resident aliens: the Tc1/mariner superfamily of transposable elements. *Trends in genetics : TIG* **15**, 326-332, doi:10.1016/s0168-9525(99)01777-1 (1999).
- 25 Dubrana, K., Le Mouel, A. & Amar, L. Deletion endpoint allele-specificity in the developmentally regulated elimination of an internal sequence (IES) in *Paramecium*. *Nucleic acids research* **25**, 2448-2454, doi:10.1093/nar/25.12.2448 (1997).
- 26 Allen, S. E. *et al.* Circular Concatemers of Ultra-Short DNA Segments Produce Regulatory RNAs. *Cell* **168**, 990-999 e997, doi:10.1016/j.cell.2017.02.020 (2017).
- 27 Hoehener, C., Hug, I. & Nowacki, M. Dicer-like Enzymes with Sequence Cleavage Preferences. *Cell* **173**, 234-247 e237, doi:10.1016/j.cell.2018.02.029 (2018).
- 28 Lepere, G. *et al.* Silencing-associated and meiosis-specific small RNA pathways in *Paramecium tetraurelia*. *Nucleic acids research* **37**, 903-915, doi:10.1093/nar/gkn1018 (2009).
- 29 Mochizuki, K., Fine, N. A., Fujisawa, T. & Gorovsky, M. A. Analysis of a piwi-related gene implicates small RNAs in genome rearrangement in tetrahymena. *Cell* **110**, 689-699, doi:10.1016/s0092-8674(02)00909-1 (2002).
- 30 Mochizuki, K. & Gorovsky, M. A. Small RNAs in genome rearrangement in Tetrahymena. *Current opinion in genetics & development* **14**, 181-187, doi:10.1016/j.gde.2004.01.004 (2004).
- 31 Chalker, D. L. & Yao, M. C. Nongenic, bidirectional transcription precedes and may promote developmental DNA deletion in *Tetrahymena thermophila*. *Genes & development* **15**, 1287-1298, doi:10.1101/gad.884601 (2001).
- 32 Sandoval, P. Y., Swart, E. C., Arambasic, M. & Nowacki, M. Functional diversification of Dicer-like proteins and small RNAs required for genome sculpting. *Developmental cell* **28**, 174-188, doi:10.1016/j.devcel.2013.12.010 (2014).
- 33 Bouhouche, K., Gout, J. F., Kapusta, A., Betermier, M. & Meyer, E. Functional specialization of Piwi proteins in *Paramecium tetraurelia* from post-transcriptional gene silencing to genome remodelling. *Nucleic acids research* **39**, 4249-4264, doi:10.1093/nar/gkq1283 (2011).

-
- 34 Lepere, G., Betermier, M., Meyer, E. & Duharcourt, S. Maternal noncoding transcripts antagonize the targeting of DNA elimination by scanRNAs in *Paramecium tetraurelia*. *Genes & development* **22**, 1501-1512, doi:10.1101/gad.473008 (2008).
- 35 Nowacki, M., Zagorski-Ostojka, W. & Meyer, E. Nowa1p and Nowa2p: novel putative RNA binding proteins involved in trans-nuclear crosstalk in *Paramecium tetraurelia*. *Current biology : CB* **15**, 1616-1628, doi:10.1016/j.cub.2005.07.033 (2005).
- 36 Betermier, M., Duharcourt, S., Seitz, H. & Meyer, E. Timing of developmentally programmed excision and circularization of *Paramecium* internal eliminated sequences. *Molecular and cellular biology* **20**, 1553-1561, doi:10.1128/MCB.20.5.1553-1561.2000 (2000).
- 37 Furrer, D. I., Swart, E. C., Kraft, M. F., Sandoval, P. Y. & Nowacki, M. Two Sets of Piwi Proteins Are Involved in Distinct sRNA Pathways Leading to Elimination of Germline-Specific DNA. *Cell reports* **20**, 505-520, doi:10.1016/j.celrep.2017.06.050 (2017).
- 38 Marmignon, A. *et al.* Ku-mediated coupling of DNA cleavage and repair during programmed genome rearrangements in the ciliate *Paramecium tetraurelia*. *PLoS genetics* **10**, e1004552, doi:10.1371/journal.pgen.1004552 (2014).
- 39 Chen, D. *et al.* Condensed mitotic chromatin is accessible to transcription factors and chromatin structural proteins. *The Journal of cell biology* **168**, 41-54, doi:10.1083/jcb.200407182 (2005).
- 40 Paweletz, N. Walther Flemming: pioneer of mitosis research. *Nature reviews. Molecular cell biology* **2**, 72-75, doi:10.1038/35048077 (2001).
- 41 Hirano, T. Chromosome cohesion, condensation, and separation. *Annual review of biochemistry* **69**, 115-144, doi:10.1146/annurev.biochem.69.1.115 (2000).
- 42 Cobbe, N. & Heck, M. M. Review: SMCs in the world of chromosome biology- from prokaryotes to higher eukaryotes. *Journal of structural biology* **129**, 123-143, doi:10.1006/jsbi.2000.4255 (2000).
- 43 Cobbe, N. & Heck, M. M. The evolution of SMC proteins: phylogenetic analysis and structural implications. *Molecular biology and evolution* **21**, 332-347, doi:10.1093/molbev/msh023 (2004).
- 44 Ou, H. D. *et al.* ChromEMT: Visualizing 3D chromatin structure and compaction in interphase and mitotic cells. *Science* **357**, doi:10.1126/science.aag0025 (2017).
- 45 Haering, C. H., Lowe, J., Hochwagen, A. & Nasmyth, K. Molecular architecture of SMC proteins and the yeast cohesin complex. *Molecular cell* **9**, 773-788, doi:10.1016/s1097-2765(02)00515-4 (2002).
- 46 Hopfner, K. P. *et al.* The Rad50 zinc-hook is a structure joining Mre11 complexes in DNA recombination and repair. *Nature* **418**, 562-566, doi:10.1038/nature00922 (2002).
- 47 Griese, J. J., Witte, G. & Hopfner, K. P. Structure and DNA binding activity of the mouse condensin hinge domain highlight common and diverse features of SMC proteins. *Nucleic acids research* **38**, 3454-3465, doi:10.1093/nar/gkq038 (2010).
- 48 Hirano, T. At the heart of the chromosome: SMC proteins in action. *Nature reviews. Molecular cell biology* **7**, 311-322, doi:10.1038/nrm1909 (2006).
- 49 Barysz, H. *et al.* Three-dimensional topology of the SMC2/SMC4 subcomplex from chicken condensin I revealed by cross-linking and molecular modelling. *Open biology* **5**, 150005, doi:10.1098/rsob.150005 (2015).
- 50 Walker, J. E., Saraste, M., Runswick, M. J. & Gay, N. J. Distantly related sequences in the alpha- and beta-subunits of ATP synthase, myosin, kinases and other ATP-requiring enzymes and a common nucleotide binding fold. *The EMBO journal* **1**, 945-951, doi:10.1002/j.1460-2075.1982.tb01276.x (1982).

-
- 51 Hirano, M. & Hirano, T. Opening closed arms: long-distance activation of SMC ATPase by hinge-DNA interactions. *Molecular cell* **21**, 175-186, doi:10.1016/j.molcel.2005.11.026 (2006).
- 52 Jeppsson, K., Kanno, T., Shirahige, K. & Sjogren, C. The maintenance of chromosome structure: positioning and functioning of SMC complexes. *Nature reviews. Molecular cell biology* **15**, 601-614, doi:10.1038/nrm3857 (2014).
- 53 Hopfner, K. P. *et al.* Structural biology of Rad50 ATPase: ATP-driven conformational control in DNA double-strand break repair and the ABC-ATPase superfamily. *Cell* **101**, 789-800, doi:10.1016/s0092-8674(00)80890-9 (2000).
- 54 Lowe, J., Cordell, S. C. & van den Ent, F. Crystal structure of the SMC head domain: an ABC ATPase with 900 residues antiparallel coiled-coil inserted. *Journal of molecular biology* **306**, 25-35, doi:10.1006/jmbi.2000.4379 (2001).
- 55 Hirano, M. & Hirano, T. Hinge-mediated dimerization of SMC protein is essential for its dynamic interaction with DNA. *The EMBO journal* **21**, 5733-5744, doi:10.1093/emboj/cdf575 (2002).
- 56 Fousteri, M. I. & Lehmann, A. R. A novel SMC protein complex in *Schizosaccharomyces pombe* contains the Rad18 DNA repair protein. *The EMBO journal* **19**, 1691-1702, doi:10.1093/emboj/19.7.1691 (2000).
- 57 Hirano, T., Kobayashi, R. & Hirano, M. Condensins, chromosome condensation protein complexes containing XCAP-C, XCAP-E and a *Xenopus* homolog of the *Drosophila* Barren protein. *Cell* **89**, 511-521, doi:10.1016/s0092-8674(00)80233-0 (1997).
- 58 Yamazoe, M. *et al.* Complex formation of MukB, MukE and MukF proteins involved in chromosome partitioning in *Escherichia coli*. *The EMBO journal* **18**, 5873-5884, doi:10.1093/emboj/18.21.5873 (1999).
- 59 Schleiffer, A. *et al.* Kleisins: a superfamily of bacterial and eukaryotic SMC protein partners. *Molecular cell* **11**, 571-575, doi:10.1016/s1097-2765(03)00108-4 (2003).
- 60 Gruber, S., Haering, C. H. & Nasmyth, K. Chromosomal cohesin forms a ring. *Cell* **112**, 765-777, doi:10.1016/s0092-8674(03)00162-4 (2003).
- 61 Melby, T. E., Ciampaglio, C. N., Briscoe, G. & Erickson, H. P. The symmetrical structure of structural maintenance of chromosomes (SMC) and MukB proteins: long, antiparallel coiled coils, folded at a flexible hinge. *The Journal of cell biology* **142**, 1595-1604, doi:10.1083/jcb.142.6.1595 (1998).
- 62 Jessberger, R., Frei, C. & Gasser, S. M. Chromosome dynamics: the SMC protein family. *Current opinion in genetics & development* **8**, 254-259, doi:10.1016/s0959-437x(98)80149-4 (1998).
- 63 Hirano, T. The ABCs of SMC proteins: two-armed ATPases for chromosome condensation, cohesion, and repair. *Genes & development* **16**, 399-414, doi:10.1101/gad.955102 (2002).
- 64 Yoshinaga, M. & Inagaki, Y. Ubiquity and Origins of Structural Maintenance of Chromosomes (SMC) Proteins in Eukaryotes. *Genome biology and evolution* **13**, doi:10.1093/gbe/evab256 (2021).
- 65 Jessberger, R. The many functions of SMC proteins in chromosome dynamics. *Nature reviews. Molecular cell biology* **3**, 767-778, doi:10.1038/nrm930 (2002).
- 66 Hagstrom, K. A. & Meyer, B. J. Condensin and cohesin: more than chromosome compactor and glue. *Nature reviews. Genetics* **4**, 520-534, doi:10.1038/nrg1110 (2003).
- 67 Ono, T., Fang, Y., Spector, D. L. & Hirano, T. Spatial and temporal regulation of Condensins I and II in mitotic chromosome assembly in human cells. *Molecular biology of the cell* **15**, 3296-3308, doi:10.1091/mbc.e04-03-0242 (2004).

-
- 68 Ono, T. *et al.* Differential contributions of condensin I and condensin II to mitotic chromosome architecture in vertebrate cells. *Cell* **115**, 109-121, doi:10.1016/s0092-8674(03)00724-4 (2003).
- 69 Ohta, S. *et al.* The protein composition of mitotic chromosomes determined using multiclassifier combinatorial proteomics. *Cell* **142**, 810-821, doi:10.1016/j.cell.2010.07.047 (2010).
- 70 Csankovszki, G. *et al.* Three distinct condensin complexes control *C. elegans* chromosome dynamics. *Current biology : CB* **19**, 9-19, doi:10.1016/j.cub.2008.12.006 (2009).
- 71 Howard-Till, R., Tian, M. & Loidl, J. A specialized condensin complex participates in somatic nuclear maturation in *Tetrahymena thermophila*. *Molecular biology of the cell* **30**, 1326-1338, doi:10.1091/mbc.E18-08-0487 (2019).
- 72 Collette, K. S., Petty, E. L., Golenberg, N., Bembenek, J. N. & Csankovszki, G. Different roles for Aurora B in condensin targeting during mitosis and meiosis. *Journal of cell science* **124**, 3684-3694, doi:10.1242/jcs.088336 (2011).
- 73 Shintomi, K. & Hirano, T. The relative ratio of condensin I to II determines chromosome shapes. *Genes & development* **25**, 1464-1469, doi:10.1101/gad.2060311 (2011).
- 74 Hirano, T. Chromosome Dynamics during Mitosis. *Cold Spring Harbor perspectives in biology* **7**, doi:10.1101/cshperspect.a015792 (2015).
- 75 Hirano, T. & Mitchison, T. J. A heterodimeric coiled-coil protein required for mitotic chromosome condensation in vitro. *Cell* **79**, 449-458, doi:10.1016/0092-8674(94)90254-2 (1994).
- 76 Lee, B. G. *et al.* Cryo-EM structures of holo condensin reveal a subunit flip-flop mechanism. *Nature structural & molecular biology* **27**, 743-751, doi:10.1038/s41594-020-0457-x (2020).
- 77 Kalitsis, P., Zhang, T., Marshall, K. M., Nielsen, C. F. & Hudson, D. F. Condensin, master organizer of the genome. *Chromosome research : an international journal on the molecular, supramolecular and evolutionary aspects of chromosome biology* **25**, 61-76, doi:10.1007/s10577-017-9553-0 (2017).
- 78 Schoenfelder, S. *et al.* Preferential associations between co-regulated genes reveal a transcriptional interactome in erythroid cells. *Nature genetics* **42**, 53-61, doi:10.1038/ng.496 (2010).
- 79 Tsang, C. K., Wei, Y. & Zheng, X. F. Compacting DNA during the interphase: condensin maintains rDNA integrity. *Cell cycle* **6**, 2213-2218, doi:10.4161/cc.6.18.4733 (2007).
- 80 Kobayashi, T. Strategies to maintain the stability of the ribosomal RNA gene repeats--collaboration of recombination, cohesion, and condensation. *Genes & genetic systems* **81**, 155-161, doi:10.1266/ggs.81.155 (2006).
- 81 Wood, A. J., Severson, A. F. & Meyer, B. J. Condensin and cohesin complexity: the expanding repertoire of functions. *Nature reviews. Genetics* **11**, 391-404, doi:10.1038/nrg2794 (2010).
- 82 Gerlich, D., Hirota, T., Koch, B., Peters, J. M. & Ellenberg, J. Condensin I stabilizes chromosomes mechanically through a dynamic interaction in live cells. *Current biology : CB* **16**, 333-344, doi:10.1016/j.cub.2005.12.040 (2006).
- 83 Hartl, T. A., Smith, H. F. & Bosco, G. Chromosome alignment and transvection are antagonized by condensin II. *Science* **322**, 1384-1387, doi:10.1126/science.1164216 (2008).

-
- 84 Joyce, E. F., Williams, B. R., Xie, T. & Wu, C. T. Identification of genes that promote or antagonize somatic homolog pairing using a high-throughput FISH-based screen. *PLoS genetics* **8**, e1002667, doi:10.1371/journal.pgen.1002667 (2012).
- 85 Iwasaki, O., Tanaka, A., Tanizawa, H., Grewal, S. I. & Noma, K. Centromeric localization of dispersed Pol III genes in fission yeast. *Molecular biology of the cell* **21**, 254-265, doi:10.1091/mbc.E09-09-0790 (2010).
- 86 Haeusler, R. A., Pratt-Hyatt, M., Good, P. D., Gipson, T. A. & Engelke, D. R. Clustering of yeast tRNA genes is mediated by specific association of condensin with tRNA gene transcription complexes. *Genes & development* **22**, 2204-2214, doi:10.1101/gad.1675908 (2008).
- 87 Lau, A. C. & Csankovszki, G. Condensin-mediated chromosome organization and gene regulation. *Frontiers in genetics* **5**, 473, doi:10.3389/fgene.2014.00473 (2014).
- 88 Nasmyth, K. Disseminating the genome: joining, resolving, and separating sister chromatids during mitosis and meiosis. *Annual review of genetics* **35**, 673-745, doi:10.1146/annurev.genet.35.102401.091334 (2001).
- 89 Akai, Y. *et al.* Opposing role of condensin hinge against replication protein A in mitosis and interphase through promoting DNA annealing. *Open biology* **1**, 110023, doi:10.1098/rsob.110023 (2011).
- 90 Dixon, J. R. *et al.* Topological domains in mammalian genomes identified by analysis of chromatin interactions. *Nature* **485**, 376-380, doi:10.1038/nature11082 (2012).
- 91 Gibcus, J. H. *et al.* A pathway for mitotic chromosome formation. *Science* **359**, doi:10.1126/science.aao6135 (2018).
- 92 Alipour, E. & Marko, J. F. Self-organization of domain structures by DNA-loop-extruding enzymes. *Nucleic acids research* **40**, 11202-11212, doi:10.1093/nar/gks925 (2012).
- 93 Terakawa, T. *et al.* The condensin complex is a mechanochemical motor that translocates along DNA. *Science* **358**, 672-676, doi:10.1126/science.aan6516 (2017).
- 94 Ganji, M. *et al.* Real-time imaging of DNA loop extrusion by condensin. *Science* **360**, 102-105, doi:10.1126/science.aar7831 (2018).
- 95 Kschonsak, M. *et al.* Structural Basis for a Safety-Belt Mechanism That Anchors Condensin to Chromosomes. *Cell* **171**, 588-600 e524, doi:10.1016/j.cell.2017.09.008 (2017).
- 96 Shaltiel, I. A. *et al.* A hold-and-feed mechanism drives directional DNA loop extrusion by condensin. *Science* **376**, 1087-1094, doi:10.1126/science.abm4012 (2022).
- 97 Davidson, I. F. & Peters, J. M. Genome folding through loop extrusion by SMC complexes. *Nature reviews. Molecular cell biology* **22**, 445-464, doi:10.1038/s41580-021-00349-7 (2021).
- 98 Yanagida, M. Clearing the way for mitosis: is cohesin a target? *Nature reviews. Molecular cell biology* **10**, 489-496, doi:10.1038/nrm2712 (2009).
- 99 Heale, J. T. *et al.* Condensin I interacts with the PARP-1-XRCC1 complex and functions in DNA single-strand break repair. *Molecular cell* **21**, 837-848, doi:10.1016/j.molcel.2006.01.036 (2006).
- 100 Kimura, K. & Hirano, T. ATP-dependent positive supercoiling of DNA by 13S condensin: a biochemical implication for chromosome condensation. *Cell* **90**, 625-634, doi:10.1016/s0092-8674(00)80524-3 (1997).
- 101 Tsao, Y. P., Wu, H. Y. & Liu, L. F. Transcription-driven supercoiling of DNA: direct biochemical evidence from in vitro studies. *Cell* **56**, 111-118, doi:10.1016/0092-8674(89)90989-6 (1989).

-
- 102 Bazett-Jones, D. P., Kimura, K. & Hirano, T. Efficient supercoiling of DNA by a single condensin complex as revealed by electron spectroscopic imaging. *Molecular cell* **9**, 1183-1190, doi:10.1016/s1097-2765(02)00546-4 (2002).
- 103 Guacci, V., Hogan, E. & Koshland, D. Chromosome condensation and sister chromatid pairing in budding yeast. *The Journal of cell biology* **125**, 517-530, doi:10.1083/jcb.125.3.517 (1994).
- 104 Cervantes, M. D., Coyne, R. S., Xi, X. & Yao, M. C. The condensin complex is essential for amitotic segregation of bulk chromosomes, but not nucleoli, in the ciliate *Tetrahymena thermophila*. *Molecular and cellular biology* **26**, 4690-4700, doi:10.1128/MCB.02315-05 (2006).
- 105 Howard-Till, R. & Loidl, J. Condensins promote chromosome individualization and segregation during mitosis, meiosis, and amitosis in *Tetrahymena thermophila*. *Molecular biology of the cell* **29**, 466-478, doi:10.1091/mbc.E17-07-0451 (2018).
- 106 Mitra, R., Fain-Thornton, J. & Craig, N. L. piggyBac can bypass DNA synthesis during cut and paste transposition. *The EMBO journal* **27**, 1097-1109, doi:10.1038/emboj.2008.41 (2008).
- 107 Dubois, E. *et al.* Multimerization properties of PiggyMac, a domesticated piggyBac transposase involved in programmed genome rearrangements. *Nucleic acids research* **45**, 3204-3216, doi:10.1093/nar/gkw1359 (2017).
- 108 Guerineau, M. *et al.* The unusual structure of the PiggyMac cysteine-rich domain reveals zinc finger diversity in PiggyBac-related transposases. *Mobile DNA* **12**, 12, doi:10.1186/s13100-021-00240-4 (2021).
- 109 Bischerour, J. *et al.* Six domesticated PiggyBac transposases together carry out programmed DNA elimination in *Paramecium*. *eLife* **7**, doi:10.7554/eLife.37927 (2018).
- 110 de Vanssay, A. *et al.* The *Paramecium* histone chaperone Spt16-1 is required for Pgm endonuclease function in programmed genome rearrangements. *PLoS genetics* **16**, e1008949, doi:10.1371/journal.pgen.1008949 (2020).
- 111 Abello, A. *et al.* Functional diversification of *Paramecium* Ku80 paralogs safeguards genome integrity during precise programmed DNA elimination. *PLoS genetics* **16**, e1008723, doi:10.1371/journal.pgen.1008723 (2020).
- 112 Lieber, M. R. The mechanism of double-strand DNA break repair by the nonhomologous DNA end-joining pathway. *Annual review of biochemistry* **79**, 181-211, doi:10.1146/annurev.biochem.052308.093131 (2010).
- 113 Bhullar, S. *et al.* A mating-type mutagenesis screen identifies a zinc-finger protein required for specific DNA excision events in *Paramecium*. *Nucleic acids research* **46**, 9550-9562, doi:10.1093/nar/gky772 (2018).
- 114 Hirano, T. Condensin-Based Chromosome Organization from Bacteria to Vertebrates. *Cell* **164**, 847-857, doi:10.1016/j.cell.2016.01.033 (2016).
- 115 Anderson, D. E., Losada, A., Erickson, H. P. & Hirano, T. Condensin and cohesin display different arm conformations with characteristic hinge angles. *The Journal of cell biology* **156**, 419-424, doi:10.1083/jcb.200111002 (2002).
- 116 Chan, R. C., Severson, A. F. & Meyer, B. J. Condensin restructures chromosomes in preparation for meiotic divisions. *The Journal of cell biology* **167**, 613-625, doi:10.1083/jcb.200408061 (2004).
- 117 Nishide, K. & Hirano, T. Overlapping and non-overlapping functions of condensins I and II in neural stem cell divisions. *PLoS genetics* **10**, e1004847, doi:10.1371/journal.pgen.1004847 (2014).

-
- 118 Green, L. C. *et al.* Contrasting roles of condensin I and condensin II in mitotic chromosome formation. *Journal of cell science* **125**, 1591-1604, doi:10.1242/jcs.097790 (2012).
- 119 Sakai, A., Hizume, K., Sutani, T., Takeyasu, K. & Yanagida, M. Condensin but not cohesin SMC heterodimer induces DNA reannealing through protein-protein assembly. *The EMBO journal* **22**, 2764-2775, doi:10.1093/emboj/cdg247 (2003).
- 120 Sutani, T. & Yanagida, M. DNA renaturation activity of the SMC complex implicated in chromosome condensation. *Nature* **388**, 798-801, doi:10.1038/42062 (1997).
- 121 Festuccia, N., Gonzalez, I., Owens, N. & Navarro, P. Mitotic bookmarking in development and stem cells. *Development* **144**, 3633-3645, doi:10.1242/dev.146522 (2017).
- 122 Beisson, J. *et al.* Mass culture of *Paramecium tetraurelia*. *Cold Spring Harbor protocols* **2010**, pdb prot5362, doi:10.1101/pdb.prot5362 (2010).
- 123 Beisson, J. *et al.* Maintaining clonal *Paramecium tetraurelia* cell lines of controlled age through daily reisolation. *Cold Spring Harbor protocols* **2010**, pdb prot5361, doi:10.1101/pdb.prot5361 (2010).
- 124 Katoh, K., Rozewicki, J. & Yamada, K. D. MAFFT online service: multiple sequence alignment, interactive sequence choice and visualization. *Briefings in bioinformatics* **20**, 1160-1166, doi:10.1093/bib/bbx108 (2019).
- 125 Marchler-Bauer, A. *et al.* CDD: a Conserved Domain Database for the functional annotation of proteins. *Nucleic acids research* **39**, D225-229, doi:10.1093/nar/gkq1189 (2011).
- 126 Arnaiz, O. *et al.* Improved methods and resources for *paramecium* genomics: transcription units, gene annotation and gene expression. *BMC genomics* **18**, 483, doi:10.1186/s12864-017-3887-z (2017).
- 127 Trifinopoulos, J., Nguyen, L. T., von Haeseler, A. & Minh, B. Q. W-IQ-TREE: a fast online phylogenetic tool for maximum likelihood analysis. *Nucleic acids research* **44**, W232-235, doi:10.1093/nar/gkw256 (2016).
- 128 Fire, A. *et al.* Potent and specific genetic interference by double-stranded RNA in *Caenorhabditis elegans*. *Nature* **391**, 806-811, doi:10.1038/35888 (1998).
- 129 Arnaiz, O. & Sperling, L. *ParameciumDB* in 2011: new tools and new data for functional and comparative genomics of the model ciliate *Paramecium tetraurelia*. *Nucleic acids research* **39**, D632-636, doi:10.1093/nar/gkq918 (2011).
- 130 Denby Wilkes, C., Arnaiz, O. & Sperling, L. ParTIES: a toolbox for *Paramecium* interspersed DNA elimination studies. *Bioinformatics* **32**, 599-601, doi:10.1093/bioinformatics/btv691 (2016).
- 131 Bechara, S., Kabbani, L., Maurer Alcalá, X. & Nowacki, M. Identification of novel, functional long non-coding RNAs involved in programmed, large scale genome rearrangements. *Rna*, doi:10.1261/rna.079134.122 (2022).
- 132 Rzeszutek, I., Swart, E. C., Pabian-Jewula, S., Russo, A. & Nowacki, M. Early developmental, meiosis-specific proteins - Spo11, Msh4-1, and Msh5 - Affect subsequent genome reorganization in *Paramecium tetraurelia*. *Biochimica et biophysica acta. Molecular cell research* **1869**, 119239, doi:10.1016/j.bbamcr.2022.119239 (2022).
- 133 Beisson, J. *et al.* DNA microinjection into the macronucleus of *paramecium*. *Cold Spring Harbor protocols* **2010**, pdb prot5364, doi:10.1101/pdb.prot5364 (2010).
- 134 Reuter, M. *et al.* Loss of the Mili-interacting Tudor domain-containing protein-1 activates transposons and alters the Mili-associated small RNA profile. *Nature structural & molecular biology* **16**, 639-646, doi:10.1038/nsmb.1615 (2009).

-
- 135 Uhlmann, F. SMC complexes: from DNA to chromosomes. *Nature reviews. Molecular cell biology* **17**, 399-412, doi:10.1038/nrm.2016.30 (2016).
- 136 De Piccoli, G., Torres-Rosell, J. & Aragon, L. The unnamed complex: what do we know about Smc5-Smc6? *Chromosome research : an international journal on the molecular, supramolecular and evolutionary aspects of chromosome biology* **17**, 251-263, doi:10.1007/s10577-008-9016-8 (2009).
- 137 Michelini, F. *et al.* From "Cellular" RNA to "Smart" RNA: Multiple Roles of RNA in Genome Stability and Beyond. *Chemical reviews* **118**, 4365-4403, doi:10.1021/acs.chemrev.7b00487 (2018).
- 138 Thattikota, Y. *et al.* Cdc48/VCP Promotes Chromosome Morphogenesis by Releasing Condensin from Self-Entrapment in Chromatin. *Molecular cell* **69**, 664-676 e665, doi:10.1016/j.molcel.2018.01.030 (2018).
- 139 Burmann, F. *et al.* An asymmetric SMC-kleisin bridge in prokaryotic condensin. *Nature structural & molecular biology* **20**, 371-379, doi:10.1038/nsmb.2488 (2013).
- 140 Murarka, P. & Srivastava, P. An improved method for the isolation and identification of unknown proteins that bind to known DNA sequences by affinity capture and mass spectrometry. *PLoS One* **13**, e0202602, doi:10.1371/journal.pone.0202602 (2018).
- 141 Gilmour, D. S. & Lis, J. T. In vivo interactions of RNA polymerase II with genes of *Drosophila melanogaster*. *Molecular and cellular biology* **5**, 2009-2018, doi:10.1128/mcb.5.8.2009-2018.1985 (1985).
- 142 Gade, P. & Kalvakolanu, D. V. Chromatin immunoprecipitation assay as a tool for analyzing transcription factor activity. *Methods in molecular biology* **809**, 85-104, doi:10.1007/978-1-61779-376-9_6 (2012).
- 143 Belaghzal, H., Dekker, J. & Gibcus, J. H. Hi-C 2.0: An optimized Hi-C procedure for high-resolution genome-wide mapping of chromosome conformation. *Methods* **123**, 56-65, doi:10.1016/j.ymeth.2017.04.004 (2017).
- 144 Gluck, F. *et al.* EasyProt--an easy-to-use graphical platform for proteomics data analysis. *Journal of proteomics* **79**, 146-160, doi:10.1016/j.jpro.2012.12.012 (2013).
- 145 Cox, J. & Mann, M. MaxQuant enables high peptide identification rates, individualized p.p.b.-range mass accuracies and proteome-wide protein quantification. *Nature biotechnology* **26**, 1367-1372, doi:10.1038/nbt.1511 (2008).
- 146 Mi, H., Muruganujan, A., Casagrande, J. T. & Thomas, P. D. Large-scale gene function analysis with the PANTHER classification system. *Nature protocols* **8**, 1551-1566, doi:10.1038/nprot.2013.092 (2013).
- 147 McCarthy, F. M. *et al.* AgBase: a unified resource for functional analysis in agriculture. *Nucleic acids research* **35**, D599-603, doi:10.1093/nar/gkg1936 (2007).
- 148 Thomas, P. D. *et al.* PANTHER: a browsable database of gene products organized by biological function, using curated protein family and subfamily classification. *Nucleic acids research* **31**, 334-341, doi:10.1093/nar/gkg115 (2003).
- 149 Galvani, A. & Sperling, L. RNA interference by feeding in *Paramecium*. *Trends in genetics : TIG* **18**, 11-12, doi:10.1016/s0168-9525(01)02548-3 (2002).
- 150 Cora, E. *et al.* The MID-PIWI module of Piwi proteins specifies nucleotide- and strand-biases of piRNAs. *Rna* **20**, 773-781, doi:10.1261/rna.044701.114 (2014).

8. Appendix

Supplementary Table S1. Differential expression genes between SMC4-2 and EV KD at late time point.

	baseMean	log2FoldChange	lfcSE	stat	pvalue	padj
PTET.51.1.G5220002	40.71833	21.51369	4.408693	4.879833	1.06E-06	0.000284
PTET.51.1.G0080326	32.65949	21.2026	4.409016	4.808918	1.52E-06	0.000358
PTET.51.1.G0210128	32.02327	21.17525	4.409048	4.802681	1.57E-06	0.000363
PTET.51.1.G2560008	26.69836	20.92597	4.409379	4.745786	2.08E-06	0.000443
PTET.51.1.G5840001	25.66103	20.87199	4.40946	4.733457	2.21E-06	0.000465
PTET.51.1.G0120376	32.64916	8.401617	1.600445	5.249551	1.52E-07	6.30E-05
PTET.51.1.G4230002	19.04111	7.654903	1.626836	4.705393	2.53E-06	0.000521
PTET.51.1.G0950057	56.83275	6.652865	1.21276	5.485721	4.12E-08	1.97E-05
PTET.51.1.G0460269	685.057	5.30066	0.505258	10.49099	9.50E-26	1.06E-21
PTET.51.1.G0680082	56.55277	5.202766	0.892612	5.828701	5.59E-09	3.67E-06
PTET.51.1.G1780066	56.55277	5.202766	0.892612	5.828701	5.59E-09	3.67E-06
PTET.51.1.G0190324	656.2619	4.513589	0.473992	9.522507	1.69E-21	1.42E-17
PTET.51.1.G0950056	168.0462	4.440877	0.549309	8.084484	6.24E-16	2.32E-12
PTET.51.1.G0910133	184.057	4.315784	0.572903	7.533182	4.95E-14	9.21E-11
PTET.51.1.G1290040	214.7117	4.310907	0.56506	7.629118	2.36E-14	5.28E-11
PTET.51.1.G0760010	130.2862	4.293149	0.684386	6.272989	3.54E-10	3.39E-07
PTET.51.1.G0740074	223.7873	4.251348	0.559518	7.598226	3.00E-14	6.28E-11
PGML5a	2031.005	4.249252	0.544829	7.799236	6.23E-15	1.60E-11
PTET.51.1.G1560014	523.7589	4.194562	0.469851	8.927437	4.36E-19	2.62E-15
PTET.51.1.G1410098	134.8058	4.194174	0.57794	7.257112	3.95E-13	6.62E-10
PTET.51.1.G0700198	84.95626	4.149045	0.728964	5.691697	1.26E-08	7.26E-06
PTET.51.1.G0690142	4122.739	3.936999	0.470598	8.36594	5.96E-17	2.50E-13
PTET.51.1.G0920152	346.0847	3.923691	0.589339	6.65778	2.78E-11	3.58E-08
PTET.51.1.G0370120	70.66986	3.877675	0.678655	5.71376	1.11E-08	6.49E-06
PTET.51.1.G0930036	1387.979	3.808416	0.567336	6.71281	1.91E-11	2.66E-08
PTET.51.1.G1660105	339.0518	3.804513	0.570187	6.672397	2.52E-11	3.37E-08
PTET.51.1.G1550066	3913.099	3.788689	0.501772	7.550612	4.33E-14	8.53E-11
PTET.51.1.G0020221	178.2637	3.774387	0.679003	5.558722	2.72E-08	1.52E-05
PTET.51.1.G1760029	33.51372	3.766921	0.833364	4.520137	6.18E-06	0.001072
PTET.51.1.G1240104	30.24863	3.744827	0.80014	4.680214	2.87E-06	0.000582
PTET.51.1.G0080272	861.277	3.732785	0.4637	8.049995	8.28E-16	2.77E-12

PTET.51.1.G0360075	38.99482	3.722471	0.880888	4.225816	2.38E-05	0.003097
PTET.51.1.G2080006	104.4516	3.659177	0.755907	4.840776	1.29E-06	0.000323
PTET.51.1.G0130368	705.9818	3.612385	0.456568	7.912037	2.53E-15	7.07E-12
PTET.51.1.G1300031	1316.057	3.535777	0.602317	5.870294	4.35E-09	3.10E-06
PTET.51.1.G1390004	70.81666	3.514586	0.858046	4.096035	4.20E-05	0.004939
PTET.51.1.G0890016	81.87751	3.460816	0.639799	5.40922	6.33E-08	2.94E-05
PTET.51.1.G0230275	113.3842	3.459901	0.591881	5.845599	5.05E-09	3.45E-06
PTET.51.1.G1270118	30.75336	3.459795	0.805711	4.294087	1.75E-05	0.002437
PTET.51.1.G0740032	29.85139	3.458307	0.779958	4.433964	9.25E-06	0.001434
PTET.51.1.G0970093	909.4569	3.455094	0.461216	7.491267	6.82E-14	1.20E-10
PTET.51.1.G0350183	224.8513	3.45189	0.622481	5.545376	2.93E-08	1.58E-05
PTET.51.1.G1570125	222.3059	3.438796	0.843702	4.075842	4.58E-05	0.005281
PTET.51.1.G1790053	141.6275	3.416503	0.589884	5.791819	6.96E-09	4.32E-06
PTET.51.1.G1190058	132.3896	3.387229	0.700372	4.836327	1.32E-06	0.000326
PTET.51.1.G0140247	454.6272	3.340586	0.51995	6.424821	1.32E-10	1.52E-07
PTET.51.1.G1030082	35.09834	3.303252	0.722917	4.569336	4.89E-06	0.000891
PTET.51.1.G1590019	2632.748	3.28974	0.671642	4.89806	9.68E-07	0.000265
PTET.51.1.G0860044	105.1833	3.288363	0.641295	5.127694	2.93E-07	0.000105
PTIWI08	805.5734	3.285098	0.475292	6.911751	4.79E-12	7.29E-09
PTET.51.1.G1090151	68.56817	3.283213	0.642023	5.113857	3.16E-07	0.00011
PTET.51.1.G1000012	582.4541	3.280811	0.59635	5.501489	3.77E-08	1.83E-05
PTET.51.1.G0210235	338.4711	3.27581	0.591792	5.535412	3.10E-08	1.65E-05
PTET.51.1.G0260271	197.0646	3.269804	0.637142	5.13199	2.87E-07	0.000104
PTET.51.1.G0150061	230.1202	3.268416	0.553312	5.907001	3.48E-09	2.60E-06
PTET.51.1.G1340123	1197.373	3.252477	0.682486	4.765629	1.88E-06	0.000409
PTET.51.1.G0860006	250.6767	3.213096	0.526024	6.108273	1.01E-09	9.12E-07
PTET.51.1.G1300051	65.29121	3.200415	0.633153	5.054726	4.31E-07	0.000142
PGML5b	840.5487	3.191825	0.531636	6.003776	1.93E-09	1.70E-06
PTET.51.1.G0740009	5603.293	3.187419	0.633586	5.030757	4.89E-07	0.000152
PTET.51.1.G0050231	68.92674	3.164081	0.595836	5.310322	1.09E-07	4.70E-05
PTET.51.1.G0550043	899.7438	3.147149	0.493723	6.374325	1.84E-10	1.99E-07
PTET.51.1.G0080273	538.5461	3.142084	0.621969	5.051834	4.38E-07	0.000142
PTET.51.1.G0950020	519.1471	3.12217	0.654368	4.771275	1.83E-06	0.000403
PTET.51.1.G0180198	1381.869	3.110291	0.468988	6.631923	3.31E-11	4.11E-08
PTET.51.1.G0360066	77.95532	3.094268	0.639124	4.841424	1.29E-06	0.000323
PTET.51.1.G0200051	701.4204	3.092402	0.520896	5.936696	2.91E-09	2.50E-06

PTET.51.1.G0860046	336.6854	3.069771	0.556678	5.514444	3.50E-08	1.75E-05
PTET.51.1.G0560201	54.09134	3.068474	0.664301	4.619102	3.85E-06	0.000742
PTET.51.1.G1500004	833.7234	3.055053	0.672208	4.544802	5.50E-06	0.000974
PTET.51.1.G1410092	213.4016	3.031674	0.623238	4.864391	1.15E-06	0.000298
PGML3a	514.2986	3.019893	0.582971	5.18018	2.22E-07	8.44E-05
PTET.51.1.G1500021	228.1698	3.019433	0.704807	4.284054	1.84E-05	0.002498
PTET.51.1.G1400105	160.2507	3.008773	0.654409	4.597696	4.27E-06	0.000795
PTET.51.1.G2630002	288.132	2.999124	0.596295	5.029597	4.92E-07	0.000152
PIE2	280.2876	2.978457	0.554192	5.374415	7.68E-08	3.48E-05
PTET.51.1.G0120140	1265.478	2.969349	0.471013	6.304177	2.90E-10	2.94E-07
PTET.51.1.G3820001	31.06187	2.966221	0.689143	4.304215	1.68E-05	0.002358
PTET.51.1.G1020165	2146.4	2.951828	0.534945	5.518002	3.43E-08	1.74E-05
PTET.51.1.G0070281	90.18804	2.946778	0.624989	4.714924	2.42E-06	0.000503
PTET.51.1.G1620005	211.9253	2.945819	0.498813	5.905655	3.51E-09	2.60E-06
PTMB.203, PTETG100132001	92.07212	2.925432	0.605446	4.831861	1.35E-06	0.000328
PTET.51.1.G0270188	30.78304	2.924083	0.719234	4.065552	4.79E-05	0.00544
PTET.51.1.G0030402	324.3273	2.922524	0.568282	5.142733	2.71E-07	9.96E-05
PTET.51.1.G0650036	552.0582	2.910121	0.454679	6.40038	1.55E-10	1.73E-07
PTET.51.1.G0070261	152.9081	2.874669	0.563474	5.101686	3.37E-07	0.000114
PTET.51.1.G1770066	33.27577	2.852072	0.693217	4.114252	3.88E-05	0.004629
PTET.51.1.G0120377	1037.544	2.85097	0.547239	5.209731	1.89E-07	7.62E-05
PTET.51.1.G1300067	329.2038	2.846041	0.549652	5.177901	2.24E-07	8.44E-05
sAG_51g	61.73219	2.843252	0.634583	4.480507	7.45E-06	0.001225
PTET.51.1.G1530121	725.1364	2.841345	0.48061	5.911958	3.38E-09	2.60E-06
ku70-1	766.8925	2.837117	0.594759	4.7702	1.84E-06	0.000403
PTET.51.1.G0260286	1532.243	2.832844	0.449056	6.308436	2.82E-10	2.94E-07
PTET.51.1.G0950019	1311.486	2.831603	0.69686	4.063376	4.84E-05	0.005472
PTET.51.1.G2860001	334.7067	2.830554	0.533893	5.301728	1.15E-07	4.86E-05
PTET.51.1.G1520043	5367.705	2.827908	0.489797	5.773638	7.76E-09	4.72E-06
PTET.51.1.G0810201	203.6296	2.820272	0.519775	5.425949	5.76E-08	2.72E-05
PGML4a	128.8772	2.819598	0.579477	4.86576	1.14E-06	0.000298
PTET.51.1.G0280071	156.729	2.815108	0.578502	4.866205	1.14E-06	0.000298
PTET.51.1.G0750201	87.73424	2.809246	0.610999	4.597792	4.27E-06	0.000795
PTET.51.1.G0970158	351.81	2.805533	0.720953	3.891421	9.97E-05	0.009933
PTET.51.1.G0400261	1200.415	2.798471	0.474077	5.902992	3.57E-09	2.60E-06

PTET.51.1.G1670111	547.2172	2.793773	0.481728	5.799487	6.65E-09	4.21E-06
PTET.51.1.G0820079	53.43555	2.787327	0.608543	4.58033	4.64E-06	0.000854
PGML2	372.3613	2.783207	0.517235	5.380929	7.41E-08	3.40E-05
SETb1	329.1162	2.782301	0.620196	4.486161	7.25E-06	0.001222
PTMB.205, PTETG100130001	113.2494	2.780495	0.603566	4.606776	4.09E-06	0.00077
PTET.51.1.G1590093	91.18207	2.778736	0.610625	4.550639	5.35E-06	0.000953
PGML3c	54.86999	2.775097	0.604637	4.589692	4.44E-06	0.000821
PTET.51.1.G1410101	96.85685	2.773006	0.609259	4.551444	5.33E-06	0.000953
PTET.51.1.G1440089	5924.881	2.769054	0.501817	5.518052	3.43E-08	1.74E-05
PTET.51.1.G0620172	346.0612	2.754072	0.62407	4.413082	1.02E-05	0.001544
PTET.51.1.G0160234	101.0379	2.749016	0.570449	4.819035	1.44E-06	0.000345
PTET.51.1.G1550035	208.6115	2.740887	0.5253	5.217754	1.81E-07	7.40E-05
PTET.51.1.G0920155	131.1203	2.726684	0.554091	4.921005	8.61E-07	0.000241
PTET.51.1.G0020207	51.01128	2.718359	0.599136	4.537133	5.70E-06	0.001005
PTET.51.1.G1580082	958.9166	2.715114	0.45831	5.924185	3.14E-09	2.56E-06
PTET.51.1.G0060408	1794.571	2.713553	0.551472	4.920569	8.63E-07	0.000241
PTET.51.1.G0970059	429.1529	2.707744	0.543015	4.986499	6.15E-07	0.000184
PTET.51.1.G1410093	1167.943	2.699896	0.456568	5.91346	3.35E-09	2.60E-06
PTET.51.1.G0020442	196.284	2.698962	0.533732	5.056776	4.26E-07	0.000141
NOWA2	2567.751	2.691485	0.558237	4.821399	1.43E-06	0.000343
PTET.51.1.G0440127	766.8217	2.682755	0.462616	5.799103	6.67E-09	4.21E-06
PTET.51.1.G0910001	53.78835	2.679645	0.654026	4.097151	4.18E-05	0.004932
PTET.51.1.G0050297	419.5044	2.67641	0.457695	5.847585	4.99E-09	3.45E-06
PTET.51.1.G0120047	63.96908	2.654335	0.576064	4.607709	4.07E-06	0.00077
PTET.51.1.G0040217	127.0865	2.649768	0.51921	5.103464	3.33E-07	0.000114
PTET.51.1.G0510207	46.75858	2.645398	0.666315	3.97019	7.18E-05	0.007587
PTET.51.1.G0440203	583.3799	2.640862	0.471728	5.598276	2.16E-08	1.23E-05
PTET.51.1.G0040036	1592.522	2.640707	0.494962	5.335167	9.55E-08	4.21E-05
PTET.51.1.G1280098	204.5025	2.639252	0.479603	5.50299	3.73E-08	1.83E-05
PTET.51.1.G1190050	493.1198	2.637954	0.639295	4.126348	3.69E-05	0.004479
PTET.51.1.G1070131	218.6531	2.634468	0.534803	4.926054	8.39E-07	0.000238
PiRPB1	2460.999	2.630865	0.625569	4.205554	2.60E-05	0.003355
PTET.51.1.G0120198	649.9158	2.627062	0.50006	5.25349	1.49E-07	6.25E-05
PTET.51.1.G6710001	134.7625	2.611914	0.581985	4.487937	7.19E-06	0.001222
PTET.51.1.G0570172	251.7891	2.611164	0.524902	4.974572	6.54E-07	0.000193

PTET.51.1.G2740007	768.0912	2.604055	0.489847	5.31606	1.06E-07	4.61E-05
PTET.51.1.G0580153	225.031	2.602068	0.523338	4.972063	6.62E-07	0.000193
PTET.51.1.G0320111	95.68941	2.596914	0.594487	4.368325	1.25E-05	0.001847
PTET.51.1.G0140243	508.2914	2.593007	0.560574	4.625627	3.73E-06	0.000727
PTET.51.1.G0110239	6606.55	2.582082	0.46509	5.551787	2.83E-08	1.55E-05
PTET.51.1.G0490010	125.5337	2.580456	0.513584	5.024412	5.05E-07	0.000155
PTET.51.1.G1210169	23468.07	2.579541	0.616348	4.185204	2.85E-05	0.003628
PTET.51.1.G0500162	328.0773	2.577497	0.502433	5.130031	2.90E-07	0.000104
PTET.51.1.G0400276	622.208	2.564517	0.477437	5.37142	7.81E-08	3.49E-05
PTET.51.1.G0100167	326.9162	2.556505	0.462731	5.524819	3.30E-08	1.73E-05
PTET.51.1.G0370143	61.06252	2.544095	0.618104	4.115964	3.86E-05	0.004627
PTET.51.1.G0110132	1969.304	2.519988	0.524264	4.806716	1.53E-06	0.000359
PTET.51.1.G1500049	43.70777	2.500593	0.634021	3.944026	8.01E-05	0.008257
PTET.51.1.G0730142	111.9686	2.497814	0.628727	3.972813	7.10E-05	0.007528
PTET.51.1.G0730048	45.69381	2.497235	0.634579	3.935264	8.31E-05	0.008511
NOWA1	1244.285	2.496632	0.55738	4.479223	7.49E-06	0.001225
PTET.51.1.G1130106	344.9909	2.483521	0.480796	5.165441	2.40E-07	8.93E-05
PTET.51.1.G0970003	486.3809	2.475304	0.483251	5.122193	3.02E-07	0.000106
PTET.51.1.G0680057	40.00062	2.473119	0.629147	3.930911	8.46E-05	0.00864
PTET.51.1.G1250162	97.15832	2.468204	0.531193	4.646526	3.38E-06	0.000673
PTET.51.1.G0610198	194.0407	2.465366	0.550048	4.482091	7.39E-06	0.001225
PTET.51.1.G0400181	1623.94	2.455199	0.59472	4.128329	3.65E-05	0.004466
DCL5	391.1537	2.454135	0.547896	4.479197	7.49E-06	0.001225
PTET.51.1.G0040071	116.5924	2.453062	0.515181	4.761555	1.92E-06	0.000412
PTET.51.1.G0940013	201.6209	2.445154	0.480517	5.088595	3.61E-07	0.000121
PTET.51.1.G0530225	218.4427	2.444252	0.552322	4.425412	9.63E-06	0.001479
PTET.51.1.G1180014	351.1036	2.442894	0.527688	4.629431	3.67E-06	0.000718
PTET.51.1.G0370136	74.22967	2.442789	0.574356	4.253094	2.11E-05	0.002791
PTET.51.1.G0440244	872.8997	2.437151	0.615563	3.959224	7.52E-05	0.007837
PTET.51.1.G1390096	305.243	2.435998	0.538761	4.521486	6.14E-06	0.001071
PTET.51.1.G0280060	116.5327	2.433382	0.57365	4.24193	2.22E-05	0.00291
PTET.51.1.G1130040	301.94	2.428765	0.499168	4.865631	1.14E-06	0.000298
PTET.51.1.G0380064	269.0768	2.422327	0.584566	4.143807	3.42E-05	0.00419
PTET.51.1.G1670070	603.9813	2.420244	0.487359	4.966034	6.83E-07	0.000197
PTET.51.1.G2550004	406.8497	2.42016	0.579875	4.173592	3.00E-05	0.003775
PTET.51.1.G0580061	650.3978	2.41614	0.493432	4.8966	9.75E-07	0.000265

PTET.51.1.G1660029	5517.256	2.414408	0.582067	4.147993	3.35E-05	0.00413
PTET.51.1.G0430272	130.2183	2.40415	0.50487	4.76192	1.92E-06	0.000412
PTET.51.1.G0120094	187.4943	2.388572	0.482202	4.953471	7.29E-07	0.000209
PTET.51.1.G0070139	1168.461	2.387628	0.552254	4.323425	1.54E-05	0.002171
H3P4	9110.24	2.382971	0.477626	4.989194	6.06E-07	0.000183
PTET.51.1.G0070416	146.5691	2.37141	0.582101	4.073882	4.62E-05	0.005303
PTET.51.1.G1250095	328.0021	2.371047	0.470652	5.037791	4.71E-07	0.000149
PTET.51.1.G0230221	206.7634	2.350453	0.496496	4.734083	2.20E-06	0.000465
PTET.51.1.G0630147	1865.088	2.339471	0.52224	4.47969	7.48E-06	0.001225
PTET.51.1.G0230023	559.1881	2.330033	0.456544	5.103634	3.33E-07	0.000114
PTET.51.1.G1180067	269.0999	2.325907	0.478994	4.85582	1.20E-06	0.000309
PTMB.219, PTETG100122001	1213.072	2.317893	0.445815	5.199227	2.00E-07	7.70E-05
epsilon-51D	66.14468	2.312644	0.58419	3.958722	7.54E-05	0.007837
PTET.51.1.G0660068	290.3745	2.31078	0.490484	4.711228	2.46E-06	0.000509
PTET.51.1.G0230328	717.4595	2.310656	0.477241	4.841701	1.29E-06	0.000323
PTET.51.1.G1530110	372.8879	2.310105	0.483309	4.779769	1.75E-06	0.000389
PTET.51.1.G2090002	443.2323	2.300989	0.476078	4.833215	1.34E-06	0.000328
PTET.51.1.G0350166	117.0893	2.29998	0.565598	4.066455	4.77E-05	0.005437
PTET.51.1.G0730130	487.829	2.299647	0.492079	4.673325	2.96E-06	0.000598
PtKu80-3	1586.418	2.294639	0.512947	4.473442	7.70E-06	0.001245
PTET.51.1.G1290041	211.0183	2.291167	0.494021	4.637795	3.52E-06	0.000694
PTET.51.1.G0660063	211.2992	2.288728	0.485106	4.717992	2.38E-06	0.000499
PTET.51.1.G0410123	2478.354	2.284122	0.467316	4.887751	1.02E-06	0.000275
PTET.51.1.G1560117	418.6633	2.28406	0.518736	4.403129	1.07E-05	0.00161
PTET.51.1.G0730088	122.5067	2.279981	0.547195	4.166669	3.09E-05	0.003834
PTET.51.1.G0550130	4679.534	2.26818	0.435724	5.205542	1.93E-07	7.62E-05
PTET.51.1.G0360089	198.4496	2.267642	0.509254	4.452871	8.47E-06	0.001338
PTET.51.1.G0120071	729.7377	2.26284	0.46792	4.835954	1.33E-06	0.000326
PTET.51.1.G0900199	641.9858	2.262316	0.472568	4.787284	1.69E-06	0.000383
PGML1	496.6463	2.255236	0.50389	4.475652	7.62E-06	0.001238
PTET.51.1.G0720026	277.3071	2.253309	0.460172	4.896661	9.75E-07	0.000265
PTET.51.1.G0320284	228.7547	2.252531	0.504406	4.465711	7.98E-06	0.001279
PTET.51.1.G0430206	471.3678	2.252493	0.446703	5.042483	4.60E-07	0.000147
PTET.51.1.G0430205	282.4239	2.248925	0.484349	4.643195	3.43E-06	0.00068
PTET.51.1.G0590028	72.74106	2.242661	0.565833	3.96347	7.39E-05	0.007779

PTET.51.1.G0460076	916.3596	2.242076	0.537508	4.171243	3.03E-05	0.003795
PTET.51.1.G1040164	136.3426	2.240305	0.562013	3.986217	6.71E-05	0.00716
PTET.51.1.G0030168	341.4735	2.232553	0.550964	4.052086	5.08E-05	0.005667
PTET.51.1.G0370037	494.6388	2.230852	0.459642	4.853458	1.21E-06	0.00031
PTET.51.1.G0990129	440.0647	2.2296	0.50411	4.422849	9.74E-06	0.00149
PTET.51.1.G0350295	849.363	2.224485	0.564676	3.939399	8.17E-05	0.008392
PTET.51.1.G1080182	546.8664	2.212443	0.493962	4.478976	7.50E-06	0.001225
PTET.51.1.G1000101	351.9914	2.211109	0.535955	4.125552	3.70E-05	0.004479
PTET.51.1.G0480017	223.4175	2.192723	0.511163	4.289675	1.79E-05	0.002456
PTET.51.1.G0900069	245.2465	2.189541	0.536429	4.081694	4.47E-05	0.005181
PTET.51.1.G0950081	2961.64	2.18286	0.43299	5.041365	4.62E-07	0.000147
PTET.51.1.G0030393	1942.252	2.180625	0.523033	4.169195	3.06E-05	0.003806
PTET.51.1.G0540171	359.3771	2.178693	0.542121	4.018832	5.85E-05	0.006422
PTET.51.1.G1830010	180.3891	2.17165	0.553591	3.92284	8.75E-05	0.008881
PTET.51.1.G0380169	560.3811	2.170141	0.471084	4.606692	4.09E-06	0.00077
PTET.51.1.G1300152	250.7813	2.169912	0.535997	4.048368	5.16E-05	0.005738
PTET.51.1.G0120304	501.0776	2.168201	0.518348	4.182908	2.88E-05	0.003651
PTET.51.1.G0320285	388.4793	2.164238	0.474714	4.559039	5.14E-06	0.000925
PTET.51.1.G1460041	939.697	2.161561	0.486287	4.445031	8.79E-06	0.001375
PTET.51.1.G1720081	385.1844	2.160682	0.5038	4.288766	1.80E-05	0.002456
PTET.51.1.G0180124	191.9209	2.158871	0.484721	4.453839	8.43E-06	0.001338
PTET.51.1.G1650089	282.0665	2.152482	0.534061	4.030406	5.57E-05	0.006134
PTET.51.1.G1560077	187.3277	2.139719	0.492396	4.345526	1.39E-05	0.002006
EZL4	82.91756	2.138917	0.54733	3.907912	9.31E-05	0.009391
PTET.51.1.G1150123	614.2262	2.137212	0.472973	4.518674	6.22E-06	0.001074
PTET.51.1.G0650095	1181.983	2.136757	0.479234	4.458697	8.25E-06	0.001315
PTET.51.1.G1170173	136.9032	2.134201	0.540341	3.949732	7.82E-05	0.008087
PTET.51.1.G0750138	1195.485	2.133276	0.444233	4.802155	1.57E-06	0.000363
PTET.51.1.G0160206	189.8574	2.132465	0.542708	3.929306	8.52E-05	0.008672
PTET.51.1.G0710091	270.7601	2.131505	0.505028	4.220569	2.44E-05	0.003151
PTET.51.1.G0080258	363.179	2.130887	0.489716	4.351269	1.35E-05	0.001962
PTET.51.1.G0800198	7233.238	2.119321	0.521089	4.067096	4.76E-05	0.005437
PTET.51.1.G0930087	653.1718	2.119229	0.474088	4.470113	7.82E-06	0.001259
PTET.51.1.G0680147	231.4977	2.118286	0.482961	4.386038	1.15E-05	0.001718
PTET.51.1.G0560236	219.31	2.108102	0.532219	3.960969	7.46E-05	0.007812
PTET.51.1.G0120102	228.5704	2.108008	0.517222	4.075638	4.59E-05	0.005281

PTET.51.1.G0630048	366.4367	2.103531	0.525748	4.001027	6.31E-05	0.006858
PTET.51.1.G0710159	304.3996	2.0932	0.487561	4.293209	1.76E-05	0.002437
PTET.51.1.G0560087	471.2201	2.091788	0.45269	4.620791	3.82E-06	0.00074
PTET.51.1.G1120122	258.908	2.080446	0.47328	4.395801	1.10E-05	0.00165
PTET.51.1.G1670032	192813.1	2.074888	0.511053	4.060025	4.91E-05	0.005514
PTET.51.1.G0730049	329.3651	2.073011	0.485438	4.27039	1.95E-05	0.002614
PTET.51.1.G0490131	118.5305	2.072974	0.502517	4.125178	3.70E-05	0.004479
PTET.51.1.G0910136	264.4539	2.069992	0.477622	4.333953	1.46E-05	0.002078
mtGb	747.1749	2.052756	0.499064	4.113213	3.90E-05	0.004634
PTET.51.1.G0090337	1038.254	2.046414	0.50969	4.015018	5.94E-05	0.006506
PTET.51.1.G0930132	249.2437	2.042952	0.478296	4.271313	1.94E-05	0.002614
PTET.51.1.G0740177	1565.875	2.036402	0.469124	4.340861	1.42E-05	0.00204
PTET.51.1.G1900001	274.9885	2.035641	0.47904	4.249415	2.14E-05	0.002826
PTET.51.1.G0980174	226.7236	2.029533	0.483448	4.198038	2.69E-05	0.003455
PTET.51.1.G0070099	1279.256	2.024488	0.456012	4.439553	9.01E-06	0.001404
PTET.51.1.G0480186	335.04	2.021889	0.478517	4.225322	2.39E-05	0.003097
PTET.51.1.G1640109	567.4071	2.020518	0.497368	4.062423	4.86E-05	0.005476
PTET.51.1.G0230268	868.5775	2.016391	0.471363	4.277786	1.89E-05	0.002549
PTET.51.1.G1210101	138.9781	2.007073	0.503484	3.986373	6.71E-05	0.00716
PTET.51.1.G0160137	121.1726	-2.01259	0.482558	-4.17067	3.04E-05	0.003795
PTET.51.1.G1330058	413.0646	-2.05203	0.47826	-4.29061	1.78E-05	0.002456
PTET.51.1.G1470167	398.0095	-2.05435	0.474002	-4.33404	1.46E-05	0.002078
PTET.51.1.G0260144	429.584	-2.08087	0.47325	-4.39697	1.10E-05	0.001649
PTET.51.1.G0620217	127.9542	-2.1171	0.488349	-4.33522	1.46E-05	0.002078
PTET.51.1.G0250252	247.7278	-2.12006	0.476252	-4.45156	8.52E-06	0.00134
PTET.51.1.G0800029	234.6636	-2.15313	0.527023	-4.08546	4.40E-05	0.005115
PTET.51.1.G1070064	1072.941	-2.16781	0.479905	-4.51718	6.27E-06	0.001076
PTET.51.1.G0230099	205.8165	-2.18512	0.48712	-4.4858	7.26E-06	0.001222
PTET.51.1.G0090176	771.705	-2.18894	0.468603	-4.6712	2.99E-06	0.000601
PTET.51.1.G0850039	401.906	-2.2259	0.570228	-3.90352	9.48E-05	0.009506
PTET.51.1.G0170227	236.0226	-2.2955	0.506151	-4.5352	5.75E-06	0.001009
PTET.51.1.G1160096	275.9696	-2.30286	0.521351	-4.41711	1.00E-05	0.001523
PTET.51.1.G0970001	51.83007	-2.37503	0.587607	-4.04186	5.30E-05	0.00588
PTET.51.1.G0590129	84.6369	-2.38701	0.523011	-4.56397	5.02E-06	0.000909
PTET.51.1.G0080386	59.27146	-2.38891	0.546799	-4.3689	1.25E-05	0.001847
PTET.51.1.G0580014	354.508	-2.41508	0.578287	-4.17626	2.96E-05	0.003745

PTET.51.1.G0880185	129.606	-2.43207	0.507082	-4.79619	1.62E-06	0.000371
PTET.51.1.G0930099	56.63102	-2.46537	0.548413	-4.49547	6.94E-06	0.001186
PTET.51.1.G0240243	636.4707	-2.48265	0.528552	-4.69708	2.64E-06	0.000539
PTET.51.1.G1650093	255.3306	-2.51486	0.505706	-4.97296	6.59E-07	0.000193
PTET.51.1.G1650045	45.56399	-2.51798	0.58523	-4.30254	1.69E-05	0.002366
PTET.51.1.G0750147	133.806	-2.56041	0.600603	-4.26306	2.02E-05	0.00268
PTET.51.1.G0970152	180.4474	-2.56528	0.512942	-5.00111	5.70E-07	0.000174
PTET.51.1.G0520074	156.2173	-2.59246	0.63399	-4.08912	4.33E-05	0.005053
PTET.51.1.G0760223	99.27008	-2.62027	0.503869	-5.2003	1.99E-07	7.70E-05
PTET.51.1.G0870018	50.07805	-2.6512	0.664547	-3.98949	6.62E-05	0.007131
PTET.51.1.G1540003	76.45525	-2.65376	0.553512	-4.79441	1.63E-06	0.000372
PTET.51.1.G0820146	96.50806	-2.7874	0.665356	-4.18934	2.80E-05	0.003576
PTET.51.1.G0290167	769.3246	-2.79062	0.535886	-5.2075	1.91E-07	7.62E-05
PTET.51.1.G0160050	53.28775	-2.84703	0.652296	-4.36464	1.27E-05	0.00187
PTET.51.1.G0020281	145.9975	-2.88207	0.504211	-5.716	1.09E-08	6.49E-06
PTET.51.1.G0010175	145.4726	-2.88557	0.599856	-4.81043	1.51E-06	0.000358
PTET.51.1.G0050186	60.00411	-2.89247	0.653542	-4.42584	9.61E-06	0.001479
PTET.51.1.G0020367	36.78415	-2.95233	0.617151	-4.7838	1.72E-06	0.000387
PTET.51.1.G0600108	2013.863	-3.00222	0.752746	-3.98835	6.65E-05	0.007142
PTET.51.1.G1210173	22.04244	-3.07927	0.719033	-4.28252	1.85E-05	0.002506
PTET.51.1.G0690122	28.35534	-3.12044	0.789109	-3.95438	7.67E-05	0.007956
PTET.51.1.G1270004	74.27108	-3.21308	0.697039	-4.60961	4.03E-06	0.00077
PTET.51.1.G1410005	25.50615	-3.21889	0.760336	-4.23351	2.30E-05	0.00301
PTET.51.1.G4980001	54.2862	-3.50393	0.590704	-5.93178	3.00E-09	2.51E-06
PTET.51.1.G0650058	574.3621	-3.58073	0.500155	-7.15925	8.11E-13	1.29E-09
PTET.51.1.G0690117	1159.077	-3.59992	0.534368	-6.73678	1.62E-11	2.36E-08
PTET.51.1.G0760177	87.57607	-3.65167	0.579859	-6.2975	3.02E-10	2.98E-07
PTET.51.1.G0230294	19.93125	-3.79325	0.793167	-4.78241	1.73E-06	0.000387
PTET.51.1.G0120225	16.4522	-4.04168	0.926857	-4.36063	1.30E-05	0.001897
PTET.51.1.G0400056	86.44225	-4.10707	0.631697	-6.50165	7.94E-11	9.50E-08
PTET.51.1.G1540004	14.93137	-5.021	1.097103	-4.5766	4.73E-06	0.000865
PTIWI10	2443.73	-5.15723	0.578201	-8.91943	4.69E-19	2.62E-15
PTIWI11	1734.302	-5.21111	0.447931	-11.6337	2.78E-31	4.65E-27
PTET.51.1.G0710033	81.41969	-5.49578	0.692059	-7.9412	2.00E-15	6.10E-12
PTIWI07	126.6251	-5.92237	0.695432	-8.5161	1.65E-17	7.89E-14
PTIWI06	998.904	-6.12354	0.525005	-11.6638	1.95E-31	4.65E-27

PTET.51.1.G4270003	24.03736	-8.21054	1.342599	-6.11541	9.63E-10	8.96E-07
Ptccn_icl9d	83.32795	-10.0037	1.295224	-7.7235	1.13E-14	2.71E-11

Supplementary Table S2. Differential expression of proteins identified by mass spectrometry from SMC4-1 and SMC4-2 Co-IP experiments at late time point.

Leading_Protein	Synonyms	Description	Score	OnOff WT vs SMC4_1	OnOff WT vs SMC4_2	OnOff SMC4_1 vs SMC4_2	Top3 log2FC SMC4_1 - WT	Top3 log2FC SMC4_2 - WT	Top3 log2FC SMC4_2 - SMC4_1
PTET.51.1.P0010184	PTMB.323, PTETG100077001	Nucleic acid-binding, OB-fold	17.419	SMC4_1		SMC4_1			
PTET.51.1.P0010254	PTMB.266	Surfeit locus 1/Shyl	31.621	SMC4_1	SMC4_2				-2.452939601
PTET.51.1.P0010279	PTMB.248c, PTETG100038001	P-loop containing nucleoside triphosphate hydrolase	61.028				2.107835054	1.104759802	-1.003075252
PTET.51.1.P0010297	PTMB.233	Rossmann-like alpha/beta/alpha sandwich fold	31.245				-	-	1.384103669
PTET.51.1.P0010326	PTMB.208	UvrABC system protein C	36.981	SMC4_1	SMC4_2				-0.178349541
PTET.51.1.P0010348	mag3, PTMB.190c	G surface protein, allelic form 156	21.388				1.989942861	3.963007169	1.973064308
PTET.51.1.P0010379	PTMB.166c, PTETG100158001	tRNA methyltransferase complex GCD14 subunit	51.496				1.955001852	2.71942523	0.764423378
PTET.51.1.P0010479	PTMB.81, PTETG100101001	2-oxoglutarate dehydrogenase E1 component	55.85		WT	SMC4_1	2.891235338		
PTET.51.1.P0010562	PTMB.14c, PTETG100074001	GrpE	18.65	SMC4_1	SMC4_2				-1.193046312
PTET.51.1.P0010572	PTETG100018001, PTMB.08c	Fibrinogen alpha/beta chain family	18.024	SMC4_1		SMC4_1			
PTET.51.1.P0020102		DNA/RNA-binding protein Alba-like	23.593				-	-	-0.257615102
							1.561043039	1.818658142	
PTET.51.1.P0020184		Calcineurin-like phosphoesterase	55.323				1.608248666	1.454068232	-0.154180435
PTET.51.1.P0020273		Carbon-nitrogen hydrolase	18.822	SMC4_1	SMC4_2				0.717268812
PTET.51.1.P0020350		TLDe domain	32.144	SMC4_1	SMC4_2				-3.875236638
PTET.51.1.P0020475		V-type ATP synthase subunit E	14.041	SMC4_1		SMC4_1			
PTET.51.1.P0030003		Isopenicillin N synthase-like	93.124				0.446955028	0.516986776	0.070031748
PTET.51.1.P0030017		Ulp1 protease family, C-terminal catalytic domain	26.117	SMC4_1		SMC4_1			
PTET.51.1.P0030065		Nucleoside diphosphate kinase B	25.866				-	0.317893291	1.777941479
							1.460048189		
PTET.51.1.P0030131		Protein kinase domain	38.952				0.390049091	-	-1.500058669
								1.110009578	
PTET.51.1.P0030193		Eukaryotic initiation factor 3, gamma subunit	11.329	SMC4_1		SMC4_1			
PTET.51.1.P0030205		NADP transhydrogenase, beta subunit	40.143				1.561873229	0.381939853	-1.179933376
PTET.51.1.P0030248		S-adenosyl-L-methionine-dependent methyltransferase-like	33.344	SMC4_1	SMC4_2				-1.196441278
PTET.51.1.P0030254			13.629	SMC4_1	SMC4_2				-2.672132695
PTET.51.1.P0030381		Protein transport protein Sec23B	26.467	SMC4_1	SMC4_2				0.331888012

PTET.51.1.P0030393	PTETG300037001	Transcription elongation factor Spt6	106.78			0.280491455	-	-1.015088396
							0.734596941	
PTET.51.1.P0040135		Peptidase M16 inactive domain	76.731			2.842187056	3.161357131	0.319170074
PTET.51.1.P0040137		Nascent polypeptide-associated complex subunit alpha	34.396			0.434630979	0.206621515	-0.228009464
PTET.51.1.P0040233	PTETG400003001	Biotin synthase	35.47	SMC4_1	SMC4_2			-0.38740496
PTET.51.1.P0040314		Alpha/beta hydrolase family	12.944	SMC4_1	SMC4_2			-1.433886732
PTET.51.1.P0040332		tRNA synthetases class I (W and Y)	79.117			0.180198757	0.483183437	0.30298468
PTET.51.1.P0040350		Peptidase C1-like family	12.816	WT	WT			
PTET.51.1.P0050055		Aldehyde dehydrogenase family	30.504	SMC4_1	SMC4_2			-2.158637257
PTET.51.1.P0050154		Cyclic nucleotide-binding domain	23.366	SMC4_1	SMC4_1			
PTET.51.1.P0050179		WD domain, G-beta repeat	73.8			0.156462689	0.550973586	0.394510897
PTET.51.1.P0050419		Coiled coil domain	11.82	WT	WT			
PTET.51.1.P0060018		Nop domain	18.445	SMC4_1	SMC4_1			
PTET.51.1.P0060034	PTIWI06	Piwi-like protein 1	24.925	SMC4_1	SMC4_1			
PTET.51.1.P0060144	PTETG600028001	Chloramphenicol acetyltransferase-like domain	41.118		WT			
						-	2.324672857	
PTET.51.1.P0060199		YTH domain-containing protein ECT3	13.86	SMC4_1	SMC4_1			
PTET.51.1.P0060205		High mobility group nucleosome-binding domain-containing protein 5	12.133	SMC4_1	SMC4_1			
PTET.51.1.P0060411		Serine/threonine-protein phosphatase 2A 65 kDa regulatory subunit A alpha isoform	19.92			1.162876546	-	-1.278753184
							0.115876638	
PTET.51.1.P0070001		Isopenicillin N synthase-like	59.826			0.233963125	-0.22944554	-0.463408665
PTET.51.1.P0070020	PTETG700003001	Ubiquitin-conjugating enzyme/RWD-like	24.448			0.25256362	-1.30899206	-1.56155568
PTET.51.1.P0070092		Glycylpeptide N-tetradecanoyltransferase 2	44.888			-0.72925668	-2.15732847	-1.42807179
PTET.51.1.P0070145		Coiled coil domain	11.286	SMC4_1	SMC4_1			
PTET.51.1.P0070153		Ribosome biogenesis protein BRX1	18.028	WT	SMC4_2		1.584180061	
PTET.51.1.P0070340		S-adenosylmethionine synthetase	13.921			1.255192661	0.841024053	-0.414168608
PTET.51.1.P0070404		Mitochondrial substrate/solute carrier	54.414			6.556738303	4.561035413	-1.99570289
PTET.51.1.P0080015		Glycosyl hydrolases family 25	25.693	SMC4_1	SMC4_2			-1.489272596
PTET.51.1.P0080040		Pyroline-5-carboxylate reductase 1, mitochondrial	40.169			1.791039032	1.270707694	-0.520331339
PTET.51.1.P0080054		Metallo-dependent phosphatase-like	20.565			0.432367747	-	-0.583155066
							0.150787319	
PTET.51.1.P0080095		Prohibitin	30.648	SMC4_1	SMC4_1			
PTET.51.1.P0080169		Putative purine permease 20	11.397	SMC4_1	SMC4_1			
PTET.51.1.P0080174		Chaperonin Cpn60/TCP-1	82.126			-	-	0.083532473
						0.383829878	0.300297405	
PTET.51.1.P0080218		Citrate synthase, C-terminal domain	14.147	SMC4_1	SMC4_2			1.233861029
PTET.51.1.P0080260	PTETG800018001	Ubiquitin-conjugating enzyme	23.617			1.009567552	1.537666678	0.528099126
PTET.51.1.P0080295		Succinate dehydrogenase	73.57			1.889751223	3.001087723	1.1113365
PTET.51.1.P0080397	PTETG800045001	2-oxoglutarate dehydrogenase, mitochondrial	12.771	SMC4_1	SMC4_1			

PTET.51.1.P0080438		Lipoyl synthase, chloroplastic	19.087	SMC4_1	SMC4_2				-1.061753821
PTET.51.1.P0090053		40S ribosomal protein SA	13.042			-	0.981609103	0.448734959	1.430344062
PTET.51.1.P0090086		ATPase, V1/A1 complex, subunit E	34.584			1.521022788	1.639750351		0.118727563
PTET.51.1.P0090113		Translation elongation factor IF5A	47.885			-	0.07714448	0.034150444	0.111294923
PTET.51.1.P0090195		Alpha/Beta hydrolase fold	17.436	SMC4_1					SMC4_1
PTET.51.1.P0090213	PTETG900022001	Spliceosome-associated protein 130 B	154.53			-	0.795713227	0.808181324	1.603894551
PTET.51.1.P0090252		Structural maintenance of chromosomes protein 1	18.356		SMC4_2				SMC4_2
PTET.51.1.P0090255		Vacuolar protein sorting-associated protein 26	11.81		WT			-	SMC4_1
PTET.51.1.P0100002		Replication protein A 70 kDa DNA-binding subunit	30.691			0.590355933	-0.61280584		-1.203161774
PTET.51.1.P0100009		Putative F-box protein At3g21170	251.07			-	-	0.130721056	1.629018838
PTET.51.1.P0100011		Coiled coil domain	323.31			-	-1.22126825	0.405088547	-0.816179703
PTET.51.1.P0100050		Endoplasmic reticulum oxidoreductin 1	11.35	SMC4_1					SMC4_1
PTET.51.1.P0100097	PTETG1000030001	Adenosylhomocysteinase	100.08			0.042660057	2.851257011		2.808596954
PTET.51.1.P0100106		Ribosomal protein L3	36.793			0.702407944	1.131395661		0.428987717
PTET.51.1.P0100128		Regulator of chromosome condensation 1/beta-lactamase-inhibitor protein II	77.806	SMC4_1	SMC4_2				-1.606315422
PTET.51.1.P0100202		Probable enoyl-CoA hydratase echA8	25.29			-	-	1.126928877	0.101745669
PTET.51.1.P0100252	PTETG1000006001	Cytochrome c oxidase, subunit Vb	18.668	SMC4_1					SMC4_1
PTET.51.1.P0100278	PTETG1000002001	Enolase	123.51			-	-	0.337512013	1.189446027
PTET.51.1.P0100395		MORN motif	13.544		WT			0.759480328	SMC4_1
PTET.51.1.P0110022		Persulfide dioxygenase ETHE1, mitochondrial	30.063	SMC4_1					SMC4_1
PTET.51.1.P0110028		RuvB-like	18.679	SMC4_1					SMC4_1
PTET.51.1.P0110036		Armadillo-like helical	112.23			-	-	0.014427818	0.041542256
PTET.51.1.P0110039		60S ribosomal protein L10	62.998			4.552670661	3.599627459		-0.953043202
PTET.51.1.P0110119		Nucleotide-binding, alpha-beta plait	12.509	SMC4_1					SMC4_1
PTET.51.1.P0110137	PTETG1100001001	Thioredoxin domain-containing protein 3 homolog	11.612	SMC4_1					SMC4_1
PTET.51.1.P0110162		Calmodulin binding protein-like	12.439		WT			-	SMC4_1
PTET.51.1.P0110239		Uncharacterized protein YfdF	12.606	SMC4_1	SMC4_2				-0.792907888
PTET.51.1.P0110278		Succinyl-CoA ligase, alpha subunit	51.232			0.352119309	0.335368303		-0.016751006
PTET.51.1.P0110289	PIE2, PDSG2	Elongation factor Ts	46.202			1.134453695	-	1.622791075	-2.75724477
PTET.51.1.P0110362		Citrate synthase-like	69.304			1.493807884	1.834998943		0.341191059
PTET.51.1.P0110390		Protein kinase domain	11.475	SMC4_1	SMC4_2				0.822604204

PTET.51.1.P0110429		ATPase, F1 complex, delta/epsilon subunit, N-terminal	13.179			-	-	-0.346807798
						0.746699668	1.093507466	
PTET.51.1.P0120057		Protein kinase domain	17.373	SMC4_1	SMC4_1			
PTET.51.1.P0120086		T-complex protein 1 subunit beta	131.92			-	-	0.065286752
						0.109328783	0.044042031	
PTET.51.1.P0120113		Alpha/beta hydrolase domain-containing protein 11	18.855	SMC4_1	SMC4_1			
PTET.51.1.P0120119		Protein max	13.123	SMC4_1	SMC4_2			0.505966603
PTET.51.1.P0120205		Macroglobulin domain MG4	243.43	SMC4_1	SMC4_2			0.988791886
PTET.51.1.P0120274		DEAD-box ATP-dependent RNA helicase 15	45.209			2.911888405	2.891835029	-0.020053376
PTET.51.1.P0120277		Mitochondrial 2-oxoglutarate/malate carrier protein	72.134			0.849335348	-	-1.291598705
							0.442263356	
PTET.51.1.P0120293		Molybdopterin oxidoreductase	25.308	SMC4_1	SMC4_1			
PTET.51.1.P0120294		NAC domain	19.81			-	-	-0.244035951
						1.476503445	1.720539396	
PTET.51.1.P0120377		PHD-zinc-finger like domain	12.382		WT	SMC4_1	1.96136759	
PTET.51.1.P0130008		Protein STIP1 homolog	18.659	SMC4_1	SMC4_2			0.502132381
PTET.51.1.P0130113		MT-A70	11.673	SMC4_1	SMC4_1			
PTET.51.1.P0130197		Adenylate kinase	24.213	SMC4_1	SMC4_1			
PTET.51.1.P0130217	PTETG1300015001	HEAT repeats	43.859	SMC4_1	SMC4_1			
PTET.51.1.P0130319		Protein piccolo	17.033	SMC4_1	SMC4_1			
PTET.51.1.P0130320		Mannose-binding lectin	20.42	SMC4_1	SMC4_1			
PTET.51.1.P0140021		Citrate synthase-like	38.823		WT	SMC4_1	1.336657789	
PTET.51.1.P0140093		Mating-type locus allele B6 protein	18.697	SMC4_1	SMC4_1			
PTET.51.1.P0140342	arp2-1, PTETG1400002001	Actin-related protein	46.625			-	0.912499468	1.023535275
						0.111035807		
PTET.51.1.P0150014		V-type ATP synthase subunit I	13.147		WT	SMC4_1	-	
						2.497668145		
PTET.51.1.P0150066		ATP-NAD kinase-like domain	19.914			0.00894269	0.147573698	0.138631008
PTET.51.1.P0150089		Serine--tRNA ligase, cytoplasmic	70.172	SMC4_1	SMC4_2			0.252865885
PTET.51.1.P0150105		DNA/RNA-binding protein Alba-like	11.446			-	-	-1.146660891
						2.650666526	3.797327417	
PTET.51.1.P0150119		Ribosomal protein L6e	17.404	WT	SMC4_2			2.871930347
PTET.51.1.P0150223		Probable disease resistance protein At4g19520	25.131			0.372610564	-	-2.35810965
							1.985499086	
PTET.51.1.P0150275		Type III restriction enzyme, res subunit	11.555	SMC4_1	SMC4_1			
PTET.51.1.P0150343		ClpP/crotonase-like domain	49.709			-	-	0.337590239
						0.838646188	0.501055949	
PTET.51.1.P0160023		Ribosomal protein S10	14.546			1.526874572	1.913528156	0.386653584
PTET.51.1.P0160032		Ribosomal protein L30, ferredoxin-like fold domain	33.107			-	-	0.04346942
						0.563672687	0.520203266	
PTET.51.1.P0160123		WD domain, G-beta repeat	12.564	SMC4_1	SMC4_1			
PTET.51.1.P0160139		Metallopeptidase family M24	11.914			-0.64291707	0.231691677	0.874608747
PTET.51.1.P0160163		Phospholipid-transporting ATPase IG	13.741	SMC4_1	SMC4_1			
PTET.51.1.P0160240		Ultraviolet-B receptor UVR8	21.819	SMC4_1	SMC4_2			-2.031172549

PTET.51.1.P0160244		Protein disulfide-isomerase A6	30.408	WT	SMC4_1	1.886979141		
PTET.51.1.P0160330		Putative mitochondrial 2-oxoglutarate/malate carrier protein	28.014	SMC4_1	SMC4_2			-2.866191739
PTET.51.1.P0160340		Coiled-coil domain-containing protein 18	72.105			-	-	0.848192497
PTET.51.1.P0160357		Coiled coil domain	323.31			-1.0774546	-	-0.458635978
							1.536090578	
PTET.51.1.P0170077	NOWA1	Coiled coil domain	19.672	SMC4_1	SMC4_2			-1.274407887
PTET.51.1.P0170151	PTETG1700002001	GDP dissociation inhibitor	33.656			1.383357078	2.849518574	1.466161497
PTET.51.1.P0170184		Polyribonucleotide nucleotidyltransferase	32.942			1.684678508	0.124522539	-1.560155969
PTET.51.1.P0170225		Baculoviral IAP repeat-containing protein 6	39.148			2.493843364	1.625314876	-0.868528489
PTET.51.1.P0170257		Protein of unknown function (DUF541)	189.41			0.667158036	0.363964075	-0.303193961
PTET.51.1.P0190251		Rhodanese-like domain	17.345	SMC4_1			SMC4_1	
PTET.51.1.P0200201	KdB2	Cysteine synthase 2	82.37			-	2.767185277	3.416133369
						0.648948092		
PTET.51.1.P0200315		50S ribosomal protein L11	17.121	SMC4_1			SMC4_1	
PTET.51.1.P0200334		Methylmalonate-semialdehyde dehydrogenase	15.433			0.729894429	-	-1.149480216
							0.419585787	
PTET.51.1.P0210034		Ribosomal protein L10/acidic P0	22.042	SMC4_1	SMC4_2			-0.33495953
PTET.51.1.P0210041		D-isomer specific 2-hydroxyacid dehydrogenase, catalytic domain	62.109			1.590870709	1.766809321	0.175938612
PTET.51.1.P0210175		AMP-binding enzyme	37.426	SMC4_1			SMC4_1	
PTET.51.1.P0210203		Ribosomal protein S7e	13.419	SMC4_1	SMC4_2			-0.200620291
PTET.51.1.P0210280	PTETG2100008001	Leishmanolysin-like peptidase	138.25			0.979620444	-0.05456776	-1.034188204
PTET.51.1.P0210302		DNA-directed RNA polymerase subunit alpha	44.1			0.074318978	-	-1.92168343
							1.847364452	
PTET.51.1.P0220003		Gamma carbonic anhydrase 3, mitochondrial	12.902		WT		SMC4_1	1.479151769
PTET.51.1.P0220057		Protein phosphatase 2C (PP2C)-like domain	26.306	SMC4_1			SMC4_1	
PTET.51.1.P0220116		T-complex protein 1 subunit zeta	74.619			-	-	-0.813816784
						0.879052388	1.692869172	
PTET.51.1.P0220177	PTETG2200025001	Insulin-like growth factor binding protein, N-terminal	18.965	SMC4_1			SMC4_1	
PTET.51.1.P0220197		Elongation factor 1-gamma 2	26.289			-	-	0.203009686
						1.253582662	1.050572976	
PTET.51.1.P0220247		Methionine--tRNA ligase, cytoplasmic	18.269	SMC4_1	SMC4_2			-0.412404028
PTET.51.1.P0220269	PPN2	Metallo-dependent phosphatase-like	78.135			1.192614105	0.276595123	-0.916018982
PTET.51.1.P0220270		Mitochondrial carrier protein	19.657	SMC4_1			SMC4_1	
PTET.51.1.P0230160		Peptidase M16 inactive domain	11.737	SMC4_1			SMC4_1	
PTET.51.1.P0230214		AMP-binding enzyme	27.086	SMC4_1	SMC4_2			0.182906893
PTET.51.1.P0230219		Paramecium surface antigen domain	38.651	SMC4_1	SMC4_2			3.824277118
PTET.51.1.P0230221		DNA-directed RNA polymerase subunit beta	20.079	SMC4_1	SMC4_2			-0.654581522
PTET.51.1.P0230249		Chaperonin Cpn60/TCP-1	19.551	SMC4_1	SMC4_2			-1.216301179

PTET.51.1.P0230261	PTETG230007001	Intraflagellar transport protein 74 homolog	11.875	SMC4_1	SMC4_1			
PTET.51.1.P0230286		Isocitrate/isopropylmalate dehydrogenase	116.93			-	-	0.481163673
						0.631028527	0.149864854	
PTET.51.1.P0250050		Plectin/S10, N-terminal	24.205	SMC4_1	SMC4_1			
PTET.51.1.P0250100		Calcium-binding mitochondrial carrier protein SCaMC-1	49.545	SMC4_1	SMC4_1			
PTET.51.1.P0250101		small GTPase Rab1 family profile.	25.154	SMC4_1	SMC4_1			
PTET.51.1.P0250236		Coiled coil domain	104.09			0.957156873	1.123070216	0.165913343
PTET.51.1.P0250319		Ribosomal protein L32	11.239	SMC4_1	SMC4_2			-1.019550834
PTET.51.1.P0260039		Ribosomal protein S2, eukaryotic/archaeal	135.05			-	1.229495822	1.879383884
						0.649888062		
PTET.51.1.P0260174	PTETG2600021001	Spliceosome-associated protein 130 B	25.664	SMC4_1	SMC4_2			3.270369529
PTET.51.1.P0270023		DNA polymerase epsilon subunit 2	11.846	SMC4_1	SMC4_1			
PTET.51.1.P0270129		UvrABC system protein C	82.496			0.189550989	0.83097285	0.641421861
PTET.51.1.P0270186		DnaJ protein homolog	18.166	SMC4_1	SMC4_2			-2.499273707
PTET.51.1.P0270209	PTETG2700003001	P-loop containing nucleoside triphosphate hydrolase	287.66			0.658647673	0.780559098	0.121911426
PTET.51.1.P0270210		Uridine kinase-like protein 3	20.385			1.087676047	0.854083649	-0.233592398
PTET.51.1.P0270239		Enoyl-CoA hydratase, mitochondrial	46.129			0.326029743	0.553293501	0.227263758
PTET.51.1.P0280112		Porphobilinogen synthase	11.91		SMC4_2	SMC4_2		
PTET.51.1.P0280283		Eukaryotic translation initiation factor 3 subunit I	18.716	SMC4_1	SMC4_1			
PTET.51.1.P0290214		Protein kinase-like domain	11.654	SMC4_1	SMC4_1			
PTET.51.1.P0300021		Fumarate lyase family	198.11			-	-	-1.356612478
						0.139729929	1.496342407	
PTET.51.1.P0300158		Leishmanolysin-like peptidase	18.824	SMC4_1	SMC4_2			0.350665289
PTET.51.1.P0300222	PTETG3000005001	Parkin co-regulated protein	17.969	SMC4_1	SMC4_2			-0.076671389
PTET.51.1.P0300231		Calcium and integrin-binding family member 2 (Fragment)	11.863	SMC4_1	SMC4_2			-0.72900787
PTET.51.1.P0300272		Clathrin heavy chain 1	13.381	SMC4_1	SMC4_1			
PTET.51.1.P0300291		Coiled coil domain	71.174			0.422381266	0.45692988	0.034548614
PTET.51.1.P0310063		Proteasome component (PCI) domain	11.76	SMC4_1	SMC4_1			
PTET.51.1.P0310118		Aspartate/other aminotransferase	50.932			-	-	-0.843071769
						0.109647509	0.952719278	
PTET.51.1.P0310186		Peptidase C1A	62.116			0.43354445	-	-3.329598419
							2.896053969	
PTET.51.1.P0310192		60S ribosomal protein L6E	37.123			0.58052149	0.313217362	-0.267304128
PTET.51.1.P0310216		Mitochondrial carrier protein	13.157	SMC4_1	SMC4_1			
PTET.51.1.P0320031		Carbonic anhydrase 2	11.286			-	-	0.367598946
						0.544950612	0.177351666	
PTET.51.1.P0320061		Tetrapeptide repeat protein 7A	56.745			2.522862006	0.791100914	-1.731761092
PTET.51.1.P0320109		Paramecium surface antigen domain	258		SMC4_2	SMC4_2		
PTET.51.1.P0320151	act1_3	Actin-related protein	266.05			2.351626061	2.722879407	0.371253346
PTET.51.1.P0320296		Aldehyde dehydrogenase family	200.25			0.002931382	-	-1.030381103
							1.027449721	

PTET.51.1.P0330075	PtSMC2-1, SMC2	P-loop containing nucleoside triphosphate hydrolase	312.21			6.06350107	6.558768196	0.495267126
PTET.51.1.P0330130		ATP synthase subunit a	12.069	SMC4_1	SMC4_1			
PTET.51.1.P0330220	Hsp70Pt01, PTETG3300001001	Heat shock 70 kDa protein 5	57.713			2.200872247	1.996549596	-0.204322651
PTET.51.1.P0330225		ATP synthase subunit alpha, mitochondrial	225.99			0.350177958	-	-0.563397154
PTET.51.1.P0330227		Pyruvate, phosphate dikinase	11.033	SMC4_1	SMC4_1		0.213219196	
PTET.51.1.P0330250		6-phosphofructo-2-kinase/fructose-2,6-bisphosphatase 4	18.119		SMC4_2	SMC4_2		
PTET.51.1.P0330264		Thiamin diphosphate-binding fold	19.138			0.720461985	-	-1.348762054
PTET.51.1.P0340161	PTETG3400005001	Aldehyde/histidinol dehydrogenase	19.861	WT	SMC4_1	1.093478881		
PTET.51.1.P0340162	PTETG3400002001	EF-hand domain pair	74.555			0.032398142	-	-0.106889804
PTET.51.1.P0340170		Enoyl-CoA hydratase/isomerase	20.492			-	-	-1.731733771
PTET.51.1.P0340171		Armadillo-like helical	40.073			1.026576652	2.758310423	
PTET.51.1.P0340171		Armadillo-like helical	40.073			0.608533219	-	-1.457233021
PTET.51.1.P0340233		ATP-dependent 6-phosphofructokinase 7	12.872	WT	SMC4_1	1.154499788		
PTET.51.1.P0340238		Ribosomal protein S6e	25.404	SMC4_1	SMC4_2			0.302843197
PTET.51.1.P0350129		Isocitrate and isopropylmalate dehydrogenases family	23.909	SMC4_1	SMC4_2			-2.204176974
PTET.51.1.P0350184		Tubby C-terminal-like domain	27.508			-	-	-2.303016209
PTET.51.1.P0350280		Sensory histidine kinase/phosphatase NtrB	62.898			1.228503834	3.531520044	
PTET.51.1.P0360019		Isoleucine--tRNA ligase, cytoplasmic	19.017	SMC4_1	SMC4_2			0.275004612
PTET.51.1.P0360034		Delta-1-pyrroline-5-carboxylate dehydrogenase 12A1, mitochondrial	11.487			0.011311024	-	-0.275200256
PTET.51.1.P0360064		Acyl-CoA dehydrogenase/oxidase C-terminal	11.996	SMC4_1	SMC4_1			
PTET.51.1.P0360133		Coiled coil domain	12.653	SMC4_1	SMC4_1			
PTET.51.1.P0360184		GroEL-like equatorial domain	12.133	SMC4_1	SMC4_1			
PTET.51.1.P0360228		AIR synthase-related protein, C-terminal domain	12.142	WT	SMC4_2		-	0.257230755
PTET.51.1.P0370010		Cytochrome b-c1 complex subunit Rieske-2, mitochondrial	43.425			0.968822761	0.525989773	-0.442832988
PTET.51.1.P0370172		Isocitrate and isopropylmalate dehydrogenases family	86.542			1.957771629	-	-3.339697765
PTET.51.1.P0370298		Superoxide dismutase	19.22			1.381926136		
PTET.51.1.P0370298		Superoxide dismutase	19.22			-	-	-2.889250719
PTET.51.1.P0380053		High frequency lysogenization protein HflD homolog	99.343	SMC4_1	SMC4_2	0.911859892	3.801110611	
PTET.51.1.P0380053		High frequency lysogenization protein HflD homolog	99.343	SMC4_1	SMC4_2			-1.152086789
PTET.51.1.P0380073	PGML2	Transposase IS4	17.832	SMC4_1	SMC4_1			
PTET.51.1.P0380195	GAPDH	Glyceraldehyde/Erythrose phosphate dehydrogenase family	162.46			2.265369893	1.99806137	-0.267308523
PTET.51.1.P0380223		Chromo (CHR)romatin Organisation MOdifier) domain	55.977	SMC4_1	SMC4_2			-0.741023612
PTET.51.1.P0380286		Pentatricopeptide repeat-containing protein At3g29230	76.354	SMC4_1	SMC4_2			-1.02924861

PTET.51.1.P0390035	PTETG390002001	Cytochrome c oxidase subunit 1+2	12.741		SMC4_2	SMC4_2			
PTET.51.1.P0400049	Hsp70P07, PTETG4000011001	Heat shock protein 70 family	180.93				1.36269449	1.892984613	0.530290123
PTET.51.1.P0400094		o-succinylbenzoate synthase	53.822				0.628905735	0.170428294	-0.458477441
PTET.51.1.P0400246		Coiled coil domain	25.082	SMC4_1	SMC4_2				-1.62934145
PTET.51.1.P0400271		Protein kinase-like domain	86.474				0.493840028	-	-0.596261609 0.102421581
PTET.51.1.P0410006		Serine/threonine-protein phosphatase 6 catalytic subunit	13.451	SMC4_1		SMC4_1			
PTET.51.1.P0410041		T-complex protein 1 subunit epsilon	67.486				-0.43536455	-	0.275010786 0.160353763
PTET.51.1.P0410063	PtSMC4-1, SMC4	P-loop containing nucleoside triphosphate hydrolase	227.5	SMC4_1		SMC4_1			
PTET.51.1.P0410099		5-methyltetrahydropteroyltriglutamate-homocysteine methyltransferase	24.129				0.169590236	-	-1.313040149 1.143449914
PTET.51.1.P0410101		Prephenate dehydrogenase	30.759	SMC4_1	SMC4_2				-1.566692993
PTET.51.1.P0410180		NADH dehydrogenase ubiquinone Fe-S protein 4, mitochondrial	24.597	SMC4_1	SMC4_2				-1.409215414
PTET.51.1.P0410229		Agglutinin alpha chain	12.322	WT	WT				
PTET.51.1.P0420093	vATPase_B2, PTETG4200001001	P-loop containing nucleoside triphosphate hydrolase	83.715				0.94134053	0.638551971	-0.302788559
PTET.51.1.P0420119		Ribosomal protein L24e-related	51.697				2.365595125	0.065761182	-2.299833943
PTET.51.1.P0420242		NADH dehydrogenase	67.064	SMC4_1		SMC4_1			
PTET.51.1.P0430034		Aminoacyl-tRNA synthetase, class II (D/K/N)-like	99.66				4.751919598	4.584256565	-0.167663034
PTET.51.1.P0430169		Dehydrogenase E1 component	18.867	SMC4_1		SMC4_1			
PTET.51.1.P0430270		60S acidic ribosomal protein P0	26.064	SMC4_1	SMC4_2				0.009100119
PTET.51.1.P0440040		UPF0302 protein YpiB	14.147	SMC4_1		SMC4_1			
PTET.51.1.P0450025		WD40/YVTN repeat-like-containing domain	13.023	SMC4_1		SMC4_1			
PTET.51.1.P0450054		ATP-dependent helicase/nuclease subunit A	65.617	SMC4_1		SMC4_1			
PTET.51.1.P0450076		ARP2/3 complex, 16kDa subunit (p16-Arc)	32.831				-	0.128919141	0.341973635 0.213054494
PTET.51.1.P0450077	PtSMC2-2, SMC2, PTETG4500016001	Structural maintenance of chromosomes protein 2-1	26.079	SMC4_1	SMC4_2				0.194467034
PTET.51.1.P0450094		Glutathione synthetase	71.076				-	2.087092866	2.331583123 0.244490257
PTET.51.1.P0450140	PTETG4500010001	Ribosomal protein S15	35.385				-	-	0.46001534 0.747229521 0.287214182
PTET.51.1.P0450180		DNA mismatch repair protein MSH7	47.961		WT	SMC4_1	1.596631365		
PTET.51.1.P0450187		Probable cinnamyl alcohol dehydrogenase 2	13.45		SMC4_2	SMC4_2			
PTET.51.1.P0450229		Mitochondrial-processing peptidase subunit beta	30.851	SMC4_1	SMC4_2				1.066887234
PTET.51.1.P0450230		NAD(P)-binding domain	93.916				0.658565356	0.583027761	-0.075537594
PTET.51.1.P0460020		TCP-1/cpn60 chaperonin family	84.724				-	-	0.129251713 0.723045446 0.593793734
PTET.51.1.P0460022		Thioredoxin	19.246		WT	SMC4_1	0.811512224		

PTET.51.1.P0460036		Leucine-rich repeat, SDS22-like subfamily	31.763	SMC4_1	SMC4_1			
PTET.51.1.P0460041		Chaperonin Cpn60/TCP-1	28.153	SMC4_1	SMC4_2			-2.728400173
PTET.51.1.P0460076		P-loop containing nucleoside triphosphate hydrolase	38.887	SMC4_1	SMC4_2			-3.03607072
PTET.51.1.P0460136		Inorganic polyphosphate/ATP-NAD kinase	64.351			4.259209253	5.065061732	0.805852479
PTET.51.1.P0460194	PTETG4600006001	Phosphoenolpyruvate carboxykinase	53.39			1.421388448	1.814765312	0.393376863
PTET.51.1.P0470012		Ribosomal L30 N-terminal domain	12.157			0.410636505	0.461470135	0.050833631
PTET.51.1.P0470151		Trimeric LpxA-like	33.512		WT	SMC4_1	2.635407607	
PTET.51.1.P0470179		Coiled coil domain	18.36	SMC4_1		SMC4_1		
PTET.51.1.P0470190		Arsenite methyltransferase	47.969	SMC4_1	SMC4_2			-0.687532832
PTET.51.1.P0480006	PTETG4800001001	Guanine nucleotide-binding protein subunit beta-like protein	323.31			-0.46234253	-	-0.881693641
PTET.51.1.P0480063		Phosphofructokinase domain	103.1			1.062554201	-	-2.638041938
PTET.51.1.P0480070		Protein male abnormal 21	11.956	WT		SMC4_2	1.481110931	
PTET.51.1.P0480074		NADH-ubiquinone oxidoreductase, 21kDa subunit, N-terminal	11.47	SMC4_1		SMC4_1		
PTET.51.1.P0480132	PTETG4800002001	EF-hand domain pair	18.41			1.023181836	-0.67694217	-1.700124006
PTET.51.1.P0480261		Eukaryotic porin/Tom40	12.829	SMC4_1		SMC4_1		
PTET.51.1.P0490112		Calpain family cysteine protease	25.128		WT	SMC4_1	0.908134307	
PTET.51.1.P0490213		Gamma-crystallin-related	44.968			1.862257539	2.019732382	0.157474843
PTET.51.1.P0490229		Replication protein 1a	18.536	SMC4_1		SMC4_1		
PTET.51.1.P0500041		Coiled coil domain	117.83	SMC4_1	SMC4_2			-1.277202834
PTET.51.1.P0500099		40S ribosomal protein S15a	21.291			-	-	0.357009926
PTET.51.1.P0500184	GapC	Glyceraldehyde/Erythrose phosphate dehydrogenase family	20.008	SMC4_1	SMC4_2	0.816570125	0.459560199	-1.359295245
PTET.51.1.P0500227		Serine/threonine-protein kinase ATG1b	11.724	SMC4_1		SMC4_1		
PTET.51.1.P0510037		Ribosomal L28e protein family	12.482	SMC4_1	SMC4_2			1.425011988
PTET.51.1.P0510055		Ribosomal protein S3Ae	18.499	SMC4_1		SMC4_1		
PTET.51.1.P0510092		Proteasome component ECM29/Translational activator GCN1	11.148	SMC4_1		SMC4_1		
PTET.51.1.P0510120		Ribosomal protein L6	55.558			4.959577879	5.269939715	0.310361836
PTET.51.1.P0510134	PTETG5100001001, AK2	Arginine kinase	39.629		SMC4_2	SMC4_2		
PTET.51.1.P0510147	sAG_51C	Paramecium surface antigen domain	11.685		SMC4_2	SMC4_2		
PTET.51.1.P0510203		Cyclophilin-like domain	13.69			-	-	-0.180291235
PTET.51.1.P0520133		Elongation factor Tu	33.276	SMC4_1		SMC4_1		
PTET.51.1.P0520161		Cyclophilin-like domain	12.743		WT	SMC4_1	1.087725893	
PTET.51.1.P0520173	KdC1	Porin domain	112.39			2.133198112	2.417501713	0.2843036
PTET.51.1.P0530017		Armadillo-type fold	19.237					-1.554547074
PTET.51.1.P0530030		P-loop containing nucleoside triphosphate hydrolase	196.08			0.005650187	-	-0.380224053
							0.374573867	

PTET.51.1.P0530059		Skp1 family, tetramerisation domain	24.501		WT	SMC4_1	1.370356504		
PTET.51.1.P0530127		Chaperonin Cpn60/TCP-1	12.708	SMC4_1		SMC4_2			-1.555673662
PTET.51.1.P0530165		alpha/beta hydrolase fold	73.402	SMC4_1		SMC4_2			-2.066899206
PTET.51.1.P0530218		RAC serine/threonine-protein kinase	17.797	SMC4_1			SMC4_1		
PTET.51.1.P0530254		TCP-1/cpn60 chaperonin family	85.122				0.314480304	0.490167007	0.175686703
PTET.51.1.P0530256		Succinyl-CoA synthetase, beta subunit	52.085	SMC4_1			SMC4_1		
PTET.51.1.P0540213		Pyruvate/Phosphoenolpyruvate kinase-like domain	24.34		WT	SMC4_1	0.563096121		
PTET.51.1.P0550098		von Willebrand factor type A domain	11.557	SMC4_1			SMC4_1		
PTET.51.1.P0550100		Tropomyosin like	11.464		WT	SMC4_1	0.257315153		
PTET.51.1.P0550159		Protein-tyrosine phosphatase-like	27.101	SMC4_1		SMC4_2			1.570436882
PTET.51.1.P0550219		Malate dehydrogenase	116.81				0.364104663	-	-0.483569993
								0.119465331	
PTET.51.1.P0560051		Peptidase CIA	32.697				-	-	-2.479947528
							0.913941133	3.393888661	
PTET.51.1.P0560226	PTETG5600001001	Cytochrome c oxidase subunit 1+2	48.751	SMC4_1		SMC4_2			3.681874706
PTET.51.1.P0570051	PGML5a	Transposase IS4	19.074	SMC4_1			SMC4_1		
PTET.51.1.P0570068		Luc7-like protein 3	48.671	SMC4_1		SMC4_2			0.270719889
PTET.51.1.P0570074		TNF receptor-associated protein 1 homolog, mitochondrial	34.733	SMC4_1		SMC4_2			-0.649767307
PTET.51.1.P0570163		Aconitase/isopropylmalate dehydratase	24.336		WT	SMC4_1	1.909683374		
PTET.51.1.P0580041		RuvB-like	13.861	SMC4_1			SMC4_1		
PTET.51.1.P0580083		Fibrillarin	56.081	SMC4_1		SMC4_2			-1.053108113
PTET.51.1.P0580112		Saccharopine dehydrogenase C-terminal domain	65.224				0.896053335	-	-1.128672864
								0.232619529	
PTET.51.1.P0580147		Superoxide dismutase, copper/zinc binding domain	25.876				0.490457282	1.504697606	1.014240324
PTET.51.1.P0590040	PTETG5900041001	Ribosomal L27e protein family	18.356	SMC4_1		SMC4_2			1.195422691
PTET.51.1.P0590042		60S ribosomal protein L6E	24.225				2.424388281	2.142912527	-0.281475754
PTET.51.1.P0590059		Ribosomal protein L22/L17, eukaryotic/archaeal	13.811	SMC4_1		SMC4_2			0.807889943
PTET.51.1.P0590135	PtSMC4-2, SMC4	RecF/RecN/SMC, N-terminal	243.16	SMC4_1		SMC4_2			5.696556993
PTET.51.1.P0590146	DRPC1	Dynamin central region	11.664	SMC4_1		SMC4_2			0.062880742
PTET.51.1.P0590225		Ribosomal protein L14b/L23e	124.16				0.665724657	0.259025419	-0.406699238
PTET.51.1.P0600091		Ribosomal protein S9/S16	27.773				3.001018729	2.4794536	-0.521565129
PTET.51.1.P0600104	KdC2	Uncharacterized killer plasmid pGKL-2 helicase	11.171	SMC4_1		SMC4_2			0.814148221
PTET.51.1.P0600114		Cyclophilin-like domain	36.814				0.674016279	-	-1.136866316
								0.462850037	
PTET.51.1.P0600152		Prephenate dehydrogenase	19.692					-	0.622636357
PTET.51.1.P0600185		60S ribosomal protein L14	12.315	SMC4_1		SMC4_2			0.502231667
PTET.51.1.P0600189		Pyruvate dehydrogenase E1 component subunit beta	17.805	SMC4_1			SMC4_1		
PTET.51.1.P0610066	PTETG610008001	AAA domain	13.307		WT	SMC4_1	0.629025916		

PTET.51.1.P0610077	PTETG6100010001	Chloramphenicol acetyltransferase-like domain	25.011			-0.08085226	-	-2.875649093
							2.956501353	
PTET.51.1.P0610150		Glycine cleavage system P protein	26.278	SMC4_1	SMC4_2			-1.899402178
PTET.51.1.P0610190		SecY translocase	24.893			1.848137737	0.709782674	-1.138355063
PTET.51.1.P0610217		Kinesin-like protein	11.038	SMC4_1				SMC4_1
PTET.51.1.P0610254		Probable mitochondrial import receptor subunit TOM40-2	27.925	SMC4_1	SMC4_2			-2.119280759
PTET.51.1.P0620102		Staphylococcal nuclease (SNase-like), OB-fold	17.655	SMC4_1				SMC4_1
PTET.51.1.P0620182		Creatine kinase M-type	19.196	SMC4_1				SMC4_1
PTET.51.1.P0620230		Coiled coil domain	11.5	WT	WT			
PTET.51.1.P0620246		Peptidase M1, alanine aminopeptidase/leukotriene A4 hydrolase	65.156	SMC4_1	SMC4_2			1.022904209
PTET.51.1.P0620250		Ribosomal protein L31e	17.692	SMC4_1				SMC4_1
PTET.51.1.P0630027	can-A5-2, PTETG6300001001	ATP synthase delta (OSCP) subunit	50.113			1.477651728	0.616067503	-0.861584225
PTET.51.1.P0630039		2-oxoglutarate dehydrogenase E1 component	57.803		WT			SMC4_1
PTET.51.1.P0630139		Fructose-1-6-bisphosphatase, N-terminal domain	11.475	WT	WT			
PTET.51.1.P0640022	PtSERCA1, SERCA, SERCA1	Calcium-transporting ATPase 2, endoplasmic reticulum-type	92.398			1.906902643	-	-1.964586834
							0.057684191	
PTET.51.1.P0650012		Thioredoxin	49.994	SMC4_1				SMC4_1
PTET.51.1.P0650034	STO7, PtSto7, STO	Stomatin-like protein 2, mitochondrial	12.2					SMC4_2
								SMC4_2
PTET.51.1.P0660034	PTETG6600006001	Ubiquitin-like modifier-activating enzyme 1	30.16	SMC4_1	SMC4_2			0.384354978
PTET.51.1.P0660075		P-loop containing nucleoside triphosphate hydrolase	83.436			0.645849523	0.096721825	-0.549127698
PTET.51.1.P0660088		Ribosomal protein L22e	48.162			2.140610805	2.142047378	0.001436573
PTET.51.1.P0660146		Uncharacterized protein YggE	44.475			0.840886608	0.871096426	0.030209819
PTET.51.1.P0660147		Protein of unknown function DUF541	49.105			0.376209149	0.306949418	-0.069259731
PTET.51.1.P0670034	PTETG6700004001	Ubiquitin-conjugating enzyme/RWD-like	17.071			0.347719802	-	-1.01480021
							0.667080408	
PTET.51.1.P0670042		Thiol protease SEN102	13.361	SMC4_1	SMC4_2			2.037950184
PTET.51.1.P0670074		RNA recognition motif domain, eukaryote	23.026			-3.35645567	-	-0.144413722
							3.500869393	
PTET.51.1.P0670172		Ornithine aminotransferase	100.44			0.534834953	0.944850725	0.410015772
PTET.51.1.P0670236		Major vault protein, N-terminal	67.527	SMC4_1	SMC4_2			-0.201303798
PTET.51.1.P0690129		Ribosomal protein S5, C-terminal domain	72.4			1.604653985	2.079791979	0.475137993
PTET.51.1.P0700060		Insulin-like growth factor binding protein, N-terminal	39.256	SMC4_1	SMC4_2			-0.744665076
PTET.51.1.P0700131		Chaperonin Cpn60/TCP-1	82.651			-	-	-0.081273972
						0.329424262	0.410698235	
PTET.51.1.P0700138		Protein piccolo	17.095	SMC4_1				SMC4_1
PTET.51.1.P0710112	PTIWI01, PTETG7100004001	Ribonuclease H-like domain	17.432	SMC4_1				SMC4_1

PTET.51.1.P0710131	alphaPT4, tub_alphaPT4, PTETG7100002001	Tubulin alpha chain	323.31			0.457990877	1.588300465	1.130309588
PTET.51.1.P0710133		Ribosomal L22e protein family	12.684			2.129112835	1.711487111	-0.417625724
PTET.51.1.P0710140		Fe-S cluster assembly protein DRE2	13.87	SMC4_1				
PTET.51.1.P0710220		dITP/XTP pyrophosphatase	19.327	SMC4_1				
PTET.51.1.P0720056		Ribosomal protein L18e/L15P	17.482	SMC4_1	SMC4_2			-1.508538399
PTET.51.1.P0720102		Coiled coil domain	30.208			0.898986084	3.501253089	2.602267005
PTET.51.1.P0720184		Cse1	24.803	SMC4_1				
PTET.51.1.P0730164		KH domain	185.65			2.368489155	1.742818213	-0.625670943
PTET.51.1.P0740114		Zinc finger CCCH domain- containing protein 13	12.068		WT		SMC4_1	0.403114662
PTET.51.1.P0740177		Protein of unknown function DUF3546	12.886	SMC4_1			SMC4_1	
PTET.51.1.P0740192		HAD-like domain	28.31			2.557731101	2.591874429	0.034143328
PTET.51.1.P0750047		Nephrocystin-3	38.474		WT		SMC4_1	0.375292
PTET.51.1.P0750166		Protein kinase domain	14.303	SMC4_1				SMC4_1
PTET.51.1.P0750175		NAD(P)-binding domain	12.768		SMC4_2			SMC4_2
PTET.51.1.P0750181		MmgE/PrpD	89.878			1.215722326	1.516434711	0.300712386
PTET.51.1.P0760045		Phosphofructokinase domain	38.084	SMC4_1				SMC4_1
PTET.51.1.P0760195		Ornithine aminotransferase, mitochondrial	11.905	SMC4_1	SMC4_2			-0.251839819
PTET.51.1.P0760207		dTDP-4-dehydrorhamnose reductase	11.511	SMC4_1				SMC4_1
PTET.51.1.P0770007		Putative DNA-binding domain	24.534	SMC4_1				SMC4_1
PTET.51.1.P0770142		Glycine cleavage system T protein	13.142			-0.57496509	-	0.012113747
							0.562851342	
PTET.51.1.P0770143		CID domain	11.874	SMC4_1				SMC4_1
PTET.51.1.P0770145		V-ATPase subunit C	20.772	SMC4_1	SMC4_2			-0.473311621
PTET.51.1.P0770146		3-ketoacyl-CoA thiolase B, peroxisomal	135.56			0.059419468	0.770768025	0.711348557
PTET.51.1.P0770174		Aspartate/other aminotransferase	17.79			0.215110468	1.574331696	1.359221227
PTET.51.1.P0770205		Pyridine nucleotide disulphide reductase class-I signature	13.056		WT		SMC4_1	3.371753647
PTET.51.1.P0780038		ATPase, F1 complex, gamma subunit domain	12.269			2.525764859	1.480945077	-1.044819782
PTET.51.1.P0780047		Phosphoglycerate kinase	53.096			-	-	-0.088835741
						0.221356355	0.310192096	
PTET.51.1.P0780060		WD40-repeat-containing domain	11.894	SMC4_1				SMC4_1
PTET.51.1.P0780129		Uridylate kinase	18.668	SMC4_1				SMC4_1
PTET.51.1.P0790053		Heat shock protein 104	68.078			1.728400086	1.496874204	-0.231525881
PTET.51.1.P0800043	PTETG8000005001	Protein kinase-like domain	23.083		WT		SMC4_1	-
						1.817091039		
PTET.51.1.P0800091		Coiled coil domain	37.057	SMC4_1				SMC4_1
PTET.51.1.P0800119		Peptidase C1A, papain C-terminal	13.802	SMC4_1	SMC4_2			1.279702687
PTET.51.1.P0800141		60S ribosomal protein L4	90.397			2.54424805	3.109300998	0.565052947
PTET.51.1.P0800155		Endoplasmic	54.805			0.307310857	-	-0.535207151
							0.227896294	

PTET.51.1.P0800198		Chromo (CHR)romatin Organisation MOdifier domain	12.289	SMC4_1	SMC4_1			
PTET.51.1.P0810081		Pseudouridine synthase I, TruA	18.339			-	-	-0.161841734
						0.774260861	0.936102595	
PTET.51.1.P0810085		Thiolase, N-terminal domain	11.294		SMC4_2	SMC4_2		
PTET.51.1.P0810095	rab_B78	Intraflagellar transport protein 22 homolog	13.161	SMC4_1		SMC4_1		
PTET.51.1.P0810192		Phosphoribosyltransferase-like	33.115	SMC4_1		SMC4_2		0.789853101
PTET.51.1.P0820022		Tetrapeptide-like helical domain	119.42				1.182600901	1.566934307
								0.384333406
PTET.51.1.P0820041		Actin-related protein 2/3 complex subunit 4	24.108				1.098900301	1.718865598
								0.619965297
PTET.51.1.P0820051		PCI/PINT associated module	24.145	SMC4_1		SMC4_2		0.5328822
PTET.51.1.P0820072		Ribosomal protein L5 eukaryotic/L18 archaeal	50.117				3.248641374	4.097227152
								0.848585778
PTET.51.1.P0820086		Ribosomal protein L18a/LX	33.11				0.06055101	-
								0.183125824
PTET.51.1.P0820101	PTETG8200012001	Ubiquitin-related domain	16.221				0.639921203	1.586432709
								0.946511506
PTET.51.1.P0820112	rab_A30	P-loop containing nucleoside triphosphate hydrolase	12.229	SMC4_1		SMC4_1		
PTET.51.1.P0820161		Ribosomal protein S4/S9 N-terminal domain	25.139	SMC4_1		SMC4_2		1.29765986
PTET.51.1.P0820162		High-osmolarity-induced transcription protein 1	12.699				-	-
							0.664629979	0.248592501
PTET.51.1.P0820178		P-loop containing nucleoside triphosphate hydrolase	11.348	SMC4_1		SMC4_1		0.416037478
PTET.51.1.P0830027		Cilia- and flagella-associated protein 57	17.311		WT	SMC4_1	1.05023004	
PTET.51.1.P0830052		Probable 3-hydroxybutyryl-CoA dehydrogenase	46.687				1.058295185	0.685062806
								-0.373232378
PTET.51.1.P0830133		Mitochondrial carrier protein	47.981	SMC4_1		SMC4_2		-1.341912592
PTET.51.1.P0840196		Serine/threonine-protein kinase HT1	18.41		WT	SMC4_1	2.01207079	
PTET.51.1.P0850007		Heat shock protein 70 family	196.95				2.51638606	3.648594762
								1.132208703
PTET.51.1.P0850107		Clathrin adaptor, mu subunit	76.334				-	-
							0.229347848	0.207111229
PTET.51.1.P0850132		Histidine protein kinase 1	43.636	SMC4_1		SMC4_1		
PTET.51.1.P0850133	act1-5	Actin-related protein	24.665	SMC4_1		SMC4_1		
PTET.51.1.P0850169		Cysteine-rich with EGF-like domain protein 1	18.53				-	0.087977144
							0.541387637	0.62936478
PTET.51.1.P0860027		Protein NLRC5	53.957				-	1.252859145
							1.194150362	2.447009507
PTET.51.1.P0860064		Coiled coil domain	12.037		WT	SMC4_1	-	-
							1.460038451	
PTET.51.1.P0860086		Tubby C-terminal-like domain	41.528				-	-
							0.277263929	0.431123688
PTET.51.1.P0860204		Redoxin	11.313				-	0.065661712
							0.145466249	0.211127961
PTET.51.1.P0870133		Alpha-protein kinase vwkA	18.364		WT	SMC4_1		
PTET.51.1.P0870152		Acyl-coenzyme A thioesterase 9, mitochondrial	36.809	SMC4_1		SMC4_2		1.777348704
PTET.51.1.P0870166		Trichocyst matrix protein T1-B	11.421	SMC4_1		SMC4_1		

PTET.51.1.P0870174		Histone H2B type 1-M	24.358			2.051335896	2.068718942	0.017383046
PTET.51.1.P0880068		H-type lectin domain	323.31			-1.03534828	-	-0.023976612
							1.059324892	
PTET.51.1.P0880113		Protein phosphatase 2A, regulatory subunit PR55	12.358	SMC4_1	SMC4_2			-1.184663319
PTET.51.1.P0890039		Reticulocyte-binding protein 2 homolog a	31.403	SMC4_1	SMC4_1			
PTET.51.1.P0900010		Pyridine nucleotide disulphide reductase class-I signature	112.59			2.183429211	1.431544828	-0.751884383
PTET.51.1.P0900182		Ribosomal protein L7Ae/L30e/S12e/Gadd45 family	18.74	SMC4_1	SMC4_2			-1.287875511
PTET.51.1.P0900212		Isocitrate/isopropylmalate dehydrogenase	82.406			3.109820213	2.110750642	-0.999069571
PTET.51.1.P0910161	PTETG9100014001	Thiolase-like	37.306			-	-	-2.176385867
						1.419875227	3.596261095	
PTET.51.1.P0920028		Transmembrane protein 120B-A	18.749	SMC4_1	SMC4_1			
PTET.51.1.P0920068	PTETG9200004001	40S ribosomal protein S12	24.439			1.771498908	4.083573	2.312074092
PTET.51.1.P0920087		Pyridine nucleotide-disulphide oxidoreductase, FAD/NAD(P)-binding domain	26.19	SMC4_1	SMC4_1			
PTET.51.1.P0920172		Glutathione S-transferase, C-terminal-like	25.513			0.18462559	2.51529703	2.330671439
PTET.51.1.P0940124		Rcd1	12.578		WT	SMC4_1	0.950297874	
PTET.51.1.P0940159		Fructose-bisphosphate aldolase class-I, eukaryotic-type	17.417			0.468315033	0.48864932	0.020334287
PTET.51.1.P0950040		Coiled coil domain	32.226			-	-	-3.360102319
						0.236895856	3.596998175	
PTET.51.1.P0950122	KdC3	Histone-lysine N-methyltransferase SETD7	92.957			1.342372	-	-1.83408343
							0.491711431	
PTET.51.1.P0950124		JAB1/MPN/MOV34 metalloenzyme domain	13.17	SMC4_1	SMC4_1			
PTET.51.1.P0960133		Nucleotide-binding, alpha-beta plait	11.951	SMC4_1	SMC4_1			
PTET.51.1.P0970177		Pyridoxal 5'-phosphate synthase subunit PdxT	12.228	SMC4_1	SMC4_1			
PTET.51.1.P0980013		60S ribosomal protein L18	21.605			1.471434067	2.169883154	0.698449088
PTET.51.1.P0980025		Ribosomal protein S17e	16.767	SMC4_1	SMC4_2			-1.670851477
PTET.51.1.P0980041		E3 ubiquitin-protein ligase Hakai	18.056			2.271677753	0.327816346	-1.943861407
PTET.51.1.P0980107		50S ribosome-binding GTPase	60.173			1.409304793	5.111311386	3.702006593
PTET.51.1.P0980124		Lysine-specific demethylase 6A	11.712	SMC4_1	SMC4_1			
PTET.51.1.P0980168		40S ribosomal protein SA	94.167			-	0.841717292	1.628038127
						0.786320836		
PTET.51.1.P0980184	PTETG9800002001	14-3-3 protein	30.322		WT	SMC4_1	-	
							0.215862996	
PTET.51.1.P0980191		50S ribosomal protein L9	24.793	SMC4_1	SMC4_2			0.330378004
PTET.51.1.P1000056		Na(+)/H(+) antiporter 2	75.107	SMC4_1	SMC4_2			0.725208741
PTET.51.1.P1010044		Protein kinase-like domain	44.23		WT	SMC4_1	0.639295127	
PTET.51.1.P1010047		TCP-1/cpn60 chaperonin family	122.5			0.309760411	-	-0.993702455
							0.683942043	
PTET.51.1.P1010085	HSP90-1, PTETG10100003001	Heat shock protein 81-3	182.89			-	0.061835307	0.113528028
						0.051692721		

PTET.51.1.P1010086		Ribosomal protein S7e	12.609	SMC4_1	SMC4_2			0.447002848
PTET.51.1.P1010109		AMP-dependent synthetase/ligase	36.165	SMC4_1		SMC4_1		
PTET.51.1.P1010158		T-complex protein 1 subunit delta	162.25				-0.126914271	0.018558121 0.145472392
PTET.51.1.P1020022		ATP-grasp domain	51.459				0.191320437	0.226518855 0.035198418
PTET.51.1.P1020045	Hsp70P08	Luminal-binding protein 5	13.453	SMC4_1	SMC4_2			2.441626658
PTET.51.1.P1020084		40S ribosomal protein S12	12.99	SMC4_1	SMC4_2			-0.463552511
PTET.51.1.P1020090		Enoyl-CoA hydratase/isomerase	12.054	SMC4_1		SMC4_1		
PTET.51.1.P1020102		Protein phosphatase 2A, regulatory subunit PR55	95.561				0.100893338	0.438603113 0.337709775
PTET.51.1.P1020121	PTETG10200002001	WD40-repeat-containing domain	12.364	SMC4_1		SMC4_1		
PTET.51.1.P1050110		Malate dehydrogenase	28.51				1.475140728	0.851578813 -0.623561915
PTET.51.1.P1050126	PTETG10500002001	Glutathione S-transferase Mu 4	24.399	SMC4_1	SMC4_2			0.157341576
PTET.51.1.P1050161		Glutaredoxin	19.563	SMC4_1	SMC4_2			2.327755898
PTET.51.1.P1060046		WD40/YVTN repeat-like-containing domain	77.382				0.581379236	1.332501327 0.751122091
PTET.51.1.P1060077		Profilin-1A	14.246	SMC4_1	SMC4_2			1.997624453
PTET.51.1.P1060094		Phenylalanyl-tRNA synthetase	29.413		WT	SMC4_1	2.029097809	
PTET.51.1.P1060137		Superoxide dismutase	21.378		WT	SMC4_1	2.344131336	
PTET.51.1.P1060141		Major vault protein beta	58.25	SMC4_1	SMC4_2			0.081582513
PTET.51.1.P1060180	sAG_51A, PTETG10600003001	G surface protein, allelic form 168	323.31				0.022167241	6.482447954 6.460280713
PTET.51.1.P1070023		B30.2/SPRY domain	19.443	SMC4_1		SMC4_1		
PTET.51.1.P1070046		P-loop containing nucleoside triphosphate hydrolase	112.09		WT	SMC4_1	0.197453322	
PTET.51.1.P1070063		Profilin	19.3				1.187765191	1.840672946 0.652907754
PTET.51.1.P1080068		HSP20-like chaperone	26.622	SMC4_1	SMC4_2			0.486858772
PTET.51.1.P1080081		Putative amino-acid ABC transporter-binding protein PatH	28.61		WT	SMC4_1	1.570228787	
PTET.51.1.P1080104		F-box-like/WD repeat-containing protein TBL1X	89.49				-0.09690444	1.844742054 1.941646494
PTET.51.1.P1080183		Peptidase C2, calpain, catalytic domain	12.52	SMC4_1	SMC4_2			-0.299752334
PTET.51.1.P1080192	rab_C103	RanBP1 domain	20.196				-0.425457957	-0.084103902 0.341354055
PTET.51.1.P1100030		ADP-ribosylation factor family	21.865				0.674859696	-0.727734637 -1.402594333
PTET.51.1.P1110038		Homoserine O-acetyltransferase	35.16	SMC4_1	SMC4_2			-2.127433883
PTET.51.1.P1110100		Transketolase	55.305				0.694456376	-1.405371008 -2.099827384
PTET.51.1.P1110112	PCM1	NAC domain-containing protein 68	25.237	SMC4_1	SMC4_2			5.291532417
PTET.51.1.P1110113	PCM1	Gamma-crystallin D	323.31				-0.517525484	0.588232921 1.105758405
PTET.51.1.P1110150		Ribosomal protein L23	13.369	SMC4_1	SMC4_2			-0.822986529
PTET.51.1.P1120047		Vacuolar protein sorting-associated protein 35, Vps35	24.377	SMC4_1		SMC4_1		
PTET.51.1.P1120052		Ribosomal protein L44e	19.5				1.258718406	0.647902934 -0.610815472

PTET.51.1.P1120149		MmgE/PrpD family	25.535			1.338002123	-	-1.617699984
							0.279697861	
PTET.51.1.P1120155		40S ribosomal protein S15-B	29.115			3.524331024	2.100154352	-1.424176672
PTET.51.1.P1130041		Glutathione S-transferase, C-terminal-like	17.954	SMC4_1				
PTET.51.1.P1150054	TEF1, PTETG11500003001	Elongation factor Tu GTP binding domain	156.07			0.982599106	1.329231722	0.346632616
PTET.51.1.P1150082		Mitochondrial substrate/solute carrier	26.345			2.332730903	0.356298569	-1.976432334
PTET.51.1.P1150112		Mitochondrial acidic protein MAM33	16.856			0.869871225	-1.02218374	-1.892054966
PTET.51.1.P1150131		Pyridine nucleotide-disulphide oxidoreductase, FAD/NAD(P)-binding domain	151.71			1.830143446	-	-2.445922698
							0.615779252	
PTET.51.1.P1160067		Protein kinase domain	11.517			0.929878052	1.227154242	0.297276191
PTET.51.1.P1160120		15-cis-zeta-carotene isomerase, chloroplastic	20.727			1.149910628	0.352210727	-0.797699901
PTET.51.1.P1170020		Ribosomal proteins L26 eukaryotic, L24P archaeal	12.371	SMC4_1				
PTET.51.1.P1170022		Histone-fold	24.943	WT	WT			
PTET.51.1.P1170122		Mitochondrial phosphate carrier protein 3, mitochondrial	63.927			3.27310856	1.871290831	-1.401817729
PTET.51.1.P1170129		SURF1 family	21.674	SMC4_1				
PTET.51.1.P1170142		WD domain, G-beta repeat	11.841	SMC4_1				
PTET.51.1.P1180044		Transaldolase	12.623	SMC4_1				
PTET.51.1.P1180048		P-loop containing nucleoside triphosphate hydrolase	40.078	SMC4_1	SMC4_2			-0.085526657
PTET.51.1.P1180049		ATPase, F1 complex, gamma subunit domain	23.67			3.839332296	2.673869644	-1.165462652
PTET.51.1.P1180090		Thioredoxin-like fold	22.037	SMC4_1				
PTET.51.1.P1180110		Heat shock protein 70 family	201.3			0.931212543	0.466951899	-0.464260645
PTET.51.1.P1180158		Calpain family cysteine protease	22.393	SMC4_1				
PTET.51.1.P1190018		Thioredoxin-like fold	25.785	SMC4_1	SMC4_2			1.195004824
PTET.51.1.P1190028		Ribosomal protein S13-like, H2TH	19.053	SMC4_1	SMC4_2			-2.300146215
PTET.51.1.P1190058		WD40-repeat-containing domain	34.919			0.07788074	0.731801254	0.653920513
PTET.51.1.P1200007		Sec63 domain	17.646	SMC4_1				
PTET.51.1.P1210120	rab_A10	Ras-related protein Rab-1A	12.524	SMC4_1				
PTET.51.1.P1220029		Pyridine nucleotide-disulphide oxidoreductase	93.949	SMC4_1	SMC4_2			-2.971455419
PTET.51.1.P1220083		Serine hydroxymethyltransferase 2, mitochondrial	13.624	SMC4_1				
PTET.51.1.P1220095		NAD(P)-binding domain	118.86			0.585026759	-	-0.750816126
							0.165789367	
PTET.51.1.P1220101		26S proteasome, regulatory subunit Rpn7	18.411			2.803607409	1.667982254	-1.135625156
PTET.51.1.P1220116		Pyridoxal phosphate-dependent transferase	13.082		WT			
						0.203272801		
PTET.51.1.P1230083		Cingulin-like protein 1	35.152			2.290168973	1.566806791	-0.723362182
PTET.51.1.P1230130		Nucleoside phosphatase GDA1/CD39	73.737	SMC4_1	SMC4_2			-0.24888278

PTET.51.1.P1240009		Succinyl-CoA synthetase, beta subunit	12.619			0.864675047	0.374056346	-0.490618701
PTET.51.1.P1240016		Nuclear pore complex protein GP210	14.025	SMC4_1	SMC4_1			
PTET.51.1.P1240020		26S proteasome regulatory complex, non-ATPase subcomplex, Rpn1 subunit	30.79	SMC4_1	SMC4_2			-1.807403992
PTET.51.1.P1240024		Protein arginine N-methyltransferase 1.1	45.073			-	-	-0.295744234
PTET.51.1.P1240046		H-type lectin domain	16.791			1.506895769	1.802640004	
PTET.51.1.P1240098		Adenylate kinase	26.531			0.959342905	1.129090743	-0.169747837
PTET.51.1.P1250020		Protein disulfide-isomerase	13.065	SMC4_1	SMC4_1	1.917139291	-	-2.793376592
PTET.51.1.P1250118		Ubiquitin-conjugating enzyme/RWD-like	133.41		WT	0.876237301		
PTET.51.1.P1250136		Ribosomal protein L11/L12	26.78			2.316623531		
PTET.51.1.P1260091		Netrin receptor UNC5D	48.601	SMC4_1	SMC4_2	2.907491599	2.166520982	-0.740970617
PTET.51.1.P1270007		WD40-repeat-containing domain	13.339		WT	-		
PTET.51.1.P1270143	PTETG12700004001	Serine/threonine-protein kinase Nek3	16.61	SMC4_1	SMC4_1	0.685506805		
PTET.51.1.P1280037		Iron sulphur-containing domain, CDGSH-type, subfamily	24.96			0.484430327	-	-1.295926482
PTET.51.1.P1280060		Coenzyme A transferase	19.639	SMC4_1	SMC4_2	0.811496155		
PTET.51.1.P1290088		Ribonuclease P protein subunit p25-like protein	12.392			-0.165252255		
PTET.51.1.P1290090	PTETG12900002001	Ubiquitin-conjugating enzyme/RWD-like	12.842		SMC4_2	0.631763337	0.726406933	0.094643596
PTET.51.1.P1300003		Proteasome subunit Rpn10	19.785	SMC4_1	SMC4_2			2.142926869
PTET.51.1.P1300018		Glutathione S-transferase, C-terminal domain	36.052			0.372621272	1.261651879	0.889030606
PTET.51.1.P1300068		Elongation factor G-1, chloroplastic	87.093	SMC4_1	SMC4_2			-1.902561375
PTET.51.1.P1300125		Coiled coil domain	12.374	SMC4_1	SMC4_1			
PTET.51.1.P1300163		Nucleic acid-binding, OB-fold	24.228			-	-	0.78044884
PTET.51.1.P1310018		Beta/Gamma crystallin	323.31			2.269195043	1.488746203	
PTET.51.1.P1310046		Ribosomal protein L13	19.794			-	-	-0.53254491
PTET.51.1.P1320133		40S ribosomal protein S4	99.809			0.637974026	1.170518936	
PTET.51.1.P1330007		Ribonuclease T2-like	34.433			-0.22092009	0.740273385	0.961193475
PTET.51.1.P1330041	pp2r-1, PTETG13300003001	Calcineurin-like phosphoesterase	19.466			0.375382546	0.887916365	0.512533819
PTET.51.1.P1330115		haloacid dehalogenase-like hydrolase	19.574	SMC4_1	SMC4_1	1.160025841	0.826409547	-0.333616293
PTET.51.1.P1330129		Capsid protein	19.376		WT	0.135928447	-	-0.725126372
PTET.51.1.P1330138		Mercuric resistance operon regulatory protein	23.79	SMC4_1	SMC4_1	0.589197925		
PTET.51.1.P1340014		Mitochondrial carrier protein	13.184	SMC4_1	SMC4_2			-1.398398284
PTET.51.1.P1340068		BTB/POZ fold	39.8			0.613566915	-	-1.370722741
PTET.51.1.P1350053	PTETG13500002001	Intraflagellar transport protein 172 homolog	60.24		WT	0.757155826		
						0.720985075		

PTET.51.1.P1350121		Ribosomal protein L18	18.22	SMC4_1	SMC4_2			2.906453069
PTET.51.1.P1360074	PTETG13600002001	Ubiquitin-conjugating enzyme	11.824	SMC4_1	SMC4_2			1.399597445
PTET.51.1.P1360118		HAD-like domain	12.223	SMC4_1	SMC4_2			
PTET.51.1.P1370083		Adenylate kinase	11.25	SMC4_1	SMC4_2			0.021812029
PTET.51.1.P1390019		Insulin-like growth factor binding protein, N-terminal	46.094			-	-	-0.192568527
						1.240494258	1.433062785	
PTET.51.1.P1390033		26S proteasome non-ATPase regulatory subunit 11	11.658	SMC4_1			SMC4_1	
PTET.51.1.P1400024	can-A4-2, PTETG14000006001	ATPase, OSCP/delta subunit	13.619			-	-	0.427945497
						2.160970389	1.733024893	
PTET.51.1.P1400027		DNA double-strand break repair Rad50 ATPase	11.03	SMC4_1			SMC4_1	
PTET.51.1.P1400050		Uncharacterized protein C458.02c	52.702	SMC4_1			SMC4_1	
PTET.51.1.P1400060		Ribosomal protein L15e	31.687			0.095325499	1.498916489	1.40359099
PTET.51.1.P1400095	PTETG14000016001	V-type ATP synthase alpha chain	30.454			0.235037571	-	-0.624382154
							0.389344583	
PTET.51.1.P1400107		Probable mitochondrial 2-oxoglutarate/malate carrier protein	46.069	SMC4_1	SMC4_2			-1.193078776
PTET.51.1.P1420051	PCM2, PTETG14200002001	Insulin-like growth factor binding protein, N-terminal	239.05			-	-	0.633339202
						1.265557647	0.632218445	
PTET.51.1.P1420091	PTETG14200003001	ARP2/3 complex, 34kDa subunit (p34-Arc)	57.471			0.244356598	1.530006146	1.285649547
PTET.51.1.P1430120		Alanine-tRNA ligase	18.107	SMC4_1			SMC4_1	
PTET.51.1.P1440017		Oligoribonuclease	161.77		WT		SMC4_1	0.884989695
PTET.51.1.P1440071	PtCenBP1, CenBP1	Coiled coil domain	12.244	SMC4_1			SMC4_1	
PTET.51.1.P1440105	ran_B14	Ran GTPase	73.916			2.478509648	2.695605156	0.217095508
PTET.51.1.P1440125		2-acylglycerol O-acyltransferase 1	35.927	SMC4_1	SMC4_2			-1.177335223
PTET.51.1.P1440137		Oxygen-dependent choline dehydrogenase	18.957			0.047823335	-	-0.222557737
							0.174734402	
PTET.51.1.P1450009		50S ribosome-binding GTPase	11.335	SMC4_1			SMC4_1	
PTET.51.1.P1450044		Chromo (CHR)romatin Organisation MOdifier domain	22.105	SMC4_1	SMC4_2			-3.344759907
PTET.51.1.P1460073		Lipid-A-disaccharide synthetase	61.174	SMC4_1	SMC4_2			-2.969791857
PTET.51.1.P1460081		Accumulation-associated protein	85.927			3.821062816	1.982678154	-1.838384663
PTET.51.1.P1470096		Prohibitin	18.631	SMC4_1			SMC4_1	
PTET.51.1.P1470170		Protein translocase subunit SecA	35.519			1.825159106	0.813759709	-1.011399397
PTET.51.1.P1480062		54S ribosomal protein L17, mitochondrial	11.878	SMC4_1	SMC4_2			1.211895697
PTET.51.1.P1480099		Thymidine kinase	19.165			0.431361615	0.690825846	0.259464231
PTET.51.1.P1490073		Succinate dehydrogenase	59.133			4.666455542	4.285994996	-0.380460546
PTET.51.1.P1490078		Fibrillarlin	17.918	SMC4_1			SMC4_1	
PTET.51.1.P1490080		C3a anaphylatoxin chemotactic receptor	20.303	SMC4_1	SMC4_2			-2.434963222
PTET.51.1.P1490087		Branched-chain-amino-acid aminotransferase	26.418		WT		SMC4_1	2.770852094
PTET.51.1.P1500083		Ribosomal protein S3Ae	86.55			0.559399878	0.181437586	-0.377962292
PTET.51.1.P1500100		40S ribosomal protein S4	29.476	SMC4_1	SMC4_2			0.453406053

PTET.51.1.P1510028	PTETG1510006001	Peptidase C48, SUMO/Sentrin/Ubl1	11.626	SMC4_1	SMC4_2			0.494294568
PTET.51.1.P1510031		60S ribosomal protein L10a-3	68.376			2.479402854	3.037658986	0.558256132
PTET.51.1.P1510079		Ribulose biphosphate carboxylase small chain 3B, chloroplastic	18.178			0.327038715	-	-1.405072834
							1.078034119	
PTET.51.1.P1520081		Protein kinase domain	17.984	SMC4_1			SMC4_1	
PTET.51.1.P1530028		tRNA dimethylallyltransferase	26.258	SMC4_1	SMC4_2			-0.671453806
PTET.51.1.P1530088		Ribosomal protein S26e	12.72	SMC4_1			SMC4_1	
PTET.51.1.P1540048		ssDNA-binding transcriptional regulator	22.987	SMC4_1	SMC4_2			-0.306716605
PTET.51.1.P1540072		K(+) efflux antiporter 1, chloroplastic	323.31			-	-	-1.38758384
						0.440158101	1.827741941	
PTET.51.1.P1550057		ATP-dependent DNA helicase hus2/rqh1	57.515			2.826145337	2.62925964	-0.196885698
PTET.51.1.P1550131		Feline leukemia virus subgroup C receptor-related protein 1	16.231			1.051504885	-	-1.629792012
							0.578287127	
PTET.51.1.P1560087		Ribosomal protein S12/S23	12.105	SMC4_1	SMC4_2			-0.997217404
PTET.51.1.P1570010		50S ribosome-binding GTPase	33.631	SMC4_1			SMC4_1	
PTET.51.1.P1570012		Cyclin-dependent kinase 3	24.144			-	3.139649555	3.755963312
						0.616313758		
PTET.51.1.P1570072		UBA-like	11.648		WT		SMC4_1	-
								1.805547921
PTET.51.1.P1570128		ADP.ATP carrier protein	173.12			1.282219882	0.233600387	-1.048619495
PTET.51.1.P1580009		Thioredoxin-like fold	48.547			0.903770202	0.493540044	-0.410230158
PTET.51.1.P1580012		Ribosomal Proteins L2, C-terminal domain	33.415	SMC4_1	SMC4_2			0.28592987
PTET.51.1.P1580031		Ribosomal protein S17	33.724			0.002319576	0.350455343	0.348135767
PTET.51.1.P1580060		Palmitoyl-acyl carrier protein thioesterase, chloroplastic	12.935	SMC4_1	SMC4_2			-1.964528414
PTET.51.1.P1590096		Fez1	11.146	SMC4_1			SMC4_1	
PTET.51.1.P1590123	alpha-51D, sAG_alpha51D	Paramecium surface antigen	89.221	SMC4_1			SMC4_1	
PTET.51.1.P1600056		Poly(ADP-ribose) polymerase, catalytic domain	17.166	SMC4_1			SMC4_1	
PTET.51.1.P1600099		Protein kinase-like domain	32.104	SMC4_1	SMC4_2			-1.541738597
PTET.51.1.P1610030		Thiamin diphosphate-binding fold	20.535	SMC4_1	SMC4_2			-0.044620492
PTET.51.1.P1620066		CTD small phosphatase-like protein 2	11.817	SMC4_1			SMC4_1	
PTET.51.1.P1630038		Probable mitochondrial transport protein fsf1	18.25	SMC4_1			SMC4_1	
PTET.51.1.P1630088	beta-PT2, bPT2, SU3, tub_betaPT2	Tubulin	323.31			1.248976646	1.519761843	0.270785197
PTET.51.1.P1630095		Respiratory-chain NADH dehydrogenase 51 Kd subunit	24.358	SMC4_1	SMC4_2			-0.410413817
PTET.51.1.P1640075		Protein phosphatase 1 regulatory subunit 3B	18.766	SMC4_1			SMC4_1	
PTET.51.1.P1640126		SF-assemblin/beta giardin	18.857			-	0.83535631	1.585475758
						0.750119447		
PTET.51.1.P1650072		Ubiquinol-cytochrome C reductase hinge domain	12.432			-0.15242399	1.892996119	2.045420109
PTET.51.1.P1650092		Ribosomal protein L6	18.464	SMC4_1	SMC4_2			-1.157853725

PTET.51.1.P1660054	Protein kinase-like domain	56.732	SMC4_1		SMC4_1			
PTET.51.1.P1660069	60S ribosomal protein L21-B	20.026	SMC4_1	SMC4_2				0.31336729
PTET.51.1.P1660073	Heat-inducible transcription repressor HrcA	14.394				-	-	-0.251137368
						0.421504265	0.672641633	
PTET.51.1.P1670032	Eukaryotic translation initiation factor 3 subunit I	21.048	SMC4_1	SMC4_2				0.806905964
PTET.51.1.P1670039	Chalcone--flavonone isomerase	46.469				3.250695806	2.537188173	-0.713507633
PTET.51.1.P1680035	Trimeric LpxA-like	39.857				1.240003353	-	-3.136902692
							1.896899339	
PTET.51.1.P1680046	Virilizer, N-terminal	57.565				3.5619662	3.399349516	-0.162616683
PTET.51.1.P1680080	Ribosomal protein L28e	19.239	SMC4_1	SMC4_2				-0.656113316
PTET.51.1.P1680081	Ribosomal protein S4e	24.207				0.415201384	-0.22081778	-0.636019164
PTET.51.1.P1700045	Zonadhesin	323.31				2.455499603	1.142054361	-1.313445242
PTET.51.1.P1700072	Sulfide:quinone oxidoreductase, mitochondrial	55.399	SMC4_1	SMC4_2				-3.355770293
PTET.51.1.P1710013	Alcohol dehydrogenase superfamily, zinc-type	17.303		SMC4_2	SMC4_2			
PTET.51.1.P1710019	ClpP/crotonase-like domain	135.52				0.385598398	0.264768192	-0.120830205
PTET.51.1.P1710064	40S ribosomal protein S5	31.335	SMC4_1	SMC4_2				-1.992516361
PTET.51.1.P1730008	Probable butyrate kinase	18.541	SMC4_1	SMC4_2				-1.105734912
PTET.51.1.P1740041	Dynein heavy chain-like protein PF11_0240	11.894		WT	SMC4_1	-		
						0.498329767		
PTET.51.1.P1750015	Ribosomal protein L10/acidic P0	65.449				1.716416174	1.89241648	0.176000305
PTET.51.1.P1750049	Coiled coil domain	16.837	SMC4_1		SMC4_1			
PTET.51.1.P1750074	EF-hand domain pair	17.706	SMC4_1		SMC4_1			
PTET.51.1.P1780068	PCI domain	11.547	SMC4_1		SMC4_1			
PTET.51.1.P1790015	PTETG17900001001 P-loop containing nucleoside triphosphate hydrolase	50.163				2.56757276	2.268188729	-0.299384031
PTET.51.1.P1790028	Polynucleotide 3'-phosphatase ZDP	13.979				0.532951296	-	-2.343699113
							1.810747817	
PTET.51.1.P1820010	Clathrin heavy chain 1	238.04				2.865940145	1.197758278	-1.668181867
PTET.51.1.P1820013	PKHD-type hydroxylase AZC_3753	28.618	SMC4_1		SMC4_1			
PTET.51.1.P1820041	Thioredoxin-like fold	25.016		SMC4_2	SMC4_2			
PTET.51.1.P1840023	Coiled coil domain	25.332	SMC4_1		SMC4_1			
PTET.51.1.P1840047	PTETG18400001001 Protein kinase domain	323.31				4.538036906	1.1679505	-3.370086406
PTET.51.1.P1850001	DNA double-strand break repair Rad50 ATPase	12.299	SMC4_1		SMC4_1			
PTET.51.1.P2080011	Lipoamide Acyltransferase	19.841		WT	SMC4_1	-		
						2.207487422		
PTET.51.1.P2150003	6-phosphogluconate dehydrogenase, NADP-binding	37.23				0.445928526	-	-1.424736608
							0.978808082	
PTET.51.1.P2410004	Protein kinase-like domain	29.443				-	0.957945197	1.299776293
						0.341831096		
PTET.51.1.P2530004	Probable xyloglucan galactosyltransferase GT19	12.129	SMC4_1		SMC4_1			
PTET.51.1.P2550005	rRNA methyltransferase 1, mitochondrial	36.057				0.572601156	-	-1.007378971
							0.434777814	
PTET.51.1.P2710001	40S ribosomal protein S14	11.721	SMC4_1	SMC4_2				-0.327344848

PTET.51.1.P2710005	CAP domain	11.386	SMC4_1	SMC4_1			
PTET.51.1.P2740007	Homeodomain-like	30.069	SMC4_1	SMC4_1			
PTET.51.1.P3030001	Molybdopterin synthase catalytic subunit 2	44.243			2.484049115	-0.81146107	-3.295510185
PTET.51.1.P3490004	P-loop containing nucleoside triphosphate hydrolase	64.813			3.15236338	2.550851555	-0.601511825
PTET.51.1.P4420003	Cytochrome C1 family	74.259			2.448505491	-	-2.989316654
						0.540811163	
PTET.51.1.P5040001	Ribosomal protein S8e	14.449			-0.28599972	1.575060577	1.861060297
PTET.51.1.P5560008	Arginine-tRNA-protein transferase, C-terminal	25.684	WT	SMC4_1	0.786201325		
PTET.51.1.P55600045	Maintenance of mitochondrial structure and function	12.939	SMC4_1	SMC4_2			-0.323164633

TGAAAAATTTCAACAATCCTCATATTTGGATGACTTCTGCGAATTTAATTATTTCAACTAATCTTCTTACTTTCTTTTCTATTGGG
GATTTTGAATTTGAATTTCTTCTCAATAAGTTAGTTTCTTGTCTTGGATTGTAAGCAACATCTAATGGTGTGGATGTTAATTTTT
TTTTATAGAGATTTCTTTTTGACAAAATCTTTTATAAATTATAAATGGCCAACTAGATGCTACATGTAACCGCTGTGCTCCATTTTCAT
CCTGTCCAGAAGCCCATACTATTCAATTATCTTTTGTGCCGTTTTAAAATTCGCTTTACGCAGTGATTTGATTAAGTGTAAAGGCTTTTCA
AGGGAGGTGAGTTGAAGCAATGTTTCCACAATATCCCAATTATCTTATTCTGATTAATCGCGATATCAAGTGTAGTTAAATTAATTTTT
CTCAAACTTTCTTGTATTTATAATTTCAATTAATATGCTAATTTTGGCCGTTTTTGTCTGCCTAGATCAAAGCAGTGTTCCTTGATTATC
CTTATAATTGAAATCAATTTATTCTTGTATTTTTGGAAAATATTTACTTTAAAATTTATTAATGCATTATAAGTGTCTTCACTATCTCA
GTATAATAGATGCTCAACTAAGGCTTATGAAAAATTCATTATGCTGTTAATTTACTCGTATATAATCTTCAATTAACATATTACCTA
AATTTCAAATGATGTTGACTCTTGTATTAGTAAATTCGACTATTTTTTATTAGTGAATAGATTATTATACATATCGTATTTTAATAATTTAT
TTAATACATTAACAAAAATCTCATTATAATAAAACAGTCCATATATACAGATAGTCTGTTCTTAATATTCAAATATTCATAATAAAGTAAT
ATCGACTGTAATAATAAATTTAGTAAAAACAAAACTGTTTTATCAAATATGGATTGAATCAAAGTGGCTAAGGTGATTCTTATAAAATAA
GTGCTTTTGGCCGTTAGCAATATGTGATTAATTCAAATAGTCTCATGTTCCATCGAGTTCTACGTTTTCACTCTGCCACTAAGATA
GATAAATAAGGATGTAGAACTTCTTTTTTAATTAGTTTTATTAATCTATCCCAATACGTTGTGAAATAGGTTGATATGTTCTTGCA
AAAAAATTTATGGAGTATCAATTAATTTAATAAATAAATGATTTAGTGAATTTCCCAAAATTTGATATCTATAAATAGAACTACACATA
TATAAGATAATTGAAAAACAATGAATTTTATAAATTTCCATCTATATGCTCTTCTCTAGGAAAATCTTATATGCA

LEFT_PRIMER: GGTTCCTCTTAAATGGTTGTTTTAT

LEFT_PRIMER_START_LENGTH: (204, 30)

RIGHT_PRIMER: CCTAGAAGGAAGAGACATATAGATGGAAAT

RIGHT_PRIMER_START_LENGTH: (2474, 30)

PCR Product size = 2271

DraI specific 3-IES candidates

ID 377

Left IES ID=IESPGM.PTET51.1.18.134377

sequence=TAAAGCAGGCCATTTTATCTCCATAAATTTCTAACTGGAAATTCATTAACATGTATACACTTGGGTGAATTTACCTTTTG
ACAAATTAATCATTTTATTTGAAACACAAAGAATAATTTCTTATTATTTAAAGATAAATATGAAATTTGTTGGTGAATTTAATATTTAGA
AAATCATAGTAAACATTTTGTCTAAAATATTTGTTAATTCATGAATAAGAAGCTGTATATATTATAATTTTACATTTAATAATCAAAATACGA
AATATTAATTGTAATTCCTCAAAATGATTTTAATTG

Middle IES ID=IESPGM.PTET51.1.18.134388

sequence=TACACTCTTATATATTATAAATAAGTAAATTTTATAATTATATATGG

Right IES ID=IESPGM.PTET51.1.18.134467

sequence=TACAGTCGATCTTATATTATAAACATTTTGTAGTTGAACCTTTTATTCATCTGATTATTTTGACAATTTACCAAATCCTCTTTTCAT
CTACTAATTTATATTGAAATTCATAATCCAAGTTAATTTAAAATTTATAGGTGATATGTTAATGAATGGGTTTGTATGATACTTAATGTACATTG
ATTAATCCATTTATCTTTTATGCTGTTTAAAGAAAAATATGTCTTAAATCAAAAATTTTGGAGCCTTAAATTAATCAATTACATCATAAAT
ACATTTGATAAATTCATTTGAAAAATATTTCTATATAGATTTTAGATTATAACAATAAATAAATTTGGATTATCAATTTACAATTTCTAAT
TGAAAAATGTTAATAATATAAGCTCTTCTG

Region sequence

GATAAATATGAAATTTGTTGGTGAATTTAATATTTAGAAAATCATAGTAAACATTTTGCTTAAAATATTGTTAATTCATGAATAAGAAGT
GTATATATTATAATTTTACATTTAATAATCAAAAATACGAAATATTAATTGAAATTCCTCAAAATGATTTTAAATGATGTTAGTAACTACA
CTCTTATATATTATAAATAAGTTAATTTTATAATTTATATATGGTATCATCTACAAAATCTGAACTAAAACCTTATAAAGATATTAATATGAAATTT
AGATTTATTTTGAAGAAATCTTTIAGGTACAGTCGATCTTATATTATTAACATTTTGAAGTTGAACCTTTTATTCATCTGATTATTTTGACAA
TTTACCAAATCCTCTTTTCACTACTAATTTATATTGAATTCATAATCCAAGTTAA

LEFT_PRIMER: ACGAAATATTAATTGTAAATTCCTCAAAATGT

LEFT_PRIMER_START_LENGTH: (128, 33)

RIGHT_PRIMER: GATGAAAAGAGGATTTGGTAAATTTGTCAA

RIGHT_PRIMER_START_LENGTH: (395, 30)

PCR Product size = 268

PciI specific 3-IES candidates

ID 144

Left IES ID=IESPGM.PTET51.1.6.380144

sequence=TACATTCACAATTTCAATCAATAATTTTTTAATAAAAAGAGTTTATATCTCTTTTATATGAAATTTAGTTTCATAATTATACAA
GAATTATGTAATAATTAAGAAAATAGGTAATAATGCCATTAATTTAATGAAAATAAAGCAAGAAAACTTAATTTAAATTTGAACATCT
CAAAAAAATGACAAATTTTCTCATAAAAACCATGCAAAAATTTGCTCTTCGAAAATAATATAAATAAATTAATGTCATTTAAGAGATTA
GAAGATTCCTCTAAACTTTAGATGAATCTTATTTCACTAATTAAGATTTTAAATTTGATTTACGTATGTCATTGTTTATTAATGACATGTAAT
GATCTTAAGTGACATATTGCAACTATTTTGTATAAGAAAAGAAATCTTTAAATTTTGAATTTTAAACATTTTAAACATTTTAAATATCTTCA
AAATTTAATAAATAATTTAGAAAATATAGTATAAATAAATAAATAAATAAACAATTAAGAAAACATATAAATTTAACTTTCA
ATATTTTTCATATAAATAATGAAATTTACTAAAAAATAAATGTTGATTTTGCTA

Middle IES ID=IESPGM.PTET51.1.6.381684

sequence=TATAGAAGATAAGACAGAAATGAGCTA

Right IES ID=IESPGM.PTET51.1.6.382023

sequence=TATTGCTTGATTAATCACTCAGTTTGGATTACTCGATAATAAATATCAGTTTATCTAAGCTAATTTGAAATATAAATCCATATTA
GTTAATAATTTATTTAGTTAAGAGATAAATGAACATGTAATAATATAAATCTGAAAACTTATTAGTATATAAATCAAAATCTC
ATTTGGAATTTGGTTGACAA

Region sequence

AATTGATCCTTAAGTGACATATTTGCAACTATTTTGATAAGAAAGAAATCTTTAAATTTTTGAATTATTTTAAACATTTTTTAAATATCT
TCATAAATTTTAAATAAATTTAGAAAATATAGTATAAATTTAAAAAATAAATAAACAATTAAGAAAAACATATAAATTTATACT
TTCAATATTTTTTCATATAAAAATTAATGAAAATTTACTAAAAATAAATGTTGATTTTGCTATATTAGTGGATAGCAAAAATGAACTCG
CATTGCATATTTCAATTAATCAATCTTTTTCCAAACATATTTAATCAAGAAAATAATATTGAGGGTGATTAACAAGATATTAAGCTTTTT
AAGTATTGAATTCATATACGAATCAACTTAAATATTTCTTAATAGGAATCTTTTAATAAAGATGCAGATCTTAGATTGATCCATAATT
TCAATGACATAGCTTAAGAAAATTCATATAATTTAAATCTTGATAAGTATTAGAAAATGCTTTTATTAAGCTTGGATACCTTTTTCAATTTAAT
AGTTTGAATATTTATTTCTTTAGATTATCAAAAAATAAATATAAATTAATTAATTAATTTTGGATAATTTTATAACAATAAATTAATCTCAA
TCATTTTTGTTCATTGTCCTCCATATTTACTTTTCCATAAAAACTCACAAACAGCCACAGGTGCTTTTCTTTCATTTCCAAATG
AAATCCACTTTAATCAGTTGAATCTTCGAAACACACTAAAAAATCTACTTCCATTATCGTGTCTAACTTGTGGACTTAACAAGGTTT
ACTTTTTCTGGCTTATGAGGACCATTTCCTGTATTATTGTTAAGCACATTATCAACATCTTCTATATTACTATTGTTTGGTTTATCTGAA
ATTTTTCTTGAGGCTTTTCAATAATTTTTTCAGTTTTCTCAACTTATCCACTTTGTCATTGACCTTTTTTCTTTTTTTGTTCTCTAATT
TTTTCCCATTTGTTTTGATTGATAATTTAAGTGCTTTGTTTTATATGTTTTGAGGTTTAGGTTCTTGAGGGTCAATGCCCTAATGTTTTA
ATTCATAATCATGGACTAGAACCAGCATTTCAGGAGTTAATTGAGTCATGGGTTCAATTGATACTGAGTTGTACTCCATCTGAACCTTATA
CATGATGGCTTCAGGTTCAATCTTTTTCTTCAATAATTTCAACAGGATGTTTTGAATTCATAATAGATAAATTAATTAAGGAGAAGGCTCT
ATCAATGTTTATGTAGGACAATTATTGCAATGGTTTATCAAAATATTATATAACATTTATTGTTAATTTTAGTTTGCATAAAAA
TACACAATATTTGAAAATAAATAAATTTTATAATTTCTTTTTCACTTCTATAATCTGGTTATAAATTTGTTTATTTTATAAATCTTTAA
AAATGAAATAATTTAAATATAAAATGGCAATATACATAGATTGGGTGATAAATAATGATTAGTAAATAAATTAATCAGAACTTGGGGGTAAT
GGAAGACAACAGATGATTTCTATATTCGGTAAGCAAATTCATTTAAAGATATCAAGGAGGGATGGATGCAGACCCAAGAGGTGAGAATT
TTTTGATATGTTGAAAAATCAITCTGTCCAAGACTTAACTTATTTCAATTTACTACAATAGTCTCAGCATTGATTATAATCTATACATCA
CAATGTTAGGAGTTGGAGAAATAAATAAGAAGATAAGACAGAAATGAGCTATAAACATGATCGATTTTATCAGTTTATGAGAAAACCT
TGAATGATTTGGTGAAAATGATCCAGATGATGTTAAATCCAACATGAAATTTTCAGATGGGTGACATCCTTACTCTTAGTTGGAGACTT
CTATAATTAATACTTGGCAGTCTTATGATATAATATGCTATTGATATAGAAGCCACATAAGGATTGAATTTAACATTAATAGTGTTTTT
GGGGCAGGAGCATGTGGTGCCTATTTGGAGATTTGTGCAATATTTGCAAATACAGAACTTACTCTGAAACCTTTTCTGATATACGCTT
GTGATGGGTTCTTGATAGGAGTATATTGCTTGATTAATCACTAGTTTGGATTACTCGATAATAAATCAGTTTATCTAAGCTAATGTT
AAATATAAATCCATATTAGTTTAAATAATTTTATTTAGTTTAAAGAGATAAATTTGA

LEFT_PRIMER: TCTTAAGTGACATATTTGCAACTATTTTG

LEFT_PRIMER_START_LENGTH: (6, 30)

RIGHT_PRIMER: AGTTTATTATCGAGTAATCCAACTGAGTG

RIGHT_PRIMER_START_LENGTH: (2197, 30)

PCR Product size = 2192

PsiI-v2 specific 3-IES candidates

ID 799

Left IES ID=IESPGM.PTET51.1.33.359799

sequence=TATTGTTTGATATAAATTTAAATCAGAATAATTTGTTACTTTTTCAAATTTACTTTTTTAAATTAATAATTAATAAATTTCC
AATTTCTAAATTTTGGAAATGAAATTTAAATTTTTCAATCTATATTTTTAAATTTACTTTCAAATAAGCCAAAAAATTTTTACTTAAATTTATA
GCTTTACTTGAAGAATAGCAAACTAAAAAATAAGAATAAGATCTTCAGTTAATACAATTTACTCAATTATAAATTTTAACTATCTTAA
TTTACTTACTTTATCAAAAAAATTTTTAATGATAAATTTATAGATATATAGGTATAAATATAGATTGATTGAATTAACAGAATGATTAAAT
AATGATGTTTATCCCTTAAATTTGATTTCAATAATAAATAAATTTAGCATTCTTAAATAATTAGCAACCAATTAAGATTGCAATTATATAT
ATATCAAAATTAATTTATATATTTCTTCTTTATTAACAA

Middle ID=IESPGM.PTET51.1.33.361301

sequence=TATAGTCTAAAATTTTAAATATTATAGAATTAGATTCTTAGATAATAAATCATAAAATGTCATCGATTCAACTA

Right IES ID=IESPGM.PTET51.1.33.361772

sequence=TATAGATGCTGCACAAAGGAAATATGTAGTATTTAAATTTATATCTAAATTAATAATTGGAGAACCATAGTGCTAGTTTTTAAAGT
AAAACAAAAGAGTTAATTAATAAATTTAAATTTGTTTATAATAAATTTTCATGATAGAAATAGAAAGACTATTTAAATTTGATTAATAATTTAT
AATCATATTTTACCAATTATAAGTATAAATTTTTTCTATCTCAAAAATAACCATCTAGCAAAATTTCTCTGCAAACTA

Region sequence

AATTTATTAACACTATCTAATTTACTTCTTATATCAAAAACAATTTTTAATGATAAATTTATAGATATATAGGTATAAATTATAGATTGATTGAAT
TAACAGAATGATTTAATTAATGGATGTTATCCCTTAAATTTGATTTCAATAAATAAATAAATTAAGCATTCCATAAATAATTAAGCAACCAAT
AAGATTTGCTATTTATATATATATCAAAATTAATTTATATATTTCTCTTTATTAACAATAAGATTAATTAAGAAATGCAAAATCTTAGGATAA
TATTTTCAGAGGACTTTATAGAAATTTAGCTTACAAAAGCTAAAATTTAATGCTTATAAATAAATGAAATTTGTTACCCATCCAGGTTTATAC
ATCGCTATTAAAGGTGGAATGAAAATATAAGCTGAATATGAAACTAAAATAAATTTAAAAGTAAATTTCAATATATATAAATTTAGAAAT
GGGGATTTTGGTCTTATTGAAATGATCTTAAATAAAGTTAAAATTTTCTTAAATCTATAAAGAAGAAAGTCTTCTAATTTATAT
TTCAGGTGATGATTTTATCATATAAATAAAGAGGTTTACGGAGGATTATGAAAAAATGAGATTATACATGATCAATTTGCTGTTCAAGTTCA
AGTACAACGAAAATCAAATAGAAATGCTATTTTTGTTAATAATATCATGTTCTTCATAATGAAAATAAATAAATTTCAAACCTGAATTTGA
TTTTGAGAAATGAAATTTGGATGAATAAATGATAGAAGATTTTTTAAAGAGCCAATAAGAAGCACATTTTTTAAATAAGAATAAATTTCA
GAATCATCTAAAAGTTCAAATGAATTTGAAGAGTCTTTGAGATCGATCCAGTCAGTTCCAGAAATGCAAAATGAAAGATAAATCGGTAA
GAATTTTTAGGATCCATTTCTTAAATGATTGTGTGCAATCAAAAATATCCCAAGAAGGATCCCATTAATTTAACTTAGAGTTTTA
AGGTATAAGAAAAGTTAAACGTAACAAAATCAGGTAAATACAACCTTAAAGGTGAGAGTTTTAGACTTAGACAATAAGAAATTTGTCATAG
ACAATTTAAGAAATTTTAGTTTTACGATCTGTGTATAACATAGAAACTATAATCCGAAAAGTAAATAAATTTTAGAACATTGAACCTTTT
ATTATTGATGATTTTCAACATGATCAGCAACTACATCTACTGGGGTTCCAAAACACCTCCAAAGTAAAGTTGAGTCTGTATCCATCTT
CCATGCATAACAAGTTCTGTGTTAATTTGATTGTCTTCCAGTAAATCTCCATTGTCTCAATAATTATAAATTTGATAGAAATCAGCCAAAA
AGATCAATCGATATAATACCAACTTCAGTTCTAATCTTTGATGAAAATTTTATCAGTTGATCAGGATGTTTATAGGGAACTACTACT
ATTGTCATAAGCGTACGCTGCAATTTCTACTAAATCTTACTTGGCAATTTGGAACCTACGTATAATCTTTGTTTCAATTAATTTCAAACATGA
TTGGGCTCTTCTGAAGACAATCTATCGCTATCTTTATGATGGAGTGATCCAAAACATCTAGAATAGCCCATAAATTTATCCAAAGAACTC
ATGCAATCTTATAGTTTTTATCATGAGGACAACATAAAGTTGCTCCAGTGACACCTAACTGATTTTATTTGAGAGATTTCTGAGTTCT
TTTATAGTCTAAAATTTAAAATATTATAGAATTAGATTTCTAGATAAATAATCATAAATGTCATCGATTCAACTATAAATAAACAAGGTAAT
GTGGAGTTTCAIATTTGATCACTTTTTGATTGTTCAATGTGTACTCTGTTAATGAGTAGATGCAATCAAAAATATAACAATAAATATCATT
AAAATTTATGAGTGATTAATTTGATCATAAAGGAGGAGAGGTAATCCGTAGAGACCAGAAATTAATTTACTCTAAAATTTGTCAGA
AGCTAATTTCCAAATTTGATCACTTAAAGAAAGAGATATAAAGATAAAGTATTATTTTTGGAATAATCCATTAGCTAGAATCAAGCCATTAAG
ATAGTGGTTAACAAGCGAAAGATTTAAAACTGTGTATGATGATAAAGCAAACTTTGAATTAATGTGGATTTAAGAGTGGATAAGTCTT
GGTTGTAAGGACTTAGGACCTTAGATGCTTTGGATTACAGTATTTTATGCAGAATATGTGGTCCAATCTTGATGTTTGTGTTGTTACT
ATAGATGCTGCACAAAGGAAATATGTAGTATTTAAATTTATATCTAAATTAATAAATTTGGAGAACCATAGTGCTAGTTTTTAAAGTAAAAACA

AAGAGTTAATTAATAATTAAATTGGT
LEFT_PRIMER: AGCATTCTCTAAAATAATTAGCAACCAATTA
LEFT_PRIMER_START_LENGTH: (159, 30)
RIGHT_PRIMER: TAAATACTACATATTTCTTTGTGCAGCAT
RIGHT_PRIMER_START_LENGTH: (2329, 30)
PCR Product size = 2171

ID 655

Left IES ID=IESPGM.PTET51.1.88.149655
sequence=TATTGTAGATTAATCATCTCTACTCAATTTTAAATTTAATTTGTAACAAGAAATCTGATTTAAATTTATTTCTTAGTTTAGCATTAG
TATCTTAAATAATAGATTGATAAAGATTAAAAAATTTATAATTTTATTCAACTTAATGAAGAGGTTTGTATTAGTTATTAACCTATTCTGT
AATCAATTTGCTGTAAATAATTTCTGTTTCCATTTAAAAATTTCAAATTTTAAACAATTAATTTATTAATAATTTGTTTTATATTTTCACAA

Middle IES ID=IESPGM.PTET51.1.88.149727
sequence=TACTACTCAATATGAAGTGAATACAATTTAGATTATCAAATAAACTCATTTTATTG

Right IES ID=IESPGM.PTET51.1.88.151525
sequence=TATAGCTCTTACACAAAAGATTTATTCAATTTTATAGTAAATGATATGAAGAAGATTTTATAAAAAATATAAGTATCGATAA
TTTAATTTATATCAAGGATCAAAAATTAATTTATTATTCTTTAACATATAGTCAACTCAATCAATCATATTGCAATTTATTTTCCAAAT
TGTTATCATTTTACTAATTAGGATTAGAAATATTCTTAAATTTATTAAGAGATTTCTAAAAATTTATAAGTATTAATAATATAATTTTGTATTTC
TGAGTTGGAATGAAGGCAAAATGTAGATTAATTTGGGATCAGGAAAGTTTAGAATAATTGATACTTCTTTTCTAGCTAAGTTTTTAAAG
AGATCCATAACAACCTTCCAACTAAAAGGTTTAAAGTTTGCCTACTTTATCTAGCTATAAATTTATTTTCATTGTTTACATTTTCTTC
AAGGTAATTTATTTTACCATAGAGATGCTTTGTACATTATCTTATTAACAACATTTATGATTCTGAATAATAAGATAAGAGTTAATTAGAA
AATAAAATTTATACAGTAAACAATCAATGACAAGCATATTAATTTAGGTTTTCACAAATGAAAGAAATTTATATCTATTATTTTAAAAAT
GAAATTAATTTTCTAAATGGTACTACATAGATGATCTATGCAAGTGCTA

Region sequence

TTTTATCAACTTAATGAAGAGGTTTGTATTAGTTATTAACCTATTCTGTAATCAATTTGCTGTAATAATTTCTGTTTCCATTTAAAAATTT
CAAATTTTAAACAATTAATTTTAAAAATTTGTTTTATATATTTTCAATAACCAATCTACAGATTTATCACTAATTTCAAATGATGTTTATGGG
ATAACTTCTCCTTAATCAAAAAGCTGTTACACTCAATATGAAGTGAATACAATTTAGATTATCAAATAAACTCATTTTATTGTTATTTGATA
AAATATGATGAAATTTTATTTTGTGTCATCTTGTGTATGACTGATATCAATTTCACTAGAAAATAATTTACCTTCATCAAGTTATAGA
ATCGATTGAATATGATCTTTTCGATGAATTCATCACTTAGATTTCAAATATTATTGGCAAGATTAGTTTCATTTTGTTCCTTATACTAATA
TAGATCCAGAGCAAGTAACTTCCAAGAAGGTTTGTGATTTTATTACAAAAGACTTCATAATAGTTTGGTTATCCCATCTTAGTTAA
CTAATATTGTGATATGCTATCAATTAAGCATTAACTCACCATTGTAATTATTACTCCAATAAAAGTCTAATTTATGTAAGGCCTTGATGGA
AATTTTCAACAACCAATTAATCATAAGGATGATGAGATAGCTTTTCGGGATTTATTAATAAATTAATAGGTTTGTATGGAAGTATGAG
TAATATCAAAATATAGATTTTCAATGGATTGATGAATTTTATGATTTGTAGAGTTTACAACTTCTATTGATTTATAGATGTTTGTAGTGACTG
ATTGATATTAGAGTTTATAGTCTCTGAGCTTTTATTAATAAGTCATCATCTGACCCAAATGAATAGTGTAAGTCTAATTTCTCAATTTCTAA
CTGCACTGATCATAAAGACAGAAACAGGTACCAATGATTCACTTTTATTGTAATCAATGATTCTAAGGTTTCTTTTTCGAATAGAAT
TAAGGTGTCTTAAATTTCTGGATGTCAGATCTGCTTCATCATTATGACAGAAGTTCTTAACCTTCCCTCAAATAATCTAATGTCCCCGC
TTATCAATGAGACACTGATTTGAACATCAACATTTGAATAAAAGCGATATTGAGAAGACTCTGACTCACTAAAACCTTCTCCATTGAA
GATTTGCGTATAGGGTAGTCTAATACTTTTGACCCTAAAATCAATCAAACTTTACTATTCCCTTAGACGGCTGTAATTTCAATTTGAATAA
ACGCAACCCACTTTTTCGCAAGTCTTCACTTTAAATGATTTTGTATTCAACAATTTCAATCAATAAACAATGATCATAATACTAATAAT
AGTTTCATCATCAATAGACTCCAATGCTTTTGCCTGACTTACAATTTACCTTGGAAACGCAACACAATGATTTTATATTTCTTATCAATTTG
GATCATCTTAAAAATGTAATAATGAGGTATGCTTTCATGGAATAGAACATCAAATGGATAGCCAAGGAAAGCATTGACAAAATTTGCAAT
CGTCAGTATTGTAATTAATTTAAATTTACATTTCTTCTCCCAACACGCCTATGATATAATCATCTTTGCCAAATATCGATTATTCACCT
CTTATAGAAATGTAAGTTGTTCTAAAAATATGTGACCCTATTGATTAATTCAGATAGGCTGGGTCTTTAGTCTTTCCCTTTAGATATTCTA
GCATTAACAATTTACCACCTCCTTTGACATGAATATTAATTTGATCGACTTAAATCATCTTATGTTAACTGAGTTTGTAAATTTGGTTTA
ACCTTTTAAATAACGTCGATAAATAGGGTCTGATAGAGTCAATAGTTTAACTTCTTATAGACACCAATCGTATAGGTGTCATTTTAAATAA
GAGGCTCTATAGGTTAAACACGGATGTATAAAACCTAATACTTCTCAGTTTCAGGGATTGTAACCTTTAAATTTAGGTGAAATAGGAAT
GTGCTTTGATGTTTCATATCTCAGATCAGAATTTATCTTTGTTATAGCTTTACACAAAAGATTTATTCAATTTTATAGTAAATTTGATATGAA
GAAGATTTTAAATAAAATATAAGTATCGATAAATTTAATTTATATCAAGGATCAAAAATTAATTTATTTATTTCTTTAAACATATAGTC
AACTCAATCAATCATATTGCAATTTTCTCAATCTGTTATCATTTACTAATTAGGATTAGAAATTTTCTTAAATTTATTAAGAGATTTCTA
AAAAT

LEFT_PRIMER: TCAATTTGCTGTAATAATTTCTGTTTCCAT
LEFT_PRIMER_START_LENGTH: (54, 30)
RIGHT_PRIMER: AATTGCAATATGATTGATTGAGTTGACTAT
RIGHT_PRIMER_START_LENGTH: (2237, 30)
PCR Product size = 2184

SspI specific 3-IES candidates

ID 795

Left IES ID=IESPGM.PTET51.1.9.406795
sequence=TATTATTAATTTATATTTTCAACGCTTTTAAATTTTAAATATTATTAGTCATGAAATCATAAGTAATTAATAAATCTCAAAAAAC
AACAAAATCCCATACATTTAACGTTTATACAAAATAATCCAATAATTTTAAATTTGATAA

Middle IES ID=IESPGM.PTET51.1.9.406958
sequence=TATATAATTAATACTTATAAATACAT

Right IES ID=IESPGM.PTET51.1.9.407393
sequence=TATAGTTGATTCACAGATTATTTTATTTAATTTCTTAAATTTTATAAATTAATTAAGATATTAGGGTATTAAATAAATCAGTTT
GTGCTTGAGTAGTAAAGGTGATAATTTTCAATTTCTTATTAATAATATATCTTAATTTCAAGTAAGAAAAATATCAATTTTAAAAATAATTA
ATTATTGCAATTTCTATTGAATTGACTA

Region sequence

ATTTAGTCATGAAATCATAAGTAATTAATAAATCCTCAAAAAACAACAAATCCCATAACATTTAACGTTTATACAAATAAATCCAATAA
TTTTTTAATTTGATAATAGCTACGCTAAGCTTCATACAAGTAAATCAGCTTCCAAAAAGAAGCCTAATTTAATGGAATGTAAAAACTAAAT
TTAATGTACAAAAGAAACAAAAGAGATAAAAATAAATGATATTAATAAAGATTTAATCAGGGAACAAAAACAGAGTGAAACTACAGAT
TATAAATTAATAACTTATAAATACATTATACATTCAGACCCGAAAAAATGAAGTGCCAATAGATAAGTAAAAATAGCAAGGAAGAATT
AAAAATAGAAGTAGAGTATTGATCTTTGTGTCAATACAGATTTGAAGGAAATTTACATTATTAACGACTTAGATTTTATAAATAGA
TAAAAAAGAAGTCATGATGAGAATTAATTTGAATATAGACTATTTATTTAATAATGACAAATCATTATTAAATTTACTTAAAGCCTATT
ATAAATCATTATGAAGTAATAATCTTTTATTGAGTATTGCATTTCTGAAACAATCTATTTCAACCATTCCAAACCTATTTAACTG
AGGTGGCGCTGGGAATTGCACCTTTAGAATGAAAGCTCATAAACATTTAAATTAGAGATTCAATGAATTTCAATTCAGAAGATCTCTTTGT
ACTATAGTTGATTACAGATTATTTTATTTAATCTTAAATTTTATAAATTACTTAAAGATATTAGGGTATTTAAATAAATCAGTTTGTGC
TTGAGTAGTAAAAGGTGAT

LEFT_PRIMER: AACAACAAAATCCCATAACATTTAACGTTT

LEFT_PRIMER_START_LENGTH: (42, 30)

RIGHT_PRIMER: TCAAGCACAACTGATTTATTTAAATACCC

RIGHT_PRIMER_START_LENGTH: (827, 30)

PCR Product size = 786

ID 453

Left IES ID=IESPGM.PTET51.1.52.211453

sequence=TACAGCTGTAAGAGATTTCTTCATTTTTGAATAGAACAAAAATCAATATTGGATAGAGTAAGTTACTAATACTAATCTAAGTT
ATAATTAATTTTACTTCTAGTAAATAAATAGACAGTTGAAATCACTAAAAATCCTTTAAGAATGTCTA

Middle IES ID=IESPGM.PTET51.1.52.212381

sequence=TACACTACAAATAGTTCACATTTCTAATTTAAATAATTATAACAG

Right IES ID=IESPGM.PTET51.1.52.212637

sequence=TATAACTTTAGCAAACAATATATATATTTGTCTAGTAGTTCTATTAATTTAATTAGAAAATAAATAGCTAATTAATTAATAATA
ATTTATGGTGAAAAAGCAGAAAAACCTGTTAAATATTAATATTTAGCCAGCATTAAATTTATTATAAATTTATGATTTTCATTATATAAC
TCTGGAAATATCAGCTTGTGAGAACAA

Region sequence

GGATAGAGTAAGTTACTAATACTAATCTAAGTTATAATTAATAATTTTACTTCTAGTAAATAAATAGACAGTTGAAATCACTAAAAATCCTT
TAAGAATGTCTATACATTTCTCCATTATAAATCTTATTTATAGGAATTTCAACAAAATAAATCTTTCGTAATCTGGTTTTTCATACATCAT
CTTTAGATAAATCATTGTCTAAATACTCTTCAAAATCAAGAGATGAATCTGTTTTGTAAAAATGATAATCCATTATCAATCAATTTATATT
TAGAAATTTCAACAAATCTCTACATTGCCCTAAAACATGTTTAGGCATACAAATAAGAAACTAAAGGGTTTACATCTTAATCTAAATCAAC
TCCATAATCTTCTCAATTTCTGATCTAGTTTCCATTTCTTTCATCATAAGTTTTCTTCCCTTCTTCAGTTAAATTAATTTCAAGTTTTTCT
AAATAAGCCTCCTTTATAACAGCAAACAAGACTAAATTTATAAGGAATGTTGCCCTAAGCATCGCATTTGAGTTACATATCCATAATTTTGA
AAAGTGATTTCTTATCAAACTGCTTGTATATTAATTTAAGTTGATTTATTTCTTCTAAGTGTGTTACGGATTGATGTTTTTCCAATCTT
CTACACCTTTTACACGGATTGTTAATGCTAAACCCAATGGTTTTGGTAATTAAGAAGCTAGATCAGTCAATTTATTTAACTAATAAAT
GCTCCATCAGAGCTAAAACGAGTCCAAATATCAAGCATTTTGTTTTACTCATCAATCTATTGAGTTGATTTGCTCATGAAAATAAT
TTATGTCATATTGATCTAATAACAATAAGGATAAATAGATTAAGCAATAACAAAATTTAAATCAAAAATGAAGACAACCCAAAATAAAGCATT
AAAATTTGAACCATTATTCATCGTATCATACATAATCTATTCCAATCCAACCCTGTTTAAAGAAAGGAACAACAAAATGAAAGAATGATGA
AAATCTGAGAAGTTGTTAGTACTACAAATAGTTTCAATTTTAAATAATTATAACAGTATCAGATATAAATTTCCCTTCTTAATA
TCTGAAAACAAAATACTCCCAAACTGAAAAAATGAAATGGATCAAGAAAGTATAAAGCAGCCGATTATGATTGCAGGAATTGAAAA
AACTGCAGTATCTATTAGTTTTTGTAGCCCTTAAATTTTACTAATCTTAATAATCTTATAGCTCTTAAATTTCTAAACCTTTTCTTAT
AGATAATCCACTCTCATTGTTACATAATCAATAATGGATATAACTTAACTTTAGCAAACAATATATATTTTGTCTAGTAGTTTCTATTAA
TTAATTAGAAAATAAATAGCTAATTAATTAATAAATATAATTTATGGTGAAAAAGCAGAAAAACCTGTTTA

LEFT_PRIMER: ACAGTTGAAATCACTAAAAATCCTTTAAGA

LEFT_PRIMER_START_LENGTH: (67, 30)

RIGHT_PRIMER: CAGGTTTTTCTGCTTTTTCCACATAAATTA

RIGHT_PRIMER_START_LENGTH: (1447, 30)

PCR Product size = 1381

XbaI specific 3-IES candidates

ID 913

Left IES ID=IESPGM.PTET51.1.106.284913

sequence=TATTTCTAAAATTAACAAAAATACATTTTACTTTTTATAAATATTTGCTTTTGAATTTGTGAAATAATTCATATTTGAAATAAAT
AAGAAAGTAGGAAAAATTTAAAAAAGAGTATGTTATAGTGATTATTAATAATCTGATTCATAAGTTTAAAGCTTTGGCTAATAGTCATA
GAAAAGGTTACTTAATAAAAATTAATTTCAATTTCAAAAATCATATATCTAATAAAGTTCTAGATGTATAATTTGAGATTTATATCTTTTTCT
CAAATTCAGCTTGCCTATTTTGTACCTATTATTTTACAAAACATAACCGATTAAAATTTATTGAATAATCCATCATTTTATTTCTTAACTTC
TCAA

Middle IES ID=IESPGM.PTET51.1.106.286750

sequence=TATTGTGGTGTATTTTAAAAAGTAATATTTTTTAAATATTTGGTTTTCTCATAAAAAAACTTAAACCTACCA

Right IES ID=IESPGM.PTET51.1.106.286924

sequence=TACAGCTAACGTAAGAAATTTATTGTAAATATATTTTCAGCTAGATTTATTAGAAAAGAATATGAATTATCTGGAACCTTTAAT
GAGTTAACTAATGAATTTCTCATTGATTACATATTACGGTGTCTTTAAGTTATTAATTCGAGACTTCCATTATCAAGACATCTTCTAATAA
TTTTTTAAATAGTCTTTAGAATCTTTGAGACTAACACCATTTTTTTTTAATTATAATCTCCTTTCTTATCATTGAGAATAACACTGCAT

TAAAGATTCTAGAAAGCAAGGAAAATATTAATACCTGAATTTTATCCTAATTC AATCTTTGAATTATTGGATGAAAAACACGAGATTAC
TTTGAATGAAAAATTTGATTTTTGTTTAAAAATTAACCTAGTTTTTAAATGGAATGTTTACACCCTATGAAAAGAAATAGCGTTAAACA
GTAATGATATTTTCAGTAAACAACCTTTGAAAAAATAGTCAATTCAAAATACGCTATCAGATTTTTACCTTCAGAGATGATCAATTTTTAAA
TTAAATATCATAATCATTATCTTTGTTTTTAAAAACATGATGGAATTAATTAATGAAACTCTAAGGATCTGTTGATCAACTAGAATTAATA
GAATTACAAAAATAATAAATTTAGCAAAAAAAGTAAAGAAAACATAATATCTTTTTAAATTCAAAAAGTTTTGAATATCTTTTGAGTTTA
CAAATCTACTTTTATAAATGATCTTGCATTTAATATTTCTAAATAATCAATCAAAAAGGAAATCTACTATTTGAATGTAAAAAATTCATT
CATAAAAACCAAACTTAATTTGGAATTAATCAATTCAAAAAATTCATTTCTAGACTG

Region sequence

TGTATAATATTGAGATTATATCTTTTTCTCAAATTCAGCTTGCTATTTTTGTTACCTATTATTTTACAAAACTAATACCGATTAAAAATTAT
TGAATAATCCATCATTTTTATTTCTTAACTTCTCAATACCACGATCAGCTAATTTGTACAGACTATATGACACAAGCTTAATGCCATAAAACAC
TCACAAATTTAACAGCAAATGATGATTGTAATGGATTGTTGATAAATGTTATGCTACATCTAGCTTTGCTTCTGGAGCTTGACATCTTTTC
AAAGGAACTTAAACAATGTGCTAAGGATATAGAGTTGGATGCACAAATATAATTCAGCAACTTCTCTACTGCTTGTACTTTGGATTGT
ACATTA AAACTGGAACGGGCTTAGCATTTCAGATTGCTAAGCTGTAGATACTACATGCTCAGTAAATAGTACTGGAATGGATGCATA
GCTATATACTGCTGCACAGGATATGGATAAACAGCTGCTAATTTGCTTTAGATCTACAGCTGGATTATGCTGATGAATGCTGCCTCTCC
AGCAACTGCTAAGCAGTAACTTAGGCATCTGAATGTGTATTAGTACTGGAAAACTGGTTTAGATCATGCAAATGTTAAGCTTATCA
TACCTCATGCACTTCTTAAATGATGGAAGCTGGATGTTAAGAGTTAAGGCAACTTGTCTGCTTACTGGAGACGCTGCACATTGCAC
TGCCTCATAAAGGTAATGCTACTTTGAGTGGTTCGATTTGCTGCTTACTTGTGCTGCAATTTCTGGAATGGATTAACATGAT
GCTAAATGCGCAGGATATAATGCAGATTGCACTGTTAATGCTGCTGGCACTGCATGCTAAGAGTAAAAGGCTACATGTGCTGTGACTTA
ACTCAAGATTCTGCACTACATCAAAAGATACAGCAACAGCCGATAAATGTGCTTGGAGTGGAAACAGCTTGCCTTGCAGTAACAACCTGT
TGCAACTTAGTGTGCATTTGTTACAGGGTCTGGTTGGATGATACATAAATGTGCAACTTATAATGCTGGTTGTTGCTAATGCTACAGGA
ACAGCTTTGTTAAGAGAAAAAGGCAGCATGTACAGACTATACACTTCTACAGCTTGTGCAACATCTACAGCTGCCAAATGCTATTGGAA
TAGTACTACTTACCAGCTGCTTGCATTTCTATTACTACAGTGGCAACTGATTGTTAATAGTTTTGGGATCTGGTTAGATGATGCTAAAT
GTGGAGCTTACCTAACAGGCTGTGTCGCACTTTCAACCCGAGCGGGTTGTTAAGAGAAAAAGGCCACTTGTGCAGCTTACACAACCAC
TACCAGATGGAACTCAACTGCTGCCAAATGCTATTGGAATAGTCTCACCAGCTGCTGCATTTCAATTAACACTACAGCTTCCGAC
CGATTGTTAATTAGTTTTGGGATCTGGTTTAGATGATACTAAATGTGGAGCTTACCTTACAGATTGTGTTGCACTTCTACCGGAGCAGGT
TGTTAAGAGAAAAAGGCCACTTGTGCAAGTTATACAACCTCTACCCGATGTGGAACATCAACAGCTGCCAAATGCTATTGGAATAGTAC
TGCTTGATTTCAAATTTCTACAGTTGGAAGCTGATTGTTAATAAGTAAGTGAACAGGTTTAGATGATGCTAAATGCATAGCTTATAACGCT
GGTTGTGTCGCAAAATCAACAGGAACAGCTTGTGTTAAGAGAAAAAGGCAGCATGTACAGACTATACAACCTTCTACAGCTTGTGGAACATC
AACTGCTGCCAAATGCTATTGGAATAGTGTGCATCACCAGCTGCTTGCATCAAAATCCACAGTTGCAACTGATTGTTAATTAGTATTG
GGATCAGGTTTGAATGATAGTAAATGTTTACAGCTTACAACCGAGCTTGCACATCTCTAGTTGATGGTATTGTTGTTTAAAAAGTAA
TATATTTTTTAAATATTTGGTTTTCTCATAAAAAAATTAACCTTAACTTACCATACTGCTTGTGTTAAGAGAAAAAGCAACTGTAAAGATTAC
ACCACACAAAATAAATGATTTCAACTTCTAGTGAATTTGATTTGGTTTGAATGCTTGTATTCTATCACTGCAGTAAGTTGCAGTT
CAATAACTGGAATCTCTTGTATCATAAAAATGCCAAGCTTATACAGCTAACGTAAGAAATTTATTGTAATATATTTTACAGTAGATTT
ATTAGAAAAGAAATGATTAATCTGGAACCTTTAATGATTAACATAATGAATTTCTATTAGATTACATATTACGGTGCCTTTAAGTTATTA
AATTCGAGACTTCCATTAACAGACTCTTCTAATAATTTTTAATAAGTCTTTAGAACTTTTGGACTAACAACCAATTTTTTTAATAT
AATCTCTTTCTTATCATTTGAGAATAACACTGACATTAAGAT

LEFT_PRIMER: TCAGCTTGCTATTTTTGTTACCTATTATT

LEFT_PRIMER_START_LENGTH: (36, 30)

RIGHT_PRIMER: CATTAGTTAACTCATTAAAGGGTCCAGAT

RIGHT_PRIMER_START_LENGTH: (2315, 30)

PCR Product size = 2280

Dral specific inside IES

ID 798

IES ID=IESPGM.PTET51.1.23.362798

sequence=TATTGTCAAATTA AAAATACAACATTATTGTGACAATGAATACTGTTGAATAATTGGGTGCTATAAAAGCTTTAATAGAATTGTA
TCATCAAATGAAATACATTCCTACTATTCTTGTCAAATATCAGTAATTTATAGTTTAGTTGATAAACTATTATAATCAGGTATTTTAGCATAAA
TAATCGTAACTATGTCATCAGCGAAGTGA AAACTTTAACATCAATAATTAAGTGAGCTTTTTAGTTCAATTAAGAAAACCTTCAACTTAAAT
ATTATATAGGGTTGGAAAAAGTGGTGATCCTTTGAGGAAACACCATTA AAAAGTAGTATTTAATTTTCAATAAATAAGAGGCAGATTTAG
AGTAAGTTGGAATGCAATGGAAGTCTATTTACAGGTGATCTAAGATTGCTTTTTATTCTAATATATAAAAATATTCTATTAACAGATT
AACAGTATTAATAAAATCAGTTTTTATATATTTAGTAGTGAATTTATTAGATTAAATAAATCGGTTATGTTTATTAGTTGATGAGGAGG
GAATAAAAACCAATTTAATCTTTAGAAAAGTGCCTCAATCAAATAGCTTAGGCAGGAATCTGAATCTAGTAATTTGTACAAAAGCGCTAAGA
ATAGTAATAGGCTCAAAATAAAGTTTTTAGGGATATTAAGGAAAGCTTTATTAATGGTATTAATCTCGCTTTTCAACATAAATAGATTGTT
TCAATAGTGGAGTTTTTCCAAAATTAAGAAAATAAGCAGAGTTCTTTGTTGTTAATGAAAGTATCAGAAAGTCCATCATATGAAATTTG
CTTTGTTAGAAGACATATCTTATTACAGTTTTTAAAATCTATATGGTGATAAAGAGTCCGAAAGTTTTACGGATTAACCGATGATCATTGA
AAGATGCCATCTAGTTGGTTTTAAACAATTTGCAATTTGCTTCTTACCAATTTGTATATTTTTTTCATCATCTAAATAATAAGATAATTTCT
CCATCCCTTTTATTCGGCTCATGGTAATAACTTTTTGTTAAGAAAATTTATGAATTTTATTATTATTCTGAAATACTATTAAGAGCTTCTCCT
ATAACGATTTGTTATTATAATCATTGTTTTCTTGAATTTGGCACTATTCTTCTTTAATCATCTGGATGATCTTTTGCTTTCTGATGTTATTC
TAAATAATTTTATAATAGCATGTAAAATCAGTAAATTTAGATGATGCAAGTTTTTAAAGATTAGAGCATTTCTCAATCAGTTTAAAATTA
GTTTCTGGATAATATGATAGTTAGTTTACTTTCAATTTTTTCAAAATTTATATCTACTAAAAGTATTTGTTGTTAGGAATAGCTTAA
GGAAAAAGCAAAAAGGAGGACTAATAGAGTTAAAATCTCCGCAAAATTTATTTCTTGTGATGAGTTGTTTTAGTTTAAATTTCAAAATTTATTAG
AATGTTGAAACTAATAGGTGAAAACATTTCCAAGAGATTATCGAAATGGATATTTAGTTTGAATTTAGACACTTTTGGTTTATAGCTGA
GACTTTAAGATAGTTTCATATCTTAAACTCATTAATAAGTTATCCATTTAAGGATGTTGATCTGTCTTTAGGATAATTTAATAGTATTTTAT
TTTTTCTAACATTTTATTAATCTTTAGTTAAGGAGCGAGGCTCCATCTTCACTTGAAGTATTTTTCTTTTTTGTGATGATTTTATAT
TGATTAGTTGAGTTTTTTCAGCTAAGCACTAACTATCTGATAAAAATAACCTTATTAACAATTTCAAGTGCATTTTAGTCAATTTCTAAGAGT
TGCCTCTTGAAGGATTTATTTATACAGTCTTACTCAGAAATGATCTTGAAGAATTTGAAGGATATTAGTTTGTCTGATGGATTTTTTA
TTGGTTCTGTTAGGTTATTTGGATAGGTTATTTAAATGAAATTAATCATCATTTATAAGTTACCCTTGCCTGTTAACTTTATCTCAAGAA
GTGGTAACTTTGAAAGGTTTTCTATTIATGTAGAACTTACACTIATTAACAAATTTAGATAATCCAAAATGTTAAATTCATAATATTTTAA
GTATGCTTATCTGTGATGATTTGGTTTTAAGAATTAAGCAGGAAAAGCTTTAGATACTTATAAATCTTGA AAAAATCTTTTATAGTACAAT
CTTAATAAACAAGATGAAAATATGGAATATCTTCTTCCAACATAATCTTATAGCTTAACTGTTATAATGAATTTATCTTAGGTATAAGAATA
CAAATACCTAGCATATTAATCAGTTTCAAATGAAAATTAATAGCACATCTTAATCTAAAATTAATCAATTTAGCTAAAATGGATAC
CTCAACATCTTTCTGGAATGATAGCTTCTTCAATGGTAAAATTACATTTTCCATATATATAATCTTTAAGTGCAATTTCTTTCTAAAG
CTATTGAATATCTTCAAAGAACTAGAAAAGATCTATAAGGCCATTTCAAAGGTTAGTAGGTTTTTCCAAAATGTCATCGAAAACAAATTA
TTACCTATTAATTTCCCTAACTTTTGACTTTAATTA AAAAGCCCTACTCGAAAACATTAATAAGAAGTAATTTATACAAAATAACTTAAATTC

CATCATGAAATATGAATTTCCAGAAAATTAATGCAAACCAAAGTATAAGCTAAATCAATTTTGATTACCTTCTTAATAATTTATAACTT
TATTCAAATATATCTCAATATCTGTAAGAGACCAGGTAAATCTCTTCCAACATATATGAATATCATTCAAAAATATCATGCACCGAA
ATAAAAATTAICTTGAATAAAAATAAGAAAAGAGCTTAGAAAATTTTATTTCCATAATTTGAACAATATGATTTGATAGTATTCGTGTGTAA
TAAATTTAATTTTAAACCATAAAAATAATTTAGAAACCGATATCTAATATTAATAAAAATTTCTAAATTTTTTATGTAAAATAGAGAAAGCTCA
ATTTAATTTGAAACCTAGCATAAATGATCTAAGAAATCTTTCTTAATCTCAAGATCAATTAATCTTCTGATGAAATGATTCTAAGGATGG
CTACTATTTAATTTGAAATAATTTTATTTAAGGTATTAGGACTTAAAAAAAAGATAACTTACAATTTCTATAAGATTCTTTAAAAGACTTA
AAAAATCAAATTTATGATTTATAAAAATTTCAAATTTAATTTCCATTTGTATAATCTGGACAAAATTTAAAATATGGCTAATTTATTTCAAAAAAC
AAAATATAATCTTAAAAACACAAAATATTTCAGAAACCTTGACAA

IES length = 3362

length of target RE framgent 697

left_RE_position: 373696

right_RE_position: 374393

Target sequence

TTTAAAATTAAGTTTCTGGATAATATATGATATGGTTAGTTTTACTTTCAATTTTTTTCAAAAATTTATATCTACTAAAAGTATTTTGTGTTTGA
GAATAGCTTAAGGAAAAAGCAAAGGAGGACTAATAGAGTTAAAATCTCCGCAAATATATCTTTGATGAGTTGTTTTAGTTTAAT
CAAATTTATAGAATGTTTGAACCTAATAGGTGAAACATTCCAAGAGATTTCGAAATGGATATTGATTTTGAATTTGACACTTTTGGT
TTAATCTGCTGAGACTTAAAGATAGTTTCATATCCTTAAACTCATTAATAAAGTTATCCATTAAAGGTATGATCTGCTTTAGGATAATTT
AATAGTATTTATTTTTCTAACATTTTATTAATCTTTAGGTTAAGGAGCGAGGTCCATACTTCATACCTTGAAGTATTTTTCTTTTTGCA
TGTATTTTATTATTGATTAGTTGAGTTTTTCAGCTAAGCACTAACTATCTGATAAAAATAACCTTATAAACAATTTCAAGTGCATTTTAGTC
ATTTCTAAGAGTTGCCTCTTGAAGGATTGTTATTTATACAGTCTTACTCAGAATGATCTTGAAGAATTTGAAGGATATTAGTTTGTCTG
ATGGATGTTTTATTGGTTCTGTTAGGTTATTTTGGATAGGTTATTTAAA

ID 437

IES ID=IESPGM.PTET51.1.155.26437

sequence=TATTATTATGAAATAAAAATCTAGGTTTTTTTATATGAACTTGAAAAACAAAATTTTTGTTCAACATGATAGATTATTTAAAA
GTTATTTATCATTTTTCAAAACTCTTCTTTAGGAATTTATTTTAAAAATGGAACAATGGATGCAATACATTTTTTCAATTAACATTCCAG
AAATTAATTAATAAATTAATGAACATACTTATTAATATTTTAACTCATGATTTTCGATTGCTAATAAAAACTGTAAGGTTATCCACATAA
TTATATAGGATTGAGTTATGGAGAATAAAGAAAACAAAACCTTATAGTAACTACTTTAACAGTTTTTGTACCGATTTAAAAATCTTTGAA
ATCATTTGAGTTTTCCACGATCTACGATTTTTAATATGTTCCAAGAGCAAATTCATCCAAAAACAAAATACAAAGTTGAATTTTCAACGG
TATAGACTAGGTAACTATGGAGTATTAATATTTCTTTCTAGTAACTACTTTGTTTCTCTCTATCTTTTATAAGGCAATTTGGAAC
AGCATTACAATATTTCTAATCAAAAATTTGAAACTATCTTTGTCATATTTGAATGTTCAAGATTATTTAAAAATGCTCTAAAAATCTTTGGTAA
TTTCGCTACAATAAAAATTTATGTAAGAGGGATCTATTTGATGGTTCTTTAAACCATTTTGAATGGATTTCGTTCAAGTAAAACAATTTAAT
TAATCTTATTTCAATTTCTTCAATTTAGAATTTACACTTCACTTAAGATGGTTTTGTTTTAAGATGAAAGCTATAGAATATGCGAGTGAATCCA
TTTTTCAGAGTTTGACCACTATGTTAGATTTTGTAAAAATTTCAAACTAACTCTTTTTTACCACAAAATAATGGGTTAATCATAAATATT
TAGAGTCGATAAAAAATAAATAAGGCTAAGTTCCGTTATTTGAGAGGAATTAACATAATTTATTTTACTAAAAATAGAGATA
GGTTATATAGGATGGGCTGCTCACAATTTTTTTTATGATATAAATCCATATTTCTATTTTTTCAACCCTAAATGAAATATTTTTATAAGAAT
ATAATTTGAGTAATGAAAGGTATATTAGTAATTTAACTTCTCATTGACAACATCAAAGAATTTCCATCTAAATACAATTAACATTTGAACT
AAATTTGGAATGAAATGTTAATAAATTTGCTTAAAAATTAAAAAAAGGTTTTGGTTTCGTAAGTATATTGTAAAGGTTAGTAAATAACA
GTATTGTAATAGGAAATAACATTTATGGAATAATTAGACCTAACATTCGCTAGAACAAATCCAAGGAAAGGTAGTATAAATCTCTTAGA
CTCCATTTGTTCTCAGGAAAACCATATAGTAAGAAAAATCTCCTGTTTACTACCTTTACCACAAATCAGGCTAAAGAAAAATAAACGATTGA
AGAATAACTCATGAAATGTTTACATTTAATCAGCCAAGCCTCAAGCAAGCTTTCCAAAAATATAAAAAGAATGGCAACTCTAATCCT
TCAAAAAAGGAAGCTGGTATCTTTAGATGCTTCAAGGATGATCAAGATAATATAAATACTCATCCAGATACTGAATAAAATGTAAGACAA
GAATTAGACGAATCTCGCAGAGAAGTGATATCAGCCTCTTACCATACTAATTTGCCCTTATATGGAATGAAGAGATTCAGAAGCTAT
AAAAGCTCATGTCAAAAAGATAAAGCTATTACGATGGATGGTATATCAGACAATTTTATAAGGATCAAAACATCTGGACATTTTAAAGATCT
TTGGAATGATAACACTGGCTAAATAAATCAATATATTGATCAAGCTCGTGTGGTCCCACTAAATAAGGTATATCAAGAAAATACCCTCAAAA
TAGCAATTCAGACCTATCACAACAACTTAGCCATTTTTTCAAAATTTTGAATAAAGATTTTTAAACAAGACTCAAAGATTTTGGAGAGCAG
CGCTAAAATATGAACAAAATGGCTCATGTTAATAGAGGAACATAAGTAAATATAGAGAAAATTTGGTTGCTTACTTAGGTAGTGTGAATA
GAAAGGAGAGGAAATGTGTAATTTTTATAGATTTTCAAATGCATATTGCATCATGATAACAAACAAGTTGTTTTAAATATGGAAGAAATA
AGTATAACTTTGACGAATTAACATTTTCAAAAGGATTACACTACTTCTATTATTAAGACCCTAGGAAAGAAAAAGAATATGGTGGTT
TAAAATGGAGTCGTTTAAAGTATCCCTATTATCACCATCACTACTCAATATTACTTGGATACCTTTTTATAAAAATTTATCTTCAAAACTGAA
TCAGGAGCTGAACGTTAGAGCTTATGCGAGGTGATCTAGCTTTTATGTAGACGACAAAGCTGCGAAGAATTATAATTTCTTGGAAATCAA
TTTAAACAGATAAAGCTTCTACATCTAAGTATTAACAAAATAAAGGAAAGAATAATTTATATCTCCAATTAACCTAAATGGATCTTCTGA
AAAATGGATATTAGCAAAAATAATCTCTGGAATTTACATAAGGCCACTTATCACCTATTTCGAATTTAGCTATTTAAACAGCCATTA
AAAATCTCAAAGAATGATATAATAAACTATAAAGAAAATCTCTAAAGACGATAACTAGAAATGCCAAAATCTACACCAAAATCCAATCAAT
GATATATTAATCAAAATTAACAGGTATAGCCAGGTTCTTAACAACCTGGGAAAAATATGCAATATTCATAAATGCAAGATGAATGATTCACA
TATAATGAATAAGATTTGGGCTTAAATTTGAAGAATTTATGGTAATCCCCAGGGGAGAATGTAGAAAAGCAAAGCTATCAAGATGAA
AAAACGAATAGAACCAAGCGATAACAGAAAATTAATCAAAATATCAGAGAATGAAATATTAATGTGTGTTTAGGTCCTCAAAAAGGACATAA
TAATAATTATAATAAATAGGAAAATAGTAAATATAAAGATTTCAATTTATATGAAAGGATGTTAATGTTGTTTTAAATATTGTAATAAG
ATGGTTAGATAATAAATCTCGTAATTTAAAATTTAGATAAAGATTATTTATGTAATCAATCAGACTTAGCCCTTTCAAAATAATCTAAATCTCG
ATAATTTCTTTACTAA

IES length = 3211

length of target RE framgent 689

left_RE_position: 28326

right_RE_position: 29015

Target sequence

TTTAAACTTCTCATTGACAACATCAAAGAATTTCCATCTAAATACAATTACAATTTGAACCTAAATTTGGAATGAAATGTTAATAATAATTGCT
CTAAAAATTAATAAAGGTTTTGGTTTCGTAAGTATATTGTAAGGGTAGTAATAACAGTATTGTAATAGGAAAAATAACATTATGGAAT
AATTAGACCTAACATTCGTAGAACAAATCCAAGGAAAGGTAGTATAAACTCTTTAGACTCCATTTGTTCTCAGGAAAAACCATATAGTA
AGAAAAATCTCTGTTTACTACCTTTACCAAATCAGGCTAAAGAAAATAAACGATTGAAGAATAAATCATGAAATGTTTACATTTTAA
TCAGCCAAGCCTCAAGCAAGCTTTCCAAAATATAAAAAGAATGGCAACTCTTAATCTTCAAAAAGGAAAGCTGGTATCTTTAGATGCT
TCAAGGATGATCAAGATAATATAAATACTCATCCAGATACTGAATAAAAATGTAAGACAAAGAATTAGACAGAATCTCCAGAGAAGGTGAT

ATCAGCCTCTTACCCATACTAATTTGCCCTCTATATGGAATGAAGAGATTCAGAAGCTATAAAAGCTCATGTCAAAGATAAAGCTATTAC
GATGGATGGTATATCAGACAATTTTATAAGGATCAAAACATCTGGACATTTTAA

ID 670

IES ID=IESPGM.PTET51.1.174.130670

sequence=TATACTCAAATACAATTTTCACTACAACCTCAGACATCCTAATTTTTATTATAATATAAATATATTTCTATATCTAATCACAATC
AAAAACACACAAACACATAATTTAATTTTTATAATGTGAAACTATAAATAAAAAATAAAAGGCTTATTATATTGAGAGTTGGAGGGATGAAT
TAAGGAGCGAATGATTAACCTCCATTTCGATTCCAAAATTCGAAACTCTGCTTTGACTAAAATCTCCTTCAAAGTACTAAAGAATTCGAGA
CTAACAACTGCGATTGCTACGTTATTGCTATTCAAAGGAGCGGAACTTTTTGCACATTTACTTTGTGAAAATTTATATAAAACTTGA
ATTTATATAATAGCATCAGATGTATGATTGTAACCACTAATGAAATTTAAGTTTGAAGTAGAGATGTTGAACCTGGGTTGATGTATAAT
GGAGTTAAGCACAACATGTATATACAAATCTAAGGCAGTTATTGCCACTTGCTTAAGTTAAGGGCTTAAATGGAGGAAGAAAATAAATA
ATAAATAATGATAATTGATTCAGAATTTATTATATCATTGATGGAGGAATTATTCAGGACTAAGTTAAAATTTACTTCAATTTATTTTG
CTAAAAGCAGCTTAAAGGTTTCATTCAGAAATTCCTCAAATACCTATTGATTTACATTTCAATTAACCCAGAATCAAATACTAAACCTATC
GCAACCGTCAGTATCAATTACAATTTACCTTTTTAAGGTGTTGCTTATATACAACAATAGACACCTATCTGGTTGGCAACTTCATCC
AGTTTTAAAGCTAAAATGGATCCACATAGACTAATTTTTAAATCCGAGCTGAGAAAGATTAGTTAATTTTGGAAAATTCAAAATCTCTTGTTA
AAGTACATTTTTTTGAGGATTAATAACAAAATAAGTAAAGTGATAAGTATACAACCCAAAACCATTAATAAACTATTGATTACTATGAAA
ATTCACAATAATTAATATGTTTGAATTTCAAATGAGCAATATTATCTTAAACTACAATTTTTTCAATCCATAATTTGACCTATTCATCAA
ATGAAAAGCAAATTTATGACACATAGAATTAGAAAACCTGAAAACCTTAATAATTTGATATTAGCCCTTCAAATGATTTTATAAATATC
CTGTTAAAATTTAGATTTTATAGAAAATTCCTATTTCTTAAAGCAATTTACTTTGGTCCCTTTGTTAGTCTGTTAATCTTTGCATTCTTCCCTTAT
CACTATCAAATATATATGTATCATCAAAGGAATCTATTGTTGATTTACTGATGAAAATTTTTTTTTATAACAATAGGTTTATAAATAATAT
TGACAGACATCATAGCATGCAAGTATCACACATAGTTAAGTTTAAAGGCCTGCTATAGCAAATAAATAATTTACAGAGAATAAACTCATT
AAATTTAGTAAAGTAAATGAAAAGTATATATTTGTTAATTTTTGGAAAATGCTTTGAATTTAAAATAATCCAAATAAATAATGTTATGTT
ATAATTTATATAAATAATTAATTAATTTTTTTGATATATCTTTATATGTTTATTTTAAATTTGCTATAAAAGATTTTTTTTTTCAATATAA
ATTTTAGTTTTGAATGCTAAAATAAATGAGTCAAGTTTCCATTTTACAAGCAACCAAAACAAACGGTTCTGTTGAATCATTTTTATTATGGAT
TAATCTTAGCGGGATATTTTGGCCGATCCATATGTTGGAGAATACGATAATTTTTCTCAGAGTTGCTAAAATAAATCTCTTGCTCA
GAATCAAATAATGCTTAAACAGGATAATGTTTACGCAACTAAAGAGGTATTTACACAATAATTTAAGAATCTAAATGACTATATTTGGC
ATAGCAGATGAAATCTACACTCATCAAATGCGGGCTATCAATATCTTAAAGCGATGGAGCTGAATCATTCTTAATTCAGAATCAAAG
GACTAGATTAATCAAATCTAAAGCAAGATGACCTAATGCAAGATTTTACAATCAAATTTTCAATCGTTATTAGATACAAAGGTTGGA
AGAAAATAAAGTGAGATATTTTTGCAAAAAATGAAGGACAAAGTTGAGAAAATTTAAATAAGATGAAAACAAAAGCAAGTAGTCTCCCAA
AGATCTCACTAAGCAAAAACCTTACTTAAAGTAGCAAAAGATACTAAGAGTTGGATCAAATAAATTAAGGAATTTGAGAAGAAGTATA
ATAAGCGAAGTCTTTTTAAAGAAGAAATGAATAATTTAATAATAAATAAATAAAGATTAATCTTATGGATAATTTAAATTTGCTAAAT
CTGCAACCTTTTTCTGTATTCTCTACTCAAAGAAGTTTTTCATCTTCTGTTACAATCTTTATAAATAGTGCTTCAAATAAATAAATCTTGCTAGT
TGTTGCTTATGAATTTTAAATGATTTTTAGCATTCCATTTTTAGCAATTTCTTTCTTCAAATAAATAAATCTTGCTAGTATTTTTCTTT
ATCAATTTTCACTTAGTTTTAGGTGCTTGGTTTATGATTTGAAAATTTTTTGGTTTTAATTTATTAAGAGGTTTGTAAAACACACTAATCTT
TTTCATAAATTTTGTATCTTATGTTGATTTTTGCTAGTCAATCTATAACTCTGAGTCCAAATTTTTCATCAATTTGTTCACTAAAATTA
ACGATGGCATATGATTTCAATTTCCCTAAACAATACTTTCTAAGTACATTTGCTAAGTTATGGGGAAGTTGGGATATATTTTTCAGATAATTTGA
AAATAATAATGAAAATAAATAAATACACCTACATGAAATAATTTGCTATAAATGTGCGATTTTCTTTCTCATCTAATGCAAAATAGATTA
TTACCAGAAATATATAAATAATGTGCATAAAAATTAATAAATGTTAGCTAAAATATGTTTAACTA

IES length = 3001

length of target RE framgent 712

left_RE_position: 138050

right_RE_position: 138762

Target sequence

TTTAAAGCTAAATGGATCCACATAGACTAATTTTTAATCCGAGCTGAGAAGATTAGTTAATTTTTTGCAAATCAAATCTTCTTGTTAAAG
TACATTTTTTTGAGGATTAATAACAAAATAAGTAAAGTATAACAACCCAAAACCATTAATAAACTATTGATTACTGATAAAAAT
CACAATAATTTAATATGTTGATTTCAAATGAGCAATATATCTTAAACTACAATTTTTTCAATCCATAATTTGACCTATTCAAAATG
AAAAAGCAAATTTGACACATAGAATTAGAAAACCTTAAACCTTACTAATATTGATATTTAGCCCTTCAAATGATTTATTAATATCTG
TTAAAATTTAGATTTATAGAAAATTCCTATTTCTTAAAGCAATTTACTTTGGTCCCTTTGTTAGTCTGTTAATCTTTGCATTCTCCCTTATCA
CTATCAAATATATGTTATCAATCAAAGGAATCTATTGTTGATTTACTGATGAAAATTTTTTTTTATAACAATAGGTTTAAATAAATAATTTG
ACAGACATCATAGCATCAATGATTAACAACATGTTTAAAGTTTAAAGGCTGCTATAGCAAATAAATAAATTTACAGAGAATAAATAAATAA
ATTATGAGTAAGATTAATGAAAAGTATATATTTGTTAATTTTTGAAAATGCTTGAATTTAA

ID 181

IES ID=IESPGM.PTET51.1.196.12181

sequence=TATTATCAATTCAAAATTCATCATTTTTATTTTTGAAATGCAGAAGGTTCAAATAATTTTCCAACCTGATTTAGACCAAATTTATTTA
CCCTAATATTGAGTTCCCTGAGATAGCTTTCAAGAATAAATACATTCATTTTTATTCTTTAAAGAAGACAAAATTTCCCTCTTTCCCTCATGG
TAATTTTTTAAAAATCCCTTAAAAACCTCAGCCATTTGTTTAAACAATTTTCTAATTAATCATCTCTTTAAATTTGTTTGAATTTAAGG
GTTTGAACCTTAGGAAAATCGTAAGGAATTTAACTCAAGTAGTGATCCAAATAATAATTTTAGAGCAATTCAGAAAATCTACAAAATGTTT
TTTATCAGATACAAAATAAGAGGATTAGTTGTAGATTTATTAATAATTTCAAAGGGACAACCTCATTATCTGAGAAGAGTGGTATGATAGG
TGAATAATTCAGATTTGCAACTAATCAACTTAACAACAATAAATGAATGATGATAGATAAATAATAGTTTAGCCAGTTTAAACAGATA
GGAAATGGGCTATGTTAAGAAATTTGATCAAATAAATAATTTCTTAAACAAATCTTACATTAATTTGCAAAAGTTGATGCTTAGTTG
AATCATAAGGCCATGCAATACCTGATGTAACAAAAGAGGAAACGCTGAAAAATAAATAAATAAATAAATAAATAAATAAATAAATAAATAA
TGAAAATAAAGAAAAGAACAATTTGTTGAATAGATCATATTACTTGAGGTATCTATCAACAAGTACATGTTGACTCTAAATCTAGATTAA
TTTCGCTGCTCAAGGTTAACAGGTTTAAAGATCCAGAAAAGTAAACGATGCCATATATGGACGTCATTAATTTAAAAATAGGGATGCA
AAACGCATATTTGTAAGTTACATAAATTTCTGTTTGTAGATACTTTGATAGTTAAGAACAAAAAAACATGTAACAACTTATGATCTTGA
TATCTAAAGATAATATACAAAAGGACTGTGCTAAGAGGCTTCTAATTTCCATTTCTTAAATTTATACCCAGATTGTGGACAAGGATTTCAA
TAGTTTGCCTTTTGTGATACATATATAAATTAATTTCTATATAATAAATGATGGAAGTATAGAAAGTTAAGAACCAAGCAGCAG
ATAAATTAGAAAATAAATGGCTGATGCATTCAAATAGTTCTAAATTAACCATGATATTACACTTATTTAGTGGTTAAGTTACTTAGAACACA
ACCAACTACTAAAAGCTTATATTACATTTATGGAACATTGATAAATCTAAAGCATATGAAATTTTAAAGCAATAAGGGGCGATATATAGGA
CCTTATATGCAACAAAATAAAGCCCATGAGAATATATATAGAGAAATAAGATGAACAAGACTCCAAGCAGAAGTAATGTTTCAAT
CTATAAATAAATAAATAAATTTCTCATCTACTAATAACAGGATTAATTTGCAAGTTAATAAATAAAGTTGCAATTTGTTTGGTAAATTTTT
TTTAGCAACCCGACACTACTATGATCACCTTGAATGATGATGATGAAATAACGAAAAGTATTACACTAATACTAATCAATCAATCAATGAT
TAAAGTGAAGCATTAGACAGCAGATTAGGAAGAAGTTATGGAGGTTTGGACATGGGTAGTTTTTGAACAACAACCTTAAAAAGTTGAA
GGCTTGCATATCAATTTTAGGTTCAATTTGTTGATGACATGTTTAGAGTTGGCATAGCAACATTAATTTCTCTCTGATTAACAGCA
TTATGATTTGTAACCTTCTTGAATCAACTTCAACTGCACACGAAGTGTGGAACCTGTTAAATTAATCATAAGAGTGGTTAACACTGTTA

CAATTCACATTTTGTAGCTCAAATAAAATGGACATCAGTATAACTATTAGTAACAAAATTAATGCAGCAAATTGTATTGTGCTGTAGAAT
ATCATCTCTCTCAAATATTTTGGGAATTCATTATCTAAATGGAAAAATTTGAATGAGCATATTATCTTTTTTACTAATTTCTTTCCC
ATTTTATAAATCTAACTTTGGTTTTTGTGAGAGTTCCCTCCTTATTTTAAATTCCCGCTTAATATCTTCTGAAAATTAATTCGTGAGATTG
ATTTGCTAATCATTTCATCGATTATTTCTAAAATTAATTTGTATGATTTTTTATTATTTAAACATTTGATAGGAGAAGTTCATCTAATAAAT
GAATTTAATTTGATTAATAATAAAATACAAAATCTCAATTTTGGCTATAATTTATTTTCCCTTATTTTCTTTTCATATACATTTAAAA
ACATAAATAGTATCTCCATTTGAAAATAGGCTTCAACTTCTAATGCTGCTTATTGTAGCTTCAGTTGGGGTGTTCCTAGAAAGGATAGA
AATGTATTTTTTGTAGTTCCAATTAATCAAAATCTTTGTTTTAGTTTAAATTTAAAGTTTCAAATTTAATCTTAAATGTTAAAAATTTTTGTT
TTAATGGCAAATTTAATTTGATCTTTGTTTTGTTTTGTAATGACACACATGATTATGGTGCAAAAAATGCAACATTTCAATTAATGAAA
AACCTTTCCTGATCTAAAAATGATATTTATAATTTATCATCAGTATCATCATAACTGAGAACTTACAGTGTACATTACTCAAATATGATAATC
TAAATAATTTTCGTACATCAGCAATCTGTAAAGTGTGTTGTAATTTCCATTTTAAATCTTTTAAATCTTCCATAATGATATTCATCACATT
CTGAAATTTGATACAAATGTGAGAATATCTTATCTTCTTCAAAGATTTGAGAATGATGTTGTTGAGATGTTTACAAAATGTATATTTTT
GCAAAGTTACGATCTCTGGATTACACTTTGAATTAACATTTGTTGTTCTTTCCCAACAAAAGTACTTTACAAACCTTAAATGCTATG
ATTAATGTGATCAATCAATAAACTCAAATTTGCAAATTTTATCTTACATAAATAACATTGCAAATATTTATGATGATTTGTGCCAATAACA
GACCTTCATTTTCAATCAATCAAGTTTAAATATAAAACAACATAACTTTATTAATAAAGTTTAGAATTTAATTTCTTCTTCTTCTTCTATA
TTAATCTTCATCATTATTTAAAAATTTCAATTAATTTTACATAATTTATTTGAATCGAAAAAGTTATCAAAGTACTATTTCTATTAATCC
ATCTCTACACTTTTTATTCTTATCTTCTTCTTCTTCTTCTTTTTTTTTIACGATTAATCCCTCAACTTTTCCAAACATAATCTAATCATCTC
TTCGACAACAATTTCAATACCTTTTGAATCCACAATTTATCAAACTACTCCTCCACATTTCCAAATAATTTAAATTTTTTCAAATGGATT
TTAAATTAACAATTTATAATATAACTTGTCTAATACTGCTAATACATTTAATTACTTCTTCCAAACTTTCATCAAATTTATTATTATA
ATTCTCTAAGTATCTTAATTTATCCAAAATGTATTCAATATGCTGTGATGATTTGA

IES length = 5314

length of target RE fragment 1113

left_RE_position: 4999

right_RE_position: 6112

Target sequence

TTTAAACACCAGCTCATACTGCTACTCGAATCAAAAAATATCTGAAATAATTCTCATTTCACCTTTCCTGCTGATACATTTAAGATTGCTGGA
ATATTGGTGAAATCCATATAATCAATTATTGCAATAACTAAGGCTAATAAAATTTCTAACCAAAAATTTATTTAAGGAAGTTATTAATAAAGT
CTAAAAACAAGAGACAATGAATATGATATTTCTTTGTTACATTAGTTACAGGTTACATAATGTGATAGTGCATTCTGTGATCAGGTATGTGCT
TAATCATATTTCAATTTTACCCTATATTCATGATATTTGATGGCTAAGCACTTGAGGAGCTTTAATCTTCATCACAAGAATTAAGCGAAG
GATATATTTATCTTAAAGTAATACTATAAACACTATAATTTATTATTACATGTTGAATAATGTAGACAGAATCCATGAACAAAATTTAATAT
AACGGCCATCATTAAGTAAATGAACATATTTAATACGCCATAATTTTAAAGGTAGAAAGAATCATAATAGTAACGAAAAGTTACAT
CACTGAACCTTTTATTTATCAAAAGTGAAGAAAAATGAAACTCATTCAATCTAGACTACCTGCCTAATTGAATTGACATGATTGTACAT
CAGTAGAACTATTACTCCAGTTGTACAAAAGGTCCAAAACAGAATTGAAAGAATGACAAACATTAGTGTGTCAGTAACAACCAATCA
AAAAAGCTACTGCATGTTAATTGATACGTACTGTGCCAATTTACATTTTGTAGCTCAAATAAAATTTGGACATCAGTATAACTATTAGTAAC
AAAATTAATGCAGCAAATTTGTATTGTGCTGTGAGAATATCATCTCTCTCAAATTTTTGGGAATTCATTATTTCAAATGGAAAAATTTG
AATGAGCATATTATCTTTTTTACTAATTTCTTTCCATTTTATAATCTTAACTTTGTTTTTGTGAGAGTTCCCTCTTATTTAATTTCCG
CTTAATATCTCTGAAAGTATTAATTTGTGTCAGATTGATTGCTAATCATTTTCTTAAATTTAATTTGTATGATTTTTCAT
TATTTAAA

9. Acknowledgements

First of all, I would like to thank Mariusz Nowacki from the bottom of my heart for saving my research career and for taking me in this lab and giving me this constructive subject when I quitted from my last lab. So, I can happily carry out my favourite scientific work in a lab that is so harmonious. Mariusz is also very open and supportive of the direction of my research and provided very constructive guidance throughout the research process. I also thank my thesis committee for their efforts on supporting and evaluating.

I thank the members of the Nowacki lab for all the discussions and support. I would like to thank the former colleague Chundi Wang for helping me to quickly open up completely new territory when I first stepped into this lab. I would also like to thank Therese Solberg, for all her constructive comments. I would like to thank Dr. Sebastian Bechara for his efforts on bioinformatic analysis on SMC4 project. Thanks Dr. Ryuma Matsubara for his support on the PGM projects. I want to thank Dr. Victor Mason, for his efforts in bioinformatic analysis in other projects. Thanks to everyone in this lab for your kindness, support and understanding.

I would like to thanks China Scholarship Council for the chance they provide that I can study abroad.

Below, I would like to thank those people who support me in thousands of miles away in Chinese.

首先，我要感谢我的父母，感谢他们无私的抚养我长大，不遗余力的支持我追求想要的生活，感谢他们在身后默默的支持我。谨以此论文献给我的父母。其次，我要感谢我的朋友们，感谢他们在身边亦或千里之外的鼓励，支持和帮助。

自 2018 年 11 月 30 日到达德国开始，眨眼间四年已经在身后流淌而过。回首一幕幕，刚出国时的兴奋，进入第一个实验室的紧张，改派时的忐忑，到新实验室的重新振作，探讨问题时的激动，加班甚至通宵取时间点的疲惫，上班路上时隐时现的雪山的震撼，第一次攀岩，第一次漂流，第一次真正意义上的远距离徒步，第一次尝试瑞士餐厅的终身难忘，第一次见识圣诞舞会的好奇，还有数不尽的感触无法一一描述。总之，四年跌宕起伏的博士生涯告一段落，无所谓好与坏，对得起自己的付出，接下来我要砥砺前行。

10. Declaration of Consent

Declaration of consent

on the basis of Article 18 of the PromR Phil.-nat. 19

Name/First Name: Zhang Fukai

Registration Number: 19-125-343

Study program: PhD in Molecular Life Science

Bachelor Master Dissertation

Title of the thesis: Investigation of condensin related structural maintenance of chromosomes and Piggmac in Paramecium tetraueilia

Supervisor: Prof. Dr. Mariusz Nowacki

I declare herewith that this thesis is my own work and that I have not used any sources other than those stated. I have indicated the adoption of quotations as well as thoughts taken from other authors as such in the thesis. I am aware that the Senate pursuant to Article 36 paragraph 1 litera r of the University Act of September 5th, 1996 and Article 69 of the University Statute of June 7th, 2011 is authorized to revoke the doctoral degree awarded on the basis of this thesis. For the purposes of evaluation and verification of compliance with the declaration of originality and the regulations governing plagiarism, I hereby grant the University of Bern the right to process my personal data and to perform the acts of use this requires, in particular, to reproduce the written thesis and to store it permanently in a database, and to use said database, or to make said database available, to enable comparison with theses submitted by others.

Bern 26.09.2022

Place/Date

Signature 